

การศึกษาการดูดซับสีอินดิโกและสีอนุพันธ์ของอินดิโกบนเส้นไหม

นางสาวนภารัตน์ จิวลักษณ์

วิทยานิพนธ์นี้เป็นส่วนหนึ่งของการศึกษาตามหลักสูตรปริญญาวิทยาศาสตรดุษฎีบัณฑิต  
สาขาวิชาเคมี  
มหาวิทยาลัยเทคโนโลยีสุรนารี  
ปีการศึกษา 2553

**A STUDY OF THE ADSORPTION OF INDIGO  
AND INDIGO DERIVATIVES ONTO SILK**

**Naparut Jiwalak**

**A Thesis Submitted in Partial Fulfillment of the Requirements for the**

**Degree of Doctor of Philosophy in Chemistry**

**Suranaree University of Technology**

**Academic Year 2010**

**A STUDY OF THE ADSORPTION OF INDIGO  
AND INDIGO DERIVATIVES ONTO SILK**

Suranaree University of Technology has approved this thesis submitted in partial fulfillment of the requirements for the Degree of Doctor of Philosophy.

Thesis Examining Committee




(Assoc. Prof. Dr. Vichitr Rattanaphani)

Chairperson



(Assoc. Prof. Dr. Saowanee Rattanaphani)

Member (Thesis Advisor)



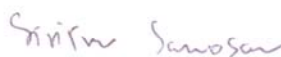
(Prof. Dr. John Barnard Bremner)

Member



(Assoc. Prof. Dr. Malee Tangsathitkulchai)

Member



(Asst. Prof. Dr. Siritron Samosorn)

Member



(Prof. Dr. Sukit Limpijumnong)

Vice Rector for Academic Affairs



(Assoc. Prof. Dr. Prapun Manyum)

Dean of Institute of Science

นภรัตน์ จิวาลักษณ์ : การศึกษาการดูดซับสีอินดิโกและสีอนุพันธ์ของอินดิโกบนเส้นไหม  
(A STUDY OF THE ADSORPTION OF INDIGO AND INDIGO DERIVATIVES  
ONTO SILK) อาจารย์ที่ปรึกษา : รองศาสตราจารย์ ดร.เสาวณีย์ รัตนพานี, 218 หน้า.

การศึกษานี้เป็นการศึกษาจลนพลศาสตร์และอุณหพลศาสตร์ของการดูดซับสีอินดิโกและอนุพันธ์ของสีอินดิโกบนเส้นไหม ซึ่งเป็นการศึกษารายละเอียดของค่าพารามิเตอร์ทางจลนพลศาสตร์และอุณหพลศาสตร์ของการย้อมไหมด้วยอินดิโกโดยเป็นวิธีการย้อมแบบเวทเป็นครั้งแรก วิธีการย้อมแบบนี้ทำได้โดยการเริ่มรีดิวซ์สีอินดิโกด้วยสาร โซเดียมไดไฮไดรไรต์เพื่อให้ได้สีในรูปของลิวโกอินดิโกซึ่งละลายน้ำได้ นำเส้นไหมไปลงในสารละลายลิวโกอินดิโกที่ได้ จากนั้นนำเส้นไหมออกมาสัมผัสอากาศเพื่อให้เกิดการออกซิไดซ์กลับไปเป็นอินดิโก จากการศึกษาพบว่าการดูดซับสีอินดิโกบนเส้นไหมเป็นกระบวนการการดูดซับทางเคมี การเปรียบเทียบผลการศึกษาทางจลนพลศาสตร์และอุณหพลศาสตร์ของการย้อมไหมด้วยสีสกัดอินดิโกจากพืชที่ได้จาก *Indigofera tinctoria* มีผลไปในทางเดียวกันกับการศึกษาการย้อมไหมด้วยสีอินดิโก ซึ่งผลการทดลองสอดคล้องกับข้อมูลการวิเคราะห์ทาง HPLC ซึ่งแสดงว่าสีสกัดจากพืชมีอินดิโกเป็นองค์ประกอบหลัก จากการศึกษาดังกล่าวแสดงว่าองค์ประกอบอื่นๆ ที่มีอยู่ในสีสกัดไม่มีผลอย่างมีนัยสำคัญต่อการศึกษาทางจลนพลศาสตร์และอุณหพลศาสตร์ของการย้อมไหมที่มีอยู่ในสีสกัดจากพืช

ได้ทำการศึกษาค่าพารามิเตอร์ทางจลนพลศาสตร์และอุณหพลศาสตร์ของการย้อมไหมโดยตรงโดยใช้สารอนุพันธ์ของสีอินดิโกที่ละลายน้ำได้ คือ อินดิโกคาร์มินที่วางขายในตลาดพบว่าการย้อมเป็นแบบการดูดซับทางเคมีชนิดคายความร้อนและเป็นปฏิกิริยาอันดับสองเสมือน นอกจากนี้ยังได้ทำการเตรียมอนุพันธ์ของสีอินดิโกซึ่งเป็นสารอนุพันธ์ตัวใหม่ที่มีสีน้ำเงิน-เขียวและละลายน้ำได้ ซึ่งมีโครงสร้างแตกต่างกับอินดิโกคาร์มิน โดยได้ทำการเพิ่มความสามารถในการละลายน้ำของสีอินดิโกด้วยการเพิ่มหมู่ฟังก์ชันที่มีขั้วบนตำแหน่งของไนโตรเจนในโมเลกุลของอินดิโก สารอนุพันธ์ที่เตรียมได้นี้ประกอบด้วยหมู่ฟังก์ชันของกรดคาร์บอกซิลิกและหมู่เอสเทอร์บนไนโตรเจนในโมเลกุลของสีอินดิโก สารอนุพันธ์ที่เตรียมได้ตัวใหม่นี้สามารถย้อมติดบนเส้นไหมภายใต้สภาวะการย้อมที่เป็นกรด

นอกจากนี้ยังได้นำเสนอวิธีการใหม่ในการเพิ่มความสามารถในการละลายน้ำของสีอินดิโกโดยการใช้สารเติมแต่ง สารเหล่านี้ได้แก่ สาร โซโคลเดกทรีนส์และอนุพันธ์ หรือสาร ไฮโดรโพรปิก เช่น ยูเรีย และนิโคตินาไมด์ ซึ่งการเติมสารเหล่านี้สามารถเพิ่มความสามารถในการละลายน้ำของสีอินดิโกและสีสกัดอินดิโกจากพืชได้ การศึกษาดังกล่าวนำไปสู่พัฒนาการย้อมเส้นไหมได้ โดยตรง

ภายใต้สภาวะการข้อมที่เป็นกรด โดยไม่จำเป็นต้องมีขั้นตอนการรีดิวซ์สีอินดิโกและขั้นตอนการออกซิไดซ์ การศึกษาทางจลนพลศาสตร์และอุณหพลศาสตร์ของการดูดซับสีอินดิโก-ยูเรียบนเส้นไหม พบว่าเป็นกระบวนการการดูดซับทางเคมีที่เป็นแบบคายความร้อน การดูดซับนี้เป็นปฏิกิริยาอันดับสองเหมือน การที่ยูเรียสามารถเพิ่มความสามารถในการละลายของอินดิโกอย่างไม่เป็นที่ทราบชัด อย่างไรก็ตามวิธีการข้อมไหมโดยตรงโดยใช้สีสกัดอินดิโกจากพืชและยูเรียดังกล่าวสามารถนำไปประยุกต์ใช้ได้ในห้องถิ่น

สาขาวิชาเคมี

ปีการศึกษา 2553

ลายมือชื่อนักศึกษา N. Jivalak.

ลายมือชื่ออาจารย์ที่ปรึกษา S. Rattaphi

ลายมือชื่ออาจารย์ที่ปรึกษาร่วม J. B. Brennan

ลายมือชื่ออาจารย์ที่ปรึกษาร่วม M. Taysathitkul

NAPARAT JIWALAK : A STUDY OF THE ADSORPTION OF INDIGO  
AND INDIGO DERIVATIVES ONTO SILK. THESIS ADVISOR : ASSOC.  
PROF. SAOWANEE RATTANAPHANI, Ph.D. 218 PP.

ADSORPTION/KINETICS/THERMODYNAMICS/INDIGO/INDIGO  
DERIVATIVES/SILK DYEING

The adsorption kinetics and thermodynamics of indigo and indigo derivative dyeing onto silk were investigated in this study. Detailed kinetic and thermodynamic parameters were determined for the first time for the dyeing of silk using indigo itself and the vat dyeing method. This method involved initial reduction of the indigo with sodium dithionite to give leuco indigo, then immersion of the silk in the aqueous solution of leuco indigo, followed by aerial oxidation to indigo *in situ*. A chemisorption process was indicated for the indigo dyeing of silk. A comparison of kinetic and thermodynamic data for silk dyeing using plant derived indigo extract obtained from *Indigofera tinctoria* was also made with the data from indigo itself and close similarities were seen. This was consistent with the HPLC analytical data which showed indigo as a major component of the extract. It also indicated that other components in the crude indigo extract were not significantly affecting the dyeing kinetics and thermodynamics.

Detailed kinetic and thermodynamic parameters have been obtained for the first time with respect to the direct dyeing of silk using the commercially available, water soluble blue dye, indigo carmine. The adsorption process with this indigo-derived dye was an exothermic chemisorption one following pseudo second order

kinetics. Another new water soluble blue-green dye was prepared in this work from indigo, which, in contrast to indigo carmine, involved the introduction of polar substituents on nitrogen in the indigo molecule. The particular compound prepared incorporated a carboxylic acid and ester group in separate substituents. In a trial experiment, this compound was shown to dye silk under acidic conditions.

New ways to increase the water solubility of indigo were found based on the use of additives. These additives included cyclodextrins and derivatives, or simple hydrotropic compounds like urea and nicotinamide. Using these compounds the water solubility of pure indigo and plant extracted indigo could be increased significantly. The addition of urea was then used to develop a new process for the direct dyeing of silk under acidic conditions without the need for an indigo reduction and subsequent oxidation step. The key kinetic and thermodynamic parameters for this dyeing process were obtained, with the kinetics fitting a pseudo second order model. Other parameters were consistent with an exothermic chemisorption process. Whether urea does more than increase the indigo solubility is as yet not known. However, direct dyeing of silk using plant extracted indigo and urea could be a potentially viable option for villagers.

School of Chemistry

Academic Year 2010

Student's Signature N. Sivalak

Advisor's Signature S. Kulkarni

Co-advisor's Signature J. B. Brennan

Co-advisor's Signature M. T. Sathyanarayana

## **ACKNOWLEDGEMENTS**

With the achievement of this degree, I am grateful to all the people that have contributed to this dissertation. First and foremost, I would like to express my sincere gratitude to Assoc. Prof. Dr. Saowanee Rattanaphani, my thesis advisor, and also extended to my co-advisor, Prof. Dr. John Barnard Bremner and Assoc. Prof. Dr. Vichitr Rattanaphani for their wonderful advice, exceptional generous support, encouragement, insightful suggestion, academic guidance and advice throughout the course of my graduate study. It has been a pleasure to work under their supervision.

My appreciation also goes to Assoc. Prof. Dr. Malee Tangsathitkulchai and Asst. Prof. Dr. Siritron Samosorn, for their kind agreement to serve on my committee and also for their many important comments and suggestions. I would also like to sincerely thank all of the academic members in the School of Chemistry and School of Chemical Engineering, Suranaree University of Technology for their teaching, encouragement, good attitude and advice.

I would like to thank the staff of the scientific equipment center F1, F2 and F6 Suranaree University of Technology for their advice and facility support. I would like to thank the members of the School of Chemistry, University of Wollongong, Australia. Special thanks go to all the spectroscopy technical staff of the Chemistry Department for their assistance, undertaking and training in IR, NMR and MS. Thanks also to Mr. Andrew Stevens for his guidance and help with molecular modeling analyses. I would like to thank the members of the Department of



Chemistry, Srinakharinwirot University. Special thanks go to Asst. Prof. Dr. Siritron Samosorn and the members of her research group for their providing assistance, undertaking, good attitude and good advice.

I would also like to thank all of my good friends in the Saowanee research group, the graduate students in the School of Chemistry and in the School of Chemical Engineering, Suranaree University of Technology, the Bremner lab, the students at the University of Wollongong, Australia and also the members in the Siritron research group, and the students in the Department of Chemistry, Srinakharinwirot University. Thanks also are due to Supunnee, Natthaya and Areeya for their good friendship and all the good help they have provided.

I wish to thank Chiang Mai Ratchabhat University, Chiang Mai, Thailand for supporting my scholarship throughout my study. I also thank Suranaree University of Technology, the University of Wollongong and the Ministry of University Affairs for partial financial support.

Finally, I would like to express my deepest gratitude to my wonderful parents and my sister for their unconditional love and support in everything and also continual encouragement during my education.

Naparat Jiwalak

# CONTENTS

	<b>Page</b>
ABSTRACT IN THAI.....	I
ABSTRACT IN ENGLISH .....	III
ACKNOWLEDGEMENTS.....	V
CONTENTS.....	VII
LIST OF TABLES.....	XVII
LIST OF FIGURES .....	XXI
LIST OF ABBREVIATIONS.....	XXXI
<b>CHAPTER</b>	
<b>I GENERAL INTRODUCTION.....</b>	<b>1</b>
1.1 Textile fibres .....	2
1.1.1 Man-made fibres .....	2
1.1.2 Natural fibres .....	3
1.2 Silk fibre.....	5
1.2.1 Physical properties .....	6
1.2.2 Chemical properties .....	7
1.3 Synthetic dyes .....	9
1.3.1 Chemical structure classification .....	9
1.3.2 Method of application classification.....	9
1.4 Natural dyes .....	19
1.5 Research objectives.....	26

**CONTENTS (Continued)**

	<b>Page</b>
1.6 Scope and limitations of the study .....	27
1.7 References .....	28
<b>II ADSORPTION KINETIC AND THERMODYNAMIC STUDIES OF INDIGO DYEING ONTO SILK BY THE CONVENTIONAL VAT- DYEING METHOD .....</b>	<b>31</b>
2.1 Abstract .....	31
2.2 Introduction .....	32
2.2.1 Physical chemistry of the dyeing process .....	40
2.2.2 Kinetic models of adsorption .....	46
2.2.3 Adsorption isotherms .....	49
2.3 Experimental .....	53
2.3.1 Materials and Chemicals .....	53
2.3.2 Instruments .....	53
2.3.3 Experimental methods .....	54
2.3.3.1 Silk yarn preparation (Chairat, 2004) .....	54
2.3.3.2 Preparation of plant extracted indigo dye powder .....	54
2.3.3.3 Analysis of indigo in plant extracted indigo dye by the HPLC method .....	55
2.3.3.4 Reduction of indigo by sodium dithionite in alkaline medium .....	56
2.3.3.5 Batch kinetic experiments of indigo dyeing onto silk by the conventional vat-dyeing method .....	57

## CONTENTS (Continued)

	<b>Page</b>
2.3.3.6 Batch equilibrium experiments of indigo dyeing onto silk by the conventional vat-dyeing method.....	58
2.3.3.7 Batch kinetic experiments of plant extracted indigo dyeing onto silk by the conventional vat-dyeing method .....	59
2.3.3.8 Batch equilibrium experiments of plant extracted indigo dyeing onto silk by the conventional vat-dyeing method.....	60
2.4 Results and Discussion .....	60
2.4.1 Analysis of indigo in plant extracted indigo dye by HPLC method .....	60
2.4.2 Kinetic and thermodynamic studies of indigo dyeing onto silk by the conventional vat-dyeing method .....	64
2.4.2.1 Effect of initial dye concentration and contact time on the adsorption of indigo onto silk .....	64
2.4.2.2 Effect of material to liquor ratio (MLR) on the adsorption of indigo onto silk .....	69
2.4.2.3 Effect of temperature on the adsorption of indigo onto silk.....	71
2.4.2.4 Activation parameters for the adsorption of indigo onto silk.....	74

## CONTENTS (Continued)

	<b>Page</b>
2.4.2.5 Adsorption isotherm for the adsorption of indigo onto silk .....	76
2.4.2.6 Thermodynamic parameters for the adsorption of indigo on silk .....	80
2.4.3 Adsorption studies of plant extracted indigo onto silk by the conventional vat-dyeing method.....	82
2.4.3.1 Effect of initial dye concentration and contact time on the adsorption of plant extracted indigo onto silk.....	82
2.4.3.2 Effect of temperature on the adsorption of plant extracted indigo onto silk.....	87
2.4.3.3 Activation parameters for the adsorption of plant extracted indigo onto silk.....	89
2.4.3.4 Adsorption isotherm for the adsorption of plant extracted indigo onto silk.....	92
2.4.3.5 Thermodynamic parameters for the adsorption of plant extracted indigo on silk .....	95
2.5 Conclusion .....	97
2.6 References.....	98

**CONTENTS (Continued)**

	<b>Page</b>
<b>III SILK DYEING WITH WATER SOLUBLE INDIGO</b>	
<b>DERIVATIVES</b> .....	104
3.1 Abstract.....	104
3.2 Introduction.....	105
3.3 Experimental.....	110
3.3.1 Materials and Chemicals.....	110
3.3.2 Instruments.....	110
3.3.3 Experimental methods .....	111
3.3.3.1 Silk yarn preparation (Chairat, 2004) .....	111
3.3.3.2 Batch kinetic experiments of indigo carmine dyeing onto silk .....	111
3.3.3.3 Batch equilibrium experiments of indigo carmine dyeing onto silk.....	112
3.3.3.4 Preparation and characterization of more water soluble <i>N,N'</i> -substituted indigo derivatives for direct dyeing of silk .....	112
3.3.3.5 Preliminary direct dyeing of silk with an <i>N,N'</i> -disubstituted indigo derivative.....	117
3.4 Results and Discussion .....	118
3.4.1 Adsorption kinetic and thermodynamic studies of indigo carmine dyeing onto silk.....	118

## CONTENTS (Continued)

	<b>Page</b>
3.4.1.1 Effect of pH on the adsorption of indigo carmine onto silk.....	118
3.4.1.2 Effect of initial dye concentration and contact time on the adsorption of indigo carmine onto silk .....	123
3.4.1.3 Effect of material to liquor ratio (MLR) on the adsorption of indigo carmine onto silk .....	126
3.4.1.4 Effect of temperature on the adsorption of indigo carmine onto silk.....	129
3.4.1.5 Activation parameters for the adsorption of indigo carmine onto silk.....	131
3.4.1.6 Adsorption isotherm for the adsorption of indigo carmine onto silk.....	134
3.4.1.7 Thermodynamic parameters for the adsorption of indigo carmine on silk.....	135
3.4.2 Preparation and characterization of more water soluble <i>N,N'</i> -indigo derivatives for direct dyeing of silk.....	137
3.4.2.1 Establishment of <i>N</i> -substitution methodology with methylation .....	137
3.4.2.2 Introduction of a water solubilising acetamido group on N .....	138
3.4.2.3 Reaction of indigo with ethyl bromopyruvate .....	139
3.4.2.4 Reaction of indigo with ethyl iodoacetate .....	140

## CONTENTS (Continued)

	<b>Page</b>
3.4.2.5 Hydrolysis of the diester .....	142
3.4.2.6 Molecular Calculations .....	144
3.4.2.7 More water soluble indigo derivatives direct dyeing of silk .....	145
3.5 Conclusion .....	146
3.6 References.....	147
<b>IV APPROACHES TO DIRECT NON-REDUCTIVE INDIGO DYEING ONTO SILK AND ASSOCIATED ADSORPTION STUDIES.....</b>	<b>151</b>
4.1 Abstract.....	151
4.2 Introduction.....	152
4.2.1 Cyclodextrins (CDs) .....	153
4.2.1.1 Natural cyclodextrins and chemically modified cyclodextrins .....	153
4.2.1.2 Cyclodextrin complexation process.....	158
4.2.1.3 Application of cyclodextrin .....	159
4.2.2 Hydrotropic agents.....	163
4.3 Experimental.....	165
4.3.1 Materials and Chemicals.....	165
4.3.2 Instruments.....	165
4.3.3 Experimental methods .....	166
4.3.3.1 Silk yarn preparation (Chairat, 2004) .....	166
4.3.3.2 Solubility studies and complex preparation.....	166



## CONTENTS (Continued)

	<b>Page</b>
4.3.3.3 Batch kinetic experiments of indigo-urea dyeing onto silk .....	167
4.3.3.4 Batch equilibrium experiments of indigo-urea dyeing onto silk.....	168
4.3.3.5 Batch kinetic experiments of plant extracted indigo-urea dyeing onto silk .....	168
4.3.3.6 Batch equilibrium experiments of plant extracted indigo-urea dyeing onto silk .....	169
4.4 Results and Discussion .....	170
4.4.1 Improvement in the water solubility of indigo dye for dyeing directly onto silk .....	170
4.4.1.1 Complex formation of indigo with cyclodextrin and cyclodextrin derivatives .....	170
4.4.1.2 Additives to modulate water solubility of indigo dye.....	173
4.4.2 Adsorption kinetic and thermodynamic studies of indigo -urea dyeing onto silk without a reduction process .....	177
4.4.2.1 Effect of initial dye concentration and contact time on the adsorption of indigo-urea onto silk.....	177
4.4.2.2 Effect of material to liquor ratio (MLR) on the adsorption of indigo-urea onto silk.....	182

## CONTENTS (Continued)

	<b>Page</b>
4.4.2.3 Effect of temperature on the adsorption of indigo-urea onto silk .....	184
4.4.2.4 Activation parameters for the adsorption of indigo-urea onto silk .....	187
4.4.2.5 Adsorption isotherm for the adsorption of indigo onto silk.....	189
4.4.2.6 Thermodynamic parameters for the adsorption of indigo-urea on silk .....	193
4.4.3 Adsorption studies of plant extracted indigo-urea direct dyeing onto silk.....	194
4.4.3.1 Effect of initial dye concentration and contact time on the adsorption of plant extracted indigo-urea onto silk.....	195
4.4.3.2 Effect of temperature on the adsorption of plant extracted indigo-urea onto silk.....	200
4.4.3.3 Activation parameters for the adsorption of plant extracted indigo-urea onto silk.....	202
4.4.3.4 Adsorption isotherm for the adsorption of plant extracted indigo-urea onto silk.....	205
4.4.3.5 Thermodynamic parameters for the adsorption of plant extracted indigo-urea on silk .....	207
4.5 Conclusion .....	209

**CONTENTS (Continued)**

	<b>Page</b>
4.6 References.....	210
<b>V CONCLUSION</b> .....	<b>215</b>
<b>CURRICULUM VITAE</b> .....	<b>218</b>

## LIST OF TABLES

Table	Page
1.1 Main amino acid composition of sericin and fibroin (Karmakar, 1999).....	7
1.2 A summary of the characteristics of the main chemical classes of dyes (Christie <i>et al.</i> , 2000).....	10
1.3 Natural dyes and pigments (Bhat <i>et al.</i> , 2005).....	20
2.1 Amount of indigo in plant extracted indigo dye by HPLC method.....	63
2.2 Comparison of the pseudo first- and pseudo second-order adsorption rate constants and the calculated and experimental $q_e$ values for different initial dye concentrations, MLR and temperature for the adsorption of indigo onto silk.....	68
2.3 Activation parameters for the adsorption of indigo onto silk at initial dye concentration 20 mg/L.....	74
2.4 Langmuir and Freundlich isotherm constants for the adsorption of indigo onto silk at different temperatures.....	79
2.5 Thermodynamic parameters for the adsorption of indigo onto silk at different temperatures.....	81
2.6 Comparison of the pseudo first- and pseudo second-order adsorption rate constants and the calculated and experimental $q_e$ values for different initial dye concentrations and temperature for the adsorption of plant extracted indigo onto silk.....	86

## LIST OF TABLES (Continued)

<b>Table</b>	<b>Page</b>
2.7	Activation parameters for the adsorption of plant extracted indigo onto silk at initial dye concentration 1.1 g/L. .... 90
2.8	Langmuir and Freundlich isotherm constants for the adsorption of plant extracted indigo onto silk at 30°C. .... 93
2.9	Thermodynamic parameters for the adsorption of plant extracted indigo onto silk at different temperatures ..... 96
3.1	Comparison of the pseudo first- and pseudo second-order adsorption rate constants and the calculated and experimental $q_e$ values for different pH, initial dye concentrations, MLR and temperature for the adsorption of indigo carmine onto silk. .... 122
3.2	Activation parameters for the adsorption of indigo carmine dye onto silk at an initial dye concentration of 46.6 mg/L and pH 4.0 ..... 132
3.3	Langmuir and Freundlich isotherm constants for the adsorption of indigo carmine dye onto silk at different temperatures ..... 135
3.4	Thermodynamic parameters for the adsorption of indigo carmine onto silk at different temperatures ..... 136
3.5	Calculated energies of formation for substituted indigo ( <i>E</i> ) and ( <i>Z</i> ) isomers ..... 145
4.1	Characteristics of the natural cyclodextrins $\alpha$ -CD, $\beta$ -CD and $\gamma$ -CD (Easton and Lincoln, 1999). .... 156
4.2	Structural and physicochemical properties of selected cyclodextrins (Figure 4.3) of pharmaceutical interest (Brewster and Loftsson, 2007). .... 157

## LIST OF TABLES (Continued)

<b>Table</b>	<b>Page</b>
4.3	Effect of CDs on the solubility of indigo (molar ratio (indigo:CDs) = 1:1, sonication time = 2 hr, bath temp. = 40 ( $\pm 5^\circ\text{C}$ )..... 171
4.4	Effect of additives on the solubility of indigo (molar ratio (indigo:additive) = 1:1, sonication time = 2 hr, bath temp. = 40 ( $\pm 5^\circ\text{C}$ )..... 174
4.5	Comparison of the pseudo first- and pseudo second-order adsorption rate constants and the calculated and experimental $q_e$ values for different initial dye concentrations, MLR and temperature for the adsorption of indigo-urea onto silk. .... 181
4.6	Activation parameters for the adsorption of indigo-urea onto silk at initial dye concentration 20 mg/L. .... 187
4.7	Langmuir and Freundlich isotherm constants for the adsorption of indigo-urea onto silk at 30°C. .... 191
4.8	Thermodynamic parameters for the adsorption of indigo-urea onto silk at different temperatures. .... 193
4.9	Comparison of the pseudo first- and pseudo second-order adsorption rate constants and the calculated and experimental $q_e$ values for different initial dye concentrations and temperatures for the adsorption of plant extracted indigo-urea onto silk..... 199
4.10	Activation parameters for the adsorption of plant extracted indigo-urea onto silk at initial dye concentration 1 g/L ..... 203

**LIST OF TABLES (Continued)**

<b>Table</b>		<b>Page</b>
4.11	Langmuir and Freundlich isotherm constants for the adsorption of plant extracted indigo-urea onto silk at 30°C.....	205
4.12	Thermodynamic parameters for the adsorption of plant extracted indigo-urea onto silk at different temperatures.....	208

## LIST OF FIGURES

Figure	Page
1.1	Examples of the chemical structures of (a) polyamide and (b) polyester chains (Donald, Gary, and George, 1976)..... 3
1.2	Molecular structure and configuration of cellulose (Karmakar, 1999)..... 4
1.3	Basic amino acid structure (Donald <i>et al.</i> , 1976)..... 5
1.4	Crystalline structure of the polypeptide chains in fibroin (Karmakar, 1999)..... 8
1.5	Structure of the protein fibres (polypeptide) (Donald <i>et al.</i> , 1976)..... 9
1.6	Examples of the structures of an azo dye, carbonyl dye and arylcarbocation dye; (a) C.I. Direct Red 28, Congo Red, an example of a diazo dye; (b) C.I. Vat Blue 1, Indigo, an example of a carbonyl dye and (c) C.I. Basic Green 4, Malachite Green, an example of an arylcarbocation dye (triphenylmethane dye) (Christie <i>et al.</i> , 2000). ..... 11
1.7	The chemical interaction of picric acid (an example of a direct dye) and wool (or silk) fibre (Donald <i>et al.</i> , 1976)..... 13
1.8	Examples of acid dyes; (a) C.I. Acid Blue 74, Indigo carmine and (b) C.I. Acid Yellow 23, Tartrazine..... 13
1.9	Examples of vat dyes; (a) Indigo, C.I. Vat Blue 1 and (b) Pyranthrone (C.I. Vat Orange 9) (Perkins, 1996)..... 17



## LIST OF FIGURES (Continued)

<b>Figure</b>	<b>Page</b>
1.10	The chemistry of vat dyeing (Christie, 2001). ..... 18
1.11	Basic structures (flavone, flavane) of most flavonoids, and two examples of flavonoid pigments: morin and rutin. .... 21
1.12	Structures of quinones, and an example of a naphthaquinone pigment (lawsone) and an anthraquinone pigment (alizarin). .... 22
1.13	Basic structure of a carotenoid molecule, and two examples of carotenoid pigments: bixin and crocin ..... 23
1.14	Chemical structure of chlorophyll ..... 24
1.15	Xanthopterin from the butterfly <i>Gonopterix rhamni</i> . .... 25
1.16	An oxidation of indoxyl forms indigo (indigotin). .... 25
2.1	(a) <i>Indigofera tinctoria</i> plant; (a1) flowering branch; (a2) fruit (Lemmens and Wulijarni, 1992) and (b) Leaves of <i>Indigofera tinctoria</i> plant from Nakhon Ratchasima, Thailand..... 34
2.2	The formation of indigo and indigo dyeing process ..... 35
2.3	Graphical representation of a dyeing process: kinetics (left) and equilibrium (right) (Zollinger, 2003). .... 41
2.4	Rate of dyeing isotherms (Perkins, 1996)..... 42
2.5	HPLC chromatograms of (a) standard indigo; (b) indigo-SUT; (b1) indigo SUT spiking with standard indigo; (c) indigo-village; (c1) indigo-village spiking with standard indigo ..... 62
2.6	Calibration curve of standard indigo from HPLC method..... 63

## LIST OF FIGURES (Continued)

<b>Figure</b>	<b>Page</b>
2.7	Effect of initial dye concentration on the adsorption of indigo onto silk (under dyeing condition MLR = 1:100, pH = 11-12, 30°C)..... 65
2.8	Application of the pseudo first order equation at different initial dye concentration on the adsorption of indigo onto silk ..... 66
2.9	Application of the pseudo second order equation at different initial dye concentration on the adsorption of indigo onto silk ..... 67
2.10	Effect of MLR on the adsorption of indigo onto silk (under dyeing condition $C_0 = 20$ mg/L, pH = 11-12, 30°C)..... 70
2.11	Application of the pseudo first order equation at different MLR on the adsorption of indigo onto silk..... 70
2.12	Application of the pseudo second order equation at different MLR to the adsorption of indigo onto silk..... 71
2.13	Effect of temperature on the adsorption of indigo onto silk (under dyeing condition $C_0 = 20$ mg/L, pH = 11-12, MLR = 1:100) ..... 72
2.14	Application of the pseudo first order equation at different temperature on the adsorption of indigo onto silk ..... 73
2.15	Application of the pseudo second order equation at different temperature on the adsorption of indigo onto silk ..... 73
2.16	Arrhenius plots for the adsorption of indigo on silk..... 75
2.17	Plot of $\ln(k/T)$ against $1/T$ for the adsorption of indigo on silk..... 76
2.18	Adsorption isotherms of indigo onto silk at 30, 40 and 50°C..... 77

## LIST OF FIGURES (Continued)

<b>Figure</b>	<b>Page</b>
2.19	Langmuir adsorption isotherm of the adsorption of indigo onto silk at 30, 40 and 50°C..... 78
2.20	Freundlich adsorption isotherm of the adsorption of indigo onto silk at 30, 40 and 50°C..... 80
2.21	The van't Hoff plots of $\ln K_C$ versus $1/T$ ..... 81
2.22	Effect of initial dye concentration on the adsorption of plant extracted indigo onto silk (under dyeing condition MLR = 1:100, pH = 11-12, 30°C)..... 83
2.23	Application of the pseudo first order equation at different initial dye concentration on the adsorption of plant extracted indigo onto silk ..... 84
2.24	Application of the pseudo second order equation at different initial dye concentration on the adsorption of plant extracted indigo onto silk ..... 85
2.25	Effect of temperature on the adsorption of plant extracted indigo onto silk (under dyeing condition $C_0 = 1.1$ g/L, pH = 11-12, MLR = 1:100). ..... 88
2.26	Application of the pseudo first order equation at different temperature on the adsorption of plant extracted indigo onto silk..... 88
2.27	Application of the pseudo second order equation at different temperature on the adsorption of plant extracted indigo onto silk..... 89

## LIST OF FIGURES (Continued)

Figure	Page
2.28	Arrhenius plots for the adsorption of plant extracted indigo on silk ..... 90
2.29	Plot of $\ln(k/T)$ against $1/T$ for the adsorption of plant extracted indigo on silk..... 91
2.30	Adsorption isotherms of plant extracted indigo onto silk at 30°C..... 93
2.31	Langmuir adsorption isotherm of the adsorption of plant extracted indigo onto silk at 30°C ..... 94
2.32	Freundlich adsorption isotherm of the adsorption of plant extracted indigo onto silk at 30°C ..... 94
2.33	The van't Hoff plots of $\ln K_C$ versus $1/T$ ..... 96
3.1	Chemical structure of indigo carmine..... 106
3.2	(a) Structure of an indigo <i>N</i> -glycoside; (b) General structures of N-substituted indigo dye derivatives ( $R, R' = H, CH_2COOEt,$ $CH_2COCOOEt, CH_2CONH_2,$ and $CH_2COOH$ ..... 109
3.3	Effect of pH on the adsorption of indigo carmine onto silk (under dyeing condition: $C_0$ 46.6 mg/L, MLR 1:100, 30°C). ..... 120
3.4	Application of the pseudo first order equation at different pH of dye solution on the adsorption of indigo carmine onto silk..... 121
3.5	Application of the pseudo second order equation at different pH of dye solution on the adsorption of indigo carmine onto silk..... 121
3.6	Effect of initial dye concentration on the adsorption of indigo carmine onto silk (under dyeing condition MLR = 1:100, pH = 4.0, 30°C). ..... 124

## LIST OF FIGURES (Continued)

<b>Figure</b>	<b>Page</b>
3.7 Application of the pseudo first order equation at different initial dye concentration on the adsorption of indigo carmine onto silk.....	125
3.8 Application of the pseudo second order equation at different initial dye concentration on the adsorption of indigo carmine onto silk.....	126
3.9 Effect of MLR on the adsorption of indigo carmine onto silk (under dyeing condition $C_0 = 46.6$ mg/L, pH = 4.0, 30°C). .....	127
3.10 Application of the pseudo first order equation at different MLR on the adsorption of indigo carmine onto silk. ....	128
3.11 Application of the pseudo second order equation at different MLR on the adsorption of indigo carmine onto silk. ....	128
3.12 Effect of temperature on the adsorption of indigo carmine onto silk (under dyeing condition $C_0 = 46.6$ mg/L, pH = 4.0, MLR = 1:100).....	130
3.13 Application of the pseudo first order equation at different temperature on the adsorption of indigo carmine onto silk. ....	130
3.14 Application of the pseudo second order equation at different temperature on the adsorption of indigo carmine onto silk. ....	131
3.15 Arrhenius plots for the adsorption of indigo carmine on silk. ....	132
3.16 Plot of $\ln(k/T)$ against $1/T$ for the adsorption of indigo carmine on silk.....	133
3.17 The van't Hoff plots of $\ln K_C$ versus $1/T$ .....	137
4.1 Structure of indigo (Alexandre, Jocilene, Wlaine, and Silvia, 2004) .....	152

## LIST OF FIGURES (Continued)

<b>Figure</b>	<b>Page</b>
4.2	(a) Chemical structures of $\alpha$ -, $\beta$ - and $\gamma$ -cyclodextrin; (b) A structural scheme of a torus-shaped cyclodextrin molecule (Easton and Lincoln, 1999).....
	155
4.3	Chemical structure of substituted cyclodextrins (Brewster and Loftsson, 2007).....
	157
4.4	Water-soluble inclusion complexes (Davis and Brewster, 2004).....
	159
4.5	UV-spectrum of indigo: 2HP- $\beta$ -CD complexes and indigo:additives (as urea, nicotinamide, and N-acetylglycine.....
	172
4.6	Effect of the amount of 2HP- $\beta$ -CD, urea, nicotinamide, and N-acetylglycine on the water solubility of indigo.....
	172
4.7	The proposed interaction of indigo with urea.....
	175
4.8	UV-spectrum of indigo:urea and plant extracted indigo:urea.....
	176
4.9	Effect of the amount of urea on the water solubility of indigo and plant extracted indigo.....
	176
4.10	Effect of initial dye concentration on the adsorption of indigo-urea onto silk (under dyeing condition MLR = 1:100, pH = 4.0, 30°C). .....
	178
4.11	Application of the pseudo first order equation at different initial dye concentration on the adsorption of indigo-urea onto silk. ....
	179
4.12	Application of the pseudo second order equation at different initial dye concentration on the adsorption of indigo-urea onto silk. ....
	180

## LIST OF FIGURES (Continued)

<b>Figure</b>	<b>Page</b>
4.13	Effect of MLR on the adsorption of indigo-urea onto silk (under dyeing condition $C_0 = 20$ mg/L, pH = 4.0, 30°C). ..... 183
4.14	Application of the pseudo first order equation at different MLRs on the adsorption of indigo-urea onto silk. .... 183
4.15	Application of the pseudo second order equation at different MLRs on the adsorption of indigo-urea onto silk. .... 184
4.16	Effect of temperature on the adsorption of indigo-urea onto silk (under dyeing condition $C_0 = 20$ mg/L, pH = 4.0, MLR = 1:100)..... 185
4.17	Application of the pseudo first order equation at different temperatures on the adsorption of indigo-urea onto silk. .... 186
4.18	Application of the pseudo second order equation at different temperatures on the adsorption of indigo-urea onto silk. .... 186
4.19	Arrhenius plot for the adsorption of indigo-urea on silk. .... 188
4.20	Plot of $\ln(k/T)$ against $1/T$ for the adsorption of indigo-urea on silk..... 189
4.21	Adsorption isotherms of indigo-urea onto silk at 30°C. .... 190
4.22	Langmuir adsorption isotherm of the adsorption of indigo onto silk at 30°C. .... 191
4.23	Freundlich adsorption isotherm of the adsorption of indigo onto silk at 30°C. .... 192
4.24	The van't Hoff plots of $\ln K_C$ versus $1/T$ . .... 194

## LIST OF FIGURES (Continued)

<b>Figure</b>	<b>Page</b>
4.25	Effect of initial dye concentration on the adsorption of plant extracted indigo-urea onto silk (under dyeing condition MLR = 1:100, pH = 4.0, 30°C). ..... 196
4.26	Application of the pseudo first order equation at different initial dye concentration on the adsorption of plant extracted indigo-urea onto silk. .... 197
4.27	Application of the pseudo second order equation at different initial dye concentration on the adsorption of plant extracted indigo-urea onto silk. .... 198
4.28	Effect of temperature on the adsorption of plant extracted indigo-urea onto silk (under dyeing condition $C_0 = 1$ g/L, pH = 4.0, MLR = 1:100). ..... 201
4.29	Application of the pseudo first order equation at different temperatures on the adsorption of plant extracted indigo-urea onto silk. .... 201
4.30	Application of the pseudo second order equation at different temperatures on the adsorption of plant extracted indigo-urea onto silk. .... 202
4.31	Arrhenius plots for the adsorption of plant extracted indigo-urea on silk. .... 203
4.32	Plot of $\ln(k/T)$ against $1/T$ for the adsorption of plant extracted indigo-urea on silk. .... 204
4.33	Langmuir adsorption isotherm of the adsorption of plant extracted-urea indigo onto silk at 30°C. .... 206



**LIST OF FIGURES (Continued)**

<b>Figure</b>	<b>Page</b>
4.34 Freundlich adsorption isotherm of the adsorption of plant extracted indigo onto silk at 30°C. ....	206
4.35 The van't Hoff plots of $\ln K_C$ versus $1/T$ . ....	208

## LIST OF ABBREVIATIONS

mg	Milligram
g	gram
kg	Kilogram
$\mu\text{L}$	Microlitre
mL	Millitre
L	Litre
nm	Nanometre
mm	Millimetre
cm	Centimetre
$^{\circ}\text{C}$	Degree celsius
K	Degree kelvin
mg/g	Milligram per gram
mg/L	Milligram per litre
g/L	gram per litre
mL/min	Millitre per minute
kJ/mol	Kilo joule per mole
w/v	Weight by volume
v/v	Volume by volume
$h_i$	The initial dye adsorption rate
$k_1$	Rate constant of pseudo first-order adsorption

**LIST OF ABBREVIATIONS (Continued)**

$k_2$	Rate constant of pseudo second-order adsorption
$q_e$	The amount of dye adsorbed per gram silk at equilibrium time
$q_t$	The amount of dye adsorbed per gram silk at time t
t	Time
$t_R$	Retention time
min	Minute
hr	hour
A	The pre-exponential factor
$E_a$	Activation energy
R	Gas constant
T	Temperature
Temp.	Temperature
mp	Melting point
$\Delta H^\#$	Enthalpy of activation
$\Delta S^\#$	Entropy of activation
$\Delta G^\#$	Free energy of activation
$\Delta H^\circ$	Enthalpy change
$\Delta S^\circ$	Entropy change
$\Delta G^\circ$	Gibbs free energy
$k_b$	Boltzmann's constant
h	Planck's constant

**LIST OF ABBREVIATIONS (Continued)**

Q	Adsorption capacity of the Langmuir isotherm
b	Langmuir constant
Q <sub>f</sub>	Adsorption capacity of the Freundlich isotherm
K <sub>c</sub>	Equilibrium constant
C	Concentration
C <sub>e</sub>	Concentration of dye left in the dye bath at equilibrium
C <sub>ad,e</sub>	Concentration of the dye adsorbed at equilibrium
C <sub>o</sub>	Initial dye concentration
C <sub>t</sub>	Concentration of dye after dyeing time t
V	Volume of dye solution
W	Weight of silk yarn used
MLR	Material to Liquor Ratio
CDs	Cyclodextrins
TLC	Thin-layer chromatography
HPLC	High Performance Liquid Chromatography
HPLC-ELSD	High performance liquid chromatography evaporative light scattering detector
FT-IR	Fourier transforms infrared spectrophotometer
<sup>1</sup> H-NMR	Proton-Nuclear Magnetic Resonance
<sup>13</sup> C-NMR	Carbon-Nuclear Magnetic Resonance
δ	Chemical shifts
J	coupling constants

**LIST OF ABBREVIATIONS (Continued)**

s	singlet
d	doublet
t	triplet
m	multiplet
MS	Mass Spectrometry
HRMS	High Resolution Mass Spectrometry
ESI	Electrospray ionization
$m/z$	mass to charge value
$\lambda_{\max}$	Maximum wavelength

# CHAPTER I

## GENERAL INTRODUCTION

The ability of natural dyes to colour textiles has been known since ancient times. The earliest written record of the use of natural dyes was found in China dated 2600 B.C. (Christie, Mather, and Wardman, 2000). Up to the end of the nineteenth century natural dyes were the main colourants available for textile dyeing procedures. The development of synthetic dyes at the beginning of the twentieth century led to better quality dyeing and more reproducible techniques of application (Bechtold, Turcanu, Ganglberger, and Geissler, 2003). However, many colourants from synthetic sources can be harmful and cause allergies in humans and may also affect aquatic life and even the food chain (Chang, Lin, Kawata, Hattori, and Namba, 1989). Therefore, interest in natural dyes for dyeing has increased considerably during the past few years (Angelini, Pistelli, Belloni, Bertoli, and Panconesi, 1997). Natural dyes can be found in many different parts of plants including roots (the red dye from *Morinda angustifolia* Roxb.), rhizomes (the orange-yellow dye from *Curcuma longa* Linn.), bark (the black substance from *Terminalia catappa* Linn.), gum-resin of the bark (the yellow dye from *Garcinia hanburyi* Hook.F.), wood (the yellow dye from *Maclura cochinchinensis* Lour. and the orange-red dye from *Caesalpinia sappan* Linn.), leaves (the indigo dye from *Indigofera tinctoria* Linn.), fruits (the purplish-black dye from *Terminalia bellirica* Roxb.), seeds (annatto from *Bixa orellana* Linn.), flowers (safflower from *Carthamus tinctorius* Linn.) and stigmas (saffron from *Crocus sativus*

Linn.) (Moeyes, 1993). The functions of these substances in plants depend on their chemical structure and location in the plant.

In the textile dyeing process, a dye is a colourant substance which is soluble in the dyeing medium during all, or during at least some stages, of the dyeing process (Perkins, 1996). It can thus diffuse into fibres and interact by intermolecular or intramolecular (non-covalent) forces which depend on the structure of the dye and the nature of the fibres (Christie *et al.*, 2000). Information with respect to the textile fibres and the dyestuffs necessary for an understanding of the principles of dyeing are discussed in the following sections.

## **1.1 Textile fibres**

The fibres used in modern textile manufacture can be classified into two main groups (a) man-made and (b) natural fibres (Cook, 1993; Warner, 1995; Karmakar, 1999). Some important information on these fibres is summarised in the following sections 1.1.1 and 1.1.2.

### **1.1.1 Man-made fibres**

Man-made polymer fibres are those in which some manufacturing process has generated the fibres from either natural products or by synthesis. These fibres fall naturally into two broad groups, depending on the origin of the fibre-forming materials from which they are produced, and are usually classified into one of two groups: natural polymer fibres and synthetic fibres. Natural polymer fibres are obtained from the modification of natural fibres for example, cellulosic fibres and cellulose ester fibres. Synthetic fibres are those in which the fibre-forming material is

made from simpler substances for example, polyamide, polyester and polyvinyl derivatives (Cook, 1993; Warner, 1995). Examples of the chemical structures of polyamide and polyester chains are illustrated in Figure 1.1

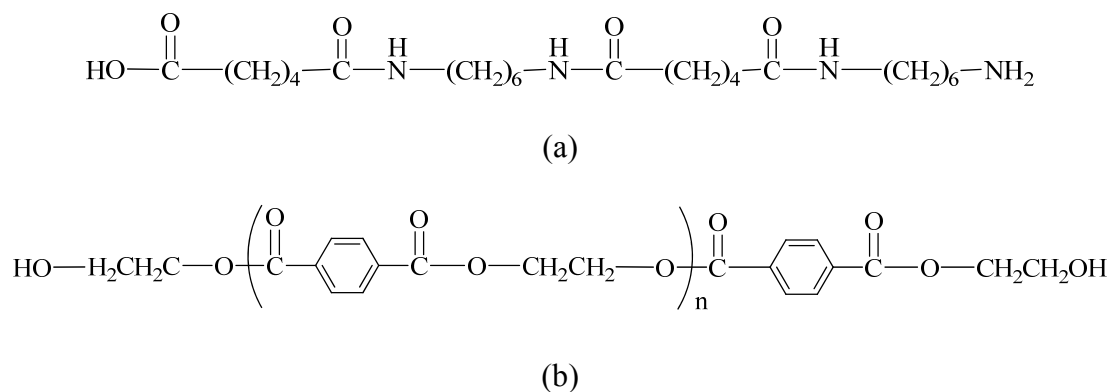


**Figure 1.1** Examples of the chemical structures of (a) polyamide and (b) polyester chains (Donald, Gary, and George, 1976).

### 1.1.2 Natural fibres

The natural fibres include cotton, linen, wool and silk which are provided by nature in a ready-made fibrous form. Natural fibres can be subdivided into three main classes, according to the nature of their source.

#### *Mineral fibres*

These fibres are of limited importance in the textile trade, and the most useful member of the group is asbestos which is made into fire-proof and industrial fabrics (Cook, 1993).



### *Vegetable fibres*

Vegetable fibres (cellulosic fibres) are a major component of textile fibres like hemp, jute, linen, cotton, paper and viscose and other fibres. These fibres are all produced by the plant and are built on the chemistry of cellulose by higher plants to reinforce their cell walls. Many of these are used in the textile industry; one of them, cotton, has become the most important textile fibre in the world (Cook, 1993; Karmakar, 1999).

The principal component of cotton fibres is cellulose (88-96%), a high molar mass, linear polymeric sugar or polysaccharide. The polymer is formed from molecules of the monosaccharide,  $\beta$ -D-glucose, linked through carbon atoms in the 1- and 4-positions (Christie *et al.*, 2000). Cotton may be described chemically as poly (1, 4- $\beta$ -D-anhydroglucopyranose) (Karmakar, 1999) (Figure 1.2). Large dye molecules can penetrate easily into the fibre because cellulose has a fairly open structure. There are three hydroxy groups in each glucose unit of the cellulose structure, two of which are secondary and one primary, and these give the cellulose molecule a considerable degree of polar character (Christie, 2001).

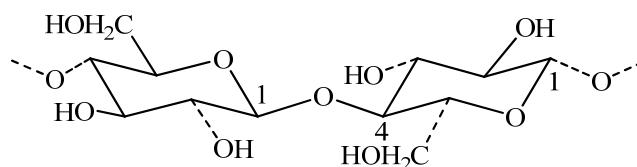


**Figure 1.2** Molecular structure and configuration of cellulose (Karmakar, 1999).

### *Animal fibres*

Animal fibres include wool, silk, and other hair-like fibres. These fibres are proteins produced by the living animal (Cook, 1993). The most prominent protein fibres are wool and silk. They are very similar in structure. They are both polypeptides, i.e., polymers made of  $\alpha$ -amino acid units (Figure 1.3). All such amino acids have the same basic structure, but differ in the nature of the substituent group, R. In naturally occurring amino acids the various possible side chain R groups consist of substituents which vary from basic ( $-\text{NH}_2$ ), to neutral ( $-\text{CH}_2\text{OH}$ ,  $-\text{CH}_3$ ), to acidic ( $-\text{COOH}$ ) (Donald *et al.*, 1976). The characteristic, physical and chemical properties of silk fibre are detailed in the next section.

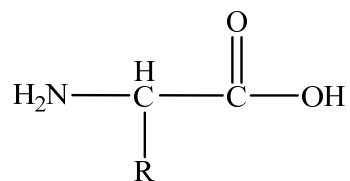


**Figure 1.3** Basic amino acid structure (Donald *et al.*, 1976).

## **1.2 Silk fibre**

Silk fibre is a natural protein fibre that is a fine continuous strand produced naturally by the moth caterpillar known as the silkworm, *Bombyx mori* (Truter, 1973; Karmakar, 1999). The silkworm spins a cocoon around its body by extruding the contents of the two silk glands through a spinnerette at its mouth. The two filaments solidify on coming in contact with air and form a composite thread. Silk has high tenacity, high luster and good dimensional stability. There are four main varieties of silkworm, namely the Mulberry, Tassar, Eri, and Muga types (Moeyes, 1993; Karmakar, 1999). All these silkworms go through four stages in their life cycles

which include eggs, larva, pupa and moth. The mulberry silkworm (*Bombyx mori*) accounts for about 95% of the world's production of silk. Raw silk thread is obtained from silk cocoons by reeling after boiling the cocoons in water.

### **1.2.1 Physical properties**

Silk is the strongest and longest natural textile fibre (1000 metres of an unbroken filament and its diameter is around 0.013 mm to 0.08 mm). Silk is lighter than cotton, with the density of silk in the raw state being 1.33 g/cc but the density of boiled-off silk is 1.25 g/cc. The cross section of silk is triangular with rounded corners, which allows light to hit at many different angles, giving shine and brightness. The texture of silk is smooth and soft but not slippery. Silk is a tough fibre with the tenacity of raw silk being about 4.5-4.8 g/denier. At the same time it is a very elastic fibre, and, if elongated, only a small amount of it remains stretched. Silk requires 0.90 gm tension per denier to stretch 1% at 65% Relative Humidity (R.H.). It is very hygroscopic and absorbs about 11% moisture under standard atmospheric conditions of 65% R.H. and 27°C but after degumming regain is only 9%. As well as this, its unique thermal properties make silk a fabric suitable for wearing in all seasons. It is used for making winter jackets, comforters and sleeping bags because it wraps the body in a layer of warm air that acts as an insulator against radiation of heat from the body to the cold surroundings. During summer, its hygroscopic nature makes it a cool body cover (Warner, 1995; Ganga, 2003).

### 1.2.2 Chemical properties

The actual silk fibre protein is called fibroin and the protein sericin is the gummy substance that holds the filament together. Raw silk has an average composition of 70-75% fibroin ( $C_{15}H_{23}N_5O_8$ ), 20-25% sericin, 2-3% waxy and 1 to 1.7% mineral matters (Karmakar, 1999). Sericin is amorphous and removed by dissolving in hot soap solution. Fibroin has the form of a filament thread and dissolves in hot 5% aqueous sodium hydroxide solution. Both fibroin and sericin are protein substances built up from 16-18 amino acids of which glycine, alanine, serine and tyrosine make up the largest part of the silk fibre; the remaining amino acids containing bulky side groups are not significant (Truter, 1973; Karmakar, 1999). The chemical composition of fibroin and sericin with respect to the four main amino acids is shown in Table 1.1.

**Table 1.1** Main amino acid composition of sericin and fibroin (Karmakar, 1999).

Amino acids	Side groups R	Sericin (% mol)	Fibroin (% mol)
Glycine	H-	14.75	45.21
Alanine	CH <sub>3</sub> -	4.72	29.16
Serine	HOCH <sub>2</sub> -	34.71	11.26
Tyrosine	<i>p</i> -OHC <sub>6</sub> H <sub>4</sub> CH <sub>2</sub> -	3.35	5.14

The structures of *Bombyx mori* silk fibroin has been studied by using solid state <sup>13</sup>C and <sup>15</sup>N-NMR spectroscopies (Kaplan, Adams, Farmer, and Viney, 1994). These studies indicated that the main sequence of silk fibroin is Gly-Ala-Gly-Ala-Gly-Ser where Gly, Ala and Ser denote glycine, alanine and

serine respectively (Kaplan *et al.*, 1994). In addition, the crystal of silk fibroin was reexamined by using newly collected intensity data. It was found that the crystalline region of silk is composed of a rather irregular stacking of the antipolar-antiparallel beta sheets with different orientations. The crystal structure of the polypeptide chains in silk fibroin is shown in Figure 1.4.

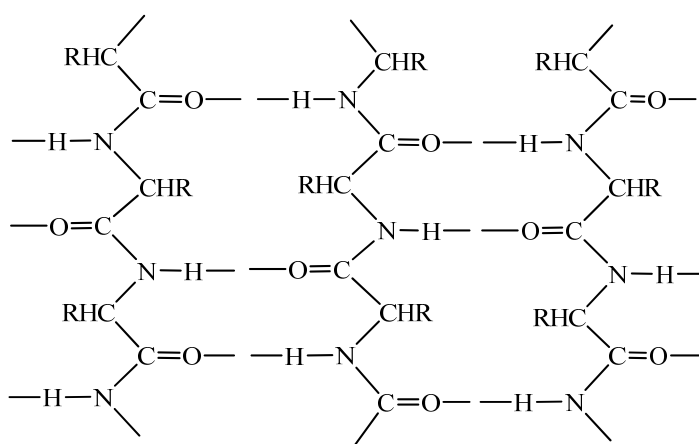


**Figure 1.4** Crystalline structure of the polypeptide chains in fibroin (Karmakar, 1999).

For the dyeing process, there are a number of ways in which a dye may bind to the silk fibre. It may make non-covalent interactions either to the terminal amino ( $-\text{NH}_2$  (basic)) or carboxylic acid ( $-\text{COOH}$  (acidic)) groups of the polypeptide chain (Figure 1.5). Dyes may also potentially interact with the backbone peptide groups or with the serine side chain hydroxyl group or the tyrosine phenolic hydroxyl group (Donald *et al.*, 1976).

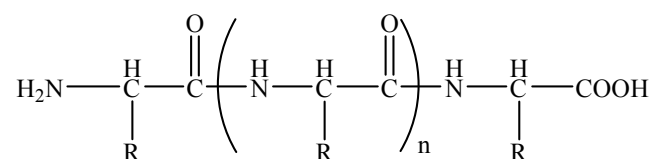


**Figure 1.5** Structure of the protein fibres (polypeptide) (Donald *et al.*, 1976).

### 1.3 Synthetic dyes

Synthetic dyes for textile fibres may be classified according to their chemical structure or according to their method of application (Perkins, 1996; Christie, 2001). Some important information on these classifications is briefly outlined in sections 1.3.1 and 1.3.2.

#### 1.3.1 Chemical structure classification

In the chemical classification method, synthetic dyes are grouped according to certain common molecular structural features. The most important organic dyes and pigments belong to the azo, carbonyl (including anthraquinones), phthalocyanine, arylcarbocation (including the triphenylmethanes), thio ether, methine and nitro chemical classes (Christie *et al.*, 2000). A summary of the principal features of each of these chemical classes is given in Table 1.2. Examples of azo, carbonyl and arylcarbocation dyes are illustrated in Figure 1.6.

#### 1.3.2 Method of application classification

The method of application of the dye is normally categorized into the following classes: direct dyes, acid dyes, basic dyes, mordant dyes, disperse dyes,

azoic dyes, sulfur dyes, reactive dyes and vat dyes (Christie, 2001). Protein fibres may be dyed using a number of these application classes, the most important of which are direct, acid, basic, mordant and vat dyes (Donald *et al.*, 1976). The characteristics of each of these classes are discussed below.

**Table 1.2** A summary of the characteristics of the main chemical classes of dyes (Christie *et al.*, 2000).

<b>Chemical class</b>	<b>Distinctive structural feature</b>	<b>General characteristics</b>	<b>Main application class(es)</b>
Azo	-N=N-	All hues, but yellow to red most important	Dominate most, but not vat dyes
Carbonyl	C=O	All hues, but blue most important	Important in most applications
Phthalocyanine	16-membered heterocyclic ring, metal complex	Blue and green only	Most important in pigments
Triarycarbocation	Positively-charged trivalent carbon species	All hues, but reds and blues most important	Cationic dyes and pigments
Sulfur dyes	Complex polymeric S-containing species	Mostly dull colours, such as blacks and browns	Often considered as an application class itself
Methine dyes	-C=	All hues, but yellows most important	Disperse, cationic
Nitro	-NO <sub>2</sub>	Mainly yellows	Disperse, hair dyes

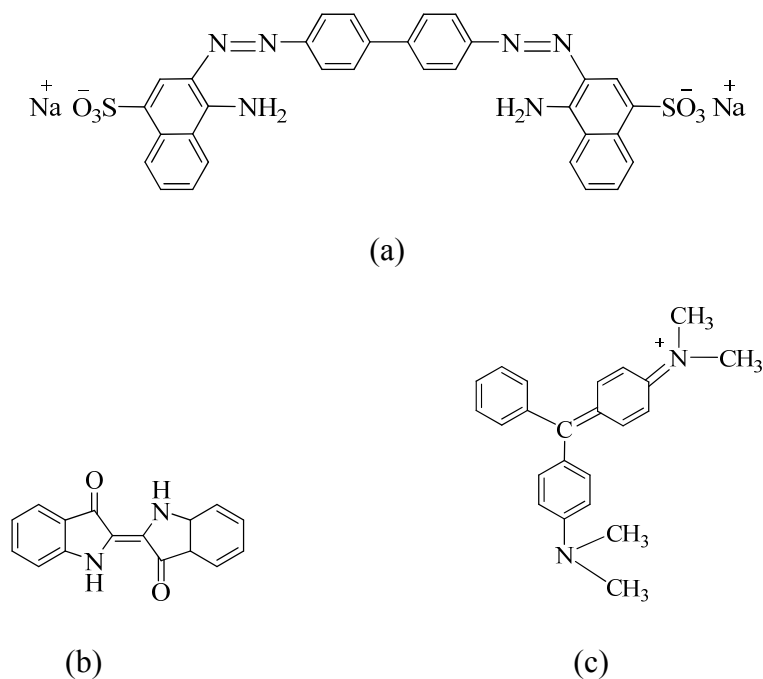


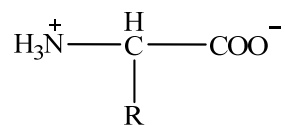
**Figure 1.6** Examples of the structures of an azo dye, carbonyl dye and arylcarbocation dye; (a) C.I. Direct Red 28, Congo Red, an example of a diazo dye; (b) C.I. Vat Blue 1, Indigo, an example of a carbonyl dye and (c) C.I. Basic Green 4, Malachite Green, an example of an arylcarbocation dye (triphenylmethane dye) (Christie *et al.*, 2000).

### *Direct dye*

Direct dyes are dyes that attach themselves to a fibre by direct chemical interaction. Picric acid is an example of a direct dye for wool or silk. Since it is a strong acid, it interacts with the basic end groups or side chains in wool or silk to form a strong salt linkage (a cation-anion electrostatic interaction) between itself and the fibre.



At biological pH, most amino acids exist in their zwitterionic form:



This means that in wool or silk there are  $\text{-NH}_3^+$  and  $\text{-COO}^-$  groups as well as  $\text{-NH}_2$  and  $\text{-COOH}$  groups. The  $\text{-NH}_2$  and  $\text{-COO}^-$  groups are basic, and the  $\text{-COOH}$  and  $\text{-NH}_3^+$  groups are acidic. The picric acid gives up its proton to some basic group on the fibre and becomes an anion which strongly bonds to a cationic group on the fibre by ionic interaction (salt formation). This interaction is illustrated in Figure 1.7.

Two other types of direct dyes for wool or silk are the anionic and cationic dyes. Anionic dyes are also called acid dyes while cationic dyes are also called basic dyes.

### *Acid dyes*

Acid dyes contain acidic groups in their structure, usually sulfonate ( $\text{-SO}_3^-$ ) groups, either as  $\text{-SO}_3\text{Na}$  or  $\text{-SO}_3\text{H}$  groups, although  $\text{-COOH}$  groups can sometimes be incorporated (Horrocks and Anand, 2000). Examples of the structures of acid dyes are illustrated in Figure 1.8. They have been used to dye protein fibres such as wool and silk. Wool, silk and other protein-based natural fibres have amino groups that can interact with acid dyes. The protein molecules carry a positive charge which attracts the acid dye conjugate base form by ionic forces. As well as this, van der Waal's forces, dipolar forces and hydrogen bonding between appropriate functionality of the dye and fibre molecules may also play a significant part in the acid-dyeing of protein fibres (Perkins, 1996; Christie *et al.*, 2000).

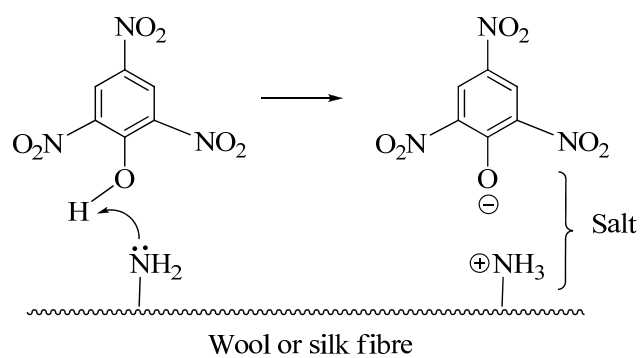


**Figure 1.7** The chemical interaction of picric acid (an example of a direct dye) and wool (or silk) fibre (Donald *et al.*, 1976).

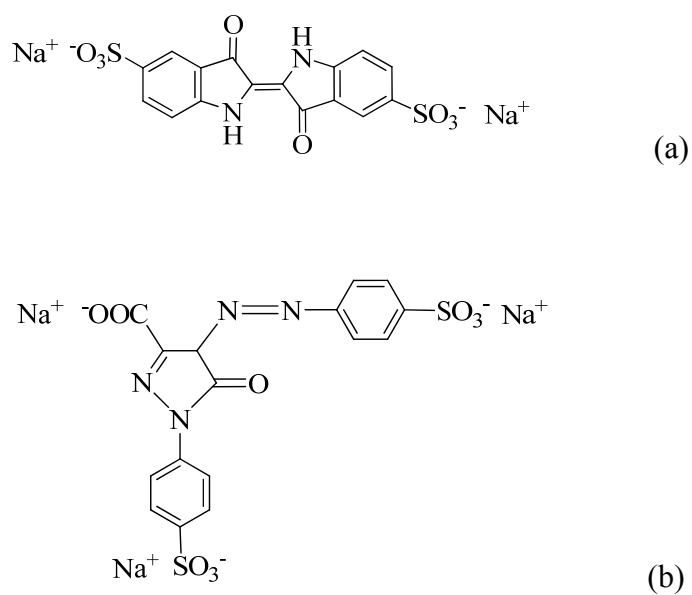
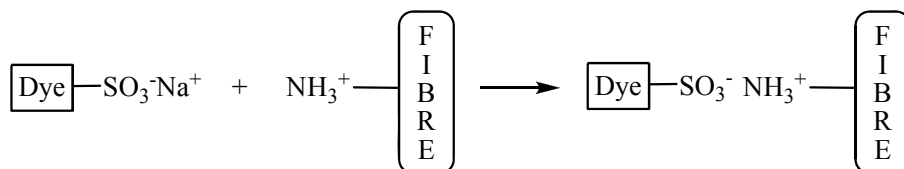


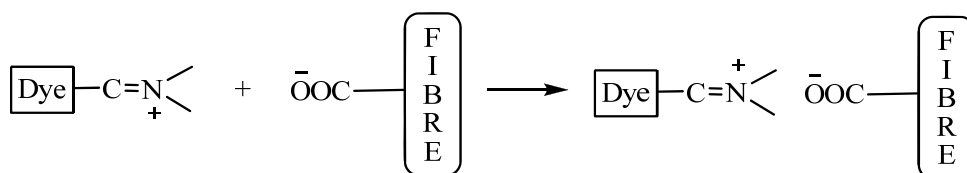
**Figure 1.8** Examples of acid dyes; (a) C.I. Acid Blue 74, Indigo carmine and (b) C.I. Acid Yellow 23, Tartrazine.

Anionic dyes may interact with the acidic  $\text{-NH}_3^+$  groups in the fibre as shown below:



### *Basic dyes*

Basic dyes are cationic dyes containing a positive charge in their structure (Horrocks and Anand, 2000). They have been used to dye fibres containing acidic groups that can interact with these cationic groups in the dye. Malachite green, a triphenylmethane dye (Figure 1.6 (c)), is an example of a basic dye that is an important dye for wool and silk. Cationic dyes interact with the  $\text{-COO}^-$  groups in the fibre illustrated below:



### *Mordant dyes*

Mordant dyes usually have incorporated within their structures groups capable of forming chelate complexes with ions of heavy metals such as copper, chromium, tin, iron, and aluminum (Donald *et al.*, 1976). The main reason for using a mordant in dyeing is to make the dyestuff adhere more strongly to the fibre, which it does through various mechanisms. The most commonly used mordant dyes have

phenolic hydroxyl and carboxyl groups and are negatively charged, i.e. anionic, mediating formation of a complex (known as a lake) with the metal ion. The incorporation of metal ions into the delocalized electron system of the dye causes a bathochromic shift in the absorption and hence a colour change. Since different metal ions have differing energy levels, the colour of the lakes may also differ. A second reason for using a mordant is that the mordant can affect the colour of the dyestuff that is used. It can deepen and intensify the colour, or it can lighten it, or it can completely change the colour. Thirdly, use of a mordant can positively influence the fastness of the dye (Bechtold *et al.*, 2003; Moeyes, 1993). The basic principle of mordanting (with metal ions) is the formation of metal ion bonds with the electron donating chromophores of dyes. For this bond formation a range of ligand groups are important, including *ortho*-dihydroxy, 3-hydroxy-4-keto-, 4-keto-5-hydroxy-, carboxyl or sulfo groups. In the dyeing process, the dye mordant complex links the dye to the fabric. For a dye to be fast when using a mordant, the complex formed between the dye, the fibre, and the mordanting metal ion must be very stable and insoluble. Different mordants (metal ions) often lead to different colours with the same dye.

Mordants are of two types: (i) Natural or organic and (ii) Inorganic (Bhat, Nagasampagi, and Sivakumar, 2005).

(i) Natural mordants consist of tannic acid, ellagic acid, tannins and sulfated and sulfonated oil obtained from vegetable oil.

(ii) Inorganic mordants include alum or potash alum  $\text{Al}_2\text{K}_2(\text{SO}_4)_4$ , ammonia alum  $(\text{Al}_2\text{NH}_4)_2(\text{SO}_4)_4 \cdot 24\text{H}_2\text{O}$ , soda alum  $\text{Al}_2(\text{Na}_2((\text{SO}_4)_4) \cdot 24\text{H}_2\text{O})$ , chrome alum  $\text{Cr}_2(\text{SO}_4)_4 \cdot 24\text{H}_2\text{O}$ , ferric alum  $\text{Fe}_2(\text{NH}_4)_2(\text{SO}_4)_4 \cdot 24\text{H}_2\text{O}$ , potassium dichromate

$K_2Cr_2O_7$ , ferrous sulfate  $FeSO_4 \cdot 7H_2O$ , cupric sulfate  $CuSO_4 \cdot 5H_2O$ , stannous chloride  $SnCl_2$ , and stannic chloride  $SnCl_4$ .

In the actual dyeing process, there are four ways of using a mordant (Moeyes, 1993; Bechtold *et al.*, 2003) as follows:

- (a) Mordanting before dyeing, or pre-mordanting;
- (b) Mordanting and dyeing at the same time, called stuffing or simultaneous mordanting;
- (c) Mordanting after dyeing, or after-mordanting or post-mordanting;
- (d) A combination of pre-mordanting and after-mordanting.

#### *Vat dyes*

Vat dyes are a type of dye that can be used for all fibres, both natural and synthetic (Donald *et al.*, 1976), and they usually have outstanding colour fastness properties. However, vat dyes are more expensive and more difficult to apply than other classes such as direct dyes and acid dyes. They are usually classified into three groups which include indigoid, anthraquinone, and fused ring polycyclic dyes (Perkins, 1996). Examples of vat dyes are shown in Figure 1.9.

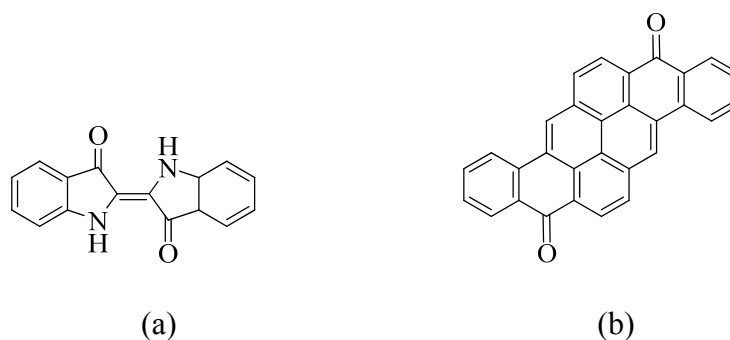


**Figure 1.9** Examples of vat dyes; (a) Indigo, C.I. Vat Blue 1 and (b) Pyranthrone (C.I. Vat Orange 9) (Perkins, 1996).

There are only a few members in the indigoid group. The parent member of the group is indigo (C.I. Vat Blue 1) which is a well-known blue vat dye (Donald *et al.*, 1976). Vat dyes are usually characterized by the presence of a conjugated diketo group that can be reduced to a dienolic or “leuco” form. Vat dyes in the diketo form are water insoluble pigments, but the dienolic form is sufficiently acidic to form a water soluble salt when reacted with strong alkali. Re-oxidation of the water soluble “leuco” form then results in the water insoluble dye (Perkins, 1996). The chemistry of the reversible reduction-oxidation process involved in vat dyeing is illustrated in Figure 1.10.

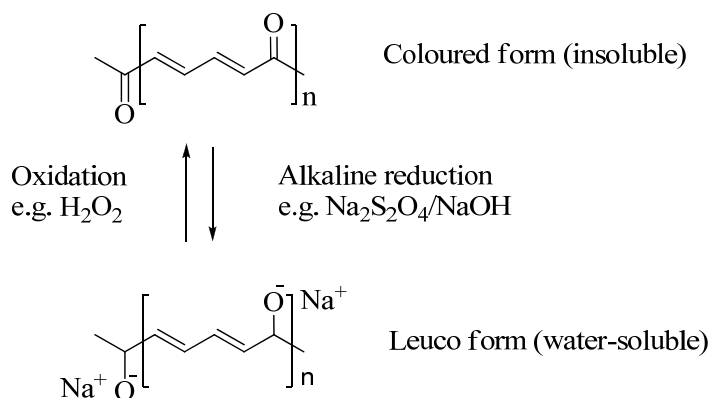


**Figure 1.10** The chemistry of vat dyeing (Christie, 2001).

As a result of the water insolubility of the vat dye but the water solubility of the corresponding reduced form, the application of these dyes is more complex and consists essentially of four stages (Christie *et al.*, 2000):

- (i) Vatting - preparation of the sodium derivative of the reduced (leuco) compound, resulting in a water soluble dye precursor.
- (ii) Impregnation of the fibres with the leuco compound.
- (iii) Oxidation in the fibres to the insoluble vat dye.
- (iv) Rinsing and soaping to remove non-adsorbed dye and non-dye reagents.

## 1.4 Natural dyes

Natural dyes originate mainly from plants, although insects and other animals may also produce useful textile colourants. In the case of plant sources, they can be obtained by fermentation, solvent extraction, or chemical treatment, the last involving chemical transformations to yield the actual dye. Sometimes the colour of the dye is already apparent in the plant material (e.g. the yellow dye curcumin is extracted from the orange-yellow coloured rhizome of *Curcuma longa* Linn.) (Moeyes, 1993). However, some important vegetable dyes originate from plant components which are not coloured in their original state such as indigo from *Indigofera tinctoria* Linn.. In this case the blue dye indigo is produced after hydrolysis and oxidation of a colourless precursor glucoside (Maugard, Enaud, Choisy, and Legoy, 2001). Substances are coloured because they absorb light that the human eye can see between about 400-800 nm wavelength. This absorption of light depends on the structure or constitution of the colourant molecules containing various chromophores which absorb light at different wavelengths to display many different colours. The chemical classification and the source and application of colourants are discussed below. Natural organic colourants can be nitrogenous and non-nitrogenous. Based on the skeleton and the chromophores they contain, broad classifications can be made as shown in Table 1.3. A brief description of some of the common natural dyes is given below.



**Table 1.3** Natural dyes and pigments (Bhat *et al.*, 2005).

Skeleton type	Common colourants
<b>Organic non-nitrogenous molecules</b>	
a) Flavonoids	i. Flavones, flavonols, flavonones, isoflavones ii. Chalcones, aurones iii. Anthocyanins iv. Anhydrobases v. Xanthones vi. Tannins
b) Quinonoids	Benzoquinones, naphthoquinones, Anthraquinones, extended anthraquinones
c) Polyenes/carotenoids	Bixin, crocin, $\beta$ -carotene, capsorubin
<b>Organic nitrogenous molecules</b>	
a) Pyrroles	Porphyrins (chlorophyll, haeme, bilirubin)
b) Pyrimidines	Pterins
c) Alkaloids	Indigo, betaine

### *Flavonoids*

Flavonoids comprise a large natural compound class with structures that are based on the flavone or flavane skeleton or isomers of these (Figure 1.11). The major subgroups of flavonoids are chalcones, flavanones, flavones, flavonols, anthocyanins and isoflavonoids. Examples of flavonoid pigments are morin (found in

several species of plants in the family Moraceae) and rutin (for example present in the flowers of *Sophora japonica* Linn.) (Figure 1.11).

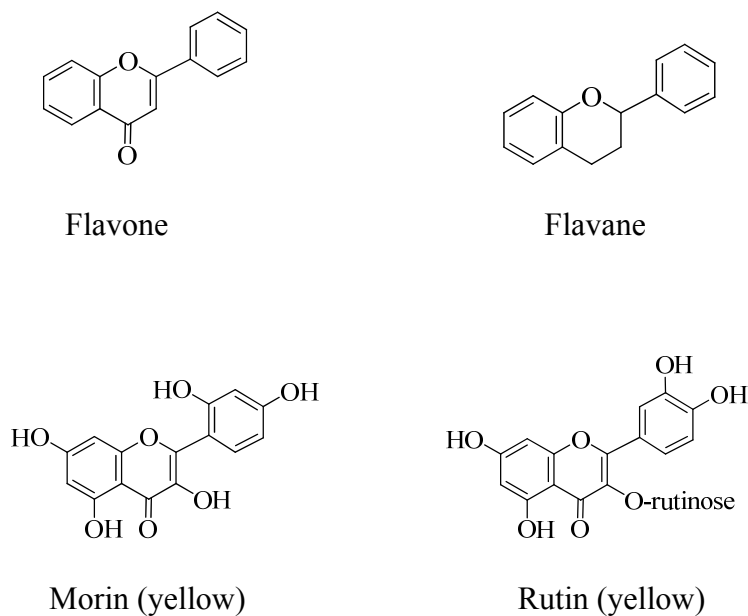


**Figure 1.11** Basic structures (flavone, flavane) of most flavonoids, and two examples of flavonoid pigments: morin and rutin.

### *Quinones*

Quinones include various compounds containing a quinone structure (Figure 1.12). The colour is usually yellow to red. Major subgroups are benzoquinones, naphthaquinones and anthraquinones. An example of a naphthaquinone pigment is lawsone from *Lawsonia inermis* L. (henna). Examples of anthraquinones are alizarin, morindin and purpurin found in species of the family Rubiaceae (Figure 1.12).

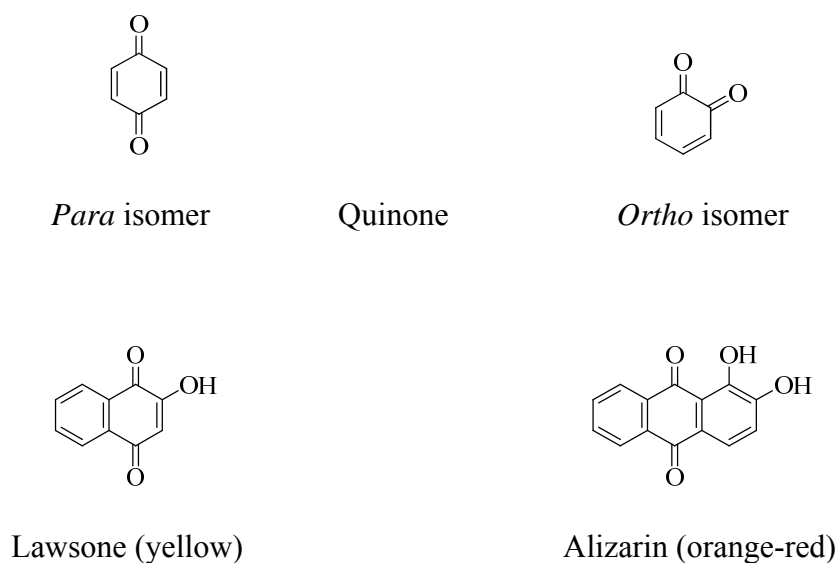
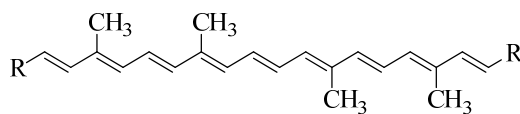


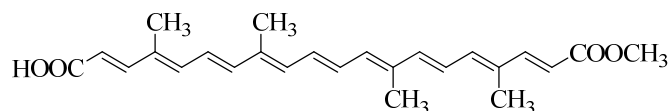
**Figure 1.12** Structures of quinones, and an example of a naphthaquinone pigment (lawsone) and an anthraquinone pigment (alizarin).

### *Carotenoids*

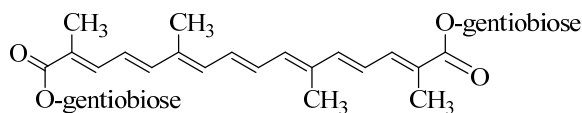
Carotenoids are chemically characterized by a long aliphatic polyene chain composed of isoprene units (Figure 1.13). They have a variety of structures and intense characteristic colours of yellow, orange, red, and purple. Examples of carotenoid pigments are bixin, obtained from *Bixa orellana* Linn. (annatto) and crocin found in *Crocus sativus* Linn. (saffron) (Figure.1.13) (Lemmens and Wulijarni, 1992).



Carotenoid molecule



Bixin (orange-purple)



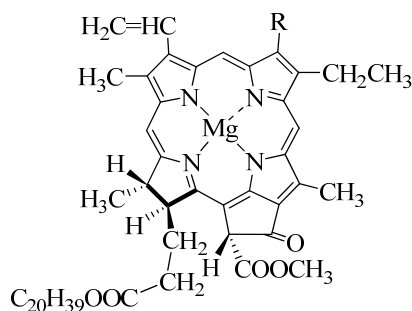
Crocin (yellow-red)

**Figure 1.13** Basic structure of a carotenoid molecule, and two examples of carotenoid pigments: bixin and crocin.

### *Pyrroles*

Pyrrole is a heterocyclic aromatic organic compound with a five-membered nitrogen-containing ring and two formal double bonds. Pyrroles are components of larger aromatic rings, including the porphyrins of heme, the chlorins and bacteriochlorins of chlorophyll, and the corrin ring of vitamin B12. There are three major groups of pyrrole dyes namely the porphyrinoids, porphyrins, and chlorophyll/hemoglobin. Chlorophyll (Figure 1.14) is a generic term for a number of closely related plant pigments responsible for the green colours in plants and are

essential components in the photosynthetic process (Bhat *et al.*, 2005). Chlorophylls are sometimes used for colouring foods and drinks.



R=CH<sub>3</sub>, Chlorophyll-a

R=CHO, Chlorophyll-b

**Figure 1.14** Chemical structure of chlorophyll.

### *Pyrimidines*

Pyrimidine is a heterocyclic aromatic organic compound similar to benzene and pyridine, containing two nitrogen atoms at positions 1 and 3 of the six membered ring. Pteridines are pyrimidine-based natural pigments that are widely distributed in butterflies (e.g. *Gonopterix rhamni*) and insects (Figure 1.15). Most of them are derived from xanthopterin, which contains a pyrimidine ring fused to a piperazine moiety (Bhat *et al.*, 2005).

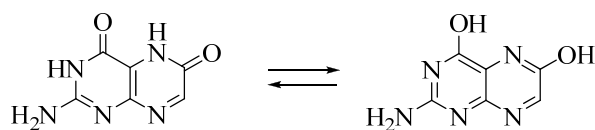


**Figure 1.15** Xanthopterin from the butterfly *Gonopterix rhamni*.

### Alkaloids

Alkaloids are naturally-occurring amines (and derivatives) produced mainly by plants, but also by animals and fungi. Many alkaloids have pharmacological effects on humans and other animals. The name derives from the word “alkaline” reflecting their basic properties; originally, the term was used to describe any nitrogen-containing base.

The famous blue dye, indigo, used to dye burial clothes during ancient times and denims in recent times, is an alkaloid occurring in the form of its glucoside, indican, in the leaves of *Indigofera tinctoria* and *Isatis tinctoria*. The leaves, on maceration with water, release an enzyme which hydrolyses the glucoside to give indoxyl and glucose. Air oxidation of two molecules of indoxyl forms indigo (indigotin), which is insoluble in water (Figure 1.16) (Steingruber, 2004).

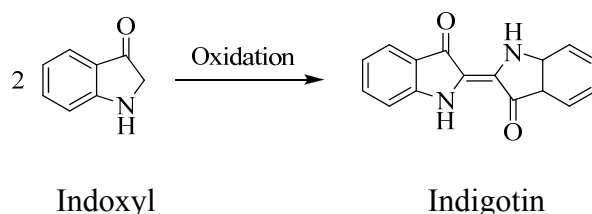


**Figure 1.16** An oxidation of indoxyl forms indigo (indigotin).

Nowadays, indigo dyeing onto silk is done in only a few places in Thailand. There are several reasons for the gradual disappearance of indigo dyeing from Thailand. Since indigo dye does not dissolve in water, it has to be converted to the water soluble leuco form by reduction and then re-oxidised to indigo (Balfour-Paul, 2006; Ricketts, 2006; Božič and Kokol, 2008; Vuorema, John, Keskitalo, Kulandainathan, and Marken, 2008). With this process it is difficult to control colour shade and uniformity of the dye on re-oxidation. Indigo dyeing is a challenging, elaborate, and time consuming process and traditionally the knowledge of indigo dyeing is transmitted in family circles (Moeyes, 1993).

The kinetics and thermodynamics of silk dyeing with indigo and indigo derivatives were to be investigated in the current work in order to obtain the parameters of indigo dyeing onto silk and to gain a better understanding of the process. As well as this, the possibility of direct dyeing of silk with indigo without the use of a reduction-oxidation sequence was also to be investigated. The successful improvement of the dyeing process using natural dyes such as indigo should help to improve the economics and well-being of villagers in Thailand.

## **1.5 Research objectives**

(a) To make indigo (or suitable derivatives) more water soluble for the direct dyeing of silk without the need for reduction and oxidation steps.

(b) To study the thermodynamics and kinetics of adsorption of standard indigo, plant-derived indigo, indigo carmine and other *N*-substituted indigo derivatives on the dyeing of silk.

(c) To investigate the application of the solubilisation techniques derived for indigo itself to crude indigo plant extracts.

## 1.6 Scope and limitations of the study

Natural plant-derived indigo dye (from *Indigofera tinctoria*) will be collected from Nakon Ratchasima and Sakonnakhon province, Thailand. Standard indigo (Vat blue, C.I. 73000) and indigo carmine (Acid blue 74, C.I. 73015) will be purchased from Sigma Aldrich and Acros Organics company respectively; other chemicals required will be purchased from Sigma Aldrich. Dyeing of natural indigo dye onto silk will use a suitable reducing agent for indigo during dyeing such as sodium hydrosulfite; other acid dyeing methods will also be assessed. Identification and structural elucidation of new more water soluble indigo derivatives will be done using different techniques such as nuclear magnetic resonance spectroscopy (NMR) and mass spectrometry (MS). Complex formation studies of indigo with 2-hydroxypropyl- $\beta$ -cyclodextrin in order to improve the water solubility of indigo will be performed using UV-visible spectroscopy. The effect of hydrotropic additives (such as urea, nicotinamide, and aceturic acid) on the water solubility of indigo will be assessed together with the acid dyeing of silk at *ca* pH 4 with these solutions. Kinetic and thermodynamic studies of indigo, indigo carmine, and other indigo derivatives onto silk will be performed and monitored using UV-visible spectroscopic techniques. For comparison purposes, some aspects of these studies will also be repeated with crude indigo extracts from the fermentation of *Indigofera tinctoria* leaves.



## 1.7 References

- Angelini, L. G., Pistelli, L., Belloni, P., Bertoli, P. and Panconesi, S. (1997). *Rubia tinctorum* a Source of Natural Dyes: Agronomic Evaluation, Quantitative Analysis of Alizarin and Industrial Assays. **Industrial Crops and Products**. 6: 303-311.
- Balfour-Paul, J. (2006). **Indigo-a Unique Dye with a Colour Story, In Indirubin, the Red Shade of Indigo**. Meijer, L., Guyard, N., Skaltsounis, L. A., Eisenbrand, G. Ed. Life in Progress Edition: France.
- Bechtold, T., Turcanu, A., Ganglberger, E. and Geissler, S. (2003). Natural dyes in modern textile dyehouses-how to combine experiences of two centuries to meet the demands of the future. **Journal of Cleaner Production**. 11: 499-509.
- Bhat, S. V., Nagasampagi, B. A. and Sivakumar, M. (2005). **Chemistry of natural products**. New Delhi: Narosa Publishing House.
- Božič, M. and Kokol, V. (2008). Ecological alternatives to the reduction and oxidation processes in dyeing with vat and sulphur dyes. **Dyes and Pigments**. 76: 299-309.
- Chang, C. H., Lin, C. C., Kawata, Y., Hattori, M. and Namba, T. (1989). Prenylated xanthenes from *Cudrania cochinchinensis*. **Phytochemistry**. 28: 2823-2826.
- Christie, R. M., Mather, M. M. and Wardman, R. H. (2000). **The Chemistry of Colour Application**. Oxford: Blackwell Science.
- Christie, R. M. (2001). **Colour Chemistry**. Cambridge: Royal Society of Chemistry.
- Cook, J. G. (1993). **Handbook of Textile Fibres**. Shildon: Merrow.

- Donald, L. P., Gary, M. L. and George, S. K. (1976). **Introduction in Organic Laboratory Techniques: A Contemporary Approach**. U.S.A.: W.B. Saunders.
- Ganga, G. (2003). **Comprehensive Sericulture Volume 2 Silkworm Rearing and Silk Reeling**. New Hampshire: Science Publishers.
- Horrocks, A. R. and Anand, S. C. (2000). **Handbook of Technical Textiles**. Cambridge: Woodhead.
- Kaplan, D., Adam, W. W., Farmer, B. and Viney, C. (1994). **Silk Polymers: Materials Science and Biotechnology**. Washington: American Chemical Society.
- Karmakar, S. R. (1999). **Chemical Technology in the Pre-Treatment Processes of Textile**. Netherlands: Elsevier Science.
- Lemmens, R. H. M. J. and Wulijarni, S. N. (1992). **Plant Resources of South-East Asia No.3, Dye and Tannin-Producing Plants**. Bogor: Indonesia.
- Maugard, T., Enaud, E., Choisy, P. and Legoy, M. D. (2001). Identification of an indigo precursor from leaves of *Isatis tinctoria* (Woad). **Phytochemistry**. 58(6): 897-904.
- Moeyes, M. (1993). **Natural Dyeing in Thailand**. Bangkok: White Lotus.
- Perkins, W. S. (1996). **Textile Colouration and Finishing**. North Carolina: Carolina Academic Press.
- Ricketts, R. (2006). ***Polygonum tinctorium*: Contemporary Indigo Farming and Processing in Japan In Indirubin, the Red Shade of Indigo**. Meijer, L., Guyard, N., Skaltsounis, L. A., Eisenbrand, G. Eds. Life in Progress Edition: France.

- Steingruber, E. (2004). **Indigo and Indigo Colorants: Ullmann's Encyclopedia of Industrial Chemistry**. Weinheim, Germany: Wiley-VCH.
- Truter, E. V. (1973). **Introduction to Natural Protein Fibres: Basic Chemistry**. London: Elek Science.
- Vuorema, A., John, P., Keskitalo, M., Kulandainathan, M. A. and Marken, F. (2008). Electrochemical and sonoelectrochemical monitoring of indigo reduction by glucose. **Dyes and Pigments**. 76: 542-549.
- Warner, S. B. (1995). **Fibre Science**. New Jersey: Prentice Hall.

## **CHAPTER II**

# **ADSORPTION KINETIC AND THERMODYNAMIC STUDIES OF INDIGO DYEING ONTO SILK BY THE CONVENTIONAL VAT-DYEING METHOD**

### **2.1 Abstract**

Detailed kinetic and thermodynamic parameters were determined for the first time for the dyeing of silk using indigo itself and the vat dyeing method. This method involved initial reduction of the indigo with sodium dithionite to give leuco indigo, then immersion of the silk in the aqueous solution of leuco indigo, followed by aerial oxidation to indigo *in situ*. A chemisorption process was indicated for the indigo dyeing of silk. A comparison of kinetic and thermodynamic data for silk dyeing using plant derived indigo extract obtained from *Indigofera tinctoria* was also made with the data from indigo itself and close similarities were seen. This was consistent with the HPLC analytical data which showed indigo as a major component of the extract. It also indicated that other components in the crude indigo extract were not significantly affecting the dyeing kinetics and thermodynamics.

## 2.2 Introduction

Indigo is one of the oldest known dyes that was used for textile dyeing and printing (Vuorema, John, Keskitalo, Kulandainathan, and Marken, 2008). The natural indigo dye has been obtained from a variety of plant sources, such as *Indigofera tinctoria* (Africa, Asia, East India and South America), *Indigofera suffruticosa* (South and Central America), *Polygonum tinctorium* (China, Korea, and Japan) and *Isatis tinctoria* (Woad) (Europe), since ancient times (Balfour-Paul, 1998; Maugard, Enaud, Choisy, and Legoy, 2001; Steingruber, 2004; Cooksey, 2007). There are a several researchers using different methods to identify and quantify the components of indigo natural sources. The HPLC technique was used to investigate indigo precursors from leaves of *Isatis tinctoria* (woad) (Maugard *et al.*, 2001). In this study, *cis*- and *trans*-isomers of indigo and indirubin were detected, together with isatan B (indoxyl-5-ketogluconate), indican (indoxyl- $\beta$ -D-glucoside), and a new precursor, isatan C that was a dioxindole ester with a molecular weight of 395. Isatan C reacted with isatan B, increasing the red pigment production. The indigoid pigments produced in *Indigofera tinctoria* were separated into five compounds, of which two were blue (HPLC  $t_R$ : 34-36 min), two were red/purple (HPLC  $t_R$ : 23 min, HPLC  $t_R$ : 37.5 min) and one was brown (HPLC  $t_R$ : 24.5 min). The Raman spectra of three sources of indigo (the synthetic pigment, the pigment from the woad plant *Isatis tinctoria*, and the pigment from the indigo plant, *Indigofera tinctoria*) have also been described (Vandenabeele and Moens, 2003). Although chemically identical, it was shown that Raman spectroscopy, in combination with suitable chemometric methods, can discriminate between synthetic and natural indigo samples. Angelini, Campeol, Tozzi, Gilbert, Cooke, and John (2003) developed a new HPLC-ELSD method to quantify the indigo

precursor indican (indoxyl- $\beta$ -D-glucoside) in *Polygonum tinctorium*. Plant material was extracted in deionized water and indican was identified and quantified. Analysis by HPLC-ELSD methodology of extracts from two woad species (*Isatis tinctoria* and *Isatis indigotica*) and *Polygonum tinctorium* were investigated (Gilbert, Maule, Rudolph, Lewis, Vandenburg, Sales, Tozzi, and Cooke, 2004). The results revealed that only one indigo precursor (indican) was present in *Polygonum*, but two precursors, indican and isatan B, were found in *Isatis spp.* in different proportions.

In Thailand, *Indigofera tinctoria* (Figure 2.1) and *Baphicacanthus cusia* are the plants which have been used as a natural source of indigo dye and are available in North-Eastern and Northern part of Thailand. However, *Indigofera tinctoria* is widely used as a source of indigo dye in Thailand. Indigo plants have a single semi-woody stem, dark green leaves that are oval-shaped in most species, and clusters of red flowers that look like butterflies and turn into pea pods. The plants can grow from two to six feet in height and the dye is obtained mainly from the leaves through a process of fermentation in water that gives the blue colour (Moeyes, 1993).

In the water fermentation process, the source for indigo production is indican **(1)** (indoxyl  $\beta$ -D-glucoside) (Figure 2.2), a colourless glucoside representing a major leaf secondary metabolite present in the vacuoles of the leaves. It is water-extracted from leaves and degraded to indoxyl **(2)** and glucose by the action of a native  $\beta$ -glucosidase. Dimerization of indoxyl by air oxidation then occurs, leading to the formation of indigo **(3)** (Angelini, Tozzi, and Nasso, 2004).

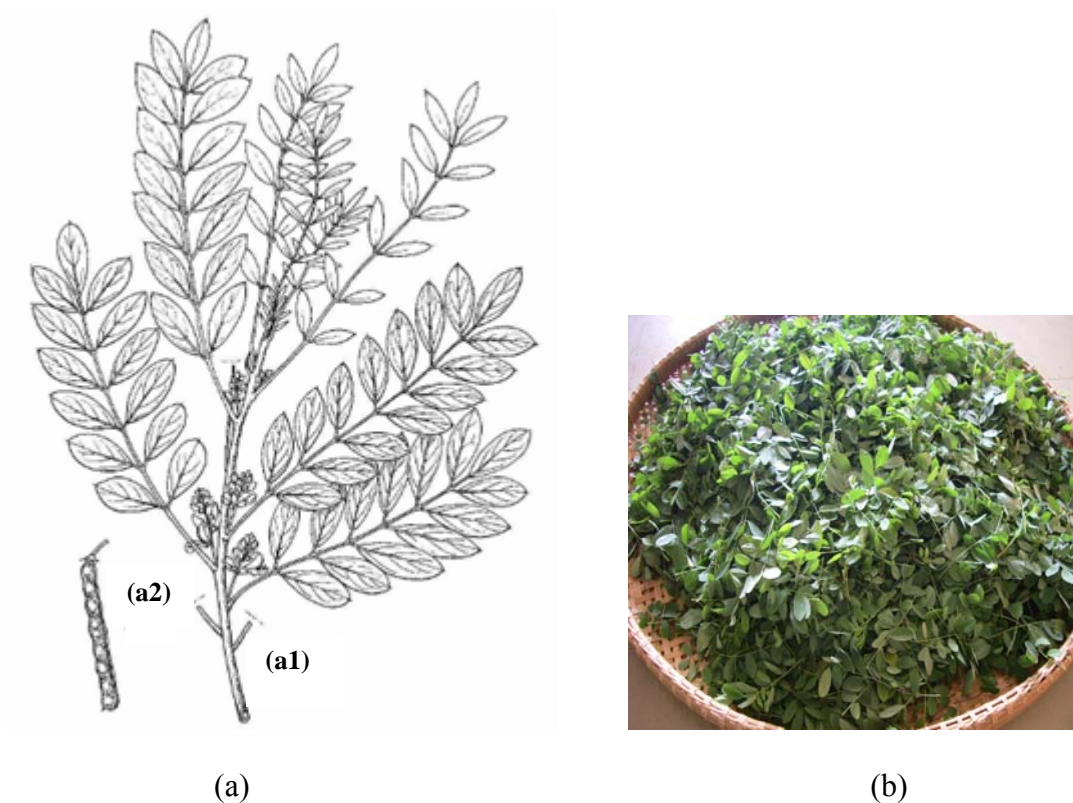


**Figure 2.1** (a) *Indigofera tinctoria* plant; (a1) flowering branch; (a2) fruit (Lemmens and Wulijarni, 1992) and (b) Leaves of *Indigofera tinctoria* plant from Nakhon Ratchasima, Thailand.

Indigo is a vat dye, which means that it needs to be reduced to its water soluble leuco-form before dyeing. Indigo can be reduced in alkaline medium with reducing agent (e.g. sodium dithionite) to the water soluble leuco indigo salt (**4**). The reduced form (**4**) is absorbed into the fibres, and when oxidised back to its blue form, indigo (Figure 2.2) it stays within the fibre. Since the indigo is insoluble in aqueous solutions, the dye is generally wash fast but not abrasion fast (Donald, Gary, and George, 1976).

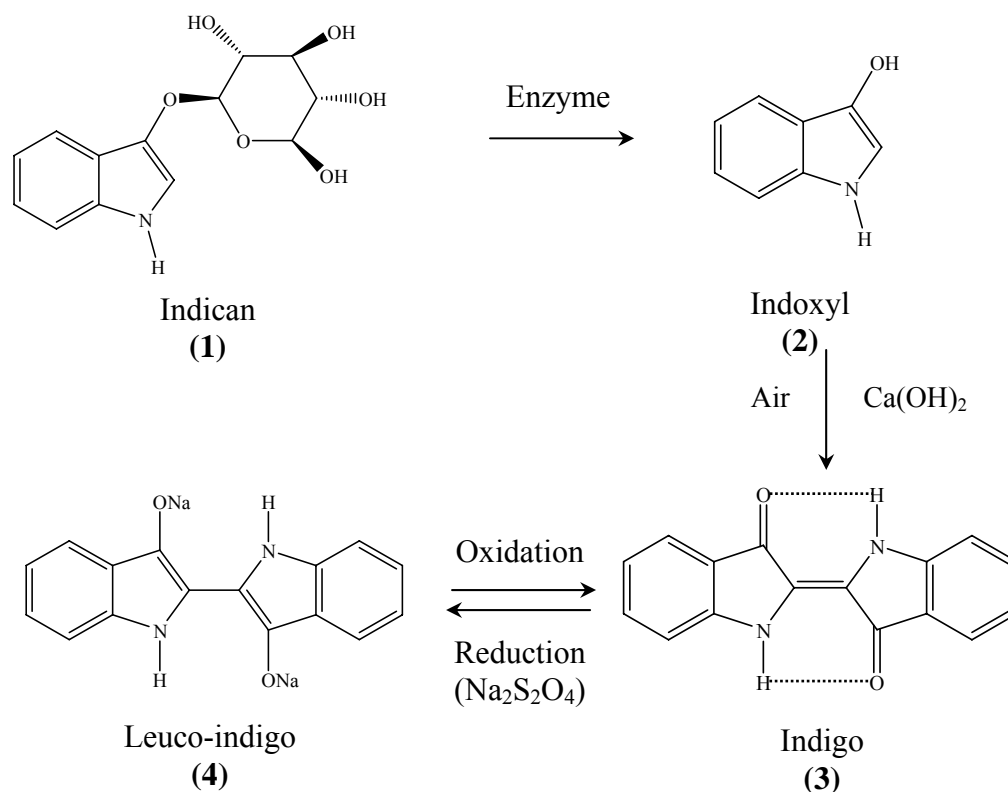


**Figure 2.2** The formation of indigo and indigo dyeing process.

The reduced form is called the leuco compound, leuco coming from the Greek word leucos meaning white, which refers to the change of colour of the vatting liquid after reduction (Božič and Kokol, 2008). With indigo the colour of the leuco-indigo solution is yellow green when reduced with sodium dithionite.

Various reducing systems for vat dyes have been proposed and used. The most common type of reducing agent used for dyeing with vat dyes is sodium hydrosulphite, commonly known as “hydros” but more correctly known as sodium dithionite, which has the chemical formula Na<sub>2</sub>S<sub>2</sub>O<sub>4</sub>. Although a part of the hydros is used up in the reduction of vat dyes, a large part of it may be destroyed by its reaction



with oxygen in the air (oxidation), particularly at higher temperatures. The advantage with sodium dithionite is that it causes swift reduction of indigo, as well as other vat dyes, and it enables very short fixing times in various dyeing methods and produces levelness in continuous dyeing. On the other hand, sodium dithionite is very easily oxidised by atmospheric oxygen affecting its stability in aqueous alkaline solution (Christie, 2001; Polenov, Pushkina, Budanov, and Khilinskaya, 2001; Roessler and Crettenand, 2004; Zanoni, Sousa, de Lima, Carneiro, and Fogg, 2006). An alternative reducing agent such as thiourea dioxide can be used instead of sodium dithionite and is more stable. Son, Lim, Hong and Kim (2005) examined the dyeing behavior of indigo dye with thiourea dioxide as a reducing agent on polyester fibres. In order to improve the build-up characteristic of indigo on to both conventional and microfibre substrates, the acid leuco technique involving an addition of acetic, formic or citric acids in the leuco indigo bath was considered. In addition, the effect of urea addition to enhance dye exhaustions and wash fastness properties was also investigated. The colour strength of indigo dyeing on to both polyester substrates generally increased with increasing application temperatures. In particular, the acid leuco moiety using formic acid exhibited greater colour strength values. Enhanced dye build-up was obtained by urea addition due to higher dye solubility and greater ease of access of indigo molecules to all parts of the swollen polyester substrates; this swelling occurs on interaction of the polyester with urea. For both conventional and microfibre polyester, the wash fastness properties of indigo dyeing were more effective than those of comparable depth of disperse dyeing. A further group of reducing agents was discovered (Bechtold and Burtscher, 2001) in the class of iron (II) complexes with triethanolamine, triisopropanolamine and also aliphatic hydroxy compounds

containing a number of hydroxyl groups. Chavan and Chakraborty (2001) examined the use of iron (II) salts complexed with such ligands as tartaric acid and citric acid in the presence of sodium hydroxide, for the reduction of indigo at room temperature and subsequent cotton dyeing.

Many attempts are being made to replace the environmentally unfavourable sodium dithionite by ecologically more attractive alternatives. Investigations have either focused on the replacement of sodium dithionite by glucose (Vuorema *et al.*, 2008), by an organic reducing agent (i.e.  $\alpha$ -hydroxyketones) with biodegradable oxidation products or on the use of ultrasound to accelerate the vatting procedure and increase the conversion of leuco indigo. Catalytic hydrogenation processes and also electrochemical reduction techniques were studied (Roessler, Crettenand, Dossenbach, Marte, and Rys, 2002; Roessler, Dossenbach, Marte, and Rys, 2002). However, it is impossible to use some of the above techniques directly in dyeing facilities due to the high explosion and fire risk or because of their unsuitability for application in the village situation.

As indicated in Chapter I, silk fibres are made up of a protein called fibroin. This protein is constructed from layers of anti-parallel beta pleated sheets which run parallel to the silk fibre axis. Each chain of fibroin is made up of multiple repeats of the sequence (Gly-Ser-Gly- Ala-Gly-Ala)<sub>n</sub> (Kaplan, Adam, Farmer, and Viney, 1994). Like wool, silk fibres contain carboxyl and protonated amino groups which result in its amphoteric characteristics (Carr, 1995). Under acid conditions the carboxyl groups are unionized, leaving a net positive charge which enables dye anions to be adsorbed (Carr, 1995). Many studies have been undertaken to investigate protein fibre dyeing. For instance, the crude water extract of saffron stigmas and crocin were used for

dyeing wool fibre after enzymatic treatment (Tsatsaroni, Liakopoulou-Kyriakides, and Elefthiadis, 1998). The results showed that wash and light fastness values were satisfactory. In addition, emodin and dermocybin natural anthraquinones as mordant dyes for wool and polyamide have been investigated (Raisanen, Nousiainen, and Hynninen, 2001). It was found that wool and polyamide have a high uptake for the pure natural anthraquinones.

To understand the silk dyeing process more fully, the adsorption kinetic and thermodynamics of dyeing have been studied. Thermodynamics of adsorption of laccic acid on silk were investigated (Kongkachuichay, Shitangkoon, and Chinwongamorn, 2002). It was found that the adsorption isotherm obtained was identified to be a Langmuir type. The values of heat and entropy of dyeing were also reported. Chairat, Rattanaphani, Bremner, and Rattanaphani (2005) have also studied the adsorption and kinetic studies of lac dyeing on silk. It was found that the experimental data fitted well to the Langmuir and Freundlich isotherms with a high correlation coefficient ( $R^2$ ). The pseudo second order kinetic model was indicated with the activation energy of 47.5 kJ/mol. It was suggested the overall rate of lac dye adsorption is likely to be controlled by the chemical process. Septhum, Rattanaphani, Bremner, and Rattanaphani (2009) have studied adsorption of alum-morin dyeing onto silk yarn. The results indicated that the adsorption capacities were significantly affected by pH, the initial dye concentration, and temperature. The pseudo second order kinetic model was indicated for alum-morin dyeing (with simultaneous mordanting) of silk at pH 4.0 with an activation energy of 45.26 kJ/mol. Also, the free energy ( $\Delta G^\circ$ ) and entropy changes ( $\Delta S^\circ$ ) for alum-morin dyeing on silk were -17.73 kJ/mol and -45.7 J/mol K, respectively, consistent with a spontaneous and exothermic

adsorption process. In addition, the thermodynamic and kinetic parameters of the dyeing process of silk with indigo carmine (as a water soluble indigo derivative) were studied (Jiwalak, Rattanaphani, Bremner, and Rattanaphani, 2010). The initial dye concentration, contact time, pH, material to liquor ratio (MLR), and temperature were significant parameters of the adsorption capacities of indigo carmine onto silk. The adsorption kinetics was found to follow a pseudo second order kinetic model with an activation energy of 51.06 kJ/mol. The equilibrium adsorption data of indigo carmine dye on silk were analyzed by the Langmuir and Freundlich models. The results indicated that the Langmuir model provided the best correlation. Adsorption isotherms were also used to obtain thermodynamic parameters such as free energy ( $\Delta G^\circ$ ), enthalpy ( $\Delta H^\circ$ ), and entropy ( $\Delta S^\circ$ ) of adsorption. The negative values of  $\Delta G^\circ$  and  $\Delta H^\circ$  confirmed the overall adsorption process as a spontaneous and exothermic one.

Nowadays, indigo dyeing onto silk is done in only a few places in Thailand. There are several reasons for the gradual disappearance of indigo dyeing from Thailand. Since indigo dye does not dissolve in water, it has to be converted to the water soluble leuco form and then re-oxidised to indigo (Balfour-Paul, 2006; Ricketts, 2006). With this process it is difficult to control colour shade and uniformity of the dye on re-oxidation. Indigo dyeing by the conventional vat-dyeing method is a challenging, elaborate and time consuming process. Dyers must have a great deal of experience in caring for the dye pots. Only one or two persons in a village can be indigo dyers. The knowledge of indigo dyeing is transmitted in family circles. Improvements and research on the chemistry of dyeing and the adsorption mechanism could help to solve some of the problems of indigo dyeing of silk. The successful

improvement of the dyeing process using natural indigo dyes would help to preserve indigo dyeing and also improve the economics and well-being of villagers in Thailand.

The aims of the work discussed in this chapter were to extract and analyze by HPLC indigo derived from the indigo plant, *Indigofera tinctoria*. The kinetics and thermodynamics of silk dyeing with indigo (standard indigo and plant extracted indigo) by the conventional vat-dyeing process were then to be investigated and compared in order to obtain the key adsorption parameters for indigo dyeing onto silk and thus to gain a better understanding of the process. It also was to provide benchmark data to inform later projected direct dyeing studies with indigo and derivatives.

### **2.2.1 Physical chemistry of the dyeing process**

The scientific investigation of the dyeing process involves two experimental methods which can be described by dyeing kinetics and dyeing equilibria (Zollinger, 2003). The dyeing process involves the distribution of a dye between at least two phases, namely dye bath and substrate. The distribution process is called adsorption if the substance which is to be distributed is retained by a surface (e.g. gas on a solid). If the substance does not stay at the surface but enters the interior of a body (e.g. gas in liquid), the process is termed sorption. Dyeing processes of water soluble dyes in aqueous dye baths with any substrate always requires a distribution process between two phases (dye bath and substrate) (Perkins, 1996). The kinetics of dyeing is represented by dye uptake curves which give the rate of transfer of dye in solution from the dye bath into the substrate. The position of adsorption

versus desorption after infinite time is represented by the dyeing equilibria of the dyeing process. Graphical representations of a dyeing process are shown in Figure 2.3, by the dye uptake curves (left hand side) and dyeing isotherms (right hand side).

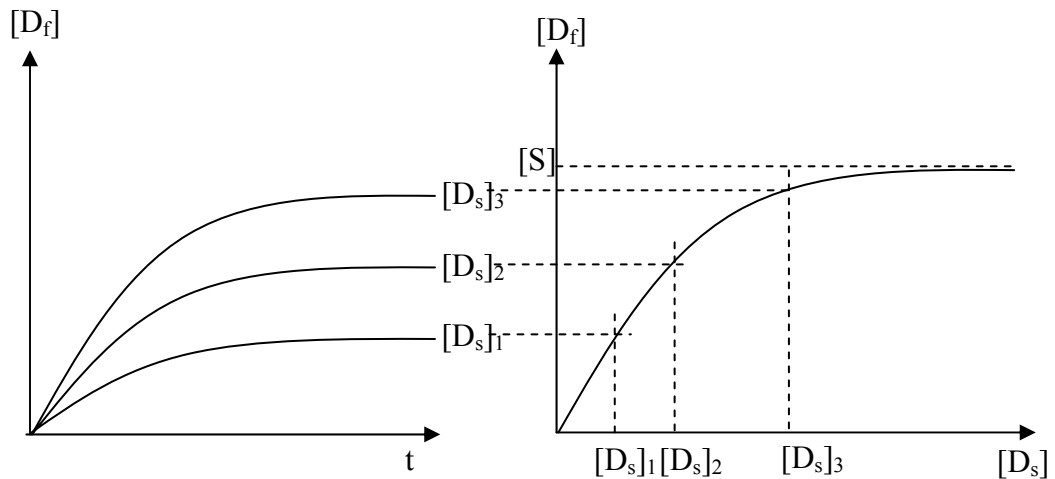


**Figure 2.3** Graphical representation of a dyeing process: kinetics (left) and equilibrium (right) (Zollinger, 2003).

$[D_s]$ : concentration of dye in solution

$[D_f]$ : concentration of dye in substrate

$t$ : time

$[S]$ : saturation value

If the dyeing process is done under different isothermal conditions, a series of curves (Perkins, 1996) are given, as shown in Figure 2.4. The initial adsorption rate increases with an increasing in dyeing temperature. This can be explained by the fact that the dye adsorption by fibres at higher temperature is faster than that at lower temperature and hence leads to an increase in the initial rate constant. The slope of curve varies depending on the temperature, type of fibre, type of dye, amount of agitation of the dye bath, amount and type of dyeing auxiliaries used and other

factors. As the amount of dye on the fibres increases, the sites being covered, and as a result the dye must leave the surface and diffuse toward the interior of the fibre before additional dye molecules can be adsorbed from the dye bath.

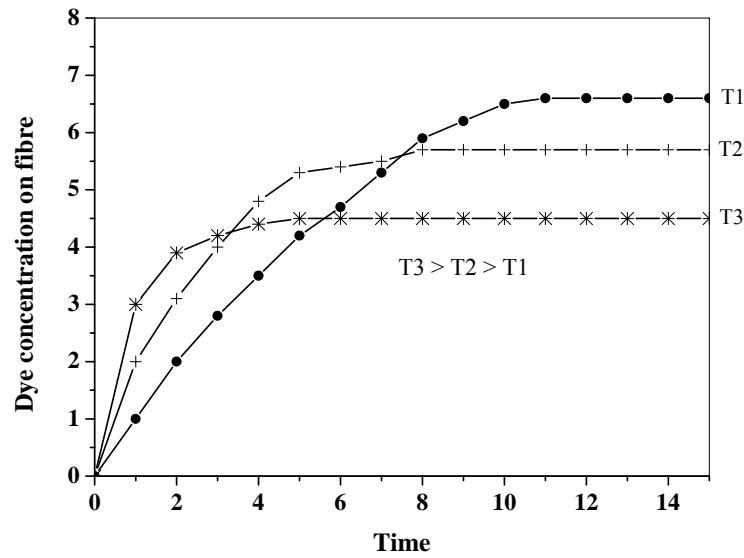


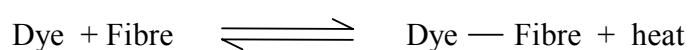
**Figure 2.4** Rate of dyeing isotherms (Perkins, 1996).

The kinetic behaviour of a dye in the dyeing of a textile material comprises at least four stages (Zollinger, 2003):

- (a) convectonal diffusion to the fibre surface, occurring in the dye bath;
- (b) molecular diffusion through the hydrodynamic boundary layer;
- (c) adsorption at the outer surface;
- (d) molecular diffusion into the fibre (sorption).

The stages (a), (c) and (d) are important for the kinetics of the overall dyeing process. After some period of time, the slope of the isotherm becomes flat indicating that the system has reached equilibrium. The time required to reach equilibrium is always shorter at higher dyeing temperature. It is mainly due to the fibres containing

more dye at higher temperatures in the early stages but less dye in the latter stages of dyeing. Therefore, an increase in the temperature leads to an increase in the dyeing rate but a decrease in the ultimate exhaustion after the equilibrium time, as shown in Figure 2.4. This shows that dye molecules can adsorb to a greater degree at a lower temperature because the dyeing reaction is exothermic.



Desorption of dye molecules from fibres to the dye bath takes place at higher dyeing temperatures because of more heat in the dyeing process. Thus, the equilibrium position of this process is shifted to the left hand side.

There are several different intermolecular and intramolecular interactions that are essential for understanding the chemistry of textile dyeing. The four main types of interactions are ionic forces, Van der Waal's forces, hydrogen bonds and dipole-dipole interactions (Christie, 2001; Zollinger, 2003) and will be described below:

#### *Ionic forces*

An ionic bond is formed by electron transfer from one atom to another atom or atoms. The atom that loses electrons becomes a positive-charged species or cation. The atom that gains the electrons becomes a negative-charged species or anion. Ionic bonds are the resulting electrostatic attraction between these oppositely charged ions. In the dyeing of wool, silk and polyamides with anionic dyes, these fibres contain amino and carboxyl groups. Depending on the pH value in dyeing



process, under lower pH these fibres have an overall positive charge ( $\text{NH}_3^+$ ) because the carboxyl groups in the side chains are hardly ionized under acid conditions. Therefore, anionic dyes are attracted towards the positively charged amino acid by ionic forces.

#### *Van der Waal's forces*

Van der Waal's forces or dispersion forces are the forces of attraction involved between non-polar molecules. The distances between molecules have an important effect on the strength of van der Waals forces. They are the weakest intermolecular forces. Although in a non-polar molecule there is no overall charge distribution, the electrons are in constant motion so that at any instant, small dipoles will be present. These instantaneous dipoles in turn induce oppositely-oriented dipoles in neighbouring molecules and a weak attraction between the molecules results. Van der Waals forces are therefore only effective for sorption of dyes to fibre molecules if the distance between the dye and the fibre molecules is small. The influence of Van der Waal's forces particularly important in dyeing of cellulosic fibres.

#### *Hydrogen bonding*

Hydrogen bonding is a strong type of dipole-dipole interaction. This interaction occurs between molecules containing a hydrogen atom which can interact with a nitrogen, oxygen, or fluorine atom. A partially positive hydrogen atom of one molecule is attracted to the unshared pair of electrons of the electronegative atom of another molecule. Intermolecular and intramolecular hydrogen bonding between

functional groups on dye molecules and fibre molecules play important role in many interaction dye-fibre systems.

#### *Covalent forces*

Covalent forces result from the sharing of a pair of electrons by two atoms. An especially important use of covalent bonding in colour application technology is the application of reactive dyes to cellulosic and protein textile fibres. After dyeing fibres with reactive dyes, the dyes interact chemically with the fibres to form a covalent bond.

#### *Dipole-dipole interactions*

Dipole-dipole interactions may make a contribution to the forces of attraction between dye and fibre molecules. Dipolar intermolecular forces involve the attraction of the positive centers in one polar molecule for the negative centers in another. As a result of these forces, polar molecules are generally attracted to each other more strongly than non-polar molecules of comparable molecular size. Non-polar molecules are attracted to each other by weak dipole-dipole interactions called London forces. London forces arise from dipoles induced in one molecule by another so a weak attraction between the molecules results. However, as the charges are only partial, dipolar-dipole interactions are weaker than ionic forces.

### 2.2.2 Kinetic models of adsorption

In order to examine the controlling mechanism of the adsorption process, pseudo first order and pseudo second order equations were used to test the experimental data. The best-fit model was selected based on the linear regression correlation coefficient,  $R^2$  values.

A simple kinetic analysis of adsorption is the pseudo first-order rate expression of the Lagergren equation (Lagergren, 1898). The Lagergren equation, a pseudo first order equation, describes the kinetics of the adsorption process as follows:

$$\frac{dq_t}{dt} = k_1(q_e - q_t) \quad (2.1)$$

where  $k_1$  is the rate constant of pseudo first-order adsorption ( $s^{-1}$ ), and  $q_e$  and  $q_t$  are the amount of dye adsorbed per gram silk (mg/g silk) at equilibrium and time  $t$ , respectively. Integration by applying the initial conditions  $q_t = 0$  at  $t = 0$  and  $q = q_t$  at  $t = t$ , then leads to the following equation:

$$\ln(q_e - q_t) = \ln q_e - k_1 t \quad (2.2)$$

A straight line of  $\ln(q_e - q_t)$  versus  $t$  suggests the applicability of this kinetic model to fit the experimental data. The first order rate constant  $k_1$  and equilibrium adsorption density  $q_e$  were calculated from the slope and intercept of this line.

In addition, the pseudo second order kinetic model (Ho and McKay, 1999; Wu, Tseng, and Juang, 2001; Chiou and Li, 2002; Dogan and Alkan, 2003; Chairat *et al.*, 2005; Lakshmi, Srivastava, Mall, and Lataye, 2009) is based on adsorption equilibrium capacity and can be expressed as:

$$\frac{dq_t}{dt} = k_2(q_e - q_t)^2 \quad (2.3)$$

where  $k_2$  (g silk/mg min) is the rate constant for pseudo second-order adsorption. Integrating equation (2.3) and applying the initial conditions gives:

$$\frac{1}{(q_e - q_t)} = \frac{1}{q_e} + k_2 t \quad (2.4)$$

or equivalently,

$$\frac{t}{q_t} = \frac{1}{k_2 q_e^2} + \frac{1}{q_e} t \quad (2.5)$$

and

$$h_i = k_2 q_e^2 \quad (2.6)$$

where  $h_i$  (Chiou and Li, 2002; Chairat *et al.*, 2005) is the initial dye adsorption rate (mg/g silk min). If the pseudo second order kinetics is applicable, the plot of  $t/q_t$  versus  $t$  shows a linear relationship. The slope and intercept of  $(t/q_t)$  versus  $t$  were used to calculate the pseudo second-order rate constant  $k_2$  and  $q_e$ . It is likely that the

behaviour over the whole range of adsorption is in agreement with the chemisorption mechanism being the rate-controlling step (Chiou and Li, 2002).

In general, the rates of chemical reactions increase with an increase in the temperature. In the rate law, temperature dependence appears in the rate constant. The dependence of rate constants on temperature over a limited range can usually be represented by an empirical equation van't Hoff and Arrhenius equation (Laidler, Meiser, and Sanctuary, 2003):

$$k = Ae^{-E_a/RT} \quad (2.7)$$

where A is the pre-exponential factor and  $E_a$  is the activation energy and R is the gas constant, equal to  $8.3145 \text{ J K}^{-1} \text{ mol}^{-1}$ . The pre-exponential factor A has the same units as the rate constant. An alternative form is obtained by taking the logarithm of each side.

$$\ln k = \ln A - \frac{E_a}{RT} \quad (2.8)$$

$E_a$  can be obtained by plotting (Arrhenius plot)  $\ln k$  against the reciprocal of the absolute temperature T. The magnitude of  $E_a$  may then give an indication of whether a physical or chemical adsorption process is in operation. In physical adsorption (physisorption) the interaction is easily reversible, equilibrium is rapidly attained and its energy requirements are small so  $E_a$  is usually no more than 5-40 kJ/mol, because usually weak intermolecular forces are involved. However, with

chemical adsorption (chemisorption) much stronger bonding forces are involved and  $E_a$  values range from 40-800 kJ/mol (Nollet, Roels, Lutgen, Meeren, and Verstraete, 2003).

The enthalpy ( $\Delta H^\#$ ), entropy ( $\Delta S^\#$ ) and free energy ( $\Delta G^\#$ ) of activation can be also calculated using the Eyring equation (Laidler *et al.*, 2003): as follows:

$$\ln\left(\frac{k}{T}\right) = \ln\left(\frac{k_b}{h}\right) + \frac{\Delta S^\#}{R} - \frac{\Delta H^\#}{RT} \quad (2.9)$$

where  $k_b$  and  $h$  refer to Boltzmann's constant and Planck's constant, respectively. The enthalpy ( $\Delta H^\#$ ) and entropy ( $\Delta S^\#$ ) of activation were calculated from the slope and intercept of a plot of  $\ln(k/T)$  versus  $1/T$ . Gibbs energy of activation ( $\Delta G^\#$ ) can be written in terms of enthalpy and entropy of activation (Laidler *et al.*, 2003):

$$\Delta G^\# = \Delta H^\# - T\Delta S^\# \quad (2.10)$$

### 2.2.3 Adsorption isotherms

The equilibrium adsorption is fundamental in describing the interaction behaviour between solutes and adsorbents, and is important in the design of an adsorption system. The relationship between the amounts of a substance adsorbed at constant temperature and its concentration in the equilibrium solution is called the adsorption isotherm (Ahmad, Hameed, and Aziz, 2007). Adsorption isotherm data are commonly fitted to the Langmuir isotherm and the Freundlich isotherm as follows:

### 2.2.3.1 The Langmuir isotherm

A basic assumption of the Langmuir theory is that sorption takes place at specific homogeneous sites within the adsorbent. It is then assumed that once a dye molecule occupies a site, no further adsorption can take place at that site. The Langmuir adsorption isotherm has been successfully applied to many other real sorption processes (Ho and McKay, 1999; Kongkachuichay *et al.*, 2002; Chairat *et al.*, 2005; Rattanaphani, Chairat, Bremner, and Rattanaphani, 2007). Theoretically, therefore, a saturation value is reached beyond which no further sorption can take place. The saturated monolayer curve can be represented by the expression:

$$q_e = \frac{QbC_e}{1 + bC_e} \quad (2.11)$$

A linear form of this expression is:

$$\frac{C_e}{q_e} = \frac{1}{Qb} + \left(\frac{1}{Q}\right)C_e \quad (2.12)$$

For lower concentrations, the following form of Langmuir equation is found to be more satisfactory (Bhattacharyya and Sarma, 2003):

$$\frac{1}{q_e} = \frac{1}{Q} + \frac{1}{QbC_e} \quad (2.13)$$

In the above equation,  $Q$  is the maximum amount of the dye per unit weight of fibre to form complete monolayer coverage on the surface bound at high equilibrium dye concentration  $C_e$ ,  $q_e$  is the amount of dye adsorbed per unit weight of fibre at equilibrium, and  $b$  the Langmuir constant related to the affinity of binding sites. The value of  $Q$  represents a practical limiting adsorption capacity when the surface is fully covered with dye molecules and assists in the comparison of adsorption performance. The values of  $Q$  and  $b$  are calculated from the intercepts and slopes of the straight lines of plot of  $1/q_e$  versus  $1/C_e$ .

### 2.2.3.2 The Freundlich isotherm

The Freundlich isotherm (Ho and McKay, 1999; Chiou and Li, 2002) is based on an exponential relationship and is generally applicable to heterogeneous surface energy distribution. The Freundlich equation is shown:

$$q_e = Q_f C_e^{1/n} \quad (2.14)$$

where  $Q_f$  is roughly an indicator of the adsorption capacity and  $1/n$  of the adsorption intensity. A linear form of the Freundlich expression in the equation (2.15) will yield the constants  $Q_f$  and  $1/n$ .

$$\ln q_e = \ln Q_f + \frac{1}{n} \ln C_e \quad (2.15)$$



Therefore,  $Q_f$  and  $1/n$  can be determined from the linear plot of  $\ln q_e$  versus  $\ln C_e$ . The magnitude of the exponent  $1/n$  gives an indication of the favourability of adsorption. Values of  $n > 1$  obtained represent favourable adsorption conditions (Chiou and Li, 2002).

Based on fundamental thermodynamics concept, it is assumed that in an isolated system, energy cannot be gained or lost and entropy change is the only driving force. The Gibbs free energy change,  $\Delta G^\circ$ , is the fundamental criterion of spontaneity. A reaction occurs spontaneously at a given temperature if  $\Delta G^\circ$  is a negative quantity. The thermodynamic parameters for the adsorption process, namely Gibbs energy ( $\Delta G^\circ$ ), enthalpy ( $\Delta H^\circ$ ) and entropy ( $\Delta S^\circ$ ) of adsorption are evaluated using the following equations (Chiou and Li, 2003):

$$K_C = \frac{C_{ad,e}}{C_e} \quad (2.16)$$

$$\Delta G^\circ = -RT \ln K_C \quad (2.17)$$

$$\Delta G^\circ = \Delta H^\circ - T\Delta S^\circ \quad (2.18)$$

$$\ln K_C = \frac{\Delta S^\circ}{R} - \frac{\Delta H^\circ}{RT} \quad (2.19)$$

In the above equations,  $K_C$  is the equilibrium constant, and  $C_{ad,e}$  and  $C_e$  are the dye concentration adsorbed at equilibrium (mg/L) and the concentration of dye left in the

dye bath at equilibrium (mg/L), respectively.  $T$  is the solution temperature (K) and  $R$  is the gas constant. Enthalpy ( $\Delta H^0$ ) and entropy ( $\Delta S^0$ ) of the adsorption are calculated from the slope and intercept of van't Hoff plots of  $\ln K_c$  versus  $1/T$ .

## 2.3 Experimental

### 2.3.1 Materials and Chemicals

- (1) Silk yarn from Chul Thai Silk Co., Ltd in Phetchabun, Thailand
- (2) Indigo [482-89-3],  $C_{16}H_{10}N_2O_2$ , MW 262.26, Sigma Aldrich
- (3) Natural plant-derived indigo dye (from *Indigofera tinctoria*),

Nakhon Ratchasima and Sakonnakhon, Thailand

- (4) Calcium hydroxide,  $Ca(OH)_2$ , Carlo
- (5) Sodium hydroxide, NaOH, Carlo
- (6) Sodium hydrosulfite,  $Na_2S_2O_4$ , Carlo
- (7) Hydrochloric acid 37% (w/v), HCl, Merck
- (8) *N,N*-Dimethylformamide, DMF, MW 73.09, Sigma Aldrich
- (9) Methanol,  $CH_3OH$ , HPLC grade, Merck
- (10) Water plus, HPLC, Merck

### 2.3.2 Instruments

(1) High performance liquid chromatography (HPLC) from Hewlett Packard (HP 1100 model) was employed to analysis the amount of indigo in plant extracted indigo dye.

(2) An Agilent 8453 UV-Vis spectrophotometer was employed to determine the concentration of dye samples through absorbance measurements using quartz cells of path length 1 cm at the characteristic maximum wavelength.

(3) A pH meter (Laboratory pH Meter CG 842, SCHOTT, UK) was used to measure the pH values of solutions.

(4) An Ultrasonic Cleaner bath (Model-575 HT, frequency 38.5-40.0 kHz, average power 135 Watts, peak power 405 Watts, Crest Ultrasonics Corp., Trenton, NJ, USA) was used in the indigo reduction process.

(5) A thermostatted shaker bath (Type SBD-50 cold, Heto-Holten A/S, Denmark) operated at 150 strokes/min, was used to study the adsorption kinetics and thermodynamics of indigo onto silk yarn.

### **2.3.3 Experimental methods**

#### **2.3.3.1 Silk yarn preparation (Chairat, 2004)**

The silk yarn used was purchased from Chul Thai Silk Co., Ltd in Phetchabun, Thailand. Prior to using in the dyeing experiments, the silk yarn (1 kg) was treated with 0.5 M HCl (*ca* 3 L) at room temperature for 30 min and then removed and washed with deionized water until the rinsed water was neutral. The silk yarn was then dried at room temperature.

#### **2.3.3.2 Preparation of plant extracted indigo dye powder**

Plant-derived indigo used in the experiments was derived from *Indigofera tinctoria* species. Two types of plant extracted indigo dye were used in this research namely indigo-SUT and indigo-village. For indigo-SUT, *Indigofera tinctoria*

plants were grown in a field at Suranaree University of Technology (SUT), Nakhon Ratchasima. Plants were grown (to a height of about 3 feet) over six months (June-November). Fresh leaves (dark green; fresh weight 1.0 kg) were then collected and then allowed to ferment in water (3.0 L) for 24 hr. The *Indigofera tinctoria* leaves were then removed and calcium hydroxide ( $\text{Ca(OH)}_2$ ) (60.0 g) was added to the solution. Air was bubbled through the solution for 30 min and then the indigo formed was allowed to precipitate overnight. Then the supernatant was discarded and the precipitated pigment or indigo paste was rinsed with water and dried in an oven at 50°C to afford indigo powder (indigo-SUT, 8.6% of precursor material). Another plant extracted (*Indigofera tinctoria*) indigo paste sample was purchased from villagers in Sakonnakhon. This plant extracted indigo paste was rinsed with water and dried in an oven at 50°C to give the indigo powder (indigo-village).

### **2.3.3.3 Analysis of indigo in plant extracted indigo dye by the HPLC method**

This method was conducted using an HPLC system (HP 1100 model). Analyses were carried out with an Agilent C18 reverse phase column (250×4 mm, 5 μm), with a flow rate of 1.0 mL/min using a gradient made of solvent A ( $\text{CH}_3\text{OH}$ ) and solvent B ( $\text{H}_2\text{O}$ ). Program: 0-10 min: 85% B/ 15% A to 75% B/ 25% A; 10-30 min: 75 to 30% B; 30-40 min: hold at 30% B; 40-45 min: 30 to 85% B. The injected sample volume was 20 μL and the column temperature was controlled at 30°C. Products were detected and quantified using a diode array detector at 280 nm (Maugard *et al.*, 2001). Pigment concentrations and yields of indigo obtained from

plant extracted indigo dye were quantified by HPLC analysis with reference to a calibration curve of indigo dye.

The calibration curve was done using various amount of standard indigo, obtained by dissolving 0.3 mg of standard indigo in 25 mL of dimethylformamide (DMF). The solution was then diluted to different concentrations with the DMF and the peak area for the indigo peak (HPLC) measured.

For the preparation of the plant extracted indigo dye for HPLC analysis, 5.0 mg of powdered plant extracted indigo dye (indigo-SUT or indigo-village) was dissolved in 25 mL DMF. All samples were filtered through a 0.45  $\mu\text{m}$  membrane filter and analyzed by HPLC under the same conditions noted above.

#### **2.3.3.4 Reduction of indigo by sodium dithionite in alkaline medium**

Indigo dye (or plant extracted indigo) and deionized water were added into a flask with the required concentrations. This mixture was degassed by bubbling through nitrogen (99.995% purity) for 10-15 min before adding sodium dithionite ( $\text{Na}_2\text{S}_2\text{O}_4$ , as reducing agent) and sodium hydroxide (NaOH) to adjust the dye bath to an alkaline pH of 11-12 (indigo was not reduced at pH less than 10). The temperature of the solution was 35°C. The ratios by weight of indigo: $\text{Na}_2\text{S}_2\text{O}_4$ :NaOH were 1:300:300. The indigo reduction was carried out in the ultrasonic bath for 30 min at room temperature and was performed under a nitrogen atmosphere to prevent oxidation of the reducing agent or leuco indigo. The concentration of the leuco indigo solution (yellow colour) was determined by using UV-Vis spectrophotometry at the absorption maximum wavelength ( $\lambda_{\text{max}}$ ) of 405 nm.

### **2.3.3.5 Batch kinetic experiments of indigo dyeing onto silk by the conventional vat-dyeing method**

The batch technique was used to examine the dyeing process at temperatures of 30, 40 and 50°C. The conventional vat dyeing process (under a nitrogen atmosphere) was performed by taking a series of 125 mL conical flasks containing the leuco indigo dye solution over the concentration range 20 to 100 mg/L at a pH of 11-12. The dye solution in each conical flask was shaken in a thermostatted shaker bath operated at 150 strokes/min and controlled temperature. After 15 min, the silk yarn (0.50 g), which had been pre-warmed in the thermostatted bath for 15 min, was immersed in the dye solution. The silk samples were then rapidly withdrawn after different immersion times. After dyeing, the leuco indigo in the silk was air oxidized at room temperature. Excess  $\text{Na}_2\text{S}_2\text{O}_4$  and NaOH was removed from the indigo-dyed silk with deionized water until the rinsed water was neutral and then the silk was dried at room temperature. The concentration of the unadsorbed leuco indigo in the supernatant dye solution was determined at time zero and at subsequent times using a calibration curve based on absorbance at  $\lambda_{\text{max}}$  405 nm versus dye concentration. The amount of dye adsorbed per gram of silk ( $q_t$ ) (mg/g silk) at any time was calculated by a mass balance relationship (Eq. (2.20)) as follows:

$$q_t = (C_0 - C_t) \frac{V}{W} \quad (2.20)$$

where  $C_0$  and  $C_t$  are the initial and subsequent at time,  $t$  concentrations of dye, respectively (mg/L),  $V$  is the volume of the solution (L), and  $W$  is the weight of the silk yarn used (g).

### **2.3.3.6 Batch equilibrium experiments of indigo dyeing onto silk by the conventional vat-dyeing method**

The conventional vat dyeing process (under nitrogen conditions) was performed by taking a series of 125 mL conical flasks containing the leuco indigo dye solution over the required concentrations at a pH of 11-12 in the dye bath solution. The experiments were carried out by shaking silk yarn (0.50 g) with different concentrations of dye solution (50 mL) in a conical flask in a thermostatted shaker bath operated at 150 strokes/min and controlled temperature. After dyeing, the leuco indigo in the silk was air oxidised at room temperature. Excess  $\text{Na}_2\text{S}_2\text{O}_4$  and  $\text{NaOH}$  was removed from the indigo-dyed silk with deionized water until the rinsed water was neutral and then the silk was dried at room temperature. The concentration of the unadsorbed leuco indigo in the supernatant dye solution was determined at time zero and at equilibrium times using a calibration curve based on absorbance at  $\lambda_{\text{max}}$  405 nm versus dye concentration. The amount of dye adsorbed per gram of silk ( $q_e$ ) (mg/g silk) at equilibrium time was calculated by a mass balance relationship (Eq. (2.21)) as follows:

$$q_e = (C_0 - C_e) \frac{V}{W} \quad (2.21)$$

where  $C_0$  and  $C_e$  are the initial and equilibrium concentration of dye, respectively (mg/L),  $V$  is the volume of the solution (L), and  $W$  is the weight of the silk yarn used (g).

### **2.3.3.7 Batch kinetic experiments of plant extracted indigo dyeing onto silk by the conventional vat-dyeing method**

The leuco plant extracted indigo dye solution was prepared from plant extracted indigo (indigo-village) at the desired concentration. The conventional vat dyeing process (under nitrogen conditions) was performed at temperatures of 30, 40 and 50°C. The dye solution (50 mL) in each conical flask was shaken in a thermostatted shaker bath operated at 150 strokes/min and controlled temperature. After 15 min, the silk yarn (0.50 g, material to liquor ratio (MLR) 1:100), which had been pre-warmed in the thermostatted bath for 15 min, was immersed in the dye solution. The silk samples were then rapidly withdrawn after different immersion times. After dyeing, the leuco plant extracted indigo in the silk was air oxidized at room temperature. Excess  $\text{Na}_2\text{S}_2\text{O}_4$  and NaOH were removed from the indigo-dyed silk with deionized water until the rinsed water was neutral and then the silk was dried at room temperature. The concentration of the unadsorbed leuco plant extracted indigo in the supernatant dye solution was determined at time zero and at subsequent times using a calibration curve based on absorbance at  $\lambda_{\text{max}}$  405 nm versus dye concentration. The amount of dye adsorbed per gram of silk ( $q_t$ ) (mg/g silk) at any time was calculated by a mass balance relationship (Eq. (2.20)).



### **2.3.3.8 Batch equilibrium experiments of plant extracted indigo dyeing onto silk by the conventional vat-dyeing method**

The leuco plant extracted indigo dye solution was prepared from plant extracted indigo (indigo-village) at the required concentrations. The conventional vat dyeing process (under nitrogen conditions) was performed with a MLR of 1:100 and at a temperature of 30°C. The silk yarn (0.50 g) and 50 mL of the leuco plant extracted indigo dye solution were put in a 125 mL flask and were shaken for 60 min by using a thermostatted shaker bath operated at 150 strokes/min and controlled temperature. After dyeing, the leuco plant extracted indigo in the silk was air oxidized at room temperature. Excess  $\text{Na}_2\text{S}_2\text{O}_4$  and NaOH were again removed from the indigo-dyed silk with deionized water until the rinsed water was neutral and then the silk was dried at room temperature. The concentration of the unadsorbed plant extracted leuco indigo in the supernatant dye solution was determined at time zero and at equilibrium times using a calibration curve based on absorbance at  $\lambda_{\text{max}}$  405 nm versus dye concentration. The amount of dye adsorbed per gram of silk ( $q_e$ ) (mg/g silk) at equilibrium time was calculated by a mass balance relationship (Eq. (2.21)).

## **2.4 Results and Discussion**

### **2.4.1 Analysis of indigo in plant extracted indigo dye by HPLC method**

*Indigofera tinctoria* is the plant which was used as a natural source of indigo dye in this research and is available in the north-eastern part of Thailand. HPLC methodology was used as described for the qualitative and quantitative analysis of indigo in two samples of the plant extracted indigo dye (indigo-SUT and indigo-village) and the results compared with standard indigo. HPLC chromatograms

of the standard indigo, indigo-SUT and indigo-village are shown in Figure 2.5. The major compound present in the indigo-SUT and indigo-village samples were detected at the ( $t_R$ ) of 31.916 and 31.912 minutes, respectively. This result showed similar retention times to that of standard indigo ( $t_R$  31.923 min.). After spiking standard indigo in the both of the plant extracted indigo dye samples, an increase in the peak area at the retention time of 31-32 minutes were observed. This confirmed that plant extracted indigo dye contained indigo.

Quantitative determinations of the amount of indigo in the two samples of the plant extracted indigo dye (indigo-SUT and indigo-village) were performed using the HPLC method and the results referenced to standard indigo. Standard indigo content was determined by an external calibration and a validated linear relationship between peak area and indigo contents (concentration at 2.4, 6.0, 7.2, 9.6 and 12.0 mg/L) (Figure 2.6) The concentration of indigo in the plant extracted indigo dye was calculated from the following the regression equation:  $y = 181.4857x + 78.7422$  and the percentage of indigo in the plant extracted indigo dye was calculated on the basis of the initial amount of crude plant extracted indigo dye. The results are shown in Table 2.1, and it can be seen that the concentration of indigo in the plant extracted indigo dye (mg/L) samples indigo-SUT and indigo-village were 4.99 mg/L (2.50%) and 3.32 mg/L (1.66%), respectively. The higher content of indigo in the former sample may have been due to fresher leaves being processed in the initial extraction. The results from this study were then used to underpin further work calculating the initial concentration of plant extracted indigo solution for dyeing onto silk by the conventional vat-dyeing method (Section 2.4.3) and direct dyeing onto silk (Chapter IV).

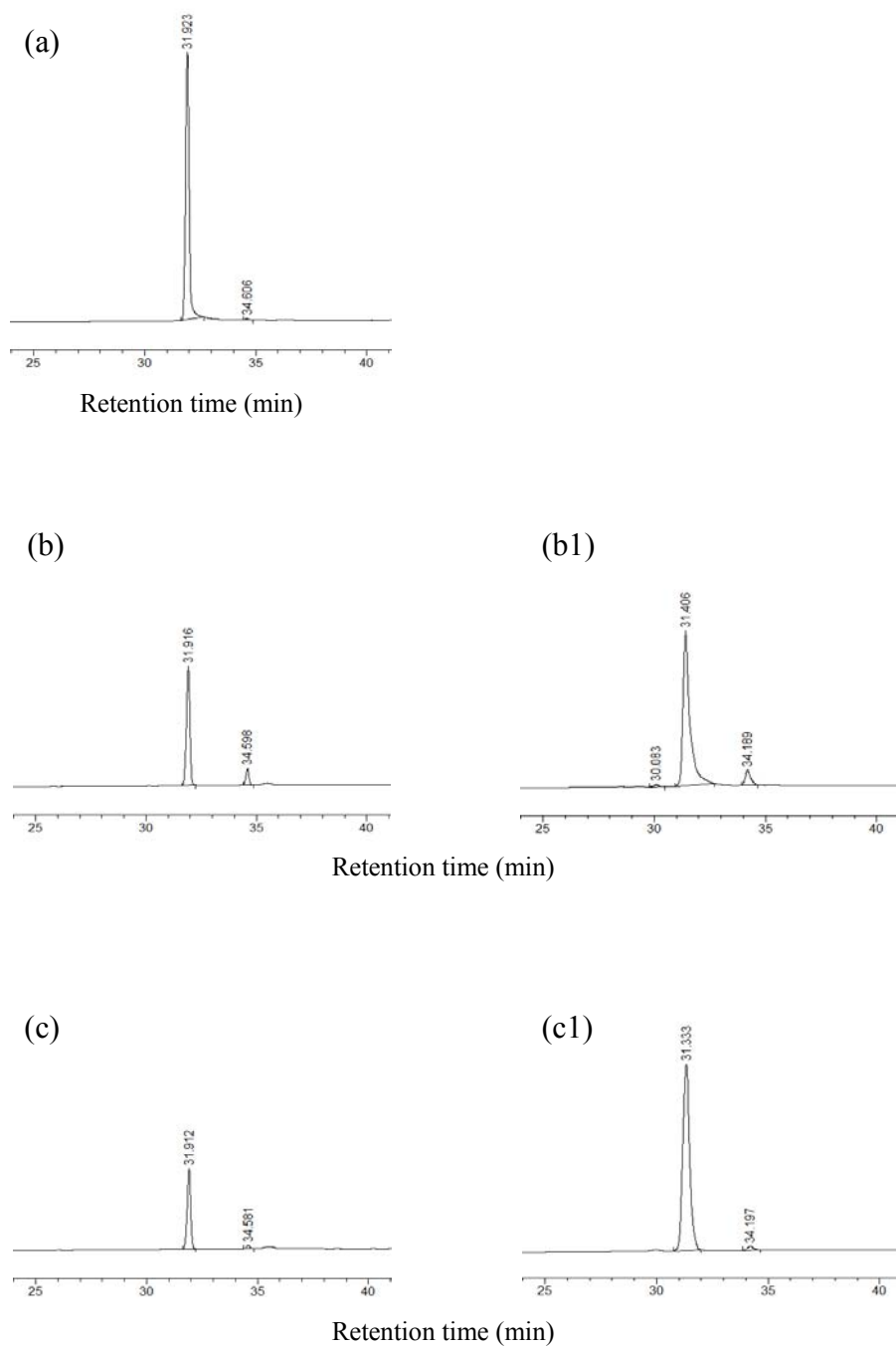


**Figure 2.5** HPLC chromatograms of (a) standard indigo; (b) indigo-SUT; (b1) indigo SUT spiking with standard indigo; (c) indigo-village; (c1) indigo-village spiking with standard indigo.

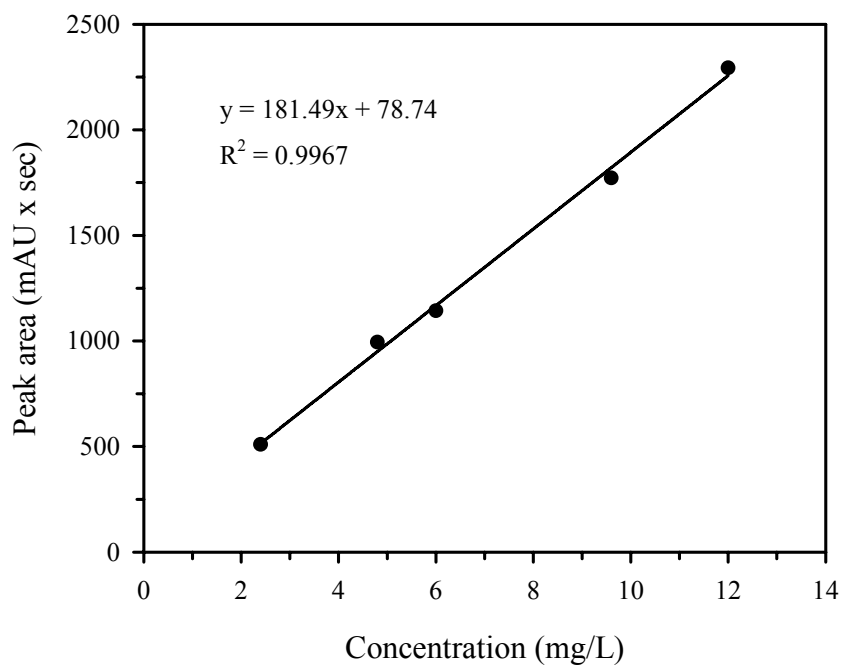


**Figure 2.6** Calibration curve of standard indigo from HPLC method.

**Table 2.1** Amount of indigo in plant extracted indigo dye by HPLC method.

Sample	$t_R$ (min)	Peak area (mAU×sec)	Concentration of indigo in plant extracted indigo dye powder (mg/L)	% of indigo in plant extracted indigo dye powder
Indigo-SUT	31.916	984.929	4.99	2.50
Indigo-village	31.912	681.819	3.32	1.66

## **2.4.2 Kinetic and thermodynamic studies of indigo dyeing onto silk by the conventional vat-dyeing method**

In order to investigate the adsorption of indigo onto silk by the conventional vat-dyeing method, the experimental parameters including initial dye concentration, contact time, material to liquor ratio (MLR), and temperature were determined to find the optimal conditions for adsorption. The mechanism of the adsorption of indigo onto silk by the conventional vat-dyeing method was investigated by using the pseudo first order and second order models. The best-fit model was selected based on the linear regression correlation coefficient,  $R^2$  values. It should be noted here that all the kinetic and thermodynamic studies were monitored indirectly through variation in the water soluble leuco indigo concentration, but this in turn should give a good reflection of indigo adsorption on the silk.

### **2.4.2.1 Effect of initial dye concentration and contact time on the adsorption of indigo onto silk**

The adsorption of indigo at different initial dye concentrations onto silk at the pH of the dye bath, MLR = 1:100 and 30°C was investigated as a function of contact time in order to determine the equilibrium time for maximum adsorption. A plot of the amount of dye adsorbed per gram silk ( $q_t$ ) (mg/g silk) at any time versus contact time ( $t$ ) is shown in Figure 2.7. It was found that the dye adsorption rate for each initial dye concentration reached equilibrium after 60 min. The equilibrium time was independent of initial dye concentrations but in the first 30 min, the initial rate of adsorption was greater for higher initial dye concentrations at the same agitation speed. An increase of the dye concentration accelerates the diffusion of dyes from the

dye solution onto silk due to the increase in the driving force of the concentration gradient (Chiou and Li, 2002; Chairat *et al.*, 2005).

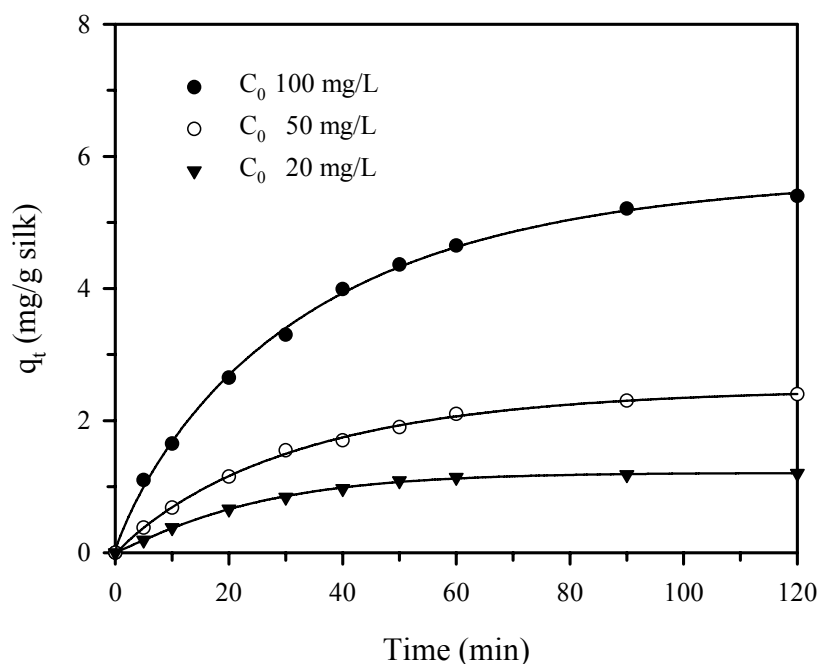


**Figure 2.7** Effect of initial dye concentration on the adsorption of indigo onto silk (under dyeing condition MLR = 1:100, pH = 11-12, 30°C).

The results of rate constant studies for different initial dye concentrations by using the pseudo first order and pseudo second order kinetic models are listed in Table 2.2 and shown in Figure 2.8 and Figure 2.9 are pseudo first order and pseudo second order plots, respectively. The pseudo second order kinetic model well described the adsorption of indigo dye onto silk over a range of desired initial dye concentrations with a high correlation coefficient ( $R^2 > 0.99$ ). This suggested that the overall rate of the indigo dye adsorption onto silk is controlled by chemisorption. A similar phenomenon has also been observed in the lac, alum-morin and indigo

carmine dyeing onto silk (Chairat *et al.*, 2005; Septhum *et al.*, 2009; Jiwalak *et al.*, 2010). The results in Table 2.2, also show  $k_2$ ,  $h_i$  and  $q_e$  as a function of initial dye concentration. The pseudo second-order rate constant ( $k_2$ ) decreased with increasing initial dye concentration whereas the initial dye adsorption rate ( $h_i$ ) increased with an increasing initial dye concentration. An increase in initial dye concentration results in a significant increase in  $q_{e,cal}$ . The  $q_{e,cal}$  for initial dye concentration also increases with an increasing of initial dye concentration.

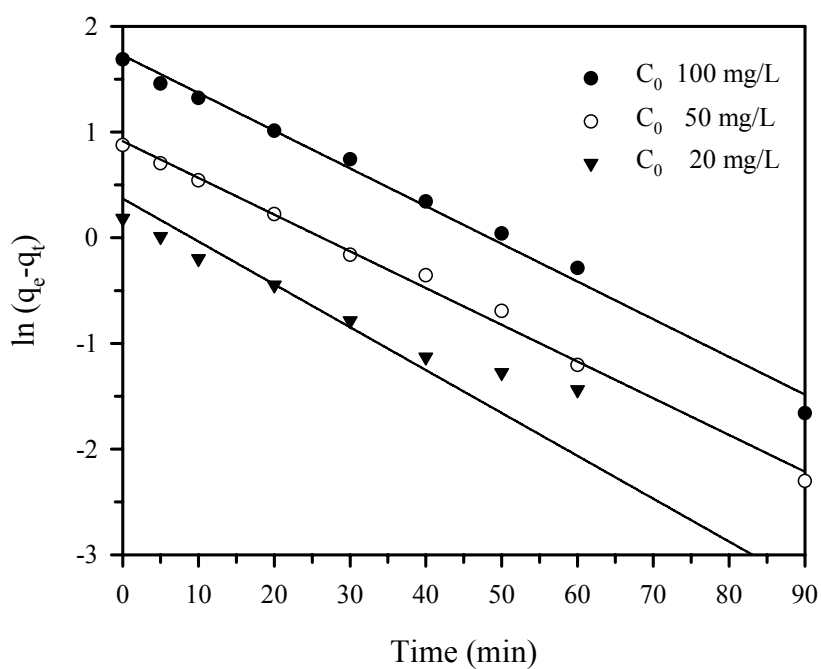


**Figure 2.8** Application of the pseudo first order equation at different initial dye concentration on the adsorption of indigo onto silk.

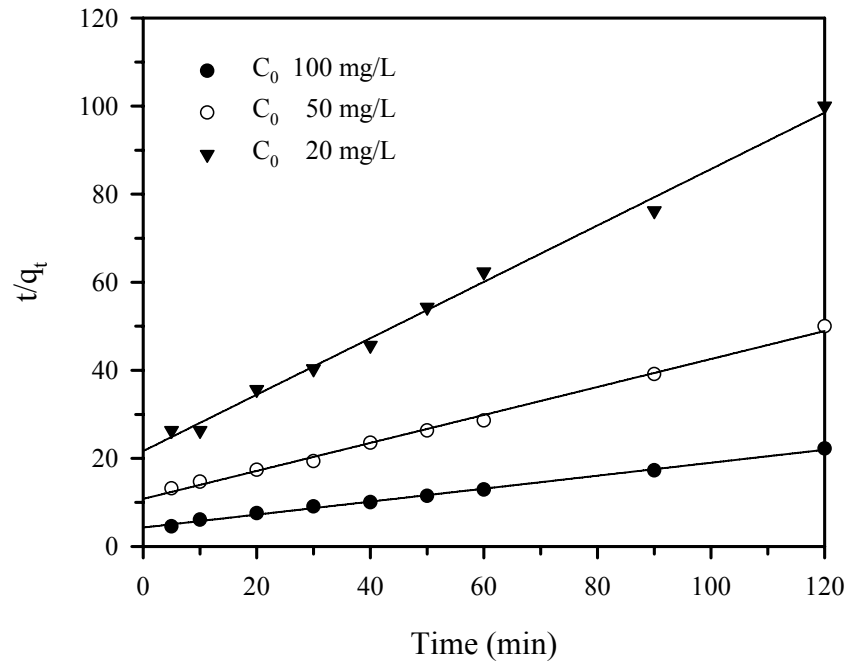


**Figure 2.9** Application of the pseudo second order equation at different initial dye concentration on the adsorption of indigo onto silk.



**Table 2.2** Comparison of the pseudo first- and pseudo second-order adsorption rate constants and the calculated and experimental  $q_e$  values for different initial dye concentrations, MLR and temperature for the adsorption of indigo onto silk.

Parameter	$q_{e,exp}$ (mg/g silk)	Pseudo first order model			Pseudo second order model			
		$k_1$ ( $\text{min}^{-1}$ )	$q_{e,cal}$ (mg/g silk)	$R^2$	$k_2$ (g silk/mg min)	$q_{e,cal}$ (mg/g silk)	$h_i$ (mg/g silk min)	$R^2$
<i>Initial dye concentration: <math>C_0</math> (mg/L): MLR 1:100, temp. 30 °C, contact time 60 min</i>								
20.3	1.24	0.0323	1.12	0.9841	0.0189	1.56	0.0462	0.9944
50.9	2.43	0.0278	2.49	0.9946	0.0094	3.15	0.0927	0.9956
101.5	5.41	0.0347	5.25	0.9974	0.0051	6.79	0.2333	0.9968
<i>MLR: <math>C_0</math> 20.3 mg/L, temp. 30 °C, contact time 60 min</i>								
1:50	0.73	0.0341	0.70	0.9947	0.0453	0.88	0.0354	0.9977
1:100	1.24	0.0278	1.12	0.9841	0.0189	1.56	0.0462	0.9944
1:150	1.48	0.0493	1.19	0.9754	0.0587	1.63	0.1564	0.9980
<i>Temperature: <math>C_0</math> 20.3 mg/L, MLR 1:100, contact time 60 min</i>								
30	1.24	0.0491	1.35	0.9863	0.0189	1.56	0.0462	0.9944
40	0.83	0.0442	0.87	0.9474	0.0577	0.94	0.0507	0.9945
50	0.64	0.0345	0.48	0.9445	0.1278	0.69	0.0610	0.9972

#### **2.4.2.2 Effect of material to liquor ratio (MLR) on the adsorption of indigo onto silk**

The aim of dyeing is to transfer the dye molecules from the dye liquor to the fibre in a uniform and efficient manner. The rate of dye uptake by the fibre is significantly increased by the increased movement of the dye liquor relative to the fibre (Christie, Mather, and Wardman, 2000). The effect of MLR on the adsorption of indigo onto silk at an initial dye concentration of 20 mg/L at pH 11-12 and 30°C is shown in Figure 2.10. It was found that an increase in volume of the dye solution resulted in an increase of the dye adsorbed onto the silk, consistent with the yarn being more loosely packed in the higher volume of dye solution. This allows the dye solution to move more readily over the silk surfaces with associated dye molecule binding, and then into the interior of the silk yarn by diffusion. Kinetic parameters from linear plots of pseudo first order (Figure 2.11) and pseudo second order (Figure 2.12) models are given in Table 2.2. The data show a good compliance with the pseudo second order equation and the regression coefficients,  $R^2$ , for the linear plot were all high ( $> 0.99$ ). The overall rate of the indigo adsorption processes appears to be controlled by the chemical process in this case in accordance with the pseudo second order reaction mechanism. The amount of dye adsorbed at MLR 1:150 was higher than that observed at MLR 1:100 and 1:50 (Figure 2.10). However, in order to minimize waste from the dyeing process, an MLR of 1:100 was used for all the kinetic experiments.

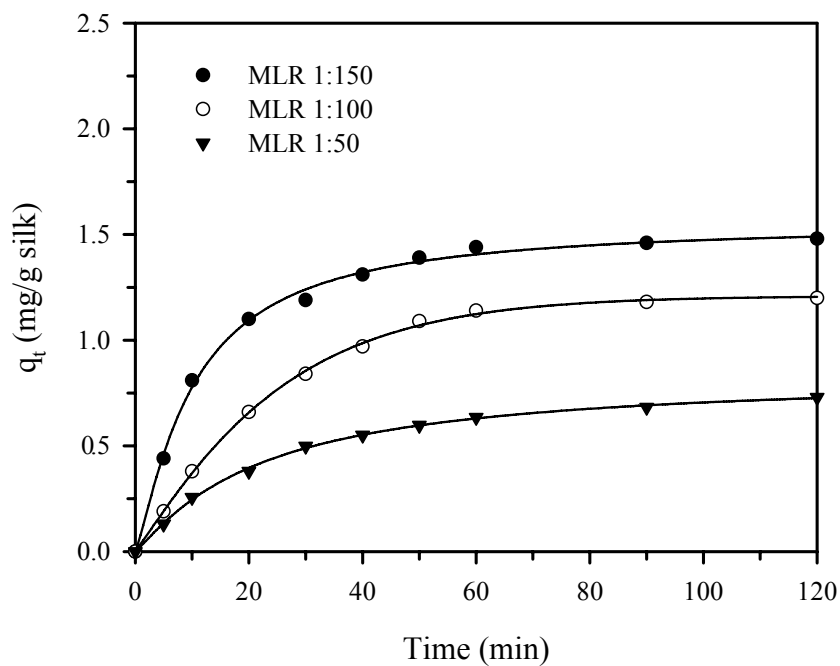


**Figure 2.10** Effect of MLR on the adsorption of indigo onto silk (under dyeing condition  $C_0 = 20$  mg/L, pH = 11-12, 30°C).

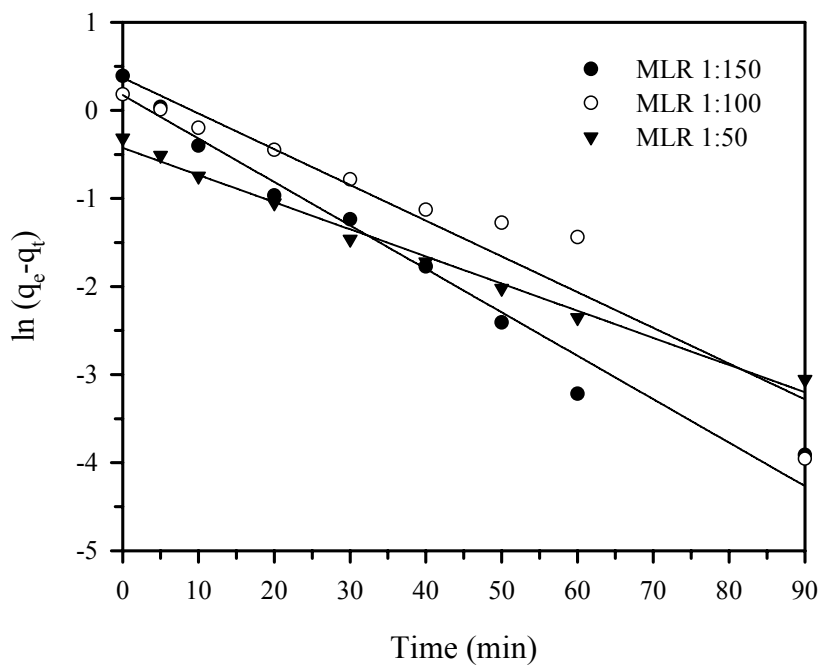


**Figure 2.11** Application of the pseudo first order equation at different MLR on the adsorption of indigo onto silk.

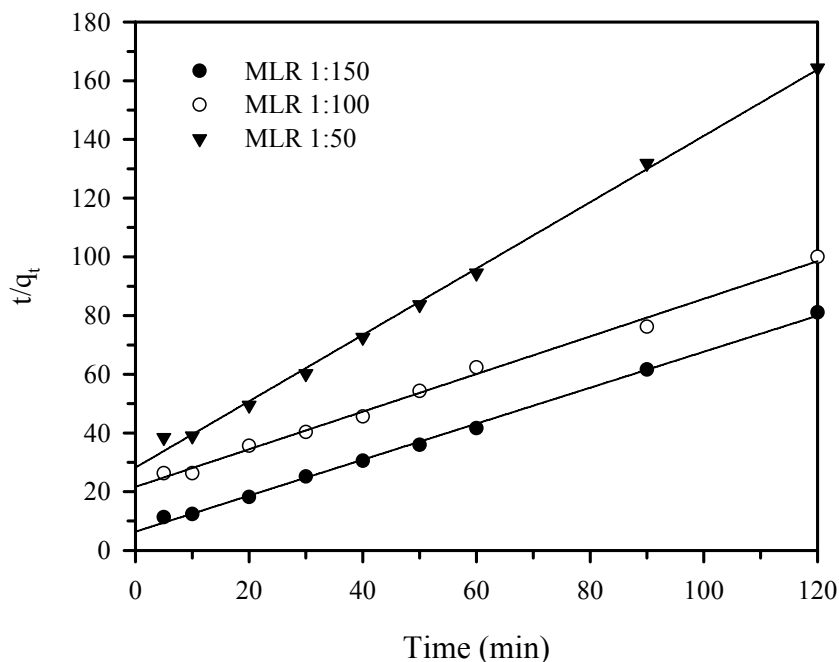


**Figure 2.12** Application of the pseudo second order equation at different MLR to the adsorption of indigo onto silk.

#### 2.4.2.3 Effect of temperature on the adsorption of indigo onto silk

The dye adsorption process was studied at different temperatures of 30, 40 and 50°C, and under the suitable conditions of pH 11-12, MLR = 1:100, and an initial dye concentration of 20 mg/L in each case. The effect of temperature on adsorption of indigo onto silk is shown in Figure 2.13. Before the equilibrium time was established, an increase in the temperature leads to an increase in dye adsorption rate indicative of a kinetically controlled process. After the equilibrium time, the amount of the dye adsorbed per gram of silk decreased with increasing the temperature suggesting that the adsorption of indigo onto silk is controlled by an exothermic process. Similar temperature effect trends on adsorption have also been

shown in the case of the lac, alum-morin and indigo carmine dyeing onto silk (Chairat *et al.*, 2005; Septhum *et al.*, 2009; Jiwalak *et al.*, 2010). Table 2.2 lists the results of rate constant and other kinetic parameter studies for different temperatures calculated by the pseudo first order (Figure 2.14) and pseudo second order (Figure 2.15) models. The correlation coefficient,  $R^2$ , for the pseudo second order adsorption model has a higher value suggesting that dye adsorption process occurs predominantly by the pseudo second order adsorption mechanism.

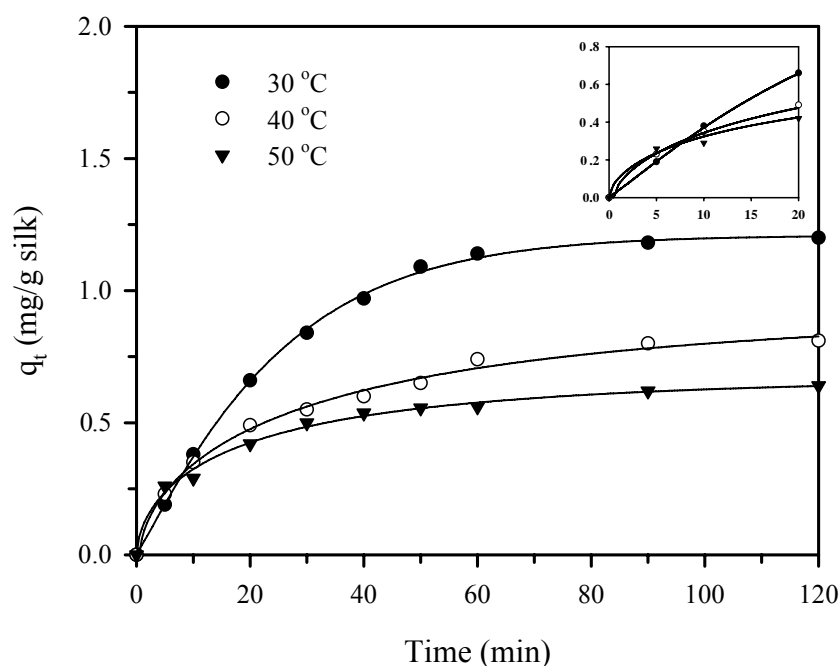


**Figure 2.13** Effect of temperature on the adsorption of indigo onto silk (under dyeing condition  $C_0 = 20$  mg/L, pH = 11-12, MLR = 1:100).

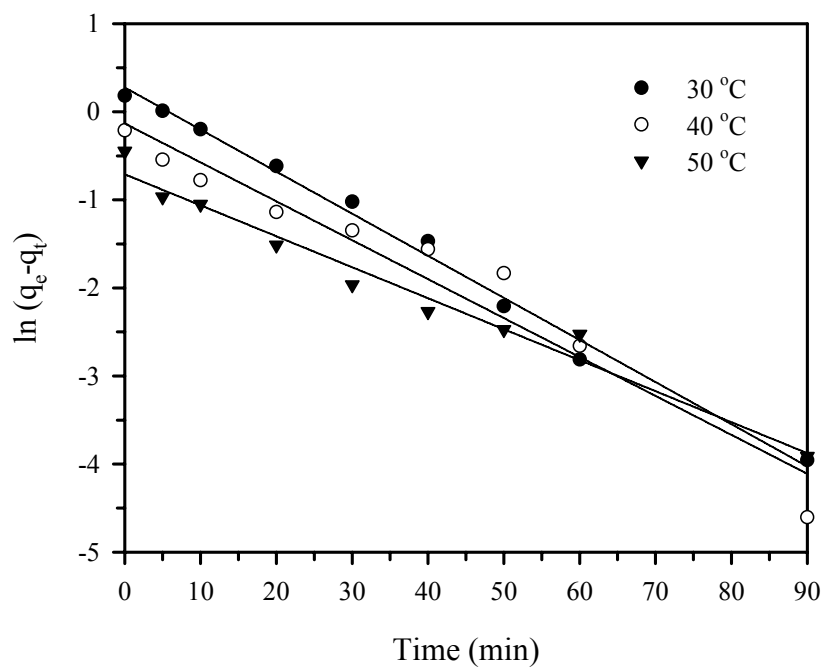


**Figure 2.14** Application of the pseudo first order equation at different temperature on the adsorption of indigo onto silk.

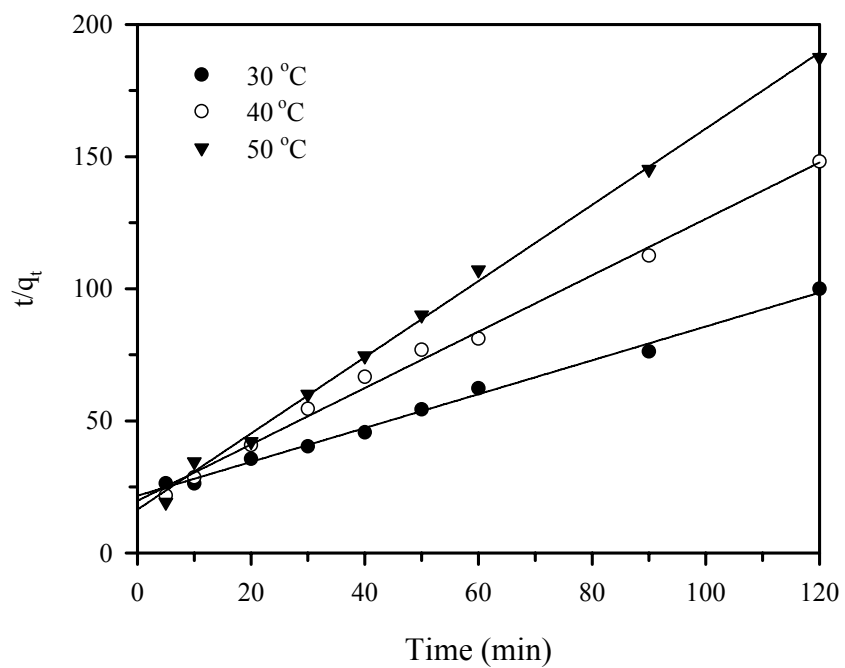


**Figure 2.15** Application of the pseudo second order equation at different temperature on the adsorption of indigo onto silk.

#### 2.4.2.4 Activation parameters for the adsorption of indigo onto silk

The rate constants  $k_2$  from the pseudo second-order model at different temperatures as listed in Table 2.2 were then applied to estimate the activation energy of the adsorption of indigo onto silk by the Arrhenius equation. The slope of the plot of  $\ln k_2$  versus  $1/T$  (Figure 2.16) was used to evaluate  $E_a$  as listed in Table 2.3.

The magnitude of  $E_a$  may then give an indication of whether a physical or chemical adsorption process is in operation. In physical adsorption (physisorption) the interaction is easily reversible, equilibrium is rapidly attained and its energy requirements are small so  $E_a$  is usually no more than 5-40 kJ/mol, because usually weak intermolecular forces are involved. However, with chemical adsorption (chemisorption) much stronger bonding forces are involved and  $E_a$  values range from 40-800 kJ/mol (Nollet *et al.*, 2003). For the  $E_a$  of 77.45 kJ/mol observed we can infer that the adsorption of leuco indigo onto silk is the most likely by a chemisorption process.

**Table 2.3** Activation parameters for the adsorption of indigo onto silk at initial dye concentration 20 mg/L.

Temp. (°C)	$k_2$ (g silk/ mg min)	$E_a$ (kJ/mol)	$R^2$	$\Delta H^\#$ (kJ/mol)	$\Delta S^\#$ (J/mol K)	$\Delta G^\#$ (kJ/mol)	$R^2$
30	0.0189					84.13	
40	0.0577	77.45	0.9935	74.85	-30.63	84.44	0.9930
50	0.1268					84.74	

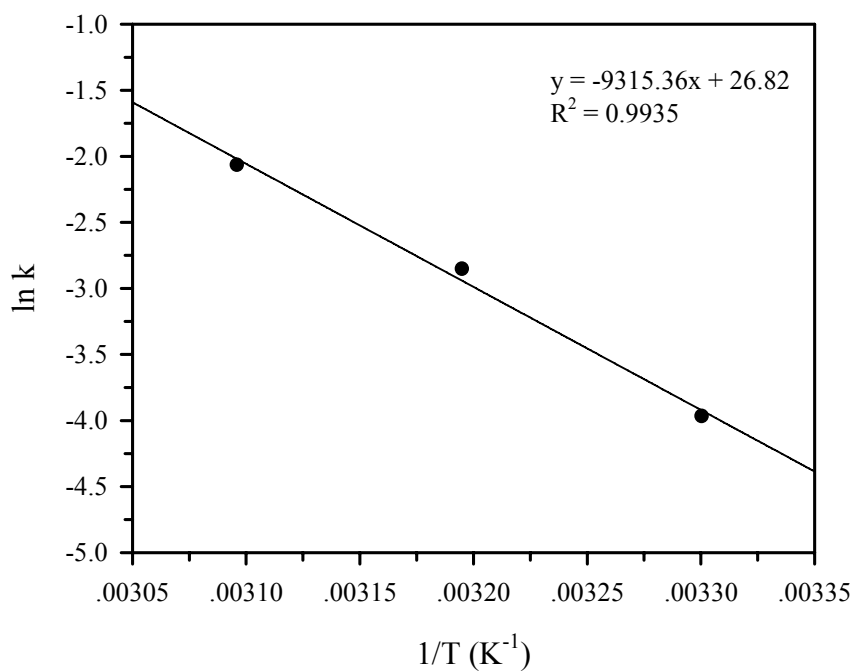


**Figure 2.16** Arrhenius plots for the adsorption of indigo on silk.

From the Eyring equation, the enthalpy ( $\Delta H^\ddagger$ ) and entropy ( $\Delta S^\ddagger$ ) of activation were calculated from the slope and intercept of a plot of  $\ln(k/T)$  versus  $1/T$  (Figure 2.17) as listed in Table 2.3. The value of  $\Delta G^\ddagger$  was calculated at 303, 313 and 323 K by using equation (2.10) and these values are listed in Table 2.3. The negative entropy value ( $\Delta S^\ddagger$ ) observed reflects more aggregation and the interaction between indigo and the silk yarn.



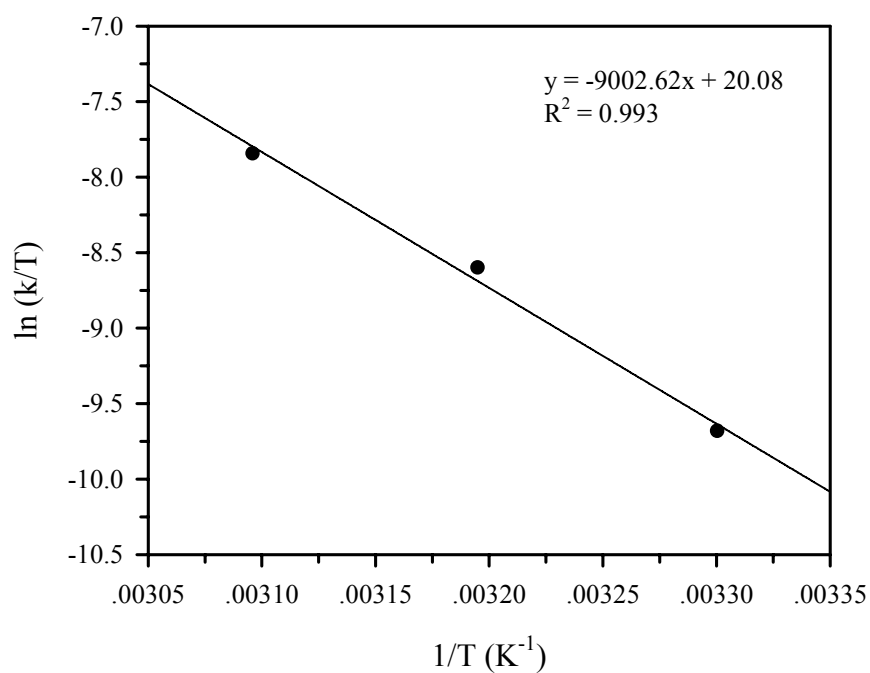


**Figure 2.17** Plot of  $\ln(k/T)$  against  $1/T$  for the adsorption of indigo on silk.

#### 2.4.2.5 Adsorption isotherm for the adsorption of indigo onto silk

The adsorption isotherm of indigo dyeing onto silk under the conditions of an MLR of 1:100 in the initial dye concentration range 20-500 mg/L at 30, 40 and 50°C is shown in Figure 2.18. It was found that the amount of dye adsorbed per unit weight of fibre at equilibrium,  $q_e$ , decreased with increasing temperature, thereby indicating the process is exothermic.

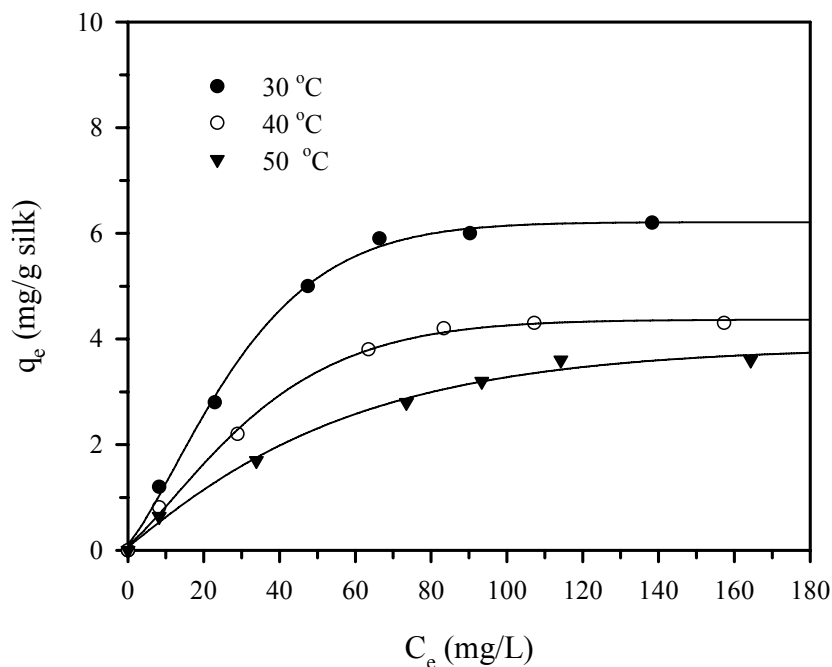


**Figure 2.18** Adsorption isotherms of indigo onto silk at 30, 40 and 50°C.

The Langmuir adsorption model was used to describe the characteristic adsorption based on the assumption that adsorption takes place at specific homogeneous sites on the surface. It is then assumed that once a dye molecule occupies a site, no further adsorption can take place at that site. When  $1/q_e$  is plotted against  $1/C_e$  according to the Eq. (2.13), the Langmuir adsorption model fitted the experimental data very well with high correlation coefficients ( $R^2 > 0.99$ ) (Figure 2.19). It was indicated that Langmuir isotherm expression in line with a monolayer coverage of indigo onto silk. The values of the maximum amount of the dye per unit weight of fibre to form complete monolayer coverage on the surface (monolayer capacities,  $Q$ ) and Langmuir constants ( $b$ ) were calculated from the slopes and intercepts of different straight lines respectively at different temperatures. The

calculated results are reported in Table 2.4. It can be seen from Table 2.4 that  $Q$  values decreased with increasing temperature. Similar observations were reported for the adsorption of lac dye on silk (Kongkachuichay *et al.*, 2002; Chairat *et al.*, 2005), and in the dyeing of silk with alum-morin dye (Septum *et al.*, 2009) and with indigo carmine (Jiwalak *et al.*, 2010). The  $b$  values indicated that the silk yarn has an affinity for indigo dye.

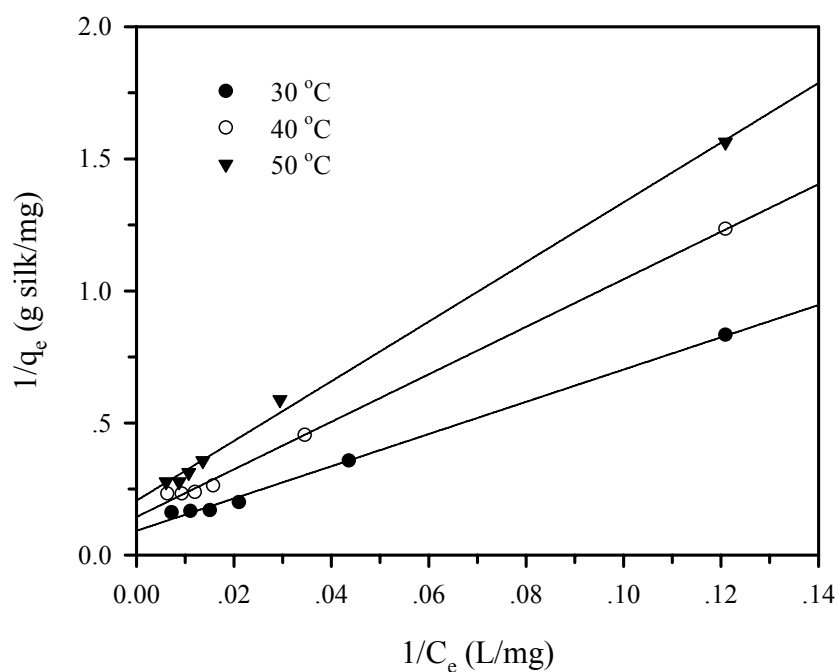


**Figure 2.19** Langmuir adsorption isotherm of the adsorption of indigo onto silk at 30, 40 and 50°C.

**Table 2.4** Langmuir and Freundlich isotherm constants for the adsorption of indigo onto silk at different temperatures.

Temp. (°C)	Langmuir			Freundlich		
	Q (mg/g silk)	b (mL/mg)	R <sup>2</sup>	Q <sub>f</sub> (mg/g silk)	n	R <sup>2</sup>
30	10.88	15.06	0.9962	0.38	1.62	0.9287
40	6.93	16.05	0.9978	0.26	1.66	0.9390
50	4.86	18.23	0.9963	0.19	1.63	0.9795

The Freundlich isotherm equation (Eq. (2.15)) was also applied to the results of the adsorption of indigo onto silk. The values of  $Q_f$  and  $1/n$  can be determined from the linear plot of  $\ln q_e$  versus  $\ln C_e$  (Figure 2.20). The magnitude of the exponent  $1/n$  gives an indication of the favourability of adsorption. Values of  $n > 1$  (Table 2.4) obtained represent favourable adsorption conditions (Chiou and Li, 2002; Chairat *et al.*, 2005). The  $Q_f$  values (Table 2.4) decreased with increasing temperature which again supported an exothermic process.

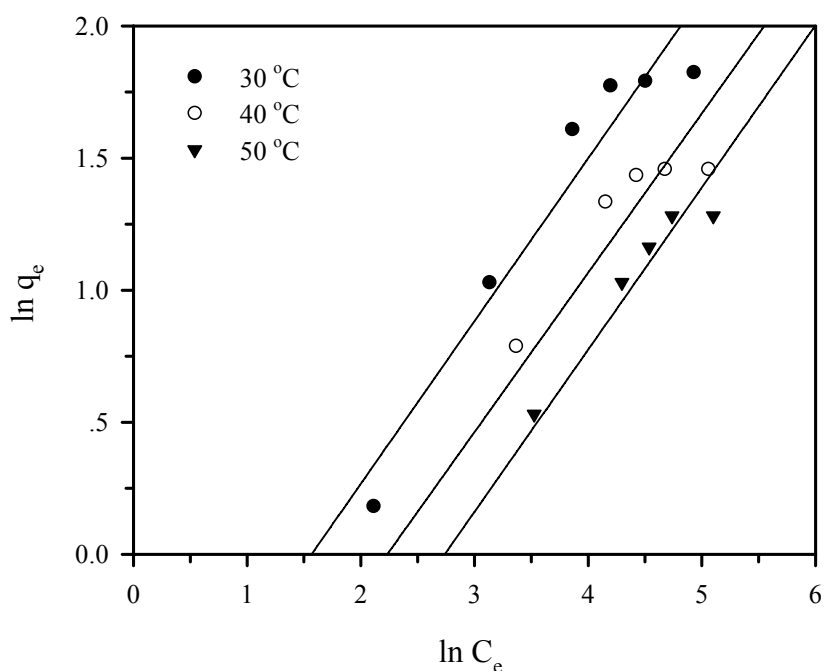


**Figure 2.20** Freundlich adsorption isotherm of the adsorption of indigo onto silk at 30, 40 and 50°C.

#### 2.4.2.6 Thermodynamic parameters for the adsorption of indigo on silk

In order to support the exothermic behaviour of the adsorption of indigo onto silk, the thermodynamic parameters,  $\Delta G^\circ$ ,  $\Delta H^\circ$  and  $\Delta S^\circ$  of indigo adsorption after reaching equilibrium were calculated by using the equations (2.16) to (2.19). Enthalpy change ( $\Delta H^\circ$ ) and entropy change ( $\Delta S^\circ$ ) of the adsorption are calculated from the slope and intercept of the van't Hoff plots of  $\ln K_c$  versus  $1/T$  (Figure 2.21). The results are listed in Table 2.5. The negative values of  $\Delta G^\circ$  indicate that the adsorption of indigo on silk is spontaneous. The negative value of  $\Delta H^\circ$  confirms that the adsorption process is an exothermic one. Furthermore, the entropy

change ( $\Delta S^\circ$ ) in dyeing represents the entropy difference of the dye molecules within the fibre (Kim, Son, and Lim, 2005). The negative value of  $\Delta S^\circ$  indicated that adsorbed indigo dye become more restrained within the silk fibre molecules than in the dyeing solution (as the leuco indigo).

**Table 2.5** Thermodynamic parameters for the adsorption of indigo onto silk at different temperatures.

Temp. (°C)	$K_C$	$\Delta G^\circ$ (kJ/mol)	$\Delta H^\circ$ (kJ/mol)	$\Delta S^\circ$ (J/mol K)	$R^2$
30	2.62	-2.38			
40	1.95	-1.72	-22.40	-66.08	0.9961
50	1.53	-1.06			

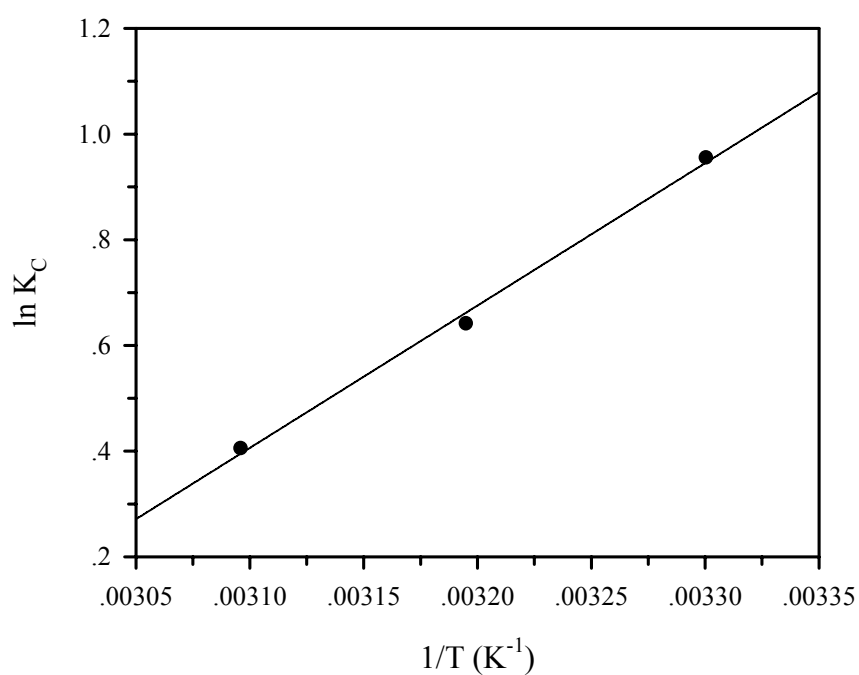


**Figure 2.21** The van't Hoff plots of  $\ln K_C$  versus  $1/T$ .

### **2.4.3 Adsorption studies of plant extracted indigo onto silk by the conventional vat-dyeing method**

The significant presence of indigo in the extract from the plant *Indigofera tinctoria* was confirmed by HPLC analysis (Section 2.4.1) and the amount of indigo in the plant extracted indigo is shown in Table 2.1. In order to investigate the adsorption of plant extracted indigo dye on silk, the experimental parameters including initial dye concentration, contact time, and temperature were determined to find the most suitable conditions for the dyeing by the conventional vat-dyeing method. The mechanism of adsorption of plant extracted indigo dyeing onto silk was investigated in the context of the pseudo first order and pseudo second order kinetic models. In addition, activation parameters and thermodynamics parameters of adsorption are discussed in this section.

#### **2.4.3.1 Effect of initial dye concentration and contact time on the adsorption of plant extracted indigo onto silk**

The effect of initial dye concentration and contact time on the adsorption of plant extracted indigo onto silk are presented in Figure 2.22. The adsorption capacities at equilibrium,  $q_{e,exp}$ , increases from 1.24-5.41 mg/g silk with an increase in initial dye concentration from 1.1-5.2 g/L (contained ~ 20-100 mg/L indigo) with an MLR of 1:100 at pH 11-12 and 30°C with equilibrium reached after 60 min. The equilibrium time is independent of initial dye concentrations. But in the first 30 min, the initial rate of adsorption was greater for higher initial dye concentrations. This is because the diffusion of dye precursor (leuco indigo) molecules through the solution to the surface of the fibre is affected by this

concentration (at a constant agitation speed). An increase of the dye concentration accelerates the diffusion of dyes from the dye solution onto the silk fibre due to the increase in the driving force of the concentration gradient.

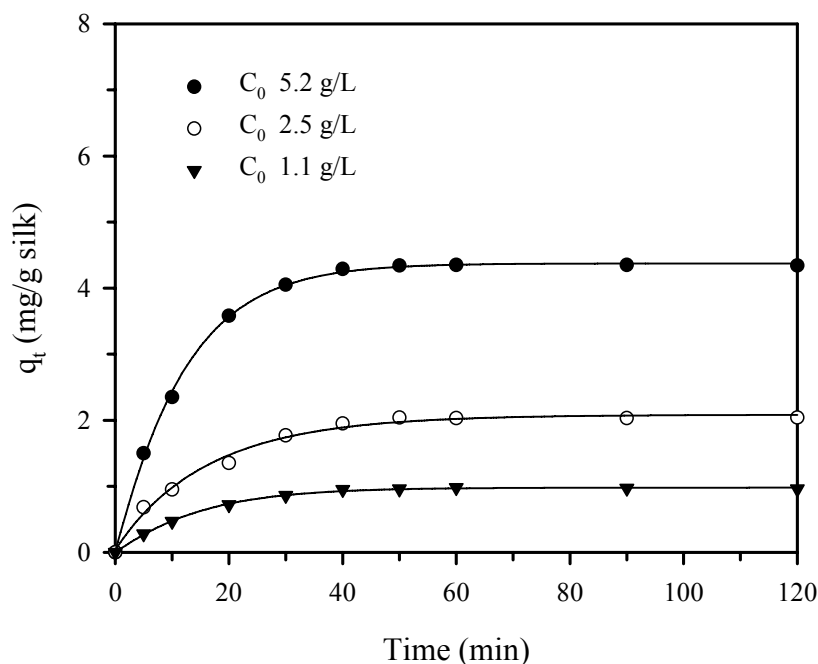


**Figure 2.22** Effect of initial dye concentration on the adsorption of plant extracted indigo onto silk (under dyeing condition MLR = 1:100, pH = 11-12, 30°C).

The characteristic parameters of the pseudo first order and pseudo second order models and correlation coefficients are tabulated in Table 2.6. Plots of the pseudo first order and pseudo second order equation at different initial dye concentration on the adsorption of plant extracted indigo onto silk are presented in Figures 2.23 and 2.24, respectively. The correlation coefficients ( $R^2$ ) for the pseudo-second order model for all concentrations are higher than for the pseudo first order model and the calculated equilibrium adsorption capacities fit well with the



experimental data in the former model. These suggest that the pseudo second order adsorption mechanism is predominant and overall the results for plant extracted indigo adsorbed onto silk were similar to the results for indigo itself as described in section 2.4.2.1. The results in Table 2.6 also show  $k_2$ ,  $h_i$  and  $q_e$  as a function of initial dye concentration. For the pseudo second order model, the rate constant decreases with increasing of initial dye concentration, while the initial adsorption rate,  $h_i$ , increases with the initial dye concentration. An increase in initial dye concentration results in a significant increase in  $q_{e,cal}$ .

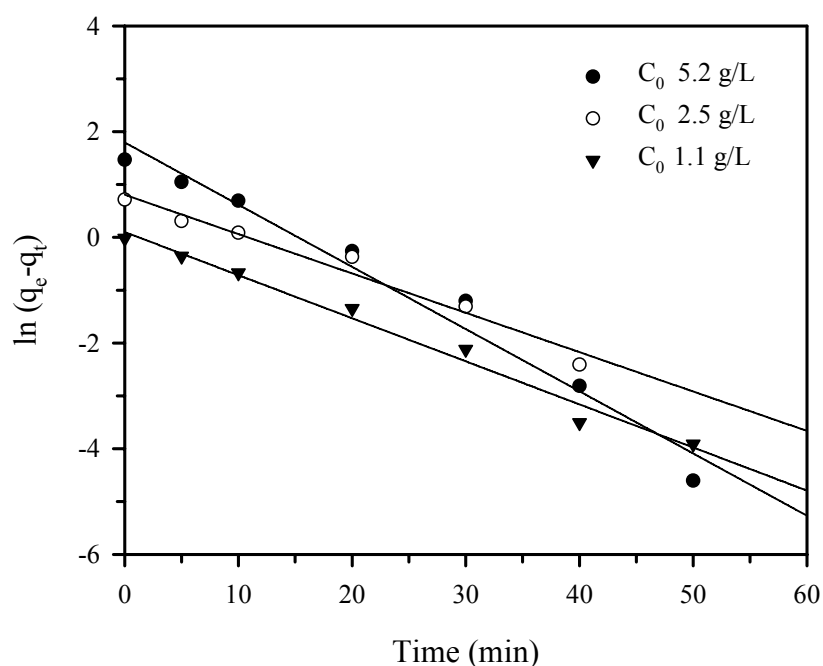


**Figure 2.23** Application of the pseudo first order equation at different initial dye concentration on the adsorption of plant extracted indigo onto silk.

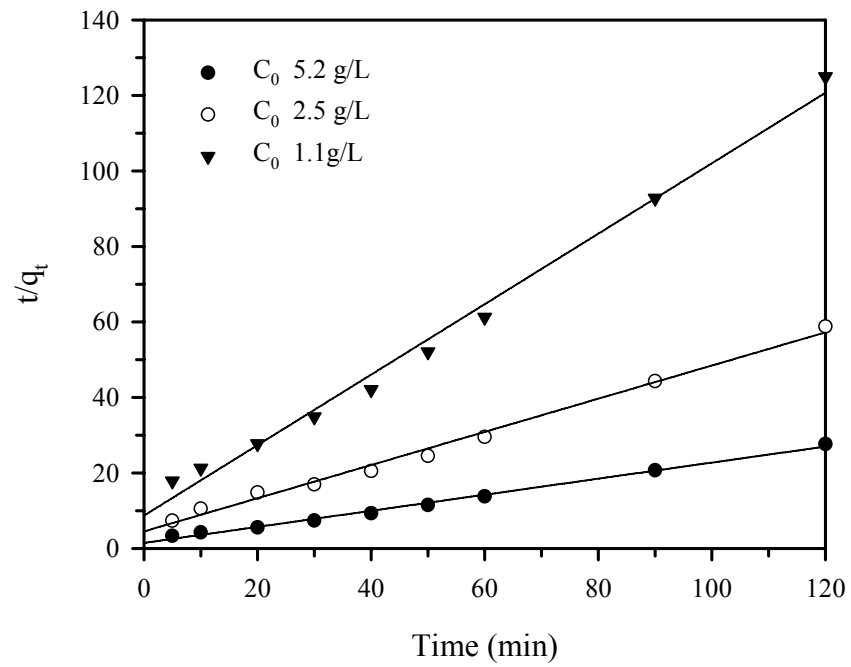


**Figure 2.24** Application of the pseudo second order equation at different initial dye concentration on the adsorption of plant extracted indigo onto silk.

**Table 2.6** Comparison of the pseudo first- and pseudo second-order adsorption rate constants and the calculated and experimental  $q_e$  values for different initial dye concentrations and temperature for the adsorption of plant extracted indigo onto silk.

Parameter	$q_{e,exp}$ (mg/g silk)	Pseudo first order model			Pseudo second order model			
		$k_1$ (min <sup>-1</sup> )	$q_{e,cal}$ (mg/g silk)	$R^2$	$k_2$ (g silk/mg min)	$q_{e,cal}$ (mg/g silk)	$h_i$ (mg/g silk min)	$R^2$
<i>Initial dye concentration: <math>C_0</math> (g/L): MLR 1:100, temp. 30 °C, contact time 60 min</i>								
1.1	1.24	0.0815	1.11	0.9737	0.1002	1.07	0.1150	0.9910
2.5	2.43	0.0745	2.24	0.9717	0.0428	2.27	0.2215	0.9926
5.2	5.41	0.1177	6.03	0.9737	0.0311	4.70	0.6869	0.9949
<i>Temperature: <math>C_0</math> 1 g/L, MLR 1:100, contact time 60 min</i>								
30	1.24	0.0427	0.94	0.9933	0.0393	1.19	0.0558	0.9902
40	0.69	0.0456	0.69	0.9846	0.0790	0.79	0.0492	0.9991
50	0.51	0.0385	0.41	0.9667	0.1660	0.55	0.0508	0.9966

#### **2.4.3.2 Effect of temperature on the adsorption of plant extracted indigo onto silk**

The effect of temperature on adsorption of plant extracted indigo onto silk has been investigated at an initial dye concentration of 1 g/L (contained ~ 20 mg/L indigo) at pH 11-12 and an MLR of 1:100. A study of the temperature dependence of adsorptions gives valuable information about the enthalpy change during adsorption. The effect of temperature on the adsorption rate was studied by carrying out a series of experiments at 30, 40 and 50°C. Before and after the equilibrium time, the adsorption capacities show a different trend at different temperatures (Figure 2.25). First 10 min, an increase in the temperature lead to an increase in dye adsorption rate which indicates a kinetically controlled process. After 10 min, the adsorption decreased with increasing the temperature indicating that the adsorption of plant extracted indigo onto silk is controlled by an exothermic process. A similar temperature effect on adsorption trend has also been shown in the case of adsorption of indigo onto silk as described in section 2.4.2.3. The results of rate constant studies for different temperatures calculated by the pseudo first order and pseudo second order models are listed in Table 2.6. The correlation coefficient,  $R^2$ , for the pseudo second order adsorption model (Figure 2.27) has a higher value suggesting the dye adsorption process is predominantly by a pseudo second order adsorption mechanism.

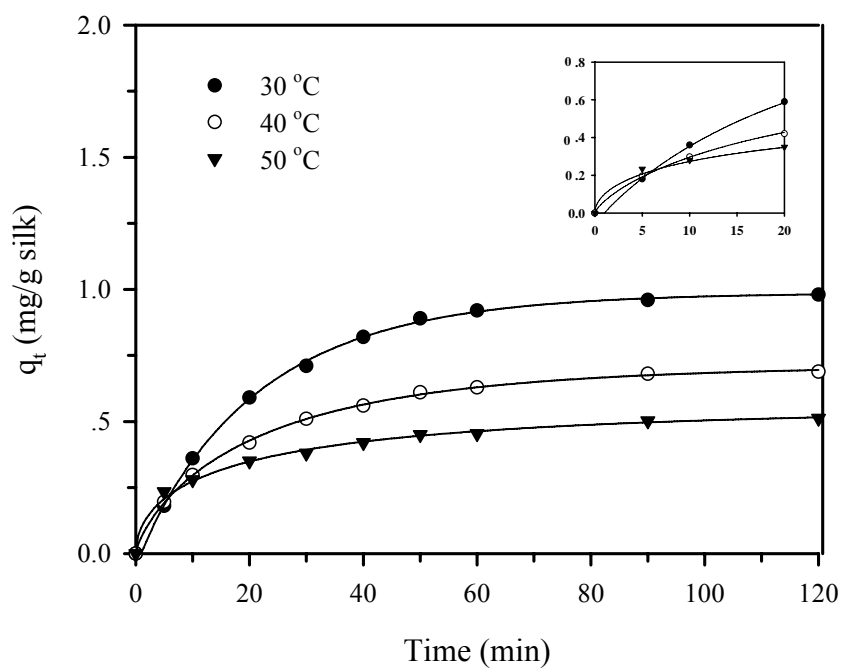


**Figure 2.25** Effect of temperature on the adsorption of plant extracted indigo onto silk (under dyeing condition  $C_0 = 1.1$  g/L, pH = 11-12, MLR = 1:100).

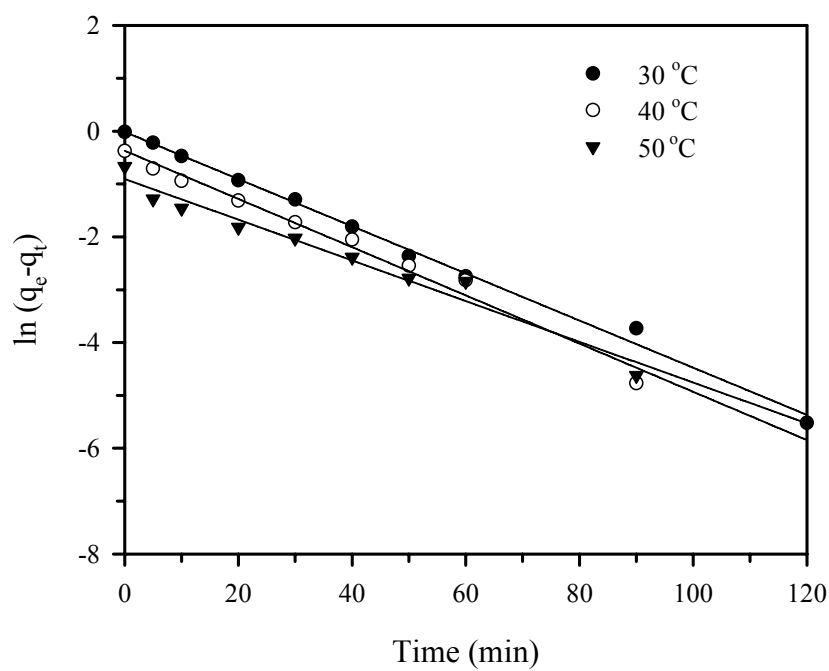


**Figure 2.26** Application of the pseudo first order equation at different temperature on the adsorption of plant extracted indigo onto silk.

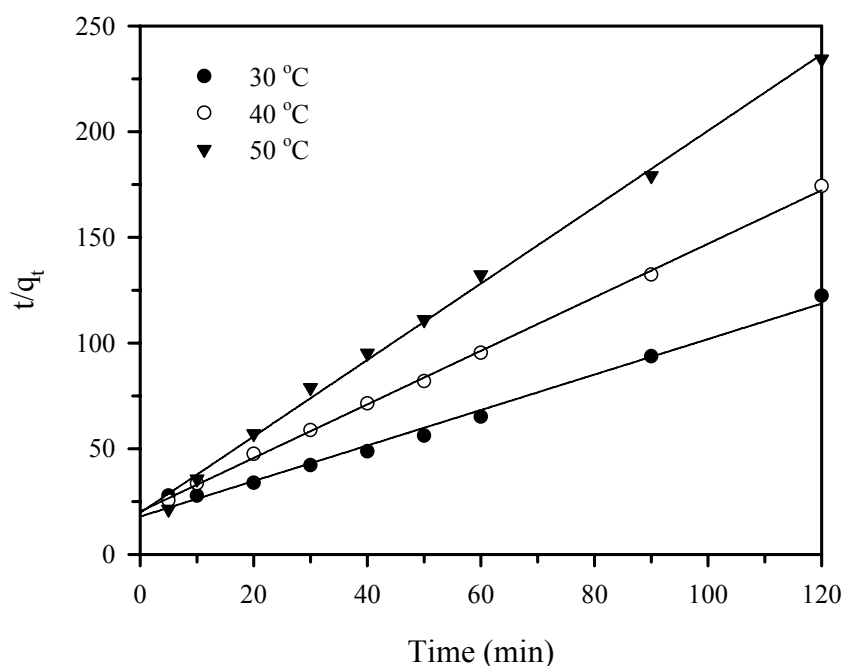


**Figure 2.27** Application of the pseudo second order equation at different temperature on the adsorption of plant extracted indigo onto silk.

#### 2.4.3.3 Activation parameters for the adsorption of plant extracted indigo onto silk

The activation energy of the diffusion describes the dependence of the diffusion coefficient on the dyeing temperature and also represents the energy barrier that the dye molecule should overcome to diffuse into the fibre molecules (Kim *et al.*, 2005). The rate constants  $k_2$  for pseudo second order model at different temperatures listed in Table 2.6 were then applied to estimate the activation energy of the adsorption of plant extracted indigo onto silk by the Arrhenius equation. The slope of the plot of  $\ln k_2$  versus  $1/T$  (Figure 2.28) was used to evaluate  $E_a$  as listed in Table 2.7 For the  $E_a$  of 58.54 kJ/mol observed we can infer that the adsorption of plant extracted

indigo onto silk is the most likely by a chemisorption process consistent with the result of the adsorption indigo onto silk as described in section 2.4.2.4.

**Table 2.7** Activation parameters for the adsorption of plant extracted indigo onto silk at initial dye concentration 1.1 g/L.

Temp. (°C)	$k_2$ (g silk/ mg min)	$E_a$ (kJ/mol)	$R^2$	$\Delta H^\#$ (kJ/mol)	$\Delta S^\#$ (J/mol K)	$\Delta G^\#$ (kJ/mol)	$R^2$
30	0.0393					82.43	
40	0.0790	58.54	0.9987	55.94	-87.45	83.31	0.9986
50	0.1660					84.18	

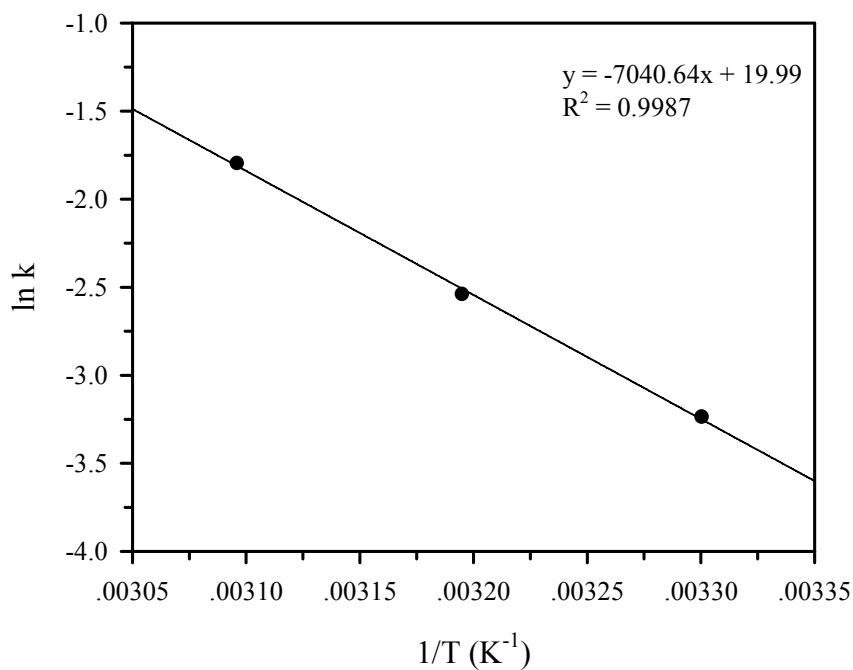


**Figure 2.28** Arrhenius plots for the adsorption of plant extracted indigo on silk.

From the Eyring equation, the enthalpy ( $\Delta H^\ddagger$ ) and entropy ( $\Delta S^\ddagger$ ) of activation were calculated from the slope and intercept of a plot of  $\ln(k/T)$  versus  $1/T$  (Figure 2.29) as listed in Table 2.7. The value of  $\Delta G^\ddagger$  was calculated at 303, 313 and 323 K by using equation (2.10) and these values are listed in Table 2.7. The negative entropy value ( $\Delta S^\ddagger$ ) reflects more aggregation and the interaction between plant extracted indigo and the silk yarn.

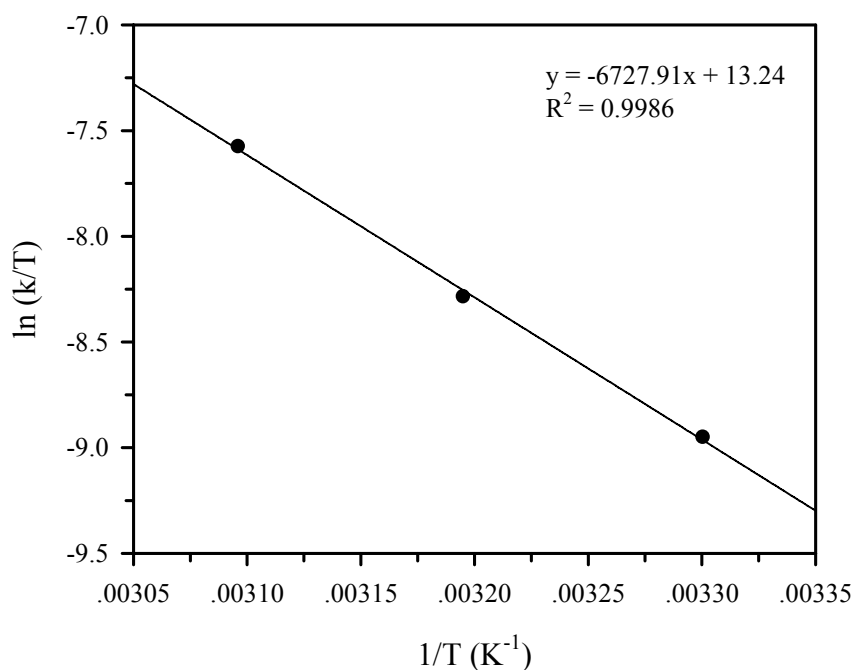


**Figure 2.29** Plot of  $\ln(k/T)$  against  $1/T$  for the adsorption of plant extracted indigo on silk.



#### **2.4.3.4 Adsorption isotherm for the adsorption of plant extracted indigo onto silk**

The adsorption isotherm of plant extracted indigo dyeing onto silk at 30°C is shown in Figure 2.30. It was found that the amount of dye adsorbed per unit weight of fibre at equilibrium,  $q_e$  rapidly increased with the initial dye concentration 1.1-7.5 g/L (contained ~ 20-150 mg/L indigo) and then reached equilibrium.

The adsorption equilibrium data were analyzed using the Langmuir (Figure 2.31) and Freundlich (Figure 2.32) expressions. The adsorption capacities and adsorption constants of plant extracted indigo onto silk are shown in Table 2.8. The experimental data were found to fit well to the Langmuir isotherm, with the former being slightly better as indicated by the higher  $R^2$  values compared with that from the Freundlich expression. The applicability of the Langmuir isotherm suggests monolayer coverage of the dye on the surface of the silk.

The Freundlich equation describes heterogeneous systems and reversible adsorption; and is not limited to the formation of a complete monolayer. It can be seen from Table 2.8 that the correlation coefficients for the Freundlich isotherms are less than those obtained from the Langmuir expression. Thus, the Freundlich isotherm cannot be totally rejected in these equilibrium studies. Also the values of  $n$  more than 1 (Table 2.8) indicate favourable adsorption.

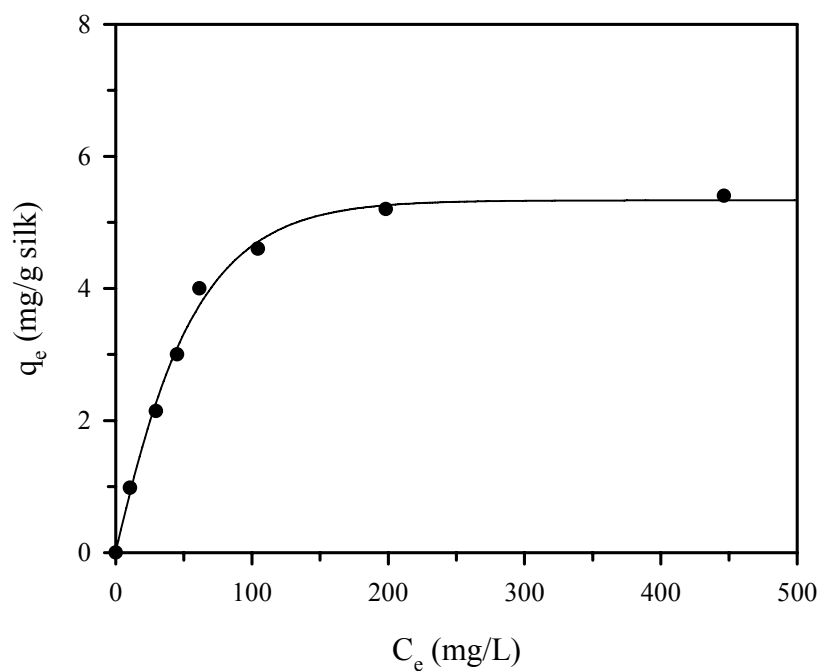


**Figure 2.30** Adsorption isotherms of plant extracted indigo onto silk at 30°C.

**Table 2.8** Langmuir and Freundlich isotherm constants for the adsorption of plant extracted indigo onto silk at 30°C.

Temp. (°C)	Langmuir			Freundlich		
	Q (mg/g silk)	b (mL/mg)	R <sup>2</sup>	Q <sub>f</sub> (mg/g silk)	n	R <sup>2</sup>
30	7.27	14.9	0.9951	0.46	2.19	0.8516

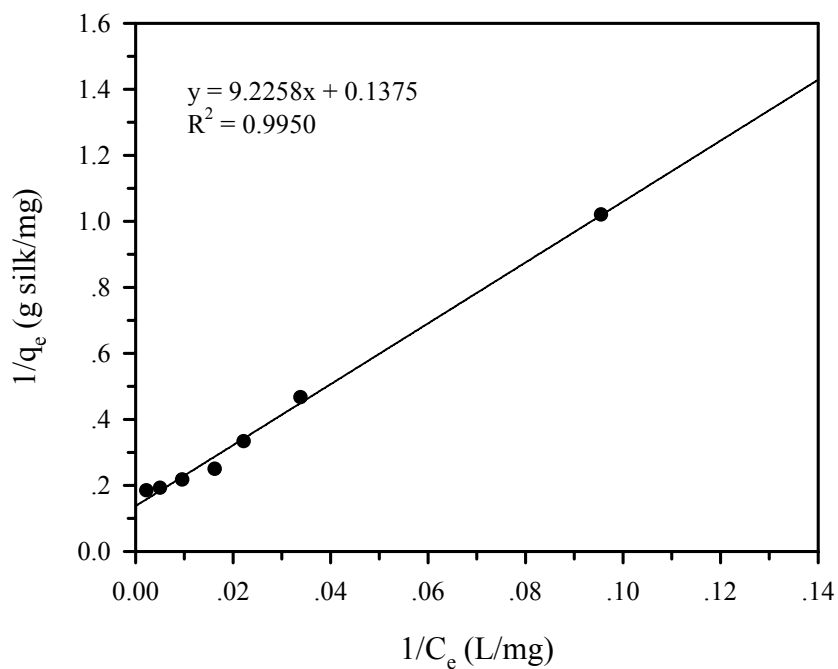


**Figure 2.31** Langmuir adsorption isotherm of the adsorption of plant extracted indigo onto silk at 30°C.

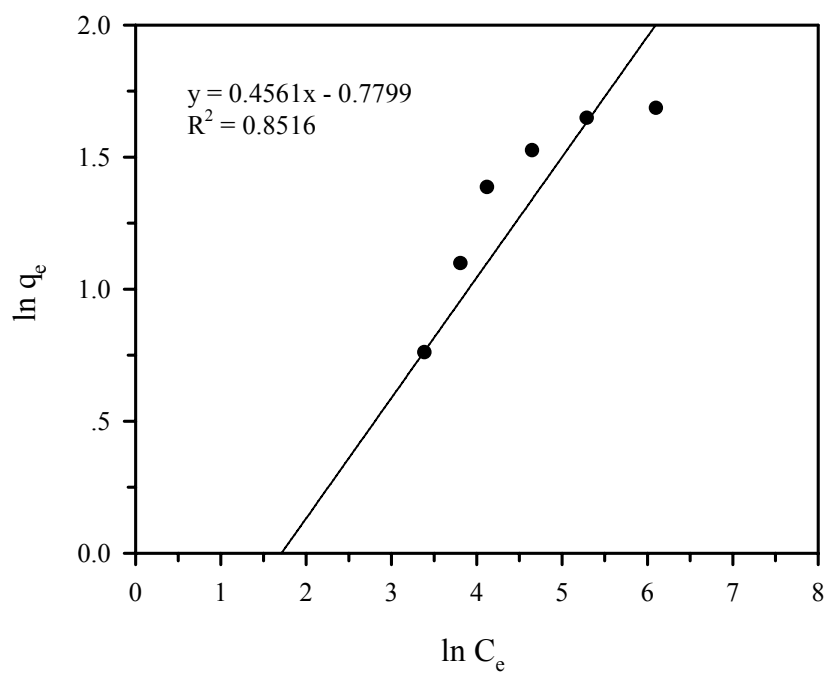


**Figure 2.32** Freundlich adsorption isotherm of the adsorption of plant extracted indigo onto silk at 30°C.

#### **2.4.3.5 Thermodynamic parameters for the adsorption of plant extracted indigo on silk**

In order to provide supporting evidence for the exothermic behaviour of plant extracted indigo adsorption onto silk, after reaching equilibrium, the thermodynamic parameters  $\Delta G^\circ$ ,  $\Delta H^\circ$  and  $\Delta S^\circ$  for this adsorption were calculated by using the equations (2.16)-(2.19). Enthalpy change ( $\Delta H^\circ$ ) and entropy change ( $\Delta S^\circ$ ) of the adsorption are calculated from the slope and intercept of the van't Hoff plots of  $\ln K_c$  versus  $1/T$  (Figure 2.33). The results are listed in Table 2.9. The negative value of  $\Delta H^\circ$  again is consistent with the adsorption of plant extracted indigo onto silk being an exothermic process. The negative values of  $\Delta G^\circ$  indicate that the adsorption process is spontaneous. The entropy change ( $\Delta S^\circ$ ) on dyeing represents the entropy difference of the dye molecules within the fibre (Kim *et al.*, 2005). The negative value of  $\Delta S^\circ$  indicates that adsorbed indigo dye becomes more restrained within the silk fibre molecules than in the dyeing solution (as the leuco form). The thermodynamic parameters for the adsorption of plant extracted indigo on silk were similar to the corresponding values for indigo itself (Table 2.5).

**Table 2.9** Thermodynamic parameters for the adsorption of plant extracted indigo onto silk at different temperatures.

Temp. (°C)	$K_C$	$\Delta G^\circ$ (kJ/mol)	$\Delta H^\circ$ (kJ/mol)	$\Delta S^\circ$ (J/mol K)	$R^2$
30	2.13	-1.88			
40	1.63	-1.33	-18.62	-55.23	0.9942
50	1.35	-0.78			

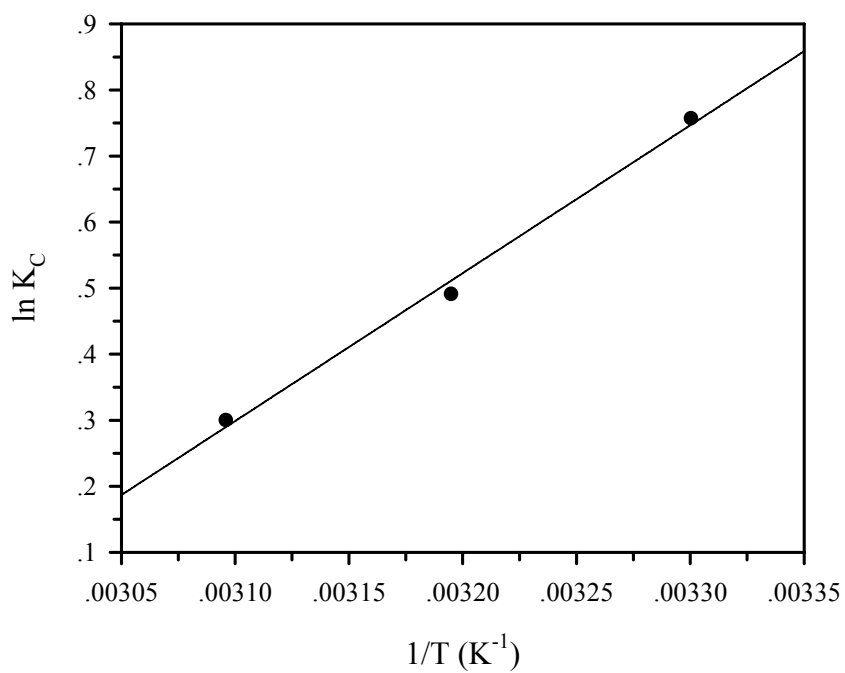


**Figure 2.33** The van't Hoff plots of  $\ln K_C$  versus  $1/T$ .

## 2.5 Conclusion

Detailed kinetic and thermodynamic parameters were determined for the first time for the dyeing of silk using indigo itself and the vat dyeing method. This method involved initial reduction of the indigo with sodium dithionite to give leuco indigo, then immersion of the silk in the aqueous solution of leuco indigo, followed by aerial oxidation to indigo *in situ*. A chemisorption process was indicated for the indigo dyeing of silk. A comparison of kinetic and thermodynamic data for silk dyeing using plant derived indigo extract obtained from *Indigofera tinctoria* was also made with the data from indigo itself and close similarities were seen. This was consistent with the HPLC analytical data which showed indigo as a major component of the extract. It also indicated that other components in the crude indigo extract were not significantly affecting the dyeing kinetics and thermodynamics. The work discussed in this chapter covered adsorption parameters for indigo dyeing onto silk and enabled a better understanding of the indigo dyeing process. The results also provided benchmark data to inform later projected direct dyeing studies with indigo and derivatives.

## 2.6 References

- Ahmad, A. A., Hameed, B. H. and Aziz, N. (2007). Adsorption of direct dye on palm ash: Kinetic and equilibrium modeling. **Journal of Hazardous Materials**. 141(1): 70-76.
- Angelini, L. G., Campeol, E., Tozzi, S., Gilbert, K. G., Cooke, D. T. and John, P. (2003). A new HPLC-ELSD method to quantify indican in *Polygonum tinctorium* L. and to evaluate beta-glucosidase hydrolysis of indican for indigo production. **Biotechnology Progress**. 19: 1792-1797.
- Angelini, L. G., Tozzi, S. and Nassi o Di Nasso, N. (2004). Environmental factors affecting productivity, indican content, and indigo yield in *Polygonum tinctorium* Ait., a subtropical crop grown under temperate conditions. **Journal of Agricultural and Food Chemistry**. 52(25): 7541-7547.
- Aobchey, P. (2007). **Production of Natural Pigments by Callus Cultures of Roots of Marinda Angustifolia Roxb. and Leaves of Indigofera Tinctoria Linn.** Ph.D. Thesis: Chiang Mai University, Thailand.
- Balfour-Paul, J. (1998). **Indigo Plants and the Marking of Their Dye: Indigo.** London: British museum press.
- Balfour-Paul, J. (2006). **Indigo-a Unique Dye with a Colour Story in Indirubin, the Red Shade of Indigo.** Meijer, L., Guyard, N., Skaltsounis, L. A., Eisenbrand, G. Ed. Life in Progress Edition: France, p1.
- Bechtold, T. and Burtscher, E. (2001). Mediator systems based on mixed metal complexes used for reducing dyes. **U.S. Patent 6790241**.
- Bhattacharyya, K. G. and Sarma, A. (2003). Adsorption characteristics of the dye, brilliant green, on neem leaf powder. **Dyes and Pigments**. 57(3): 211-222.

- Božič, M. and Kokol, V. (2008). Ecological alternatives to the reduction and oxidation processes in dyeing with vat and sulphur dyes. **Dyes and Pigments**. 76(2): 299-309.
- Carr, C. M. (1995). **Chemistry of the Textiles Industry**. Glasgow: Blackie Academic & Professional.
- Chairat, M. (2004). **Extraction and Characterization of Lac Dye from Thai Stick Lac and Development of Lac Dyeing on Silk and Cotton**. Ph.D. Thesis, Suranaree University of Technology, Thailand.
- Chairat, M., Rattanaphani, S., Bremner, J. B. and Rattanaphani, V. (2005). An adsorption and kinetic study of lac dyeing on silk. **Dyes and Pigments**. 64(3): 231-241.
- Chavan, R. and Chakraborty, J. (2001). Dyeing of cotton with indigo using iron(II) salt complexes. **Coloration Technology**. 117(2): 88-94.
- Chiou, M. S. and Li, H. Y. (2002). Equilibrium and kinetic modeling of adsorption of reactive dye on cross-linked chitosan beads. **Journal of Hazardous Materials**. B93(2): 233-248
- Chiou, M. S. and Li, H. Y. (2003). Adsorption behavior of reactive dye in aqueous solution on chemical cross-linked chitosan bead. **Chemosphere**. 50: 1095-1105.
- Christie, R. M., Mather, M. M. and Wardman, R. H. (2000). **The Chemistry of Colour Application**. Oxford: Blackwell Science.
- Christie, R. M. (2001). **Colour Chemistry**. UK: Cambridge.
- Cooksey, C. (2007). Indigo: an annotated bibliography. **Biotechnic and Histochemistry**. 82(2): 105-125.



- Dogan, M. and Alkan, M. (2003). Adsorption kinetics of methyl violet onto perlite. **Chemosphere**. 50(4): 517-528.
- Donald, L. P., Gary, M. L. and George, S. K. (1976). **Introduction in Organic Laboratory Techniques: A Contemporary Approach**. U.S.A.: W.B. Saunders.
- Gilbert, K. G., Maule, H. G., Rudolph, B., Lewis, M., Vandenburg, H., Sales, E., Tozzi, S. and Cooke, D. T. (2004). Quantitative analysis of indigo and indigo precursors in leaves of *Isatis spp.* and *Polygonum tinctorium*. **Biotechnology Progress**. 20(4): 1289-1292.
- Ho, Y. S. and McKay, G. (1999). Pseudo-second order model for sorption processes. **Process Biochemistry** 34(5): 451-465.
- Jiwalak, N., Rattanaphani, S., Bremner, J. B. and Rattanaphani, V. (2010). Equilibrium and kinetic modeling of the adsorption of indigo carmine onto silk. **Fibers and Polymers**. 11(4): 572-579.
- Kaplan, D., Adam, W. W., Farmer, B. and Viney, C. (1994). **Silk Polymers: Materials Science and Biotechnology**. Washington: American Chemical Society.
- Kim, T. K., Son, Y. A. and Lim, Y. J. (2005). Thermodynamic parameters of disperse dyeing on several polyester fibers having different molecular structure. **Dyes and Pigments**. 67(3): 229-234.
- Kongkachuichay, P., Shitangkoon, A. and Chinwongamorn, N. (2002). Thermodynamics of adsorption of laccaic acid on silk. **Dyes and Pigments**. 53: 179-185.
- Lagergren, S. (1898). Zur theorie der sogenannten adsorption gelöster stoffe. **K Sven Vetenskapsakad Handdl**. 24(1): 1-39.

- Laidler, K. J., Meiser, J. H. and Sanctuary, B. C. (2003). **Physical Chemistry**. Boston: Houghton Mifflin.
- Lakshmi, U. R., Srivastava, V. C., Mall, I. D. and Lataye, D. H. (2009). Rice husk ash as an effective adsorbent: Evaluation of adsorptive characteristics for indigo Carmine dye. **Journal of Environmental Management**. 90(2): 710-720.
- Lemmens, R. H. M. J. and Wulijarni, S. N. (1992). **Plant Resources of South-East Asia No.3, Dye and Tannin-Producing Plants**. Bogor: Indonesia.
- Maugard, T., Enaud, E., Choisy, P. and Legoy, M. D. (2001). Identification of an indigo precursor from leaves of *Isatis tinctoria* (Woad). **Phytochemistry**. 58(6): 897-904.
- Moeyes, M. (1993). **Natural Dyeing in Thailand**. Bangkok: White Lotus.
- Nollet, H., Roels, M., Lutgen, P., Van der Meeren, P. and Verstraete, W. (2003). Removal of PCBs from wastewater using fly ash. **Chemosphere**. 53(6): 655-665.
- Perkins, W. S. (1996). **Textile Coloration and Finishing**. North Carolina: Carolina Academic Press.
- Polenov, Y. V., Pushkina, V. A., Budanov, V. V. and Khilinskaya, O. S. (2001). Kinetics of heterogeneous reduction of red-Brown Zh vat dye with rongalite in the absence of diffusion hindrance. **Russian Journal of Applied Chemistry**. 74: 1301-1304.
- Raisanen, R., Nousiainen, P. and Hynninen, P. H. (2001). Emodin and dermocybin natural anthraquinones as mordant dyes for wool and polyamide. **Textile Research Journal**. 71: 1016-1022.

- Rattanaphani, S., Chairat, M., Bremner, J. B. and Rattanaphani, V. (2007). An adsorption and thermodynamic study of lac dyeing on cotton pretreated with chitosan. **Dyes and Pigments**. 72(1): 88-96.
- Ricketts, R. (2006). ***Polygonum tinctorium: Contemporary Indigo Farming and Processing in Japan In Indirubin, the Red Shade of Indigo***. Meijer, L., Guyard, N., Skaltsounis, L. A., Eisenbrand, G. Ed. Life in Progress Edition: France, p7.
- Roessler, A., Crettenand, D., Dossenbach, O., Marte, W. and Rys, P. (2002). Direct electrochemical reduction of indigo. **Electrochimica Acta**. 47(12): 1989-1995.
- Roessler, A., Dossenbach, O., Marte, W. and Rys, P. (2002). Electrocatalytic hydrogenation of vat dyes. **Dyes and Pigments**. 54(2): 141-146.
- Roessler, A. and Crettenand, D. (2004). Direct electrochemical reduction of vat dyes in a fixed bed of graphite granules. **Dyes and Pigments**. 63(1): 29-37.
- Septhum, C., Rattanaphani, S., Bremner, J. B. and Rattanaphani, V. (2009). An adsorption study of alum-morin dyeing onto silk yarn. **Fibers and Polymers**. 10(4): 481-487.
- Son, Y. A., Lim, H. T., Hong, J. P. and Kim, T. K. (2005). Indigo adsorption properties to polyester fibers of different levels of fineness. **Dyes and Pigments**. 65(2): 137-143.
- Steingruber, E. (2004). **Indigo and Indigo Colourants: Ullmann's Encyclopedia of Industrial Chemistry**. New York: Wiley-VCH.

- Tsatsaroni, E., Liakopoulou-Kyriakides, M. and Elefthriadis, I. (1998). Comparative study of dyeing properties of two yellow natural pigments-effect of enzymes and proteins. **Dyes and Pigments**. 37: 307-315.
- Vandenabeele, P. and Moens, L. (2003) Micro-Raman spectroscopy of natural and synthetic indigo samples. **Analyst**. 128: 187-193.
- Vuorema, A., John, P., Keskitalo, M., Kulandainathan, M. A. and Marken, F. (2008). Electrochemical and sonoelectrochemical monitoring of indigo reduction by glucose. **Dyes and Pigments**. 76(2): 542-549.
- Wu, F. C., Tseng, R. L. and Juang, R. S. (2001). Kinetic modeling of liquid-phase adsorption of reactive dyes and metal ions on chitosan. **Water Research**. 35(3): 613-618.
- Zanoni, M. V. B., Sousa, W. R., de Lima, J. P., Carneiro, P. A. and Fogg, A. G. (2006). Application of voltammetric technique to the analysis of indanthrene dye in alkaline solution. **Dyes and Pigments**. 68(1): 19-25.
- Zollinger, H. (2003). **Colour Chemistry**. Weinheim: Wiley-VCH.

# **CHAPTER III**

## **SILK DYEING WITH WATER SOLUBLE**

### **INDIGO DERIVATIVES**

#### **3.1 Abstract**

Detailed kinetic and thermodynamic parameters have been obtained for the first time with respect to the direct dyeing of silk using the commercially available, water soluble blue dye, indigo carmine. The adsorption process with this indigo-derived dye was an exothermic chemisorption one following pseudo second order kinetics. Another new water soluble blue-green dye was prepared in this work from indigo, which, in contrast to indigo carmine, involved the introduction of polar substituents on nitrogen in the indigo molecule. The particular compound prepared incorporated a carboxylic acid and ester group in separate substituents. In a trial experiment, this compound was shown to dye silk under acidic conditions.

### 3.2 Introduction

Indigo (**1**) has long been an important compound in the dye industry. As well known, indigo dyes belong to the group of vat dyes. They are almost insoluble in organic solvents and in water (Voss, 2006). In the dyeing process (vat dyeing), the water insoluble blue indigo dye is first reduced to a water soluble leuco indigo form to which the fibre is exposed, and then indigo is regenerated on the fibre by oxidation (Donald, Gary, and George, 1976). Leuco indigo is a water soluble form of indigo. Indigo blue is converted to the colourless, soluble, leuco indigo (Figure 2.2) by chemical reduction with a strong reducing agent such as sodium dithionite (Christie, 2001; Polenov, Pushkina, Budanov, and Khilinskaya, 2001; Roessler and Crettenand, 2004; Zanoni, Sousa, Lima, Carneiro, and Fogg, 2006) or thiourea (Son, Lim, Hong, and Kim, 2005) in alkaline medium.

More water soluble derivatives of indigo, for instance indigo carmine, can also be used as direct blue dyes. Indigo carmine (Figure 3.1; IUPAC name: disodium (2*E*)-3-oxo-2-(3-oxo-5-sulfonato-1*H*-indol-2-ylidene)-1*H*-indole-5-sulfonate) (dos Anjos, Vieira, and Cestari, 2002; Mittal, Mittal, and Kurup, 2006; Ramya, Anusha, and Kalavathy, 2008) is a blue, water soluble indigo disulfonate, in which the sulfonate groups substitute each aromatic ring. This compound has major industrial applications as a textile colouring agent (Gemeay, Mansour, El-Sharkawy, and Zaki, 2003; Lakshmi, Srivastava, Mall, and Lataye, 2009). It has also been employed as an additive in pharmaceutical tablets and capsules and as a colouring agent in confectionery items, food items, and in cosmetics industries. It also finds use as a diagnostic aid (e.g. in kidney function tests), as a redox indicator in analytical

chemistry, and as a microscopic stain in biology (Gemeay *et al.*, 2003; Mittal *et al.*, 2006; Hurlstone, George, and Brown, 2007; Lakshmi *et al.*, 2009).

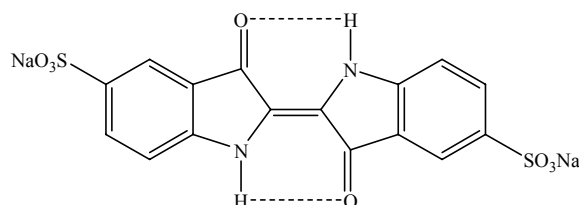


**Figure 3.1** Chemical structure of indigo carmine.

Indigo carmine is an acidic dye (Lu, Zhang, Tang, Wei, and Liu, 2005; Nakamura, Kawasaki, Tanada, Tamura, and Shimizu, 2005) and it has thus been used to dye the protein fibres, wool and silk (Donald *et al.*, 1976), including the use of alum as a mordant in the latter case (Lacasse and Baumann, 2004). Komboonchoo and Bechtold (2010) have used indigo carmine as a model for a blue natural colourant for wool and hair dyeing in a one-bath, direct procedure. The dyeing and adsorption characteristics on wool were determined on the basis of spectrophotometry and colour measurement. They found that dye adsorption and colour strength of indigo carmine dyeing on wool depends on the dyeing temperature and pH of the dye bath. Higher dye sorption and colour strength were observed at increased dyeing temperature and lower pH in the dye bath, with highest dye adsorption and colour strength occurring at dyeing bath pH 3. At pH 3 and 4, the sorption isotherms of indigo carmine can be classified as Langmuir-type isotherms. Experimental adsorption isotherms at pH 5, 6 and 7 follow the Freundlich-type behaviour. The adsorption of indigo carmine on wool proceeds as a spontaneous process. At 80°C and pH 3 the standard affinity ( $\Delta\mu^\circ$ ) as the difference between the chemical potential of the dye in its standard state on the

fibre and the corresponding chemical potential in its standard state in the dye bath. (Aspland, 1997)) was determined as  $-25.72 \text{ kJ mol}^{-1}$ . At pH 3 the heat of dyeing ( $\Delta H$ ) and entropy of dyeing ( $\Delta S$ ) were calculated as  $40.22 \text{ kJ mol}^{-1}$  and  $0.19 \text{ kJ mol}^{-1} \text{ K}^{-1}$ , respectively. However, little information is available in the literature concerning the dyeing aspects, kinetic studies, adsorption isotherms and thermodynamics of the adsorption of indigo carmine on protein fibres, particularly in relation to dye removal from textile processing effluents (dos Anjos *et al.*, 2002; Prado, Miranda, and Jacintho, 2003; Mittal *et al.*, 2006). In this context, the adsorption and thermochemical data on the interaction of the dye indigo carmine with chitosan in aqueous medium has been reported (dos Anjos *et al.*, 2002). The Gibbs energy demonstrated that the process is favourable for the interaction cited. Both Langmuir and Freundlich adsorption models seem to suggest that the interaction of indigo carmine dye with chitosan occurs on a heterogeneous surface, forming a dye monolayer. The adsorption capacity is mainly due to the protonated amino groups of chitosan, since the hydroxyl groups did not contribute to this kind of adsorption, being strongly solvated in aqueous solution. Alexandre, Jocilene, Wlaine, and Silvia (2004) have also studied the adsorption of indigo carmine dye onto chitin and chitosan from aqueous solutions in a batch system. The adsorption capacity of these materials to adsorb indigo carmine dye from aqueous solution was followed through a modified Langmuir equation. The thermodynamic data showed the dye/surface interactions are thermodynamically favourable for chitosan and are non-spontaneous for chitin. A study of the adsorption of indigo carmine on other absorbents has been reported by Alok, Jyoti, and Lisha (2006). They studied the thermodynamics and kinetics of adsorption of indigo carmine on bottom ash (a power plant waste) and de-oiled soya.



The batch adsorption process was found to be dependent upon the pH of the solution, particle size of the adsorbents, amount of adsorbent, concentration of solution, contact time and temperature for both the adsorbents. The dye uptake on to both the adsorbents was consistent with Langmuir and Freundlich adsorption isotherms, while the thermodynamic parameters obtained by the adsorption isotherm data confirmed the feasibility of the process in both cases. The kinetic investigations confirmed that, for both the adsorbents, the film diffusion mechanism was operative in the lower concentration range, whereas, at higher concentrations a particle diffusion process was operative.

However, detailed studies on the kinetics and thermodynamics of the dyeing process of silk with indigo carmine have not been undertaken previously. Such studies would be expected to supply more information on the interaction of silk with dyes. Thus the thermodynamic and kinetic parameters for the direct dyeing process of silk with indigo carmine were investigated and are reported in this Chapter. The results from this study will be used to underpin further work improving the effectiveness of dyeing of silk and also as model for the adsorption kinetic and thermodynamic studies of indigo direct dyeing onto silk without a reduction process

In a further development of the research work in this area, the possibility of preparing *N*-substituted indigo derivatives with polar groups attached to increase water solubility was also investigated. Little is known about such compounds but Hein, Phuong, Michalik, Gorls, Lalk, and Langer (2006) reported the first synthesis of deprotected indigo *N*-glycosides (blue sugars) which should be more water soluble (Figure 3.2a). They were prepared by reaction of dehydroindigo with rhamnosyl, glucosyl and mannosyl iodide generated *in situ*.

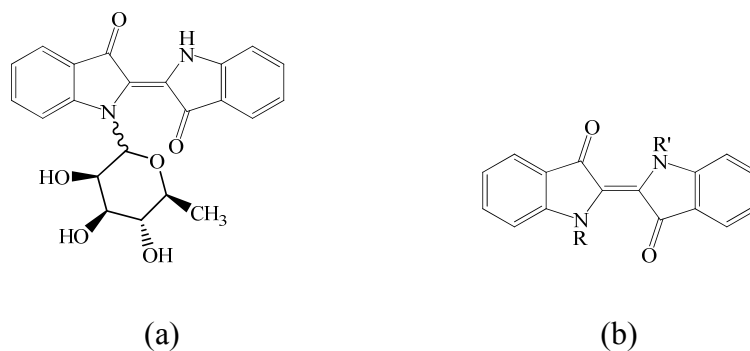


**Figure 3.2** (a) Structure of an indigo *N*-glycoside; (b) General structures of *N*-substituted indigo dye derivatives ( $R, R' = H, CH_2COOEt, CH_2COCOOEt, CH_2CONH_2,$  and  $CH_2COOH$ ).

In the current study, other water soluble *N*-substituted indigo derivatives were prepared. In exploring this approach, we wished to develop a compact route to *N*-alkyl ester and associated *N*-alkyl acid or amide derivatives (Figure 3.2b) which might be expected to retain a blue or blue green colour and, in the case of the alkyl acid derivatives, a functional group which would facilitate non-redox based direct silk dyeing under favourable acidic conditions.

### 3.3 Experimental

#### 3.3.1 Materials and Chemicals

- (1) Silk yarn from Chul Thai Silk Co., Ltd in Phetchabun, Thailand
- (2) Indigo [482-89-3],  $C_{16}H_{10}N_2O_2$ , MW 262.26, Sigma Aldrich
- (3) Indigo carmine (Acid blue 74, C.I. 73015, MW 466.34), Acros Organics
- (4) Glacial acetic acid,  $CH_3COOH$ , Merck
- (5) Ammonium acetate,  $CH_3COONH_4$ , Carlo erba
- (6) Hydrochloric acid 37% (w/v), HCl, Merck
- (7) Cesium carbonate,  $Cs_2CO_3$ , 99.9%, Aldrich.
- (8) Methyl iodide,  $CH_3I$ , 99.5%, Aldrich.
- (9) Sodium hydride, NaH, 60%dispersion in mineral oil, Aldrich.
- (10) N,N-Dimethyl formamide, anhydrous, 99.8%, DMF, Aldrich.
- (11) Iodoacetamide,  $I-CH_2CONH_2$ , Aldrich
- (12) Ethylbromoacetate,  $Br-CH_2COOCH_2CH_3$ , 98% Aldrich.
- (13) Ethylchloroacetate,  $Cl-CH_2COOCH_2CH_3$ , Fluka
- (14) Ethylbromopyruvate,  $Br-CH_2COCO_2CH_2CH_3$ , 90%, Aldrich.
- (15) Sodium iodide, NaI, Carlo

#### 3.3.2 Instruments

(1) An Agilent 8453 UV-Vis spectrophotometer was employed to determine the concentration of dye samples through absorbance measurements using quartz cells of path length 1 cm at the characteristic maximum wavelength.

(2) A pH meter (Laboratory pH Meter CG 842, SCHOTT, UK) was used to measure the pH values of solutions.

(3) A thermostatted shaker bath (Type SBD-50 cold, Heto-Holten A/S, Denmark) operated at 150 strokes/min, was used to study the adsorption kinetics and thermodynamics of indigo carmine onto silk yarn.

### **3.3.3 Experimental methods**

#### **3.3.3.1 Silk yarn preparation (Chairat, 2004)**

The silk yarn used was purchased from Chul Thai Silk Co., Ltd in Phetchabun, Thailand. Prior to using in the dyeing experiment, the silk yarn (1 kg) was treated with 0.5 M HCl (*ca* 3 L) at room temperature for 30 min and then removed and washed with deionized water until the rinsed water was neutral. The silk yarn was then dried at room temperature.

#### **3.3.3.2 Batch kinetic experiments of indigo carmine dyeing onto silk**

The batch technique was used to examine the dyeing process at temperatures of 30, 40 and 50°C. The dyeing process was scrutinized by taking a series of 125 mL conical flasks containing the aqueous solution of indigo carmine over the concentration range 23.3 to 70.0 mg/L at a fixed pH (pH range 3.0–5.0; pH adjusted by using acetic acid-acetate buffer). The dye solution in each conical flask was shaken in a thermostatted shaker bath operated at 150 strokes/min and controlled temperature. After 30 min, the silk yarn (0.50 g), which had been pre-warmed in the thermostatted bath for 30 min, was immersed in the dye solution. The silk samples were then rapidly withdrawn after different immersion times. The concentration of the unadsorbed indigo carmine in the supernatant dye solution was determined at time zero and at subsequent times using a calibration curve based on absorbance at  $\lambda_{\max}$

611 nm versus dye concentration. The amount of dye adsorbed per gram of silk ( $q_t$ ) (mg/g silk) at any time was calculated by a mass balance relationship (Eq. (2.20)).

### **3.3.3.3 Batch equilibrium experiments of indigo carmine dyeing onto silk**

Indigo carmine was dissolved in deionized water to the required concentrations and the pH of the dye solution was adjusted to 4.0 by using acetic acid-acetate buffer. The experiments were carried out by shaking silk yarn (0.50 g) with different concentrations of dye solution (50 mL) in a conical flask in a thermostatted shaker bath operated at 150 strokes/min and controlled temperature. The concentration of the unadsorbed indigo carmine in the supernatant dye solution was determined at time zero and at equilibrium times using a calibration curve based on absorbance at  $\lambda_{\max}$  611 nm versus dye concentration. The amount of dye adsorbed per gram of silk ( $q_e$ ) (mg/g silk) at equilibrium time was calculated by a mass balance relationship (Eq. (2.21)).

### **3.3.3.4 Preparation and characterization of more water soluble *N,N'*-substituted indigo derivatives for direct dyeing of silk**

#### **(1) General chemistry methods**

All chemical, solvents and reagents used were purchased from Sigma-Aldrich, Merck, Fluka, and Carlo and were used as received. Anhydrous DMF was purchased from Sigma-Aldrich Chemical Co. Inc., in a Sure-seal® bottle and was stored under an inert atmosphere. All other solvents were AR grade and were used as received, with the exception of ethyl acetate (EtOAc) and hexane that were used for

column chromatography, which were LR grade when purchased and were distilled before use. Reactions were monitored by thin-layer chromatography (TLC) on Merck Silica gel 60 F<sub>254</sub> with a thickness of 0.2 mm on aluminum sheet, and the compounds were detected by examination under ultraviolet light. Preparative TLC was performed using the same technique with 20×20 cm sheets of the same silica gel. Column chromatography was performed under medium pressure using silica gel 60 (230-400 mesh, Merck). All solvent proportions were v/v. Organic solvent extracts were dried over anhydrous sodium sulfate and solvents were removed under reduced pressure at 40°C with a Büchi rotary evaporator. All compounds were judged to be greater than 95% purity by <sup>1</sup>H NMR and TLC analysis. Melting points were obtained using a Griffin melting point apparatus and are uncorrected. UV spectra (solvent corrected) were recorded on an Agilent 8453 UV-Vis spectrophotometer. Infrared spectra were measured with an AVATAR 370 FT-IR spectrometer. NMR spectra were obtained on a Varian Unity 300 MHz spectrometer, where proton (<sup>1</sup>H) and carbon (<sup>13</sup>C) spectra were obtained at 300 MHz and 75 MHz, respectively, or on a Varian Inova 500 spectrometer, where the <sup>1</sup>H and <sup>13</sup>C were obtained at 500 MHz and 126 MHz, respectively. Spectra were recorded in CDCl<sub>3</sub> (unless otherwise indicated) and were referenced to the residual non-deuterated solvent signal. Chemical shifts of the outer peaks are given for specified multiplet patterns in the <sup>1</sup>H-NMR spectra. Hydrogen and carbon assignments were made by standard gradient correlation spectroscopy (gCOSY), gradient heteronuclear single quantum correlation (gHSQC) and gradient heteronuclear multiple bond correlation (gHMBC) spectroscopies. Superscript letters refer to interchangeable chemical shift assignments. Positive ion high resolution electrospray mass spectra, HRMS (ESI), were obtained with a Micromass Qtof 2 mass

spectrometer using a cone voltage of 30 V and polyethylene glycol (PEG) as an internal reference.

## **(2) Synthesis *N*-substituted indigo derivatives**

This work involved the preparation of new mono- or di- *N*-substituted derivatives with a carboxylic acid, ester or amide functionality present in the substituent which should increase water solubility.

### **(2.1) Establishment of *N*-substitution methodology with *N*-methylation**

Prior to making the more water soluble derivatives, the methodology for synthesis was established on a model system involving *N,N'*-methylation. Indigo (200 mg, 0.76 mmol) was suspended in anhydrous DMF (20 mL) and sonicated for 10 min. The intense dark blue mixture was then stirred and warmed to 70 °C under a nitrogen atmosphere. Anhydrous Cs<sub>2</sub>CO<sub>3</sub> (500 mg, 1.5 mmol) was added and the mixture was stirred for a further 10 min. followed by addition of CH<sub>3</sub>I (0.14 mL, 1.7 mmol). TLC analysis (DCM) showed the formation of the known *N,N'*-dimethylindigo as well as some *N*-methylindigo.

### **(2.2) Introduction of a water solubilising acetamido group on nitrogen**

Indigo (200 mg, 0.76 mmol) was suspended in anhydrous DMF (20 mL) and sonicated for 10 min. The intense dark blue mixture was then stirred and warmed to 70°C under a nitrogen atmosphere. Anhydrous Cs<sub>2</sub>CO<sub>3</sub> (500 mg, 1.5 mmol) was added and the mixture was stirred for a further 10 min. followed by

addition of I-CH<sub>2</sub>CONH<sub>2</sub> (310 mg, 1.67 mmol). TLC analysis (DCM) showed the possible formation of the N-substituted products, but no pure compound could be isolated

### **(2.3) Reaction of indigo with ethyl bromopyruvate**

Indigo (200 mg, 0.76 mmol) was suspended in anhydrous DMF (20 mL) and sonicated for 10 min. The intense dark blue mixture was then stirred and warmed to 70°C under a nitrogen atmosphere. NaH (*ca* 60% dispersion in mineral oil, 100 mg, 2.5 mmol) was added and the mixture was stirred for a further 10 min. followed by addition of Br-CH<sub>2</sub>COCO<sub>2</sub>CH<sub>2</sub>CH<sub>3</sub> (0.21 mL, 1.67 mmol). TLC analysis (DCM) showed the formation products but no pure compounds could be isolated.

### **(2.4) Reaction of indigo with ethyl iodoacetate**

To a mixture of indigo (800 mg, 3.05 mmol) and NaH (*ca* 60% dispersion in mineral oil, 400 mg, 10 mmol) was added anhydrous DMF (100 mL) under a nitrogen atmosphere. The mixture was stirred for 12 hr at room temperature. More anhydrous DMF (10 mL) was added and stirring continued for a further 15 min. Ethyl iodoacetate (1 mL, 8.45 mmol; obtained by Cl/I exchange from ethyl chloroacetate with sodium iodide) was added dropwise and the mixture was heated at 70°C for 3 hr. Monitoring of the reaction by TLC (30% EtOAc/hexane) before work-up of the reaction showed the formation of the desired product as well as other coloured compounds. The mixture was filtered through celite. The filtrate was concentrated then chromatographed on silica gel (15% EtOAc in hexane) and further chromatographed on silica gel by preparative TLC (10% EtOAc in hexane) to afford



the monoester and diester products, plus the known compounds ethyl (*Z*)-3-oxo-2,3-dihydro-1*H*-indol-2-ylidene) acetate and *N*-ethoxycarbonylmethylisatin.

### **(2.5) Hydrolysis of the diester**

To a mixture of the indigo diester (200 mg, 0.46 mmol) and anhydrous MgI<sub>2</sub> (513 mg, 4.0 mmol) was added dry xylene (10 mL) under a nitrogen atmosphere. The mixture was heated at reflux at 130°C for 3 days. An aqueous solution of 10% NaHCO<sub>3</sub> (50 mL) was added and the mixture then extracted with DCM (3×20 mL) to remove neutral products. The aqueous layer was acidified with 15% HCl and then stirred vigorously with solid NaCl for 3 hr. The solution was extracted with DCM (3×20 mL). The combined DCM extracts were washed with water, dried and evaporated. The crude product was chromatographed on silica gel by preparative TLC (20% EtOH/EtOAc) to afford the indigo monoacid-monoester derivative and a trace amount of the corresponding diacid derivative.

### **(3) Molecular Calculations**

All calculations (AM 1) were performed using Spartan '08 Version 1.0.0, licensed with local HASP, run on an AMD Athlon™ 64 processor 3800+, 2.41 GHz, with 1.00 GB of RAM. The operating system used was Microsoft Windows XP Professional, Version 2002, Service Pack 3.

### 3.3.3.5 Preliminary direct dyeing of silk with an *N,N'*-disubstituted indigo derivative

One small scale dyeing experiment of silk was undertaken by the batch technique at 30°C to examine the new blue-green indigo derivative with monoacid-monoester functionality present. An aqueous solution of this water soluble indigo derivative was prepared by dissolving in deionized water at a concentration of 0.59 mg/mL (the pH of the solution was 4.7). In the experiment, 0.1 g of silk and 5.0 mL of dye solution was put in a flask and was shaken for 60 min using a thermostatted shaker bath operated at 150 strokes/min and controlled temperature. The concentration of the unadsorbed water soluble indigo derivative in the supernatant dye solution was determined at time zero and at 60 min from a calibration curve based on absorbance at  $\lambda_{\max}$  652 nm versus dye concentration. The amount of dye adsorbed per gram of silk ( $q_t$ ) (mg/g silk) was calculated by a mass balance relationship (Eq. (2.20)).

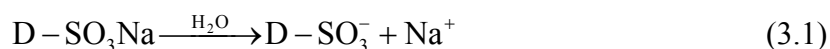
## **3.4 Results and Discussion**

### **3.4.1 Adsorption kinetic and thermodynamic studies of indigo carmine dyeing onto silk**

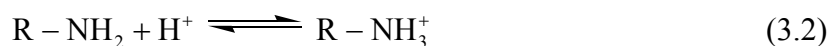
In order to investigate the adsorption of indigo carmine onto silk, the experimental parameters including initial dye concentration, contact time, pH, material to liquor ratio (MLR) and temperature were determined to find the optimal conditions for adsorption. These conditions were a pH of 4.0, an MLR of 1:100 and a temperature of 30°C. These conditions were then used for the subsequent kinetic and thermodynamic studies.

#### **3.4.1.1 Effect of pH on the adsorption of indigo carmine onto silk**

The pH of the dye solution is one of the most important parameters controlling the adsorption capacity of dye onto silk (Moeyes, 1993; Christie, Mather, and Wardman, 2000). The effect of pH on the adsorption of indigo carmine onto silk at 30°C with an initial dye concentration of 46.6 mg/L and MLR of 1:100 is shown in Figure 3.3. This showed that the adsorption capacity clearly increased with decreasing pH over the pH range 5.0-3.0. The possible mechanisms for the effect of pH on adsorption of the acid dye indigo carmine (Donald *et al.*, 1976) are likely to be ionic interactions of the dye anions with the protonated amino groups on the silk fibre (Wong, Szeto, Cheung, and McKay, 2003). Given the strongly acidic nature of arylsulfonic acids (benzenesulfonic acid  $pK_a$  -6.5) (Serjeant and Dempsey, 1979), the anionic sulfonate groups present on dissolution of the sodium salts in water (3.1) at pH 4.0 would be fully ionized.



Also, at pH 4.0, the basic amino groups of silk protein ( $\text{R}-\text{NH}_2$ ) would be essentially fully protonated (3.2) while the acidic carboxylic acid groups in the side chains or the C-terminii would be expected to be largely unionized.



The adsorption process then proceeds due to the strong electrostatic attractions between the ammonium and sulfonate ion residues (3.3).



Therefore, indigo carmine dye solution at pH 4.0 was used to study the kinetics and thermodynamics of the adsorption process throughout this study. In order to examine the controlling mechanism of the adsorption process, pseudo first order and pseudo second order equations were used to test the experimental data. The best fit model was selected based on the linear regression correlation coefficient,  $R^2$  values. Table 3.1 lists the results of rate constant and other kinetic parameters studies for different pH of dye solution calculated by the pseudo first order (Figure 3.4) and pseudo second order (Figure 3.5) models. The  $q_{e,\text{exp}}$  and the  $q_{e,\text{cal}}$  values from the pseudo second order kinetic model were very close to each other, and, the calculated correlation coefficients,  $R^2$  were also closer to unity for pseudo second order kinetics

than those for the pseudo first order kinetics. These suggested that the pseudo second-order adsorption mechanism is predominant and that the overall rate of the indigo carmine dye adsorption process is most likely to be controlled by the chemisorption process (Chairat, Rattanaphani, Bremner, and Rattanaphani, 2005).

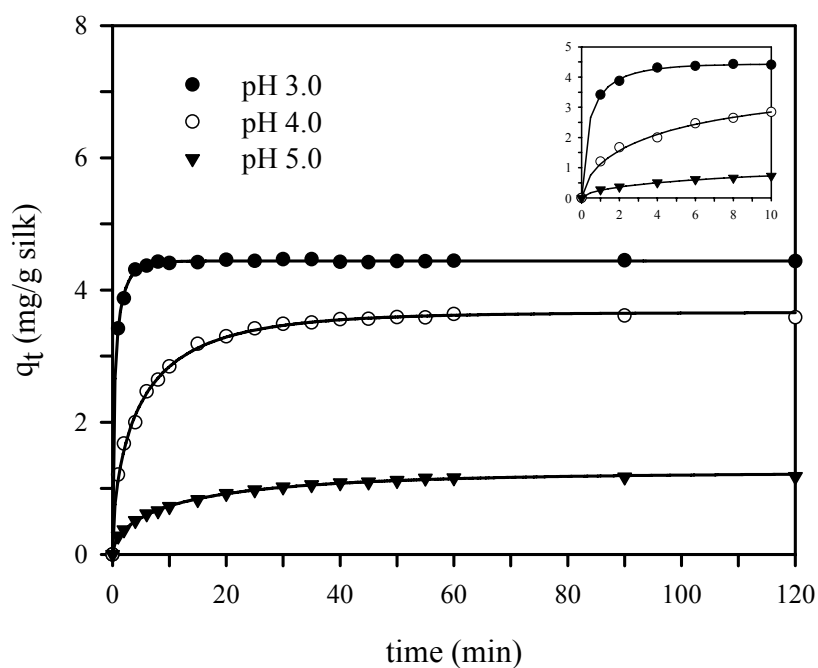


**Figure 3.3** Effect of pH on the adsorption of indigo carmine onto silk (under dyeing condition:  $C_0$  46.6 mg/L, MLR 1:100, 30°C).

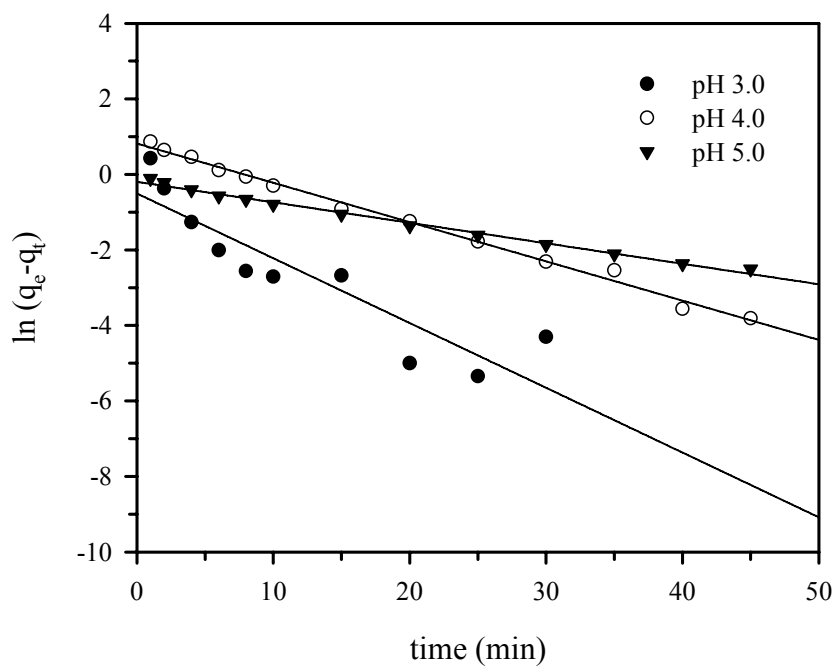


**Figure 3.4** Application of the pseudo first order equation at different pH of dye solution on the adsorption of indigo carmine onto silk.

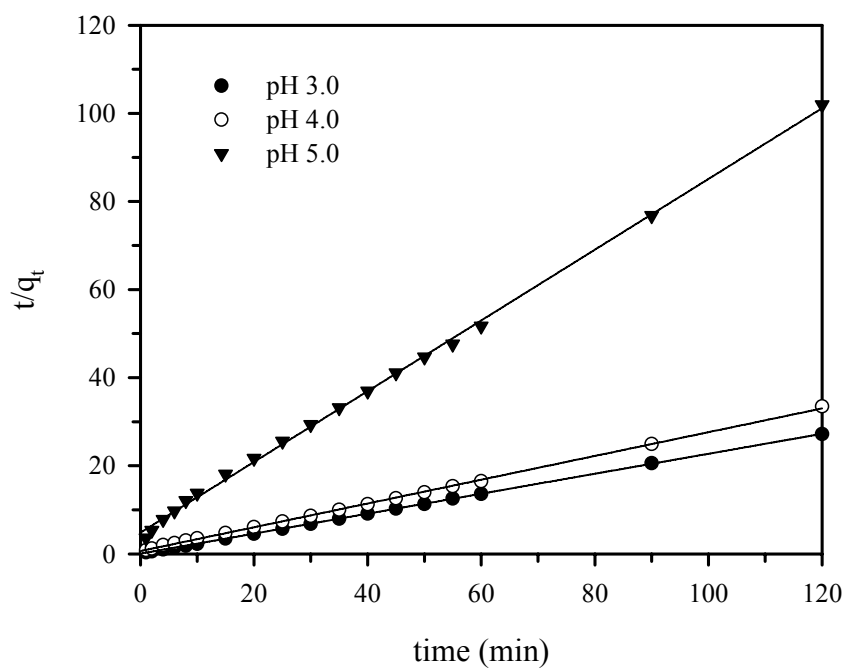


**Figure 3.5** Application of the pseudo second order equation at different pH of dye solution on the adsorption of indigo carmine onto silk.

**Table 3.1** Comparison of the pseudo first- and pseudo second-order adsorption rate constants and the calculated and experimental  $q_e$  values for different pH, initial dye concentrations, MLR and temperature for the adsorption of indigo carmine onto silk.

Parameter	$q_{e,exp}$ (mg/g silk)	Pseudo first order model			Pseudo second order model			
		$k_1$ (min <sup>-1</sup> )	$q_{e,cal}$ (mg/g silk)	$R^2$	$k_2$ (g silk/mg min)	$q_{e,cal}$ (mg/g silk)	$h_i$ (mg/g silk min)	$R^2$
<i>pH: <math>C_0</math> 46.6 mg/L, MLR 1:100, temp. 30 °C, contact time 60 min</i>								
3.0	4.44	0.34	1.10	0.7484	1.80	4.45	35.59	1.0000
4.0	3.64	0.10	2.67	0.9205	0.09	3.81	1.27	0.9996
5.0	1.16	0.06	0.88	0.9842	0.13	1.26	0.20	0.9966
<i>Initial dye concentration: <math>C_0</math>(mg/L): pH 4.0, MLR 1:100, temp. 30 °C, contact time 60 min</i>								
23.3	1.95	0.10	0.99	0.9464	0.26	2.10	1.07	0.9998
46.6	3.64	0.10	2.67	0.9205	0.09	3.81	1.27	0.9996
70.0	4.88	0.09	2.99	0.9478	0.06	5.18	1.51	0.9994
<i>MLR: <math>C_0</math> 46.6 mg/L, pH 4.0, temp. 30 °C, contact time 60 min</i>								
1:50	2.09	0.11	0.67	0.9317	0.51	2.13	2.314	1.0000
1:100	3.64	0.10	2.67	0.9205	0.09	3.81	1.27	0.9996
1:150	5.03	0.07	3.37	0.9747	0.04	5.42	1.21	0.9990
<i>Temperature: <math>C_0</math> 46.6 mg/L, pH 4.0, MLR 1:100, contact time 60 min</i>								
30	3.64	0.10	2.67	0.9205	0.09	3.81	1.27	0.9996
40	3.38	0.08	1.13	0.8631	0.25	3.51	3.05	0.9996
50	3.00	0.09	0.91	0.8577	0.37	3.11	3.53	0.9998

### **3.4.1.2 Effect of initial dye concentration and contact time on the adsorption of indigo carmine onto silk**

The adsorption of indigo carmine at different initial dye concentrations onto silk at pH 4.0, MLR 1:100 and 30°C was investigated as a function of contact time in order to determine the equilibrium time for maximum adsorption. A plot of the amount of dye adsorbed per gram silk ( $q_t$ ) (mg/g silk) at any time versus contact time ( $t$ ) is shown in Figure 3.6. It was found that the dye adsorption rate for each initial dye concentration was quite rapid in the first 15 min, but thereafter the adsorption rate decreased gradually with equilibrium essentially being reached by 60 min (optimum contact time), with only a slight increase being noted over the next 60 min. Hence subsequent experiments were conducted for the optimum contact time only. These results showed similar trends with the adsorption of indigo onto silk by conventional vat-dyeing process (Chapter II). The higher adsorption rate at the initial period (15 min) may be due to the large number of vacant adsorption sites available on the silk at this stage. Thus an increase in the concentration of indigo carmine in solution and hence on the silk surface (concentration gradient) tends to enhance the dye adsorption rate at the initial stages. As time proceeds, this concentration gradient decreases due to the increased occupation of vacant sites by dye molecules (Chiou and Li, 2002; Chairat *et al.*, 2005; Lakshmi *et al.*, 2009). Thus the initial dye concentration plays an important role in the adsorption capacity of indigo carmine onto silk.



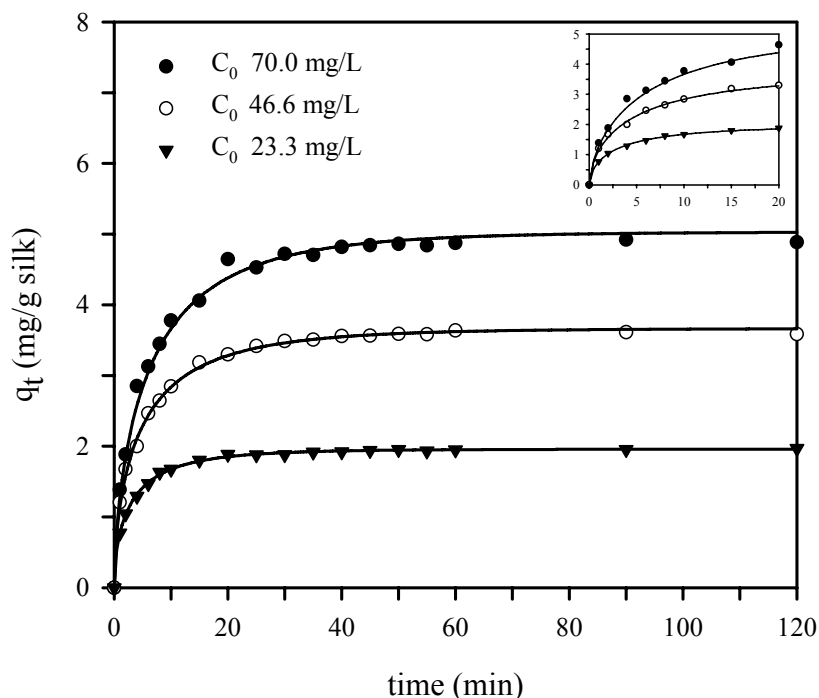


**Figure 3.6** Effect of initial dye concentration on the adsorption of indigo carmine onto silk (under dyeing condition MLR = 1:100, pH = 4.0, 30°C).

The results of rate constant studies for different initial dye concentrations by using the pseudo first order and pseudo second order kinetic models are listed in Table 3.1 and shown in Figure 3.7 and Figure 3.8 are pseudo first order and pseudo second order plots, respectively. The pseudo second order kinetic model well described the adsorption of indigo dye onto silk over range of desired initial dye concentration with a high correlation coefficient ( $R^2 > 0.99$ ). This suggested that the overall rate of the indigo dye adsorption onto silk is controlled by the chemisorption. A similar phenomenon have also been observed in the adsorption of indigo onto silk by conventional vat-dyeing process (Chapter II) and also the acid dyeing of the other dye (Chairat *et al.*, 2005; Septum, Rattanaphani, Bremner, and Rattanaphani, 2009;

Komboonchoo and Bechtold, 2010). An increase in initial dye concentration results in a significant increase in  $q_{e,cal}$ . The  $q_{e,cal}$  for initial dye concentration also increase with an increasing of initial dye concentration.

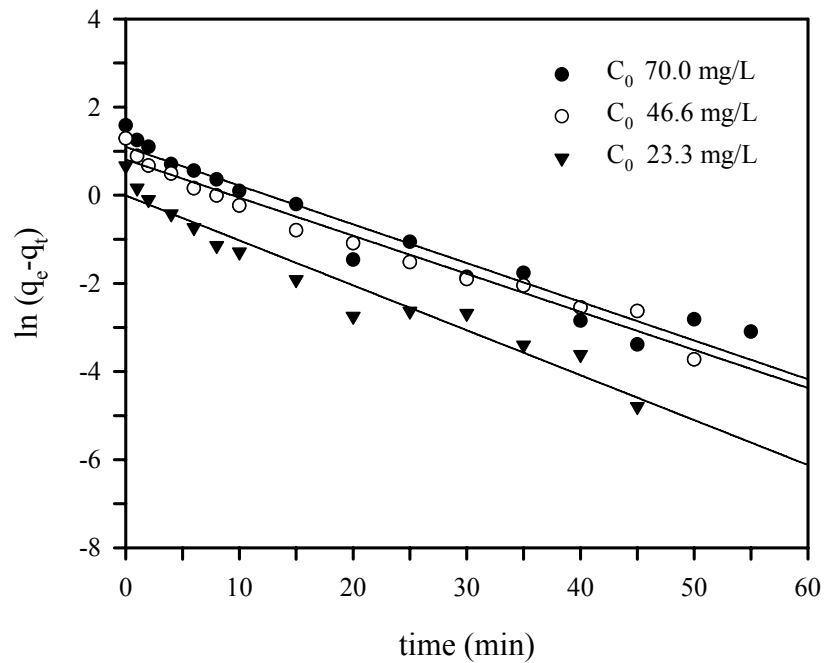


**Figure 3.7** Application of the pseudo first order equation at different initial dye concentration on the adsorption of indigo carmine onto silk.

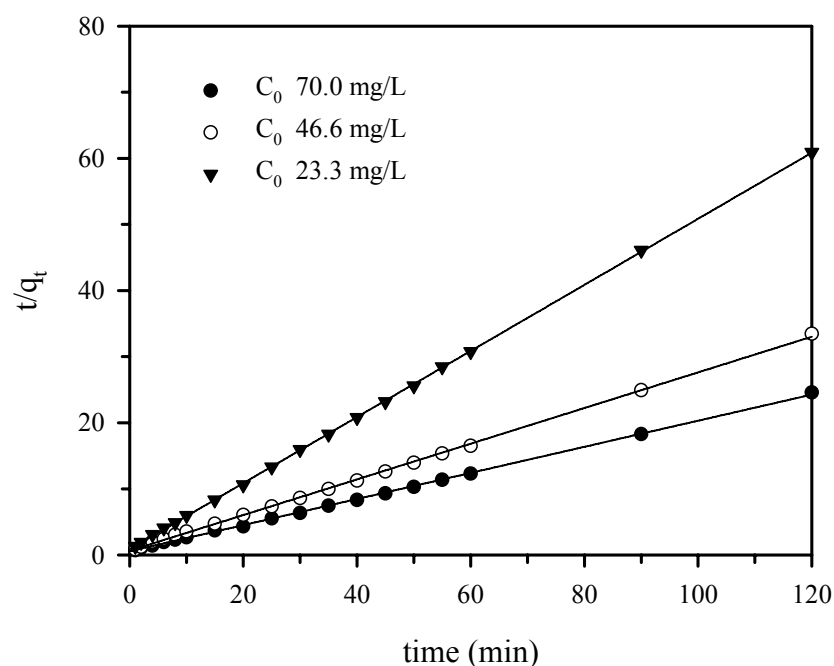


**Figure 3.8** Application of the pseudo second order equation at different initial dye concentration on the adsorption of indigo carmine onto silk.

### 3.4.1.3 Effect of material to liquor ratio (MLR) on the adsorption of indigo carmine onto silk

The aim of dyeing is to transfer the dye molecules from the dye liquor to the fibre in a uniform and efficient manner. The rate of dye uptake by the fibre is significantly increased by the increased movement of the dye liquor relative to the fibre (Christie *et al.*, 2000). The effect of material to liquor ratio (MLR) on the adsorption of indigo carmine onto silk at an initial dye concentration of 46.6 mg/L at pH 4.0 and 30°C is shown in Figure 3.9. It was found that an increase in volume of the dye solution resulted in an increase of the dye adsorbed onto the silk, consistent with the yarn being more loosely packed in such a dye solution. This allows the dye

solution to move more readily over the silk surfaces with associated dye molecule binding, and then into the interior of the silk yarn by diffusion (Chairat *et al.*, 2005). The amount of dye absorbed at MLR 1:150 was higher than for MLRs of 1:100 and 1:50. However, in order to reduce waste from the dyeing process, an MLR of 1:100 was used for all the subsequent experiments.

Kinetic parameters from linear plots of pseudo first order (Figure 3.10) and pseudo second order (Figure 3.11) models are given in Table 3.1. The data show a good compliance with the pseudo second order equation and the regression coefficients,  $R^2$ , for the linear plot were all high ( $> 0.99$ ). The overall rate of the indigo adsorption processes appears to be controlled by the chemical process in this case in accordance with the pseudo second order reaction mechanism.

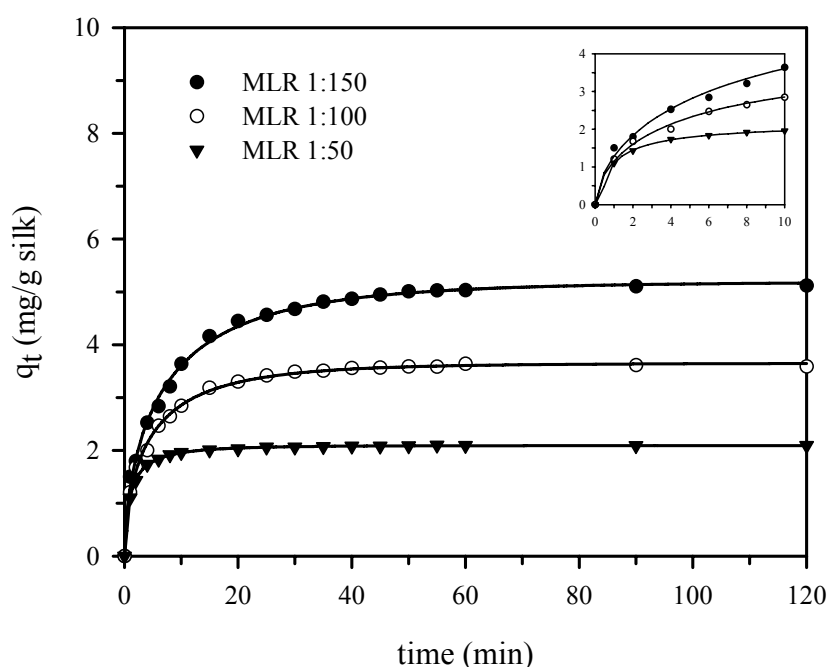


**Figure 3.9** Effect of MLR on the adsorption of indigo carmine onto silk (under dyeing condition  $C_0 = 46.6$  mg/L, pH = 4.0, 30°C).

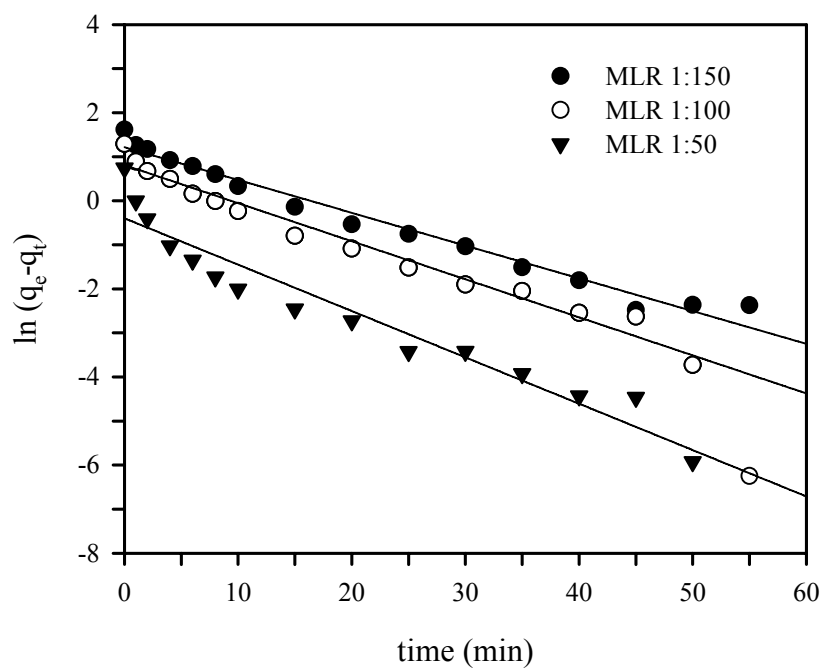


**Figure 3.10** Application of the pseudo first order equation at different MLR on the adsorption of indigo carmine onto silk.

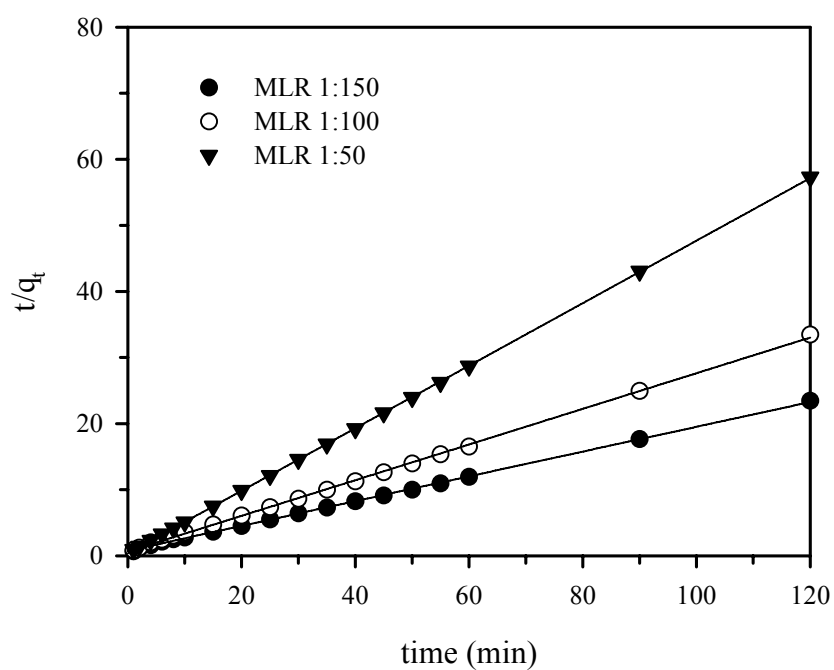


**Figure 3.11** Application of the pseudo second order equation at different MLR on the adsorption of indigo carmine onto silk.

#### **3.4.1.4 Effect of temperature on the adsorption of indigo carmine onto silk**

The dye adsorption process was studied at different temperatures of 30, 40 and 50°C, and under the optimal conditions of pH 4.0, MLR 1:100 and an initial dye concentration of 46.6 mg/L in each case. Before and after the equilibrium time, the amount of dye adsorbed per gram of silk ( $q_t$ ) showed different trends at different temperatures (Figure 3.12). Before the equilibrium time was established, an increase in the temperature leads to an increase in dye adsorption rate indicative of a kinetically controlled process. After the equilibrium time, the amount of the dye adsorbed per gram of silk decreased with increasing the temperature suggesting that the adsorption of indigo carmine onto silk is controlled by an exothermic process. Similar temperature effect trends on adsorption trend have also been shown in the case of the adsorption of indigo onto silk by conventional vat-dyeing process (Chapter II) and also the acid dyeing of the other dye (Chairat *et al.*, 2005; Septhum *et al.*, 2009). Table 3.1 lists the results of rate constant and other kinetic parameters studies for different temperatures calculated by the pseudo first order (Figure 3.13) and pseudo second order (Figure 3.14) models. The correlation coefficient,  $R^2$ , for the pseudo second order adsorption model has a higher value suggesting the dye adsorption occurs process is predominantly by the pseudo second order adsorption mechanism.

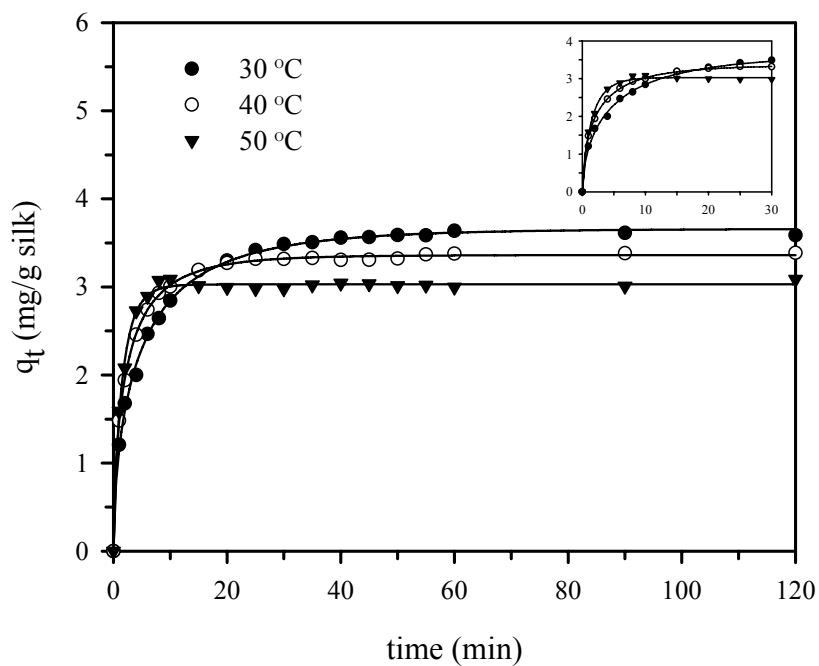


**Figure 3.12** Effect of temperature on the adsorption of indigo carmine onto silk (under dyeing condition  $C_0 = 46.6$  mg/L, pH = 4.0, MLR = 1:100).

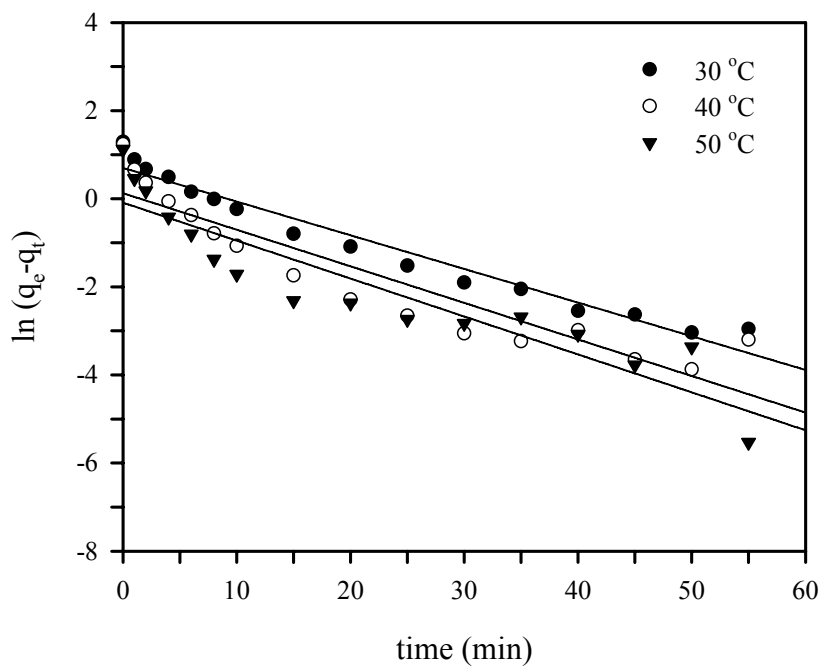


**Figure 3.13** Application of the pseudo first order equation at different temperature on the adsorption of indigo carmine onto silk.

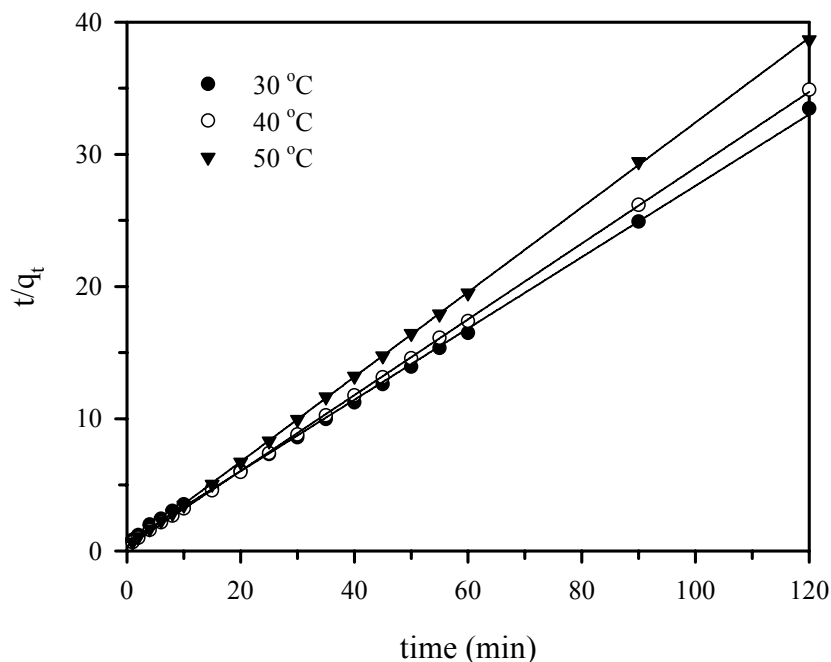


**Figure 3.14** Application of the pseudo second order equation at different temperature on the adsorption of indigo carmine onto silk.

### 3.4.1.5 Activation parameters for the adsorption of indigo carmine onto silk

The rate constants  $k_2$  for pseudo second order model at different temperatures listed in Table 3.1 were then applied to estimate the activation energy of the adsorption of indigo carmine onto silk by the Arrhenius equation. The slope of the plot of  $\ln k$  versus  $1/T$  (Figure 3.15) was used to evaluate  $E_a$  as listed in Table 3.2. For the  $E_a$  of 51.06 kJ/mol observed we can infer that the adsorption of indigo carmine onto silk most likely involves a chemisorption process consistent with strong H-bond reinforced salt bridge interactions between the dye sulfonate groups and protonated



amino groups on the silk. A similar, though lower, activation energy of 47.5 kJ/mol was noted for the chemisorption of the acidic lac dyes on silk (Chairat *et al.*, 2005).

**Table 3.2** Activation parameters for the adsorption of indigo carmine dye onto silk at an initial dye concentration of 46.6 mg/L and pH 4.0.

Temp. (°C)	$k_2$ (g silk/ mg min)	$E_a$ (kJ/mol)	$R^2$	$\Delta H^\#$ (kJ/mol)	$\Delta S^\#$ (J/mol K)	$\Delta G^\#$ (kJ/mol)	$R^2$
30	0.09					126.55	
40	0.25	51.06	0.9824	48.47	-257.72	129.13	0.9815
50	0.37					131.71	

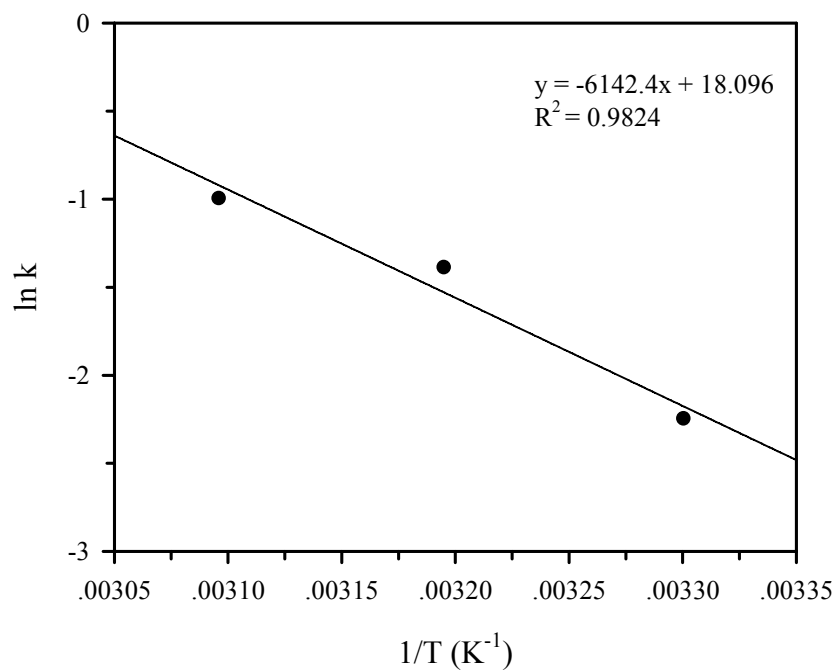


**Figure 3.15** Arrhenius plots for the adsorption of indigo carmine on silk.

From the Eyring equation, the enthalpy ( $\Delta H^\ddagger$ ) and entropy ( $\Delta S^\ddagger$ ) of activation were calculated from the slope and intercept of a plot of  $\ln(k/T)$  versus  $1/T$  (Figure 3.16) as listed in Table 3.3. The value of  $\Delta G^\ddagger$  was calculated at 303, 313 and 323 K by using equation (2.10) and these values are listed in Table 3.3, with the large negative entropy value ( $\Delta S^\ddagger$ ) being consistent with the interaction between the disulfonate dye and the silk.

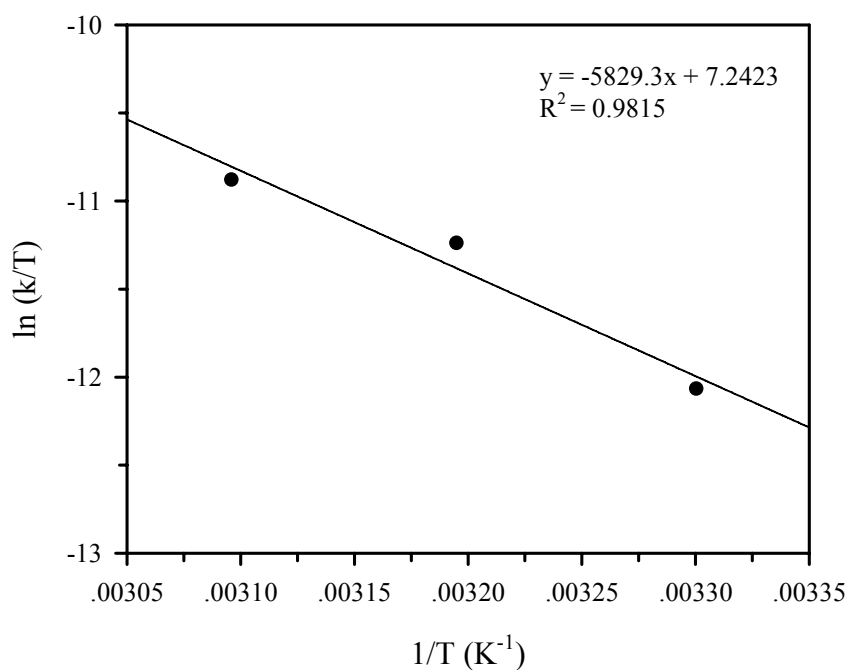


**Figure 3.16** Plot of  $\ln(k/T)$  against  $1/T$  for the adsorption of indigo carmine on silk.

### 3.4.1.6 Adsorption isotherm for the adsorption of indigo carmine onto silk

While the previous discussion focused on the kinetics of dye adsorption, further information on the dyeing process can also be obtained from studies at equilibrium. The relationship between the amounts of a substance adsorbed at constant temperature and its concentration in the equilibrium solution is called the adsorption isotherm (Ahmad, Hameed, and Aziz, 2007) Several models have been describe experimental data for adsorption isotherms, with the Langmuir (Langmuir, 1918) and Freundlich (Chiou and Li, 2002) models being the most frequently employed. In this work, both models were used to describe the relationship between the amount of indigo carmine adsorbed and its equilibrium concentration. The values of  $Q$  and  $b$  (from Eq. (2.12); Table 3.3) can be calculated from the intercepts and slopes of different straight lines representing the different temperatures. The  $R^2$  values indicated a generally good fit of the equilibrium data in the Langmuir isotherm expression in line with monolayer coverage of indigo carmine onto silk. It was observed that the adsorption of indigo carmine dye at higher temperature decreased with increasing temperature indicating that the process is exothermic. As expected, the  $Q$  values decreased with increasing temperature, while the  $b$  values indicated that the silk yarn had a maximum affinity for indigo carmine dye at lower temperature.

The Freundlich isotherm equation (Eq. (2.15)) was also applied to the results of the adsorption of indigo onto silk. The values of  $Q_f$  and  $1/n$  can be determined from the linear plot of  $\ln q_e$  versus  $\ln C_e$ . The magnitude of the exponent  $1/n$  gives an indication of the favourability of adsorption. Values of  $n > 1$  (Table 3.3) obtained represent favourable adsorption conditions (Chiou and Li, 2002; Chairat *et*

*al.*, 2005). The  $Q_f$  values decreased with increasing temperature which again supported an exothermic process. However, this model showed a lower correlation with the experimental adsorption data compared to those derived in the Langmuir model.

**Table 3.3** Langmuir and Freundlich isotherm constants for the adsorption of indigo carmine dye onto silk at different temperatures.

Temp. (°C)	Langmuir			Freundlich		
	Q (mg/g silk)	b (mL/mg)	R <sup>2</sup>	Q <sub>f</sub> (mg/g silk)	n	R <sup>2</sup>
30	15.06	55.33	0.9950	29.44	2.55	0.9163
40	17.99	25.27	0.9758	35.04	2.07	0.9484
50	18.38	22.67	0.9101	42.72	1.77	0.8960

#### 3.4.1.7 Thermodynamic parameters for the adsorption of indigo carmine on silk

In order to support the exothermic behaviour of the adsorption of indigo onto silk, the thermodynamic parameters,  $\Delta G^\circ$ ,  $\Delta H^\circ$  and  $\Delta S^\circ$  of indigo adsorption after reaching equilibrium were calculated by using the equations (2.16) to (2.19). Enthalpy change ( $\Delta H^\circ$ ) and entropy change ( $\Delta S^\circ$ ) of the adsorption are calculated from the slope and intercept of the van't Hoff plots of  $\ln K_c$  versus  $1/T$  (Figure 3.17). The complete adsorption and thermochemical data for the indigo carmine-silk interaction are given in Table 3.4. In general, all thermochemical quantities decrease when the temperature increases. This behaviour suggests a

progressive indigo carmine desorption process when the temperature increases (dos Anjos *et al.*, 2002). The negative Gibbs free energy values demonstrated that the indigo carmine dyeing on silk is a thermodynamically favourable process, for the temperature range evaluated. The obtained enthalpy value of -27.26 kJ/mol confirms that the indigo carmine dyeing of silk is an exothermic process, so raising the temperature leads to lower affinity and less dye being adsorbed at equilibrium.

**Table 3.4** Thermodynamic parameters for the adsorption of indigo carmine onto silk at different temperatures.

Temp. (°C)	$K_c$	$\Delta G^\circ$ (kJ/mol)	$\Delta H^\circ$ (kJ/mol)	$\Delta S^\circ$ (J/mol K)	$R^2$
30	4.48	-3.82			
40	3.34	-3.05	-27.26	-77.35	0.9919
50	2.29	-2.28			

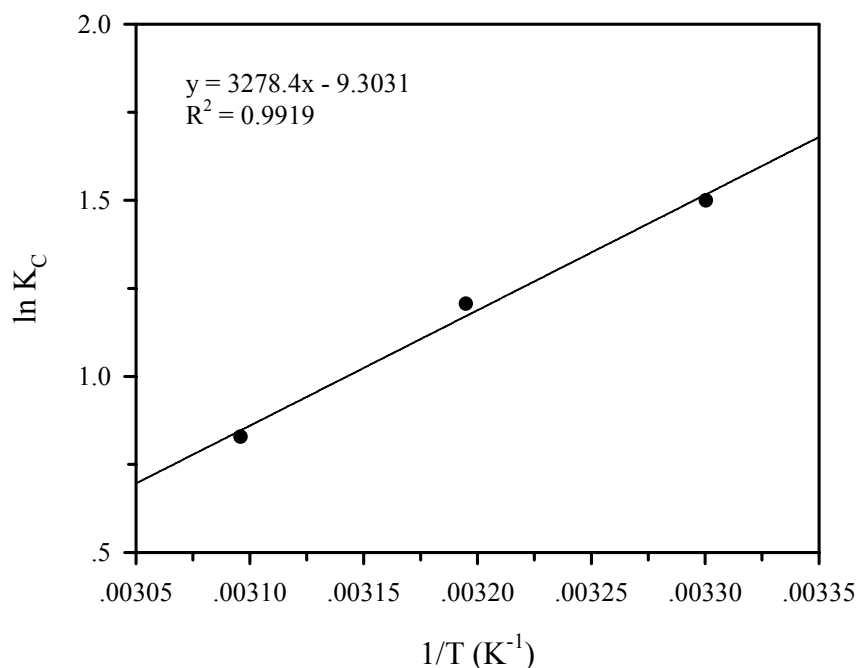


**Figure 3.17** The van't Hoff plots of  $\ln K_C$  versus  $1/T$ .

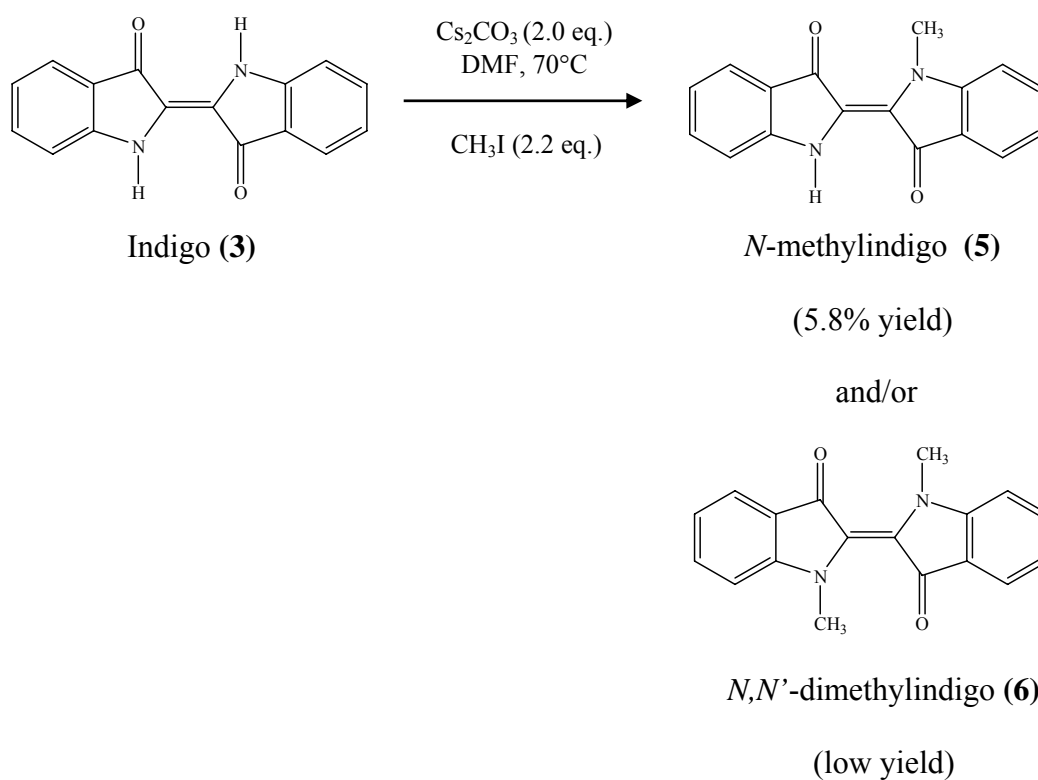
### 3.4.2 Preparation and characterization of more water soluble *N,N'*-indigo derivatives for direct dyeing of silk

This work focussed on the preparation of mono- or di- *N*-substituted indigo derivatives with a carboxylic acid, ester or amide functionality present which should increase water solubility, particularly the acid and amide groups.

#### 3.4.2.1 Establishment of *N*-substitution methodology with methylation

Prior to attempting to make the more water soluble indigo derivatives, the proposed nucleophilic substitution methodology for synthesis was established on a model system involving *N*-methylation (Scheme 3.1) with iodomethane after formation of the nucleophilic nitrogen anion by deprotonation with the base  $\text{Cs}_2\text{CO}_3$ .

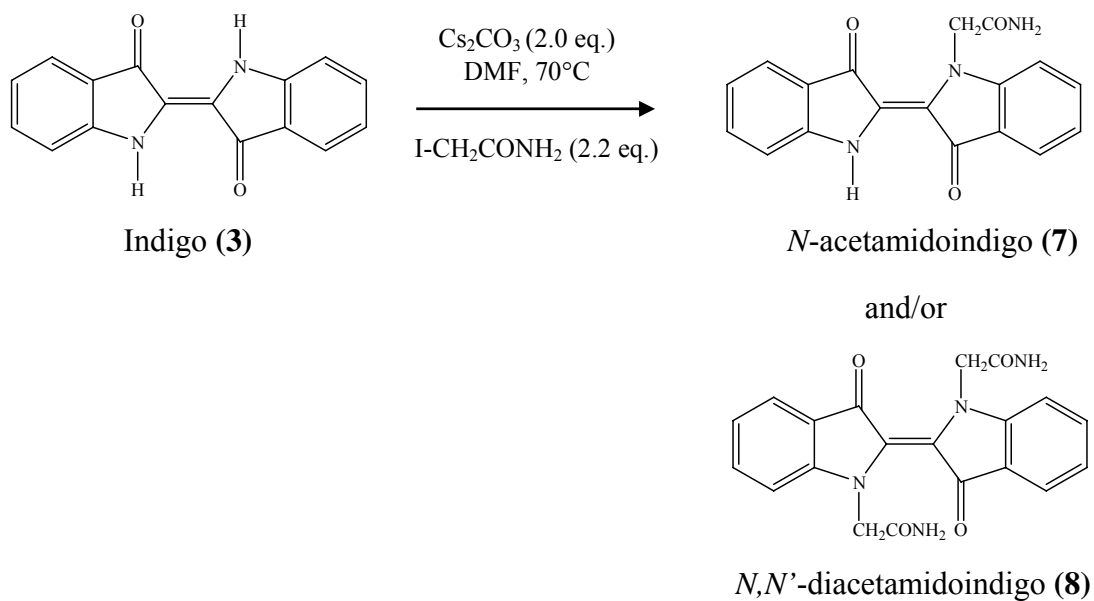
This afforded the known compounds *N*-methylindigo (**5**) (5.8% yield) and *N,N'*-dimethylindigo (**6**) (low yield). When the stronger base sodium hydride was used (in DMF at 70°C with 2.2 eq. of iodomethane) in place of Cs<sub>2</sub>CO<sub>3</sub> the yield of the latter compound improved to 49%, while the former compound was obtained in 14% yield.



**Scheme 3.1**

#### 3.4.2.2 Introduction of a water solubilising acetamido group on N

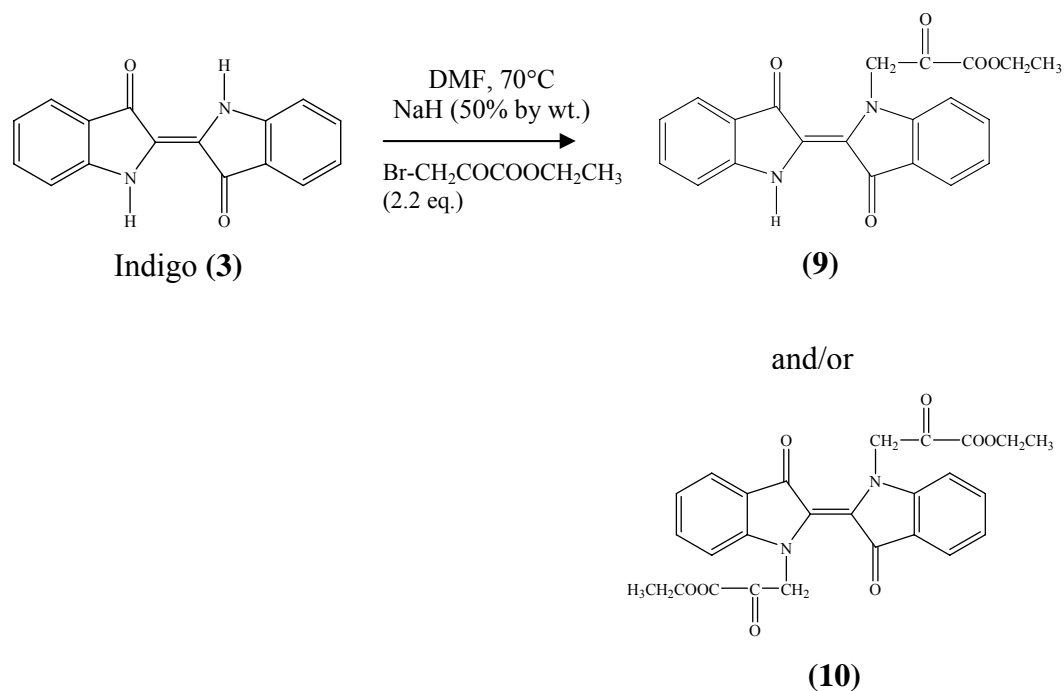
The attempted preparation of mono- or di- *N*-substituted indigo derivatives with amide functionality in the substituent is presented in Scheme 3.2, using Cs<sub>2</sub>CO<sub>3</sub> as the base and iodoacetamide as the alkylating agent. Unfortunately, no *N*-substituted acetamido products could be isolated from this reaction.

**Scheme 3.2**

### 3.4.2.3 Reaction of indigo with ethyl bromopyruvate

The attempted reaction of indigo with ethyl bromopyruvate in the presence of base is shown in Scheme 3.3. No *N*-alkylated products could be isolated from this reaction, possibly due to competing anion formation on removal of a proton from the acidic alpha-keto methylene group in the pyruvate ester.





Scheme 3.3.

#### 3.4.2.4 Reaction of indigo with ethyl iodoacetate

The general approach to the target compounds was based on the induction of nucleophilic substitution reactions at nitrogen followed by ester-acid functional group manipulation (Scheme 3.4). In order to increase the nucleophilicity at nitrogen, sodium hydride was used as a base with DMF as the solvent with a view to solubilising the indigo. Reaction of the amide sodium salt with ethyl iodoacetate then afforded the monoester and the required diester in modest yields (Scheme 3.4), together with two known minor fragmentation products (see section 3.3.3.4). Analytical and spectroscopic data for the ester compounds, which confirmed their structures, are shown below:

**Monoester (11):** blue solid; yield: 159 mg (15%);  $\lambda_{\text{max}}$  614 nm (in EtOH); IR (KBr)  $\nu$  3288 (NH), 1757 (CO), 1639 (CO)  $\text{cm}^{-1}$ .

$^1\text{H}$  NMR (300 MHz,  $\text{CDCl}_3$ )  $\delta$ : 10.58 (NH), 7.78 (d,  $J = 4.8$  Hz, 1H, H-4)<sup>a</sup>, 7.66 (d,  $J = 4.5$  Hz, 1H, H-4')<sup>a</sup>, 7.55 (t,  $J = 4.7$  Hz, 1H, H-6)<sup>b</sup>, 7.47 (t,  $J = 4.5$  Hz, 1H, H-6')<sup>b</sup>, 7.07 (t,  $J = 4.5$  Hz, 1H, H-5)<sup>c</sup>, 6.97-7.00 (m, 2H, H-7, H-7'), 6.94 (t,  $J = 4.5$  Hz, 1H, H-5')<sup>c</sup>, 5.33 (s, 2H,  $\text{NCH}_2$ ), 4.24 (q,  $J = 4.5$  Hz, 2H,  $\text{OCH}_2$ ), 1.27 (t,  $J = 4.5$  Hz, 1H,  $\text{CH}_3$ ).

$^{13}\text{C}$  NMR (300 MHz,  $\text{CDCl}_3$ )  $\delta$ : 189.2 (C-3'), 187.6 (C-3), 169.0 (CO), 152.9 (C-7a), 151.8 (C-7a'), 136.3 (C-6'), 135.9 (C-6), 124.9 (C-4'), 124.2 (C-4), 121.2 (C-5), 121.1 (C-3a), 120.7 (C-5'), 120.0 (C-3a'), 111.9 (C-7), 111.0 (C-7'), 62.6 ( $\text{OCH}_2$ ), 39.1 ( $\text{NCH}_2$ ), 14.1 ( $\text{CH}_3$ ).

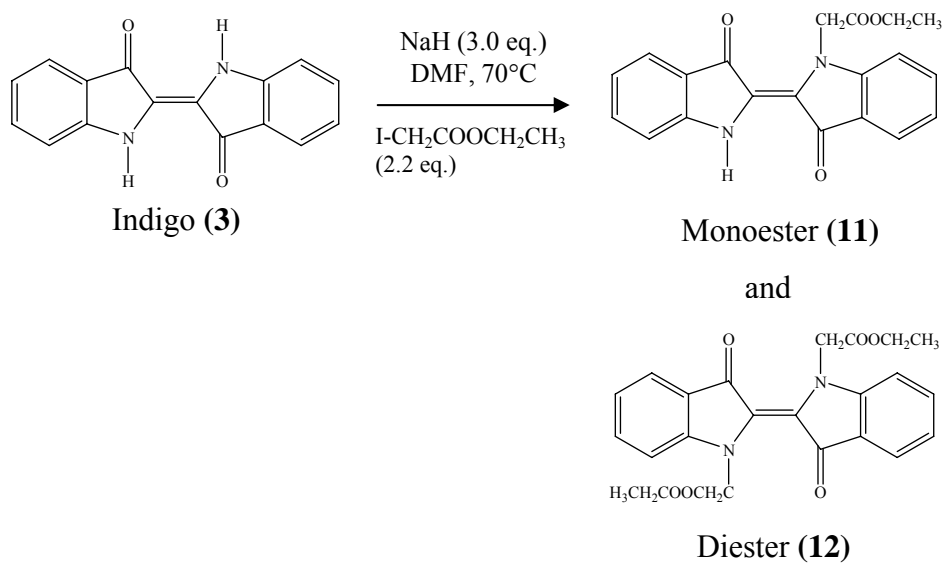
HRESIMS;  $m/z$  calcd for  $\text{C}_{20}\text{H}_{16}\text{N}_2\text{O}_4$   $[\text{M}]^+$ : 348.1110; found: 348.1104.

**Diester (12)**: Blue-green solid; yield: 305 mg (23%); mp 140-141°C;  $\lambda_{\text{max}}$  619 nm (in EtOH); IR (KBr)  $\nu$  1741 (CO), 1650 (CO)  $\text{cm}^{-1}$ .

$^1\text{H}$  NMR (500 MHz,  $\text{CDCl}_3$ )  $\delta$ : 7.73 (d,  $J = 7.5$  Hz, 2H, H-4, H-4'), 7.53 (t,  $J = 7.5$  Hz, 2H, H-6, H-6'), 7.07 (t,  $J = 7.3$  Hz, 2H, H-5, H-5'), 7.02 (d,  $J = 8.5$  Hz, 2H, H-7, H-7'), 4.82 (s, 4H,  $\text{NCH}_2$ ), 4.21 (q,  $J = 7.0$  Hz, 4H,  $\text{OCH}_2$ ), 1.25 (t,  $J = 7.0$  Hz, 6H,  $\text{CH}_3$ ).

$^{13}\text{C}$  NMR (126 MHz,  $\text{CDCl}_3$ )  $\delta$ : 186.2 (2C, C-3, C-3'), 168.8 (2C, CO), 153.6 (2C, C-7a, C-7a'), 135.6 (2C, C-6, C-6'), 127.0 (2C, C-2, C-2'), 124.3 (2C, C-4, C-4'), 122.0 (2C, C-5, C-5'), 121.9 (2C, C-3a, C-3a'), 111.0 (2C, C-7, C-7'), 61.4 (2C,  $\text{OCH}_2$ ), 51.0 (2C,  $\text{NCH}_2$ ), 14.1 (2C,  $\text{CH}_3$ ).

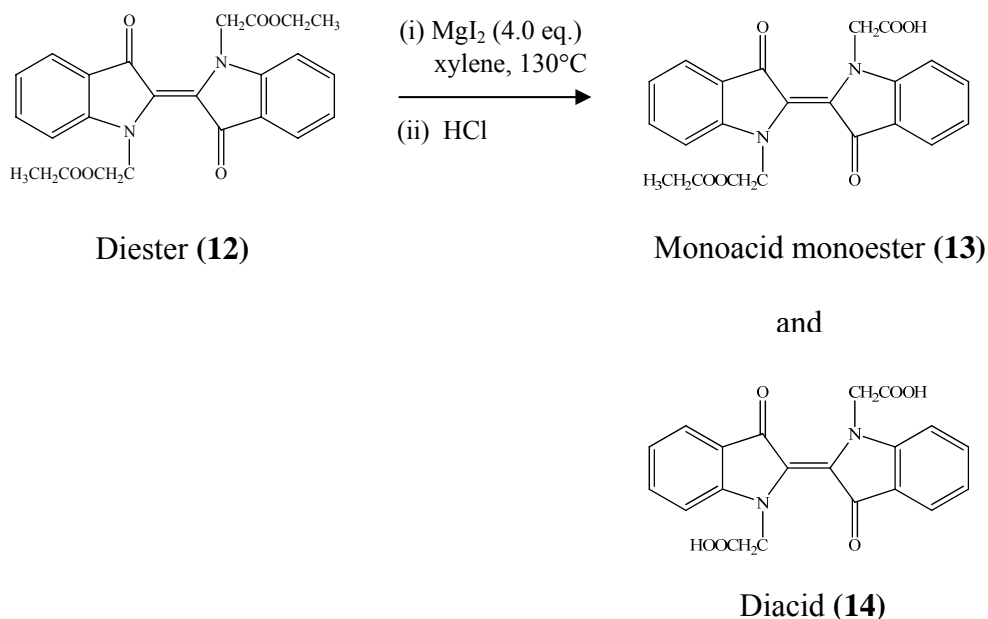
HRESIMS;  $m/z$  calcd for  $\text{C}_{24}\text{H}_{22}\text{N}_2\text{O}_6$   $[\text{M}]^+$ : 434.1478; found: 434.1481.



Scheme 3.4

#### 3.4.2.5 Hydrolysis of the diester

The hydrolysis of esters to the corresponding carboxylic acids is classically achieved by acidic or basic hydrolysis in a protic solvent medium. This procedure has the disadvantage of the potential occurrence of side reactions, particularly when complex multifunctional molecules are involved. Furthermore, sterically hindered esters can be hydrolyzed only under strong reaction conditions. Consequently, a non-hydrolytic procedure for the cleavage of esters by using magnesium iodide in toluene at reflux was assessed (García Martínez, Osío Barcinaa, Hidalgo del Veccio, Hanack, and Subramanian, 1991). In the event, the diester (see Scheme 3.4) could be converted to the mixed acid/ester product (monoacid monoester) in modest yield (Scheme 3.5), but only trace amounts of the expected diacid product were recovered. Initially the magnesium carboxylate was produced from which the carboxylic acid could be recovered by acidification with HCl.



Scheme 3.5

Analytical and spectroscopic data for these compounds are shown below:

**Monoacid monoester (13):** blue-green solid; yield: 66 mg (35.2%);  $\lambda_{\max}$  652 nm (in water); water solubility 4.0 g/L at 30°C (pH of the solution was 4.7).

<sup>1</sup>H NMR (500 MHz, CD<sub>3</sub>OD)  $\delta$ : 7.67 (d,  $J$  = 7.5 Hz, 1H, H-4)<sup>a</sup>, 7.64 (d,  $J$  = 7.5 Hz, 1H, H-4')<sup>a</sup>, 7.51-7.57 (m, 2H, H-6, H-6'), 7.17 (d,  $J$  = 8.0 Hz, 1H, H-7)<sup>b</sup>, 7.13 (d,  $J$  = 8.5 Hz, 1H, H-7')<sup>b</sup>, 7.08 (t,  $J$  = 7.5 Hz, 1H, H-5)<sup>c</sup>, 7.03 (t,  $J$  = 7.5 Hz, 1H, H-5')<sup>c</sup>, 4.73 (s, 4H, NCH<sub>2</sub>), 4.27 (q,  $J$  = 7.0 Hz, 2H, OCH<sub>2</sub>), 1.27 (t,  $J$  = 7.0 Hz, 3H, CH<sub>3</sub>).

<sup>13</sup>C NMR (126 MHz, CD<sub>3</sub>OD)  $\delta$ : 188.6 (C-3')<sup>d</sup>, 186.9 (C-3)<sup>d</sup>, 175.0 (COOH), 171.8 (COOEt), 155.6 (C-7a')<sup>e</sup>, 154.8 (C7a)<sup>e</sup>, 155.6 (C-6')<sup>f</sup>, 154.8 (C-6)<sup>f</sup>, 129.7 (C-2')<sup>g</sup>, 127.6 (C-2)<sup>g</sup>, 124.8 (C-4')<sup>h</sup>, 124.5 (C-4)<sup>h</sup>, 123.0 (3a')<sup>i</sup>, 122.8 (C-3a)<sup>i</sup>, 122.7 (C-5')<sup>j</sup>,

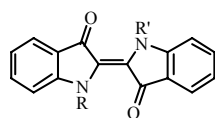
122.5 (C-5)<sup>j</sup>, 112.7 (2C, C-7, C-7'), 62.4 (OCH<sub>2</sub>), 53.7 (CH<sub>2</sub>COOH), 52.7 (CH<sub>2</sub>COOEt), 14.5 (CH<sub>3</sub>).

HRESIMS;  $m/z$  calcd for C<sub>22</sub>H<sub>19</sub>N<sub>2</sub>O<sub>6</sub> [M]<sup>+</sup>: 407.1243; found: 407.1249.

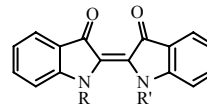
**Diacid (14)**: green solid; yield 0.7 mg (0.4%). HRESIMS;  $m/z$  calcd for C<sub>20</sub>H<sub>15</sub>N<sub>2</sub>O<sub>6</sub> [M]<sup>+</sup>: 379.0930; found: 379.0990. Insufficient compound was obtained for full NMR spectroscopic characterization.

### 3.4.2.6 Molecular Calculations

For the new *N*-alkylated ester and acid products produced it was not clear from the spectroscopic data whether (*E*) or (*Z*) isomers were produced. However, it was felt likely on steric, and in one case intramolecular H-bonding grounds, that the (*E*) geometry would be preferred. In order to gain further support for the (*E*)-stereoisomeric structures for the monoester, diester, monoacid monoester and diacid compounds, molecular modeling studies were undertaken by Mr. Andrew Stevens, School of Chemistry, University of Wollongong. These studies afforded calculated minimum energies of formation of the (*E*) and (*Z*) isomers of each compound, together with the corresponding data for indigo and methylated indigo derivatives. This data, for molecules *in vacuo*, is shown in Table 3.5. Larger negative energies of formation were obtained for all the (*E*)-isomers apart from the monoester-monoacid compound. In this case both values were very close, but the reason for this is not clear. Indigo is known to be in the (*E*)-configuration in the solid state from X-ray crystallographic analysis (Grimme, Grimme, Jones, and Boldt, 1993), and the calculated energies are also consistent with this (*E*) preference.

**Table 3.5** Calculated energies of formation for substituted indigo (*E*) and (*Z*) isomers.

(E)-isomers



(Z)-isomers

R	R'	Energy of Formation (kcal.mol <sup>-1</sup> )	R	R'	Energy of Formation (kcal.mol <sup>-1</sup> )
H	H	164.88	H	H	206.87
CH <sub>3</sub>	H	200.07	CH <sub>3</sub>	H	250.44
CH <sub>2</sub> COOEt	H	-139.23	CH <sub>2</sub> COOEt	H	-111.49
CH <sub>2</sub> COOH	H	-160.03	CH <sub>2</sub> COOH	H	-122.57
CH <sub>3</sub>	CH <sub>3</sub>	299.95	CH <sub>3</sub>	CH <sub>3</sub>	327.82
CH <sub>2</sub> COOEt	CH <sub>2</sub> COOEt	-475.90	CH <sub>2</sub> COOEt	CH <sub>2</sub> COOEt	-446.25
CH <sub>2</sub> COOEt	CH <sub>2</sub> COOH	-432.55	CH <sub>2</sub> COOEt	CH <sub>2</sub> COOH	-433.33
CH <sub>2</sub> COOH	CH <sub>2</sub> COOH	-482.29	CH <sub>2</sub> COOH	CH <sub>2</sub> COOH	-441.00

### 3.4.2.7 More water soluble indigo derivatives direct dyeing of silk

One small scale direct silk dyeing experiment was undertaken with the new water soluble monoacid-monoester indigo derivative (**13**) with an initial dye concentration of 0.59 mg/mL, at pH 4.7 (not adjusted), with an MLR of 1:100, a contact time of 60 min and at 30°C. The concentration of the unadsorbed monoacid-monoester indigo derivative in the supernatant dye solution was determined at time zero and at 60 min using a calibration curve based on absorbance at  $\lambda_{\text{max}}$  652 nm

versus dye concentration. The amount of dye adsorbed per gram of silk ( $q_t$ ) (mg/g silk) was calculated by Eq. (2.20) and was found to be 1.5 mg/g silk; the silk dyed with this solution presented an attractive blue-green colour. These results showed that new water soluble indigo derivatives could be developed by introducing a carboxylic acid group on substituents at nitrogen. The monoacid-monoester indigo derivative prepared in this initial work retained a blue-green colour and, because of its water solubility and carboxylic acid functionality, could be used to directly dye silk under acidic conditions.

### **3.5 Conclusion**

Detailed kinetic and thermodynamic parameters have been obtained for the first time with respect to the direct dyeing of silk using the commercially available, water soluble blue dye, indigo carmine. The adsorption process with this indigo-derived dye was an exothermic chemisorption one following pseudo second order kinetics. Another new water soluble blue-green dye was prepared in this work from indigo, which, in contrast to indigo carmine, involved the introduction of polar substituents on nitrogen in the indigo molecule. The particular compound prepared incorporated a carboxylic acid and ester group in separate substituents. In a trial experiment, this compound was shown to dye silk under acidic conditions. Future work could cover optimization of the dyeing process, kinetic and thermodynamic adsorption studies, colour property studies and wash and light fastness investigations. In addition, ways to prepare the diacid analogue in high yield could be further investigated, as this compound would be expected to have higher water solubility at acidic pH and more opportunities for silk-dye interactions.

### 3.6 References

- Ahmad, A. A., Hameed, B. H. and Aziz, N. (2007). Adsorption of direct dye on palm ash: Kinetic and equilibrium modeling. **Journal of Hazardous Material**. 141: 70-76.
- Alexandre, G. S. P., Jocilene, D. T., Wlaine, A. F. and Silvia, C. L. (2004). Comparative adsorption studies of indigo carmine dye on chitin and chitosan. **Journal of colloid and Interface Science**. 277: 43-47.
- Alok, M., Jyoti, M. and Lisha, K. (2006). Batch and bulk removal of hazardous dye, indigo carmine from wastewater through adsorption. **Journal of Hazardous Materials**. 137(1): 591-602.
- Aspland, J. R. (1997). **Textile Dyeing and Coloration**. USA: American association of textile chemists and colorists.
- Chairat, M. (2004). **Extraction and Characterization of Lac Dye from Thai Stick Lac and Development of Lac Dyeing on Silk and Cotton**. Ph.D. Thesis, Suranaree University of Technology, Thailand.
- Chairat, M., Rattanaphani, S., Bremner, J. B. and Rattanaphani, V. (2005). An adsorption and kinetic study of lac dyeing on silk. **Dyes and Pigments**. 64(3): 231-241.
- Chiou, M. S. and Li, H. Y. (2002). Equilibrium and kinetic modeling of adsorption of reactive dye on cross-linked chitosan beads. **Journal of Hazardous Materials**. B93(2): 233-248.
- Christie, R. M. (2001). **Colour Chemistry**. UK: Cambridge.
- Christie, R. M., Mather, R. R. and Wardman, R. H. (2000). **The Chemistry of Colour Application**. Oxford: Blackwell Science.



- Donald, L. P., Gary, M. L. and George, S. K. (1976). **Introduction to Organic Laboratory Techniques: A Contemporary Approach**. U.S.A.: W.B. Saunders.
- dos Anjos, F. S. C., Vieira, E. F. S. and Cestari, A. R. (2002). Interaction of indigo carmine dye with chitosan evaluated by adsorption and thermochemical data. **Journal of Colloid and Interface Science**. 253(2): 243-246.
- García Martínez, A., Osío Barcinaa, J., Hidalgo del Veccio, G., Hanack, M. and Subramanian, L. R. (1991). Non-hydrolytic cleavage of esters with magnesium iodide in aprotic non-polar solvents. **Tetrahedron Letters**. 32(42): 5931-5934.
- Gemeay, A. H., Mansour, I. A., El-Sharkawy, R. G. and Zaki, A. B. (2003). Kinetics and mechanism of the heterogeneous catalyzed oxidative degradation of indigo carmine. **Journal of Molecular Catalysis A: Chemical**. 193(1-2): 109-120.
- Grimme, G., Grimme, S., Jones, P. G. and Boldt, P. (1993). AM1 and X-ray studies of the structures and isomerization reactions of indigo dyes. **Chemische Berichte**. 126: 1015-1021.
- Hein, M., Phuong, N. T. B., Michalik, D., Gorls, H., Lalk, M. and Langer, P. (2006). Synthesis of the first deprotected indigo N-glycosides (blue sugars) by reductive glycosylation of dehydroindigo. **Tetrahedron Letters**. 47: 5741-5745.
- Hurlstone, D. P., George, R. and Brown, S. (2007). Novel clinical in vivo roles for indigo carmine: high-magnification chromoscopic colonoscopy. **Biotechnic and Histochemistry**. 82(2): 57-71.

- Komboonchoo, S. and Bechtold, T. (2010). Sorption characteristics of indigo carmine as a blue colourant for use in one-bath natural dyeing **Textile Research Journal**. 80(8): 734-743.
- Lacasse, K. and Baumann, W. (2004). **Textile Chemicals: Environmental Data and Facts**. New York: Springer.
- Lakshmi, U. R., Srivastava, V. C., Mall, I. D. and Lataye, D. H. (2009). Rice husk ash as an effective adsorbent: Evaluation of adsorptive characteristics for indigo carmine dye. **Journal of Environmental Management**. 90(2): 710-720.
- Langmuir, I. (1918). Adsorption of gases on plain surfaces of glass mica platinum. **Journal of the American Chemical Society**. 40: 1361-1403.
- Lu, Y., Li, J., Zhang, X., Tang, J., Wei, B. and Liu, J. (2005). Studies on the mechanism of indigo carmine removal by solvent sublation. **Journal of Colloid and Interface Science**. 292(1): 210-218.
- Mittal, A., Mittal, J. and Kurup, L. (2006). Batch and bulk removal of hazardous dye, indigo carmine from wastewater through adsorption. **Journal of Hazardous Materials**. 137(1): 591-602.
- Moeyes, M. (1993). **Natural Dyeing in Thailand**. Bangkok: White Lotus.
- Nakamura, T., Kawasaki, N., Tanada, S., Tamura, T. and Shimizu, Y. (2005). Indigo carmine removal by charcoal from rice bran as an agricultural by-product. **Toxicological & Environmental Chemistry**. 87(3): 321-327.
- Polenov, Y. V., Pushkina, V. A., Budanov, V. V. and Khilinskaya, O. S. (2001). Kinetics of heterogeneous reduction of red-brown Zh vat dye with rongalite in the absence of diffusion hindrance. **Russian Journal of Applied Chemistry**. 74: 1301-1304.

- Prado, A. G. S., Miranda, B. S. and Jacintho, G. V. M. (2003). Interaction of indigo carmine dye with silica modified with humic acids at solid/liquid interface. **Surface Science**. 542(3): 276-282.
- Ramya, M., Anusha, B. and Kalavathy, S. (2008). Decolorization and biodegradation of Indigo carmine by a textile soil isolate *Paenibacillus* larvae. **Biodegradation**. 19(2): 283-291.
- Roessler, A. and Crettenand, D. (2004). Direct electrochemical reduction of vat dyes in a fixed bed of graphite granules. **Dyes and Pigments**. 63(1): 29-37.
- Septum, C., Rattanaphani, S., Bremner, J. B. and Rattanaphani, V. (2009). An adsorption study of alum-morin dyeing onto silk yarn. **Fibers and Polymers**. 10(4): 481-487.
- Serjeant, E. P. and Dempsey, B. (1979). **Ionization Constants of Organic Acids in Solution, IUPAC Chemical Data Series**. Oxford: Pergamon Press.
- Son, Y. A., Lim, H. T., Hong, J. P. and Kim, T. K. (2005). Indigo adsorption properties to polyester fibres of different levels of fineness. **Dyes and Pigments**. 65: 137-143.
- Voss, G. (2006). Analysis of sulphur-containing indigoid dyes as leuco forms by NMR spectroscopy. **Coloration Technology**. 122: 317-323.
- Wong, Y. C., Szeto, Y. S., Cheung, W. H. and McKay, G. (2003). Equilibrium studies for acid dye adsorption onto chitosan. **Langmuir**. 19(19): 7888-7894.
- Zanoni, M. V. B., Sousa, W. R., Lima, J. P., Carneiro, P. A. and Fogg, A. G. (2006). Application of voltammetric technique to the analysis of indanthrene dye in alkaline solution. **Dyes and Pigments**. 68: 19-25.

# **CHAPTER IV**

## **APPROACHES TO DIRECT NON-REDUCTIVE INDIGO DYEING ONTO SILK AND ASSOCIATED ADSORPTION STUDIES**

### **4.1 Abstract**

New ways to increase the water solubility of indigo were found based on the use of additives. These additives included cyclodextrins and derivatives, or simple hydrotropic compounds like urea and nicotinamide. Using these compounds the water solubility of pure indigo and plant extracted indigo could be increased significantly. The addition of urea was then used to develop a new process for the direct dyeing of silk under acidic conditions without the need for an indigo reduction and subsequent oxidation step. The key kinetic and thermodynamic parameters for this dyeing process were obtained, with the kinetics fitting a pseudo second order model. Other parameters were consistent with an exothermic chemisorption process. Other effects of urea apart from increasing the indigo solubility are as yet not known. It may, for example, swell the silk fibres and act as a type of organic mordant. Direct dyeing of silk using plant extracted indigo and urea could be a potentially viable option for villagers.

## 4.2 Introduction

Indigo which is also known as indigotin, (CI Vat Blue 1), (2-(1,3-dihydro-3-oxo-2*H*-indol-2-ylidene)-1,2-dihydro-3*H*-indol-3-one) exists at ambient temperature and normal pressure as dark blue-violet needles or prisms with a distinct coppery luster (Figure 4.1) (Božič and Kokol, 2008). It is a quasiplanar molecule of approximate dimensions of  $4.8 \times 12 \text{ \AA}$  (Domenech, Domenech-Carbo, and Vazquez de Agredos Pascual, 2007). Crystals of indole are monoclinic and in the space group  $P2_1/C$ ; it sublimates above  $170^\circ\text{C}$ . Indigo is insoluble in water and poorly soluble in most of the common solvents. It is more soluble in polar organic solvents than non-polar ones (Steingruber, 2004). The poor solubility is most likely due to the strong inter- and intramolecular hydrogen bonds that are formed in indigo crystals. The hydrogen bonding also explains indigo's relatively high melting point ( $\sim 390^\circ\text{C}$ ) as well as its bathochromic shift of colour and its extremely low solubility in water (Christie, 2001). The colour of indigo is dependent on its environment. In the gas phase, where indigo is in its monomeric form, it is red, and in nonpolar solvents it is violet, but in solid form and in polar solvents as well as when it is applied to textiles as a vat dye, it is blue (Christie, 2007). Indigo has a low mammalian toxicity and there is no indication of sensitization in humans after repeated skin applications (Steingruber, 2004).

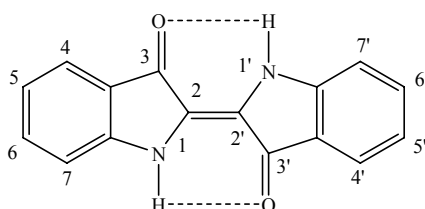


**Figure 4.1** Structure of indigo (Alexandre, Jocilene, Wlaine, and Silvia, 2004).

Thus, in the dyeing process indigo has to be converted to the water soluble leuco form, which is a salt in alkaline solution. The fibre is impregnated with the soluble leucoindigo and then re-oxidised in air to indigo (More detail in Chapter II). In this process it is difficult to control colour shade and uniformity of the dye on re-oxidation. If the water solubility of indigo dye could be improved and dyed directly onto the silk fibre this could potentially help to solve these problems of indigo dyeing.

A possible way to overcome indigo insolubility problem is by modifying the aqueous solubility of indigo dye by using cyclodextrins and their derivatives. In addition, another possible way to increase the water solubility of indigo dye is through the disruption of water structure by using a hydrotropic agent. Both these avenues were investigated in this research and are discussed in the following sections.

## **4.2.1 Cyclodextrins (CDs)**

### **4.2.1.1 Natural cyclodextrins and chemically modified cyclodextrins**

Cyclodextrins (CDs) was first discovered in 1891 by Villiers A. (Loftsson and Duchene, 2007). CDs were produced from starch by enzymatic degradation using cyclodextrin glucanotransferase (CGTase). In 1904, Schardinger characterized CDs as cyclic oligosaccharides that were composed of  $\alpha$ -1,4-glycosidic linkages. Three types of CDs:  $\alpha$ -CD,  $\beta$ -CD, and  $\gamma$ -CD have since been referred to as first generation or parent cyclodextrins (Brewster and Loftsson, 2007). CDs are cyclic oligosaccharides derived from starch containing six ( $\alpha$ -CD), seven ( $\beta$ -CD), eight ( $\gamma$ -CD), nine ( $\delta$ -CD), ten ( $\epsilon$ -CD) or more ( $\alpha$ -1,4)-linked  $\alpha$ -d-glucopyranose units. Due to the chair conformation of the glucopyranose units, the CDs take the shape of a truncated cone or torus or doughnut-shaped molecules rather than a perfect cylinder

(Figure 4.2 and Table 4.1). The hydroxyl functions are orientated to the cone exterior with the primary hydroxyl groups of the sugar residues at the narrow edge of the cone and the secondary hydroxyl groups at the wider edge. The central cavity of the CDs is lined with skeletal carbons and ethereal oxygens of the glucose residue, which gives it a relatively lipophilic character. The polarity of the cavity has been estimated to be similar to that of an aqueous ethanolic solution. In aqueous solutions, the hydroxy groups form hydrogen bonds with the surrounding water molecules resulting in a hydration shell around the dissolved CD molecules (Easton and Lincoln, 1999; Davis and Brewster, 2004; Challa, Ahuja, Ali, and Khar, 2005; Brewster and Loftsson, 2007). As a result of the hydrophilic outside surface and a polar hydrophobic cavity (Hebeish and El-Hilw, 2001), CDs can form inclusion complexes with a large variety of other guest compounds, depending on their size and shape. CDs act as a host for entrapping either totally or partially other chemical guest molecules.

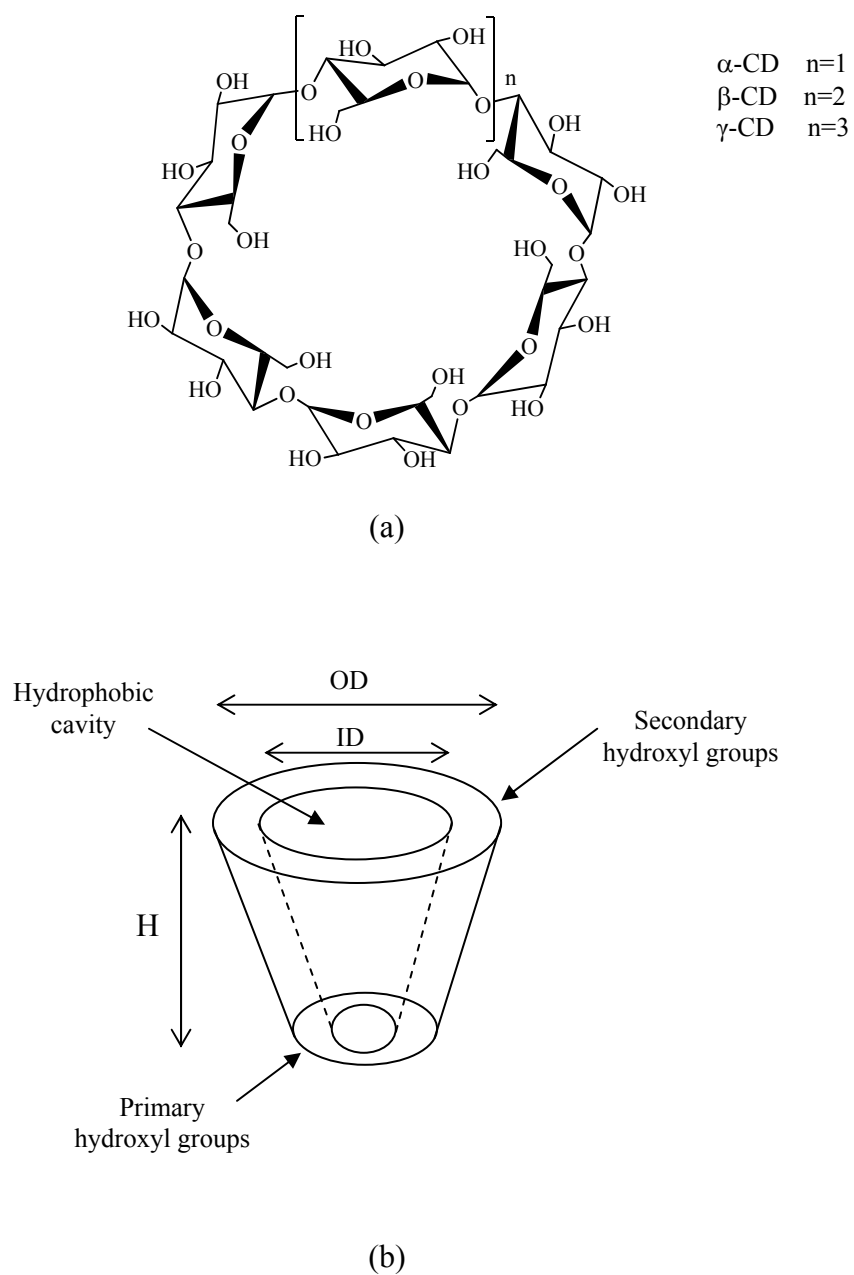


**Figure 4.2** (a) Chemical structures of  $\alpha$ -,  $\beta$ - and  $\gamma$ -cyclodextrin; (b) A structural scheme of a torus-shaped cyclodextrin molecule (Easton and Lincoln, 1999).



**Table 4.1** Characteristics of the natural cyclodextrins  $\alpha$ -CD,  $\beta$ -CD and  $\gamma$ -CD (Easton and Lincoln, 1999).

Cyclodextrins	Number of glucose units	Dimensions (nm)		
		Height of torus (H)	Outer diameter (OD)	Inner diameter (ID)
$\alpha$ -CD	6	0.78	1.37	0.57
$\beta$ -CD	7	0.78	1.53	0.78
$\gamma$ -CD	8	0.78	1.69	0.95

The natural CDs, in particular  $\beta$ -CD (Figure 4.2), are of limited aqueous solubility meaning that complexes resulting from interaction of lipophiles with these CDs may have limited water solubility although this depends also on the nature of the guest. However, substitution of any of the hydrogen bond-forming hydroxyl groups (see Figure 4.3), even by lipophilic functions, results in dramatic improvement in their aqueous solubility. Such CD derivatives of pharmaceutical interest (Figure 4.3, Table 4.2) include the hydroxypropyl derivatives of  $\beta$ -CD and  $\gamma$ -CD (i.e. HP- $\beta$ -CD and HP- $\gamma$ -CD), the randomly methylated  $\beta$ -CD (RM- $\beta$ -CD), sulfobutylether  $\beta$ -CD (SBE- $\beta$ -CD), and the so-called branched CDs such as maltosyl- $\beta$ CD (G<sub>2</sub>- $\beta$ -CD) (Brewster and Loftsson, 2007).

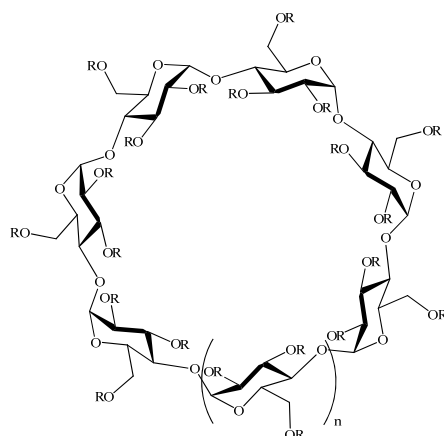


**Figure 4.3** Chemical structure of substituted cyclodextrins (Brewster and Loftsson, 2007).

**Table 4.2** Structural and physicochemical properties of selected cyclodextrins (Figure 4.3) of pharmaceutical interest (Brewster and Loftsson, 2007).

Cyclodextrins	n	R = H or	Substance <sup>a</sup>	MW <sup>b</sup> (Da)	Solubility in water <sup>c</sup> (mg/ml)	Indicative bulk price (\$US/kg) <sup>d</sup>
$\alpha$ -CD	0	-H	0	972	145	45
$\beta$ -CD	1	-H	0	1135	18.5	5
2-HP- $\beta$ -CD	1	-CH <sub>2</sub> CHOHCH <sub>3</sub>	0.65	1400	> 600	300
SBE- $\beta$ -CD	1	-(CH <sub>2</sub> ) <sub>4</sub> SO <sub>3</sub> <sup>-</sup> Na <sup>+</sup>	0.9	2163	> 500	—
RM- $\beta$ -CD	1	-CH <sub>3</sub>	1.8	1312	> 500	350
G <sub>2</sub> - $\beta$ -CD	1	Maltosyl-	0	1459	> 1500	—
$\gamma$ -CD	2	-H	0	1297	232	80
2-HP- $\gamma$ -CD	2	-CH <sub>2</sub> CHOHCH <sub>3</sub>	0.6	1576	> 500	400

<sup>a</sup> Average number of substituents per glucose repeat unit.

<sup>b</sup> MW: Molecular weight.

<sup>c</sup> Solubility in pure water at approximate 25°C.

<sup>d</sup> Approximate bulk price given as the price of 1 kg in US dollars. The price will depend on purity and technological grade of the CD.

#### 4.2.1.2 Cyclodextrin complexation process

Much of the interest in natural and modified CDs arises from their ability to include or encapsulate a substantial part of a guest molecule or ion inside their annuli to form complexes usually described as either inclusion complexes, host-guest complexes or simply as complexes.

CD inclusion is a molecular phenomenon in which usually only one guest molecule interacts with the cavity of a CDs molecule to become entrapped and form a stable association. Molecules or functional groups of molecules that are less hydrophilic than water, can be included in the CDs cavity in the presence of water. In order to complex, the “guest molecules” should fit, at least partly, into the CDs cavity. The cavity sizes as well as possible chemical modifications determine the affinity of CDs to the various molecules. In the case of some low molecular weight molecules, more than one guest molecule may fit into the cavity. Alternatively, some high molecular weight molecules may bind more than one CD molecule. Therefore a 1 to 1 molar ratio is not always achieved, which broadens the range of applications. The hydrophobic internal cavity provides the capability to form inclusion complexes with a variety of “guest” hydrophobic molecules (e.g. aromatics, alcohols, halides, fatty acids, esters, etc.) (Easton and Lincoln, 1999).

With their characteristic molecular structures, CDs are capable of forming inclusion complexes with various organic compounds which may be only sparingly soluble in water by incorporating them into the CD cavities. As a result, in aqueous solution, CDs can enhance apparent water solubility by forming dynamic, non-covalent, water-soluble inclusion complexes as depicted in Figure 4.4. This interaction is an equilibrium governed by an equilibrium constant,  $K_c$ . The nature of

the complex, as well as the numerical value of the equilibrium constant, can be derived from measuring a particular property of the complex as a function of organic compound and CD concentrations (Davis and Brewster, 2004).

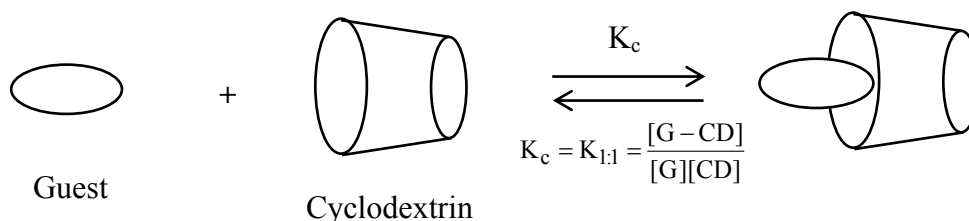


**Figure 4.4** Water-soluble inclusion complexes (Davis and Brewster, 2004).

#### 4.2.1.3 Application of cyclodextrin

CDs are able to form host-guest complexes with hydrophobic molecules given the unique nature imparted by their structure. As a result CDs have found a number of applications in a wide range of fields. The formation of the inclusion compounds greatly modifies the physical and chemical properties of the guest molecule, mostly in terms of water solubility. This is the reason why CDs have attracted much interest in many fields, such as foods, cosmetics, toiletries, agrochemicals, and especially pharmaceutical applications, because inclusion compounds of CDs with hydrophobic molecules are able to penetrate body tissues and then the biologically active guest compounds released under specific conditions. Cyclodextrin chemistry is now one of the important fields of supramolecular chemistry (Bassani, Krieger, Duchene, and Wouessidjewe, 1996; Duchene and Wouessidjewe, 1996; Szenté and Szejtli, 1999; Davis and Brewster, 2004; Challa *et al.*, 2005; Brewster and Loftsson, 2007). In the textile industry, CDs represent an

important group of auxiliaries in textile finishing. Savarino, Viscardi, Quagliotto, Montoneri, and Barni (1999) studied the reactivity and effect of CDs in textile dyeing compared to dyeing without CDs. They found that dyeing nylon 6,6 and microfibre nylon 6 fabrics in the presence of CDs improved the colour uniformity with only minor variations of colour yield. The dye molecules formed complexes with CDs and were confirmed by  $^1\text{H-NMR}$  data. They concluded that the positive effect on dyeing of CDs could be related to the relative stabilities of the dye-CDs complexes and to the relative rates of dye releasing from the complex and of diffusion through the fibre. Chemical modification of cotton cellulose in the fabric form was investigated through reaction with monochlorotriazinyl- $\beta$ -CD (Hebeish and El-Hilw, 2001). The results obtained indicated that the extent of reaction increased on increasing the reactive cyclodextrin (R-CD) concentration and on increasing the alkaline catalyst concentration, depending on the catalyst used. Crini (2003) studied the use of polymers containing  $\beta$ -CD for the sorption of dyes and found that  $\beta$ -CD polymers exhibited good adsorption properties towards dyes. The adsorption was affected through both physical adsorption and hydrogen bonding mediated via the polymer and  $\beta$ -CD host-guest interactions. The polymer strongly increased the sorption capacity. The study of the effect of the polymer particle size on dye removal showed that as the mean diameter of the polymer decreased, the adsorption capacity increased probably due to the increase in surface area. Moreover, Crini studied the influence of the  $\beta$ -CD content on the adsorption capacity. He found that the adsorption capacity increased with increasing the amount of  $\beta$ -CD, corresponding to increasing interactions between  $\beta$ -CD and the dyes. Therefore, the inclusion phenomena between  $\beta$ -CD and dyes played a major role in the adsorption mechanism. Savarino, Parlati, Buscaino,

Piccinini, Degani, and Barni (2004) used  $\beta$ -CD as a low environmental impact additive for the dyeing of nylon 6 and nylon 6,6 with a series of synthesized disperse dyes. Normally surfactants were employed as an additive but in this study  $\beta$ -CDs were used as an alternative. The low solubility of disperse dyes in water can be enhanced by the formation of complexes between  $\beta$ -CD and the dyes. Thermogravimetric analysis (TGA) and differential temperature analysis (DTA) studies were performed to evidence the formation of dye- $\beta$ -CD complexes. Dyeing tests in the presence of  $\beta$ -CD showed a positive effect on colour uniformity and intensity. Therefore,  $\beta$ -CD can be used as a leveling agent in the dyeing of polyamide fibres with disperse dyes.

Other works have been undertaken on the interaction of CDs or CD derivatives with dyes. Yuan, Zhu, and Han (1999) investigated the supramolecular inclusion complex formation and application of  $\beta$ -cyclodextrin with heteroanthracene ring cationic dyes.  $\beta$ -Cyclodextrin also forms 1:1 inclusion complexes with methylene blue, azure A, toluidine blue, resorcinol blue, neutral red, safranin T, indigo carmine and acridine orange in aqueous media. The formation constants were determined by differential pulse polarography and spectrophotometry (Yuan *et al.*, 1999). Supramolecular interaction in inclusion complexes have also been employed to immobilize dyes on an electrode. This gives high sensitivity and stable electrochemical behavior for  $\text{H}_2\text{O}_2$  detection at the  $\text{mmol L}^{-1}$  level by means of the supramolecular interaction between  $\beta$ -CD and dye molecules (Yuan *et al.*, 1999). Bikádi, Kurdi, Balogh, Szemán, and Hazai (2006) studied the complexation behavior of carotenoids with CDs using molecular-modelling and experimental methods. The aim of the investigation was to assist designing carotenoids with enhanced  $\text{H}_2\text{O}$

solubility using different CD derivatives. They found that the carotenoids interacted with  $\beta$ -CD derivatives but not with  $\alpha$ -CD or  $\gamma$ -CDs. Molecular-docking studies with carotenoid-CD complexes with a 1:1 stoichiometry could explain the capability of  $\beta$ -CDs to form complexes with carotenoids as opposed to  $\alpha$ -CDs and  $\gamma$ -CDs.

CDs can be also used to remove the dyes from aqueous solution (Crini, 2008). Batch adsorption experiments were carried out for the removal of basic dyes, namely C.I. Basic Blue 3, Basic Violet 3 and Basic Violet 10, from aqueous solutions using a CD-based polymer. The results showed that this adsorbent exhibited high adsorption capacities toward basic dyes and the kinetics of the process followed a pseudo-second order equation, suggesting that the rate limiting step may be chemisorption. The Freundlich isotherm gave the best correlation for the adsorption of basic dyes on the CD polymer material. The differences in adsorption capacities may be due to the effect of dye structure while the negative value of free energy change indicated the spontaneous nature of the adsorption.

There is no literature on possible complex formation of indigo dye and CDs to increase water solubility and use in indigo dyeing. However, the use of cyclodextrins and their derivatives as molecular reactors to template the formation of indigoid dyes has been studied (Easton, Harper, and Lincoln, 1998; Harper, Easton, and Lincoln, 2003; Easton, 2005). In this work cyclodextrin dimers were shown to bias competing reactions of indoxyl and isatin to give indigoid dyes. The effect of the cyclodextrin dimers, however, was to decrease the yield of both indigo and the isomeric dimer, indirubin. This effect of the cyclodextrin dimers to reduce the yields of the dyes is a consequence of the complexation of indoxyl and isatin increasing their effective steric bulk and reducing the frequency of their productive collisions.

The ability of CDs to form complexes with hydrophobic molecules has led to their usage in the improvement of water solubility of indigo dye in this research.

#### **4.2.2 Hydrotropic agents**

Hydrotropic agents have been used since 1916, but their mechanism of action is still under investigation. These compounds are extensively used in the detergent industry to obtain clear liquid formulations that preserve their aspect during usage and storage. These compounds can also increase the solubility of poorly water soluble organic compounds (Gonzalez, Nassar, and Zaniquelli, 2000; Mansur, Pires, Gonzalez, and Lucas, 2005). The effect of hydrotropic substances on the complexation of drugs with cyclodextrin and cyclodextrin derivatives has also been studied (Muller and Albers, 1991; Pederson, 1993). In these studies it was found that the hydrotropic agents, urea and nicotinamide, which disrupt the water structure, could help to increase the solubility of drugs. The structure disruptors such as urea and nicotinamide destabilize the water structure by destroying clusters of associated water molecules and releasing water of solvation. This is the actual hydrotropic effect, which produces a large displacement of the solubility isotherms in the direction of high complex solubility. Kongmuang (2002), who studied the aqueous solubility of riboflavin by urea, nicotinamide, and pyridine derivatives found that the aqueous solubility of riboflavin was increased by some pyridine derivatives. In these derivatives the heteroaromatic ring was important for enhancing solubility together with amide group substituents (particularly in the 3-position of the pyridine ring).



The improvement in the water solubility of indigo dye by using hydrotropic additives has been little studied. Nevertheless, Son, Lim, Hong, and Kim (2005) have investigated the effect of urea addition for indigo dyeing on polyester substrates. Urea was added to the leucoindigo dye bath at each dyeing temperature. This urea addition can impart a better solubilizing effect to leuco indigo molecules (in the acidic form) and a higher swelling effect on the fibre substrate. Thus, an increased dye build-up could be obtained by this method due to a greater ease of access of leuco indigo molecules to all parts of the swollen polyester substrate. Increased opportunities for hydrogen bonding to the leuco indigo and water molecules with urea, together with hydrogen bonding involving the polyester carbonyl groups and urea, could explain the increase in the former's solubility and the swelling effect in the latter case.

The aims of the work described in this chapter were to examine ways to improve the water solubility of indigo dye to enable direct dyeing onto silk (without the need for the reduction process). In particular, two methods to modify the water solubility of indigo dye were investigated: (i) complex formation of indigo with cyclodextrin and cyclodextrin derivatives, and (ii) the use of hydrotropic additives to modulate water solubility of the indigo dye. Also, the kinetics and thermodynamics of direct dyeing of silk with indigo (standard indigo and plant extracted indigo) by the acid dyeing process in the presence of a defined solubilizing agent (identified from the work in (i) or (ii) above) were to be investigated in order to obtain the optimized parameters for such indigo dyeing onto silk with a longer term view to potential application in the village context.

## 4.3 Experimental

### 4.3.1 Materials and Chemicals

- (1) Silk yarn from Chul Thai Silk Co., Ltd in Phetchabun, Thailand
- (2) Indigo [482-89-3],  $C_{16}H_{10}N_2O_2$ , MW 262.26, Sigma Aldrich
- (3) Natural plant-derived indigo dye (from *Indigofera tinctoria*), Nakhon Ratchasima and Sakonnakhon, Thailand
- (4) Urea,  $NH_2CONH_2$ , MW 60.06, Sigma Aldrich
- (5) Nicotinamide,  $C_6H_6N_2O$ , MW 122.12, Sigma Aldrich
- (6) N-Acetylglycine (Aceturic acid),  $CH_3CONHCH_2CO_2H$ , MW 117.10, BDH
- (7)  $\gamma$ - cyclodextrin, Aldrich
- (8) (2-Hydroxypropyl)- $\beta$ -cyclodextrin , average MW 1,540, Aldrich
- (9)  $\beta$ - cyclodextrin sulfated  $Na^+$  salt, Sigma Aldrich
- (10) Glacial acetic acid,  $CH_3COOH$ , Merck
- (11) Ammonium acetate,  $CH_3COONH_4$ , Carlo erba
- (12) Hydrochloric acid 37% (w/v), HCl, Merck

### 4.3.2 Instruments

- (1) An Agilent 8453 UV-Vis spectrophotometer was employed to determine the concentration of dye samples through absorbance measurements using quartz cells of path length 1 cm at the characteristic maximum wavelength.
- (2) A pH meter (Laboratory pH Meter CG 842, SCHOTT, UK) was used to measure the pH values of solutions.

(3) An Ultrasonic Cleaner bath (Model-575 HT, frequency 38.5-40.0 kHz, average power 135 Watts, peak power 405 Watts, Crest Ultrasonics Corp., Trenton, NJ, USA) was used to sonicate the mixture of indigo: additives.

(4) A thermostatted shaker bath (Type SBD-50 cold, Heto-Holten A/S, Denmark) operated at 150 strokes/min, was used to study the adsorption kinetics and thermodynamics of indigo-additive solution onto silk yarn.

### **4.3.3 Experimental methods**

#### **4.3.3.1 Silk yarn preparation (Chairat, 2004)**

The silk yarn used was purchased from Chul Thai Silk Co., Ltd in Phetchabun, Thailand. Prior to using in the dyeing experiment, the silk yarn (1 kg) was treated with 0.5 M HCl (*ca* 3 L) at room temperature for 30 min and then removed and washed with deionized water until the rinsed water was neutral. The silk yarn was then dried at room temperature.

#### **4.3.3.2 Solubility studies and complex preparation**

The solubility of indigo was determined by adding indigo (mg amounts) and CDs (mg amounts) with increasing concentration of CDs to deionized water and the suspension formed adjusted to a pH 4.0 with 10% v/v of acetic acid/acetate buffer (total volume 100 mL). The pH of 4.0 is the optimum pH for the comparable acid dyeing of indigo carmine (as a water soluble indigo derivative) onto silk which was investigated in Chapter III. Typically, five samples with the following molar ratio indigo:CDs were prepared, 1:1 to 1:5. The suspensions formed were sonicated for 2 hr (when equilibrium was reached) in the ultrasonic bath at a

temperature of 40°C ( $\pm 5^\circ\text{C}$ ). After cooling to room temperature, the indigo:CD complexes were filtered. The supernatant indigo:CD complex dye solutions were analyzed by using UV-visible spectrophotometry at the maximum adsorption wavelength. The concentrations of the indigo:CDs complex dye solutions were calculated from a calibration curve.

Preparation of the indigo: hydrotropic additive (urea, nicotinamide and or N-acetylglycine) solutions were prepared in the the same way as the CD complex solutions.

#### **4.3.3.3 Batch kinetic experiments of indigo-urea dyeing onto silk**

The batch technique was used to examine the dyeing process at temperatures of 30, 40 and 50°C. The dyeing process was scrutinized by taking a series of 125 mL conical flasks containing the aqueous solution of indigo-urea over the concentration range 10-40 mg/L at pH 4.0 (adjusted by using acetic acid-acetate buffer). The dye solution in each conical flask was shaken in a thermostatted shaker bath operated at 150 strokes/min and controlled temperature. After 30 min, the silk yarn (0.50 g), which had been pre-warmed in the thermostatted bath for 30 min, was immersed in the dye solution. The silk samples were then rapidly withdrawn after different immersion times. The concentration of the unadsorbed indigo-urea in the supernatant dye solution was determined at time zero and at subsequent times using a calibration curve based on absorbance at  $\lambda_{\text{max}}$  (709 nm) versus dye concentration. The amount of dye adsorbed per gram of silk ( $q_t$ ) (mg/g silk) at any time was calculated by a mass balance relationship (Eq. (2.20)).

#### **4.3.3.4 Batch equilibrium experiments of indigo-urea dyeing onto silk**

The aqueous solutions of indigo-urea were prepared to the required concentrations and the pH of the dye solution was adjusted to 4.0 by using acetic acid-acetate buffer. The experiments were carried out by shaking silk yarn (0.50 g) with different concentrations of dye solution (50 mL) in a conical flask in a thermostatted shaker bath operated at 150 strokes/min and controlled temperature. The concentration of the unadsorbed indigo-urea in the supernatant dye solution was determined at time zero and at equilibrium times using a calibration curve based on absorbance at  $\lambda_{\max}$  (709 nm) versus dye concentration. The amount of dye adsorbed per gram of silk ( $q_e$ ) (mg/g silk) at equilibrium time was calculated by a mass balance relationship (Eq. (2.21)).

#### **4.3.3.5 Batch kinetic experiments of plant extracted indigo-urea dyeing onto silk**

The plant extracted indigo-urea dye solution was prepared from plant extracted indigo (indigo-village) at the desired concentration. The dyeing process was performed at temperatures of 30, 40 and 50°C. The dye solution (50 mL) in each conical flask was shaken in a thermostatted shaker bath operated at 150 strokes/min and controlled temperature. After 30 min, the silk yarn (0.50 g), which had been pre-warmed in the thermostatted bath for 30 min, was immersed in the dye solution. The silk samples were then rapidly withdrawn after different immersion times. The concentration of the unadsorbed plant extracted indigo-urea in the supernatant dye solution was determined at time zero and at subsequent times using a calibration

curve based on absorbance at  $\lambda_{\max}$  (656 nm) versus dye concentration. The amount of dye adsorbed per gram of silk ( $q_t$ ) (mg/g silk) at any time was calculated by a mass balance relationship (Eq. (2.20)).

#### **4.3.3.6 Batch equilibrium experiments of plant extracted indigo-urea dyeing onto silk**

The plant extracted indigo-urea dye solution was prepared from plant extracted indigo (indigo-village) at the required concentration. The dyeing process was performed with a MLR of 1:100 and at a temperature of 30°C. Silk yarn (0.50 g) and 50 mL of the plant extracted indigo-urea dye solution were put in a 125 mL flask and were shaken for 60 min by using a thermostatted shaker bath operated at 150 strokes/min and controlled temperature. The concentration of the unadsorbed plant extracted indigo-urea in the supernatant dye solution was determined at time zero and at equilibrium times using a calibration curve based on absorbance at  $\lambda_{\max}$  (656 nm) versus dye concentration. The amount of dye adsorbed per gram of silk ( $q_e$ ) (mg/g silk) at equilibrium was calculated by a mass balance relationship (Eq. (2.21)).

## 4.4 Results and Discussion

### 4.4.1 Improvement in the water solubility of indigo dye for dyeing directly onto silk

In order to investigate improvement in the water solubility of indigo dye for dyeing directly onto silk, modification of indigo water solubility dye was assessed via: (i) complex formation of indigo with cyclodextrin and cyclodextrin derivatives, and (ii) additive (hydrotropic agent) addition to the aqueous solution. Complex formation studies of indigo with  $\gamma$ -cyclodextrin ( $\gamma$ -CD),  $\beta$ -cyclodextrin sulfated sodium salt ( $\beta$ -CD sulfated  $\text{Na}^+$  salt) and 2-hydroxypropyl- $\beta$ -cyclodextrin (2HP- $\beta$ -CD) and also the effect of hydrotropic additives (such as urea, nicotinamide, and N-acetylglycine) on indigo water solubility were performed at a pH 4.0 of the solution (a suitable pH for the acid dyeing of silk study discussed in sections 4.4 and 4.5). Concentrations of dye solutions were studied using UV-visible spectrophotometry.

#### 4.4.1.1 Complex formation of indigo with cyclodextrin and cyclodextrin derivatives

The effect of CDs on the water solubility of indigo at *ca* 40°C is shown in Table 4.3. The maximum water solubility of indigo itself at pH 4.0 was 0.2 mg in 100 mL of solution and this dye solution had a maximum absorption wavelength ( $\lambda_{\text{max}}$ ) at 708 nm. The water solubility of indigo was increased when various types of CDs were added in these solutions. The maximum absorption wavelengths on complex equilibria formation of indigo with  $\gamma$ -CD),  $\beta$ -CD sulfated  $\text{Na}^+$  and 2HP- $\beta$ -CD in the aqueous solution (under acid conditions) were 713, 706, and 709 nm,

respectively. The absorption spectra of the indigo-2HP- $\beta$ CD complexes are displayed in Figure 4.5, together with the effects of added hydrotropic agents (section 4.4.1.2) for comparison. A noticeable water solubility enhancement for indigo could be obtained by its complexation with 2HP- $\beta$ -CD in the molar ratio 1:1 (Figure 4.6), and this enhancement was generally better than that observed with hydrotropic additives (Figure 4.6). The good solubility of the complex makes possible the preparation of aqueous solutions of indigo. Presumably the increase in solubility is due to complexation of the water insoluble indigo by the water soluble 2HP- $\beta$ -CD, but further studies would be necessary to determine the precise details of any such complexation.

**Table 4.3** Effect of CDs on the solubility of indigo (molar ratio (indigo:CDs) = 1:1, sonication time = 2 hr, bath temp. = 40 ( $\pm$ 5 $^{\circ}$ C).

<b>Indigo (mg)</b>	<b>CDs</b>	<b>Absorbance</b>	<b><math>\lambda_{\max}</math> (nm)</b>	<b>C (mg/L)</b>
0.2	-	0.0077	708	2.20
0.5	$\gamma$ -CD (2.47 mg)	0.0257	713	7.16
0.5	$\beta$ -CD sulfated Na <sup>+</sup> salt (4.21 mg)	0.0355	706	9.91
0.5	2HP- $\beta$ -CD (2.94 mg)	0.0242	709	6.74
5.0	2HP- $\beta$ -CD (29.4 mg)	0.9375	709	46.36



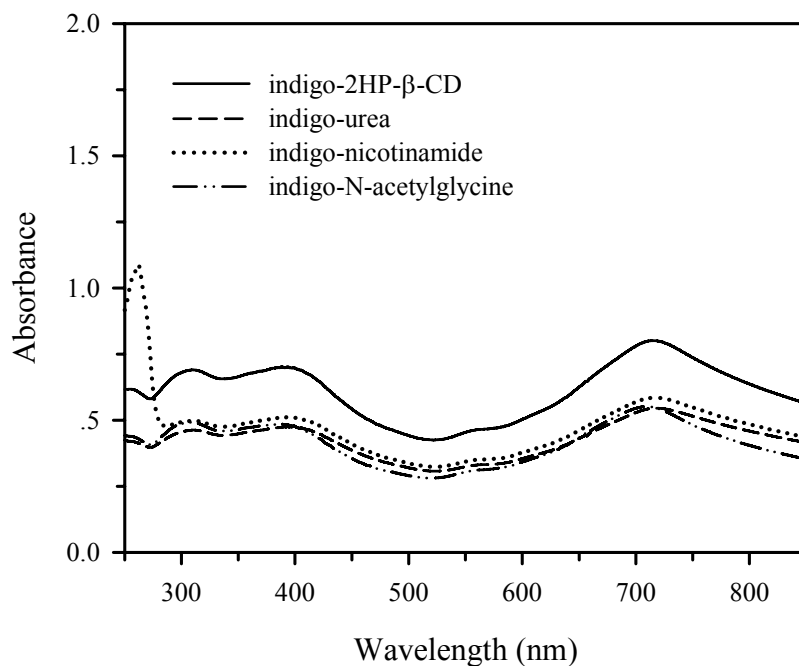


**Figure 4.5** UV-spectrum of indigo: 2HP- $\beta$ -CD complexes and indigo:additives (as urea, nicotinamide, and N-acetylglycine).

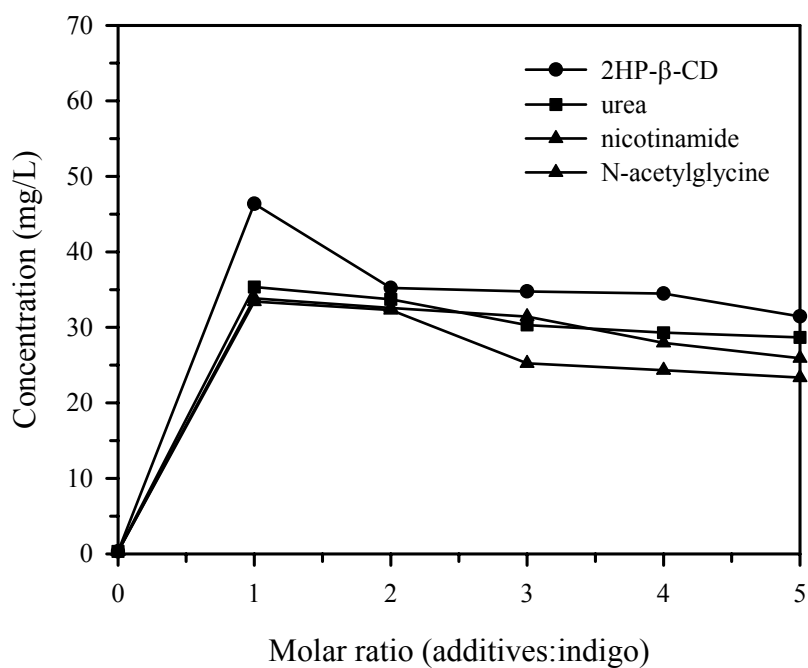


**Figure 4.6** Effect of the amount of 2HP- $\beta$ -CD, urea, nicotinamide, and N-acetylglycine on the water solubility of indigo.

#### 4.4.1.2 Additives to modulate water solubility of indigo dye

The effect of hydrotropic agents such as urea, nicotinamide and N-acetylglycine on the water solubility of indigo is shown in Table 4.4. The maximum water solubility of indigo by itself at pH 4.0 was 0.2 mg in 100 mL of solution and this dye solution gave a maximum absorption wavelength at 708 nm. The water solubility of indigo was increased when various types of hydrotropic agents were added in these solutions. The increase of the indigo dye concentration using urea, nicotinamide and N-acetylglycine as additives each showed a similar result with a 1:1 molar ratio (indigo:additive). The maximum absorption wavelengths ( $\lambda_{\max}$ ) of the indigo with urea, nicotinamide and N-acetylglycine in the aqueous solution (under acid conditions) were 709, 708, and 703 nm, respectively. The uv-visible absorption spectra for each of the mixed solutions are displayed in Figure 4.5.

The effect of the amount of urea, nicotinamide and N-acetylglycine on the water solubility of indigo was also studied. The optimum molar ratio of indigo with urea (or nicotinamide or N-acetylglycine) for the improvement of the water solubility of indigo are 1 to 1 (Figure 4.6). The water solubility of the indigo could be improved because the hydrotropic agents destabilize the water structure by breaking up the hydrogen bonding networks among water molecules by increasing H-bonding opportunities between themselves and water in view of the functional groups they contain (good H-bond acceptors and H-bond donors). This is the actual hydrotropic effect, which produces a large displacement of the solubility isotherms in the direction of high complex solubility (Muller and Albers, 1991). In addition, hydrotropic agents can act as a bridge between the solubilised dye and the aqueous media (Hamlin, Phillip, and Whiting, 1999). The proposed interaction of indigo with urea and the urea

with water is shown in Figure 4.7. The good efficacy of urea in increasing the water solubility of indigo, together with the fact it is non-expensive, resulted in its choice as a suitable additive for the preparation of the indigo aqueous solution for the adsorption kinetic and thermodynamic studies of direct dyeing onto silk (Section 4.4.2) and also for the study of plant extracted indigo direct dyeing onto silk (Section 4.4.3).

**Table 4.4** Effect of additives on the solubility of indigo (molar ratio (indigo:additive) = 1:1, sonication time = 2 hr, bath temp. = 40 ( $\pm 5^\circ\text{C}$ )).

<b>Indigo (mg)</b>	<b>Additives</b>	<b>Absorbance</b>	<b><math>\lambda_{\text{max}}</math> (nm)</b>	<b>C (mg/L)</b>
0.2	-	0.0077	708	2.20
5.0	Urea(1.15 mg)	0.7294	709	35.35
5.0	Nicotinamide(2.33 mg)	0.7717	708	33.40
5.0	N-acetylglycine(2.23 mg)	0.6987	703	33.85
250 <sup>a</sup>	Urea(1.15 mg)	0.7053	656	34.17

<sup>a</sup>Plant extracted indigo contained indigo  $\sim 5.0$  mg.

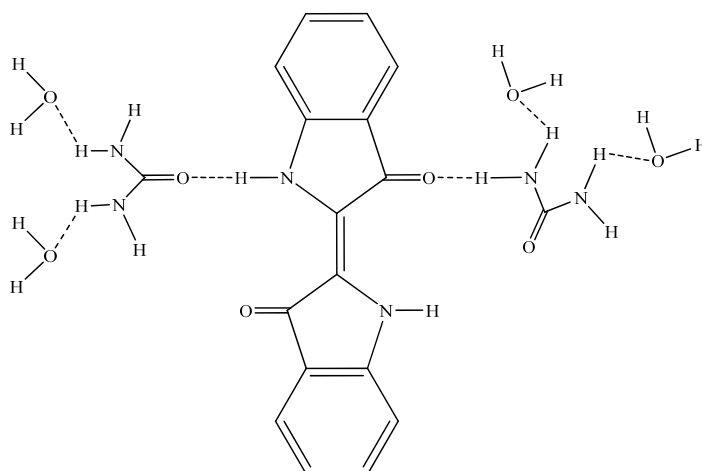


**Figure 4.7** The proposed interaction of indigo with urea.

Prior to the relevant adsorption kinetic and thermodynamic studies, the effect of urea on the water solubility of indigo compared with plant extracted indigo was also assessed. It was possible that other components present in the plant extracted indigo could influence the hydrotropic effect in some way. The absorption spectra of indigo-urea and plant extracted indigo-urea are displayed in Figure 4.8. There are clear differences between the absorption spectra in the UV region ( $\lambda < 400$  nm) but the differences between the absorption spectra in the visible region ( $\lambda > 400$  nm) were not so great. The maximum absorption wavelengths ( $\lambda_{\text{max}}$ ) of the urea with indigo and plant extracted indigo are 709 and 656 nm, respectively. Generally, natural indigo contains various impurities including indirubin (an isomer of indigo), tannin and flavonoids (Kawahito, 2006). As the indirubin is red, its absorption maximum will be at a shorter wavelength than the blue indigo (standard)-urea solution. The optimum molar ratio for the improvement of water solubility of the plant extracted indigo-urea was 1:1, the same as for indigo-urea (Figure 4.9).

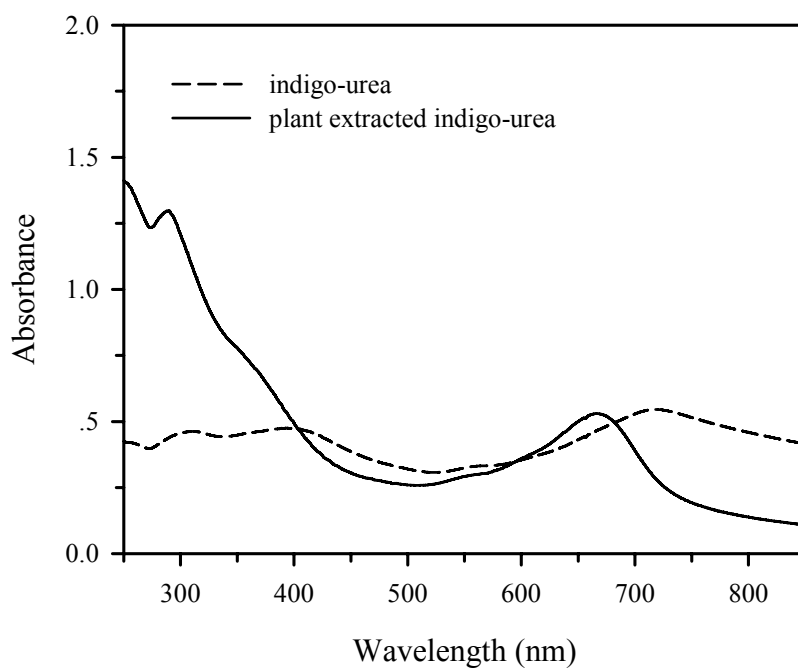


**Figure 4.8** UV-spectrum of indigo:urea and plant extracted indigo:urea.

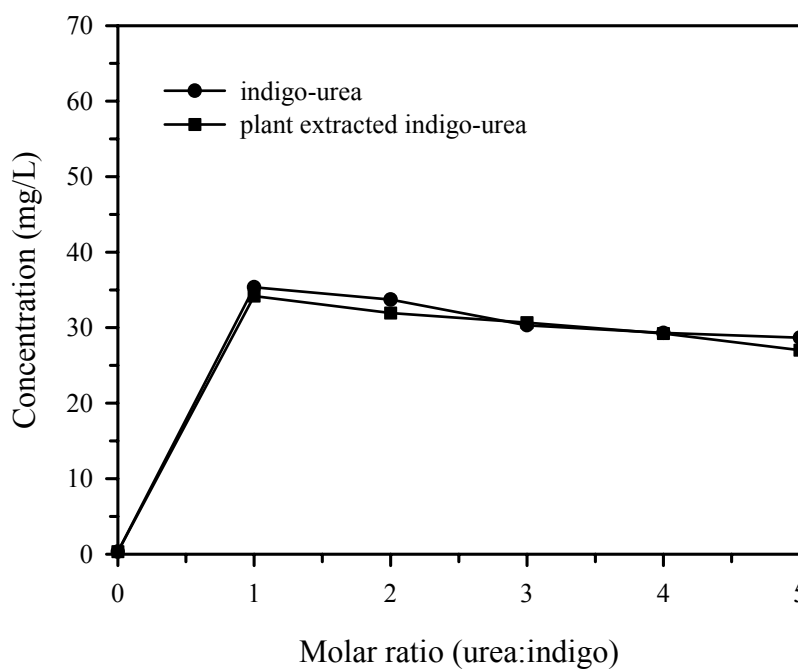


**Figure 4.9** Effect of the amount of urea on the water solubility of indigo and plant extracted indigo.

#### **4.4.2 Adsorption kinetic and thermodynamic studies of indigo-urea dyeing onto silk without a reduction process**

In order to investigate the adsorption of indigo-urea onto silk without a reduction process, the experimental parameters including initial dye concentration, contact time, material to liquor ratio (MLR), and temperature were determined to find the optimal conditions for adsorption. The general mechanism of the adsorption of indigo-urea onto silk was investigated by using the pseudo first order and pseudo second order kinetic models. The best-fit model was selected based on the linear regression correlation coefficient,  $R^2$  values. The thermodynamic parameters have been also investigated in this section.

##### **4.4.2.1 Effect of initial dye concentration and contact time on the adsorption of indigo-urea onto silk**

The adsorption of indigo-urea at different initial dye concentrations onto silk at pH 4.0 in the dye bath, MLR = 1:100 and 30°C was investigated as a function of contact time in order to determine the equilibrium time for maximum adsorption. A plot of the amount of dye adsorbed per gram silk ( $q_t$ ) (mg/g silk) at any time versus contact time ( $t$ ) is shown in Figure 4.10. It was found that the dye adsorption rate for each initial dye concentration attained equilibrium after 60 min. These result showed similar trends to those for the adsorption of indigo onto silk by the conventional vat-dyeing process (Chapter II) and with the adsorption of indigo carmine (as a water soluble indigo derivative) onto silk (Chapter III). An increase of the dye concentration accelerates the diffusion of dyes from the dye solution onto silk

due to the increase in the driving force of the concentration gradient (Chairat, Rattanaphani, Bremner, and Rattanaphani, 2005).

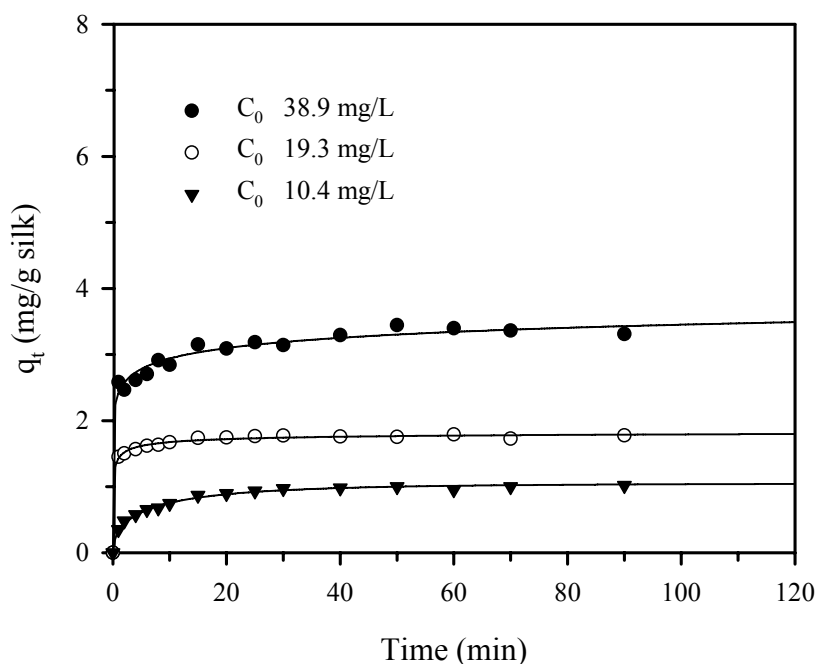


**Figure 4.10** Effect of initial dye concentration on the adsorption of indigo-urea onto silk (under dyeing condition MLR = 1:100, pH = 4.0, 30°C).

The results of rate constant studies for different initial dye concentrations by using the pseudo first order and pseudo second order kinetic models are listed in Table 4.5 and pseudo first order and pseudo second order plots are shown in Figure 4.11 and Figure 4.12 are, respectively. The pseudo second order kinetic model well described the adsorption of indigo dye onto silk over range of desired initial dye concentration with a high correlation coefficient ( $R^2 > 0.99$ ). This suggested that the overall rate of the indigo dye adsorption onto silk is controlled by chemisorption. A similar phenomenon had also been observed in the adsorption of

indigo onto silk by the conventional vat-dyeing process (Chapter II) and with the adsorption of indigo carmine onto silk (Chapter III) and also the acid dyeing with other dyes (Chairat *et al.*, 2005; Septhum, Rattanaphani, Bremner, and Rattanaphani, 2009). An increase in initial dye concentration results in a significant increase in  $q_{e,cal}$ . The  $q_{e,cal}$  for initial dye concentration also increased with an increasing of initial dye concentration.

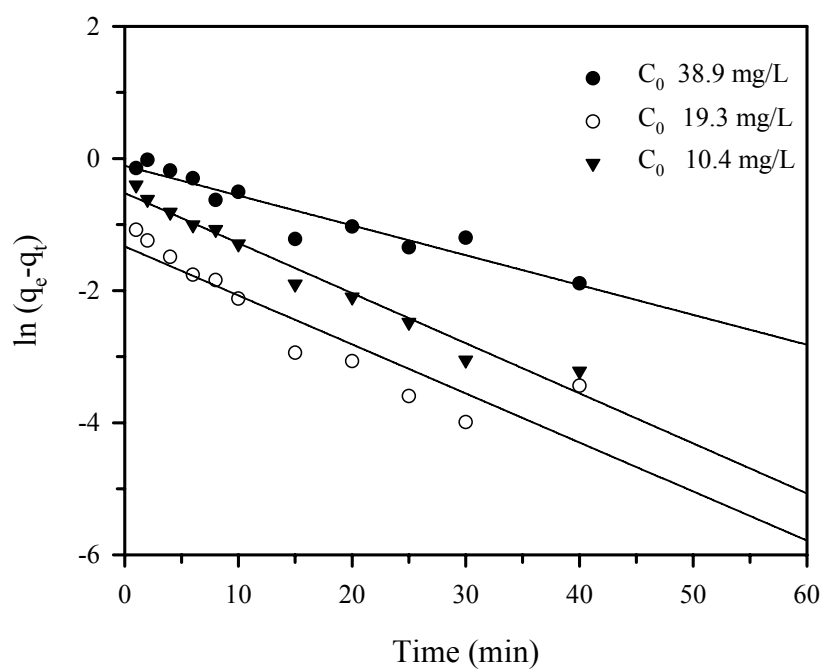


**Figure 4.11** Application of the pseudo first order equation at different initial dye concentration on the adsorption of indigo-urea onto silk.



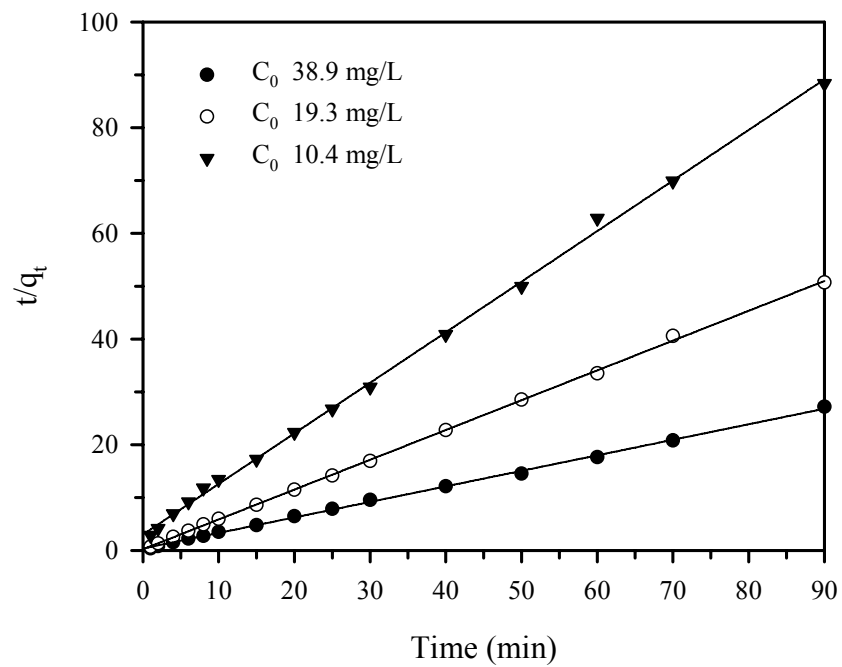


**Figure 4.12** Application of the pseudo second order equation at different initial dye concentration on the adsorption of indigo-urea onto silk.

**Table 4.5** Comparison of the pseudo first- and pseudo second-order adsorption rate constants and the calculated and experimental  $q_e$  values for different initial dye concentrations, MLR and temperature for the adsorption of indigo-urea onto silk.

Parameter	$q_{e,exp}$ (mg/g silk)	Pseudo first order model			Pseudo second order model			
		$k_1$ ( $\text{min}^{-1}$ )	$q_{e,cal}$ (mg/g silk)	$R^2$	$k_2$ (g silk/mg min)	$q_{e,cal}$ (mg/g silk)	$h_i$ (mg/g silk min)	$R^2$
<i>Initial dye concentration: <math>C_0</math> (mg/L): MLR 1:100, temp. 30 °C, contact time 60 min</i>								
10.4	1.02	0.0758	0.59	0.9700	0.3038	1.04	0.3317	0.9987
19.3	1.79	0.0742	0.26	0.8476	1.3915	1.77	4.3745	0.9996
38.9	3.44	0.0452	0.89	0.9045	0.2345	3.40	2.7152	0.9990
<i>MLR: <math>C_0</math> 19.3 mg/L, temp. 30 °C, contact time 60 min</i>								
1:50	0.84	0.0483	0.07	0.5367	1.9893	0.84	1.9893	0.9999
1:100	1.79	0.0742	0.26	0.8476	1.3915	1.77	4.3745	0.9996
1:150	2.59	0.0735	0.96	0.8532	0.2266	2.60	1.5356	0.9996
<i>Temperature: <math>C_0</math> 19.3 mg/L, MLR 1:100, contact time 60 min</i>								
30	1.79	0.0742	0.26	0.8476	1.3915	1.77	4.3745	0.9996
40	1.03	0.0676	0.32	0.8756	0.7370	1.04	0.8017	0.9995
50	0.88	0.0493	0.22	0.8100	0.4388	0.89	0.3448	0.9996

#### **4.4.2.2 Effect of material to liquor ratio (MLR) on the adsorption of indigo-urea onto silk**

The effect of MLR on the adsorption of indigo onto silk at an initial dye concentration of 20 mg/L at pH 4.0 and 30°C is shown in Figure 4.13. It was found that an increase in volume of the dye solution resulted in an increase of the dye adsorbed onto the silk, consistent with the yarn being more loosely packed in the higher volume of dye solution. This allows the dye solution to move more readily over the silk surfaces with associated dye molecule binding, and then into the interior of the silk yarn by diffusion. Kinetic parameters from linear plots of pseudo first order (Figure 4.14) and pseudo second order (Figure 4.15) models are given in Table 4.5. The data show a good compliance with the pseudo second order equation and the regression coefficients,  $R^2$ , for the linear plot were all high ( $> 0.99$ ). The overall rate of the indigo adsorption processes appears to be controlled by the chemical process in this case in accordance with the pseudo second order reaction mechanism. The amount of dye adsorbed of MLR 1:150 showed highest values when compare with MLR 1:100 and 1:50 (Figure 4.13). However, in order to minimize waste from the dyeing process, an MLR of 1:100 was used for all the kinetic experiments.

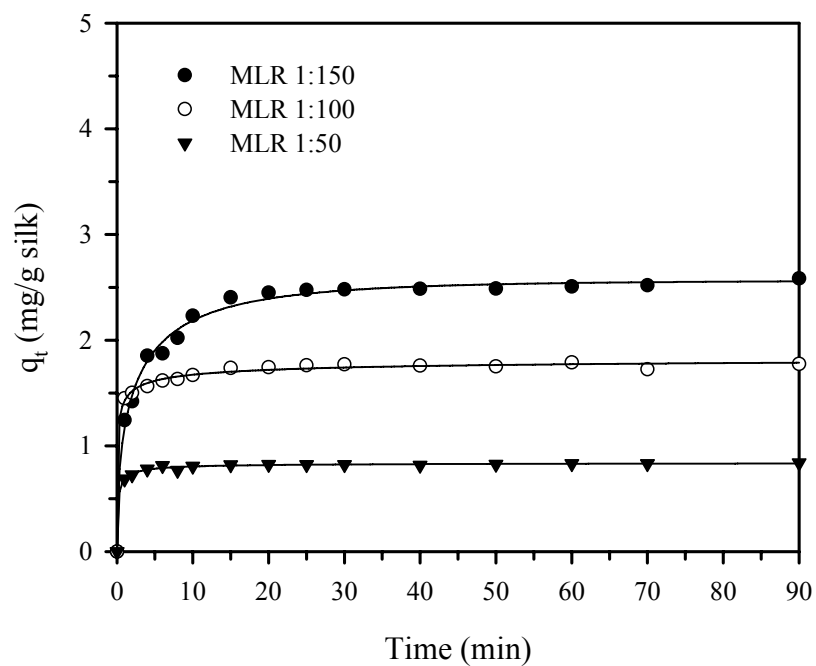


**Figure 4.13** Effect of MLR on the adsorption of indigo-urea onto silk (under dyeing condition  $C_0 = 20$  mg/L, pH = 4.0, 30°C).

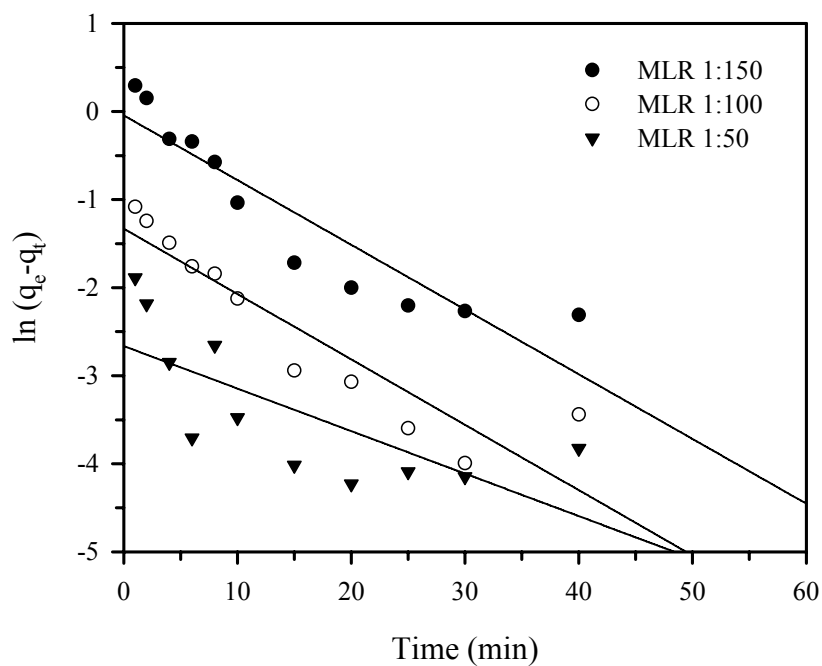


**Figure 4.14** Application of the pseudo first order equation at different MLRs on the adsorption of indigo-urea onto silk.

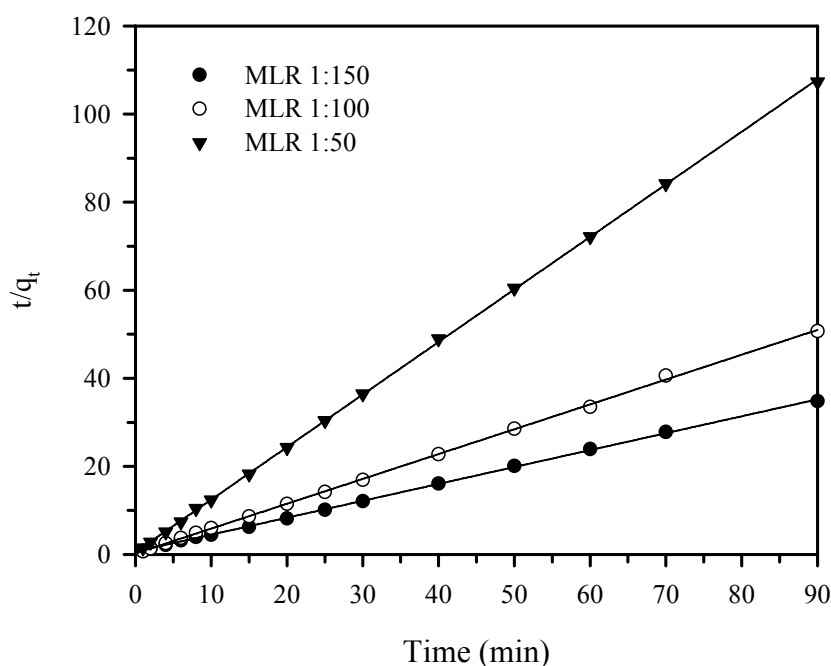


**Figure 4.15** Application of the pseudo second order equation at different MLRs on the adsorption of indigo-urea onto silk.

#### 4.4.2.3 Effect of temperature on the adsorption of indigo-urea onto silk

The dye adsorption process was studied at different temperatures of 30, 40 and 50°C, and pH 4.0, MLR = 1:100, and an initial dye concentration of 20 g/L in each case. The effect of temperature on adsorption of indigo onto silk is shown in Figure 4.16. The amount of the dye adsorbed per gram of silk decreased with increasing the temperature suggesting that the adsorption of indigo onto silk is controlled by an exothermic process. Similar temperature effect trends on adsorption were seen in the case of the adsorption of indigo onto silk by the conventional vat-dyeing process (Chapter II) and with the adsorption of indigo carmine onto silk

(Chapter III) and also the acid dyeing with other dyes (Chairat *et al.*, 2005; Septhum *et al.*, 2009). Table 4.5 lists the results of rate constant and other kinetic parameter studies for different temperatures calculated by the pseudo first order (Figure 4.17) and pseudo second order (Figure 4.18) models. The correlation coefficient,  $R^2$ , for the pseudo second order adsorption model has a higher value suggesting the dye adsorption occurs process is predominantly by the pseudo second order adsorption mechanism.

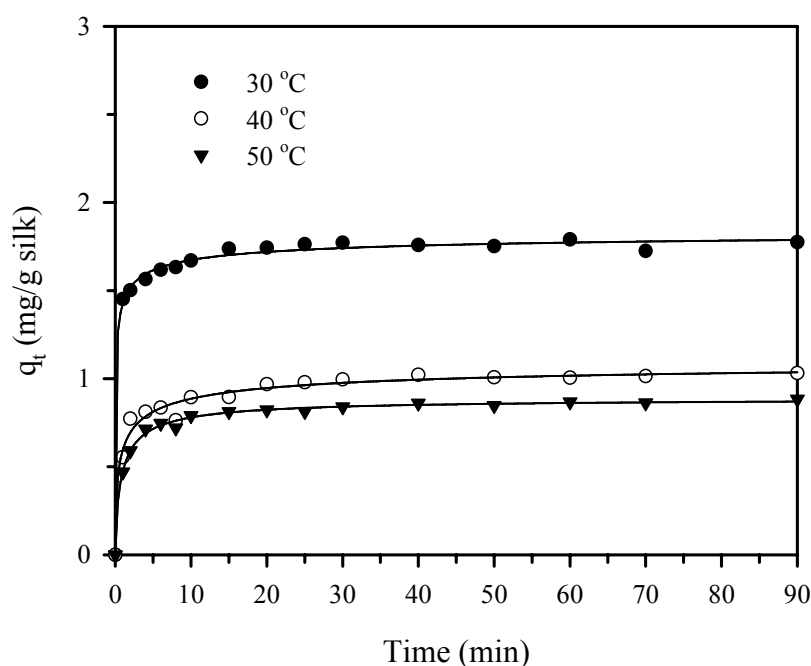


**Figure 4.16** Effect of temperature on the adsorption of indigo-urea onto silk (under dyeing condition  $C_0 = 20$  mg/L, pH = 4.0, MLR = 1:100).

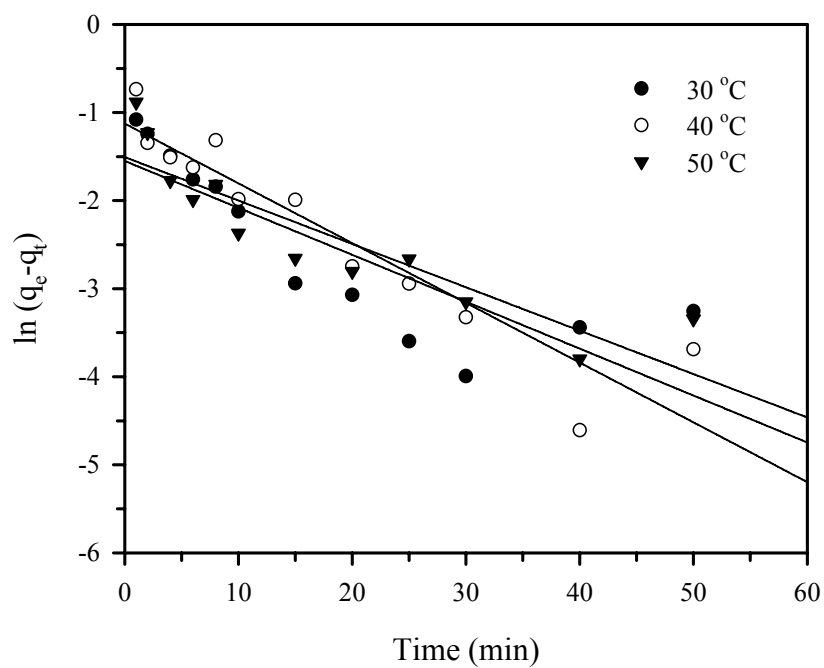


**Figure 4.17** Application of the pseudo first order equation at different temperatures on the adsorption of indigo-urea onto silk.

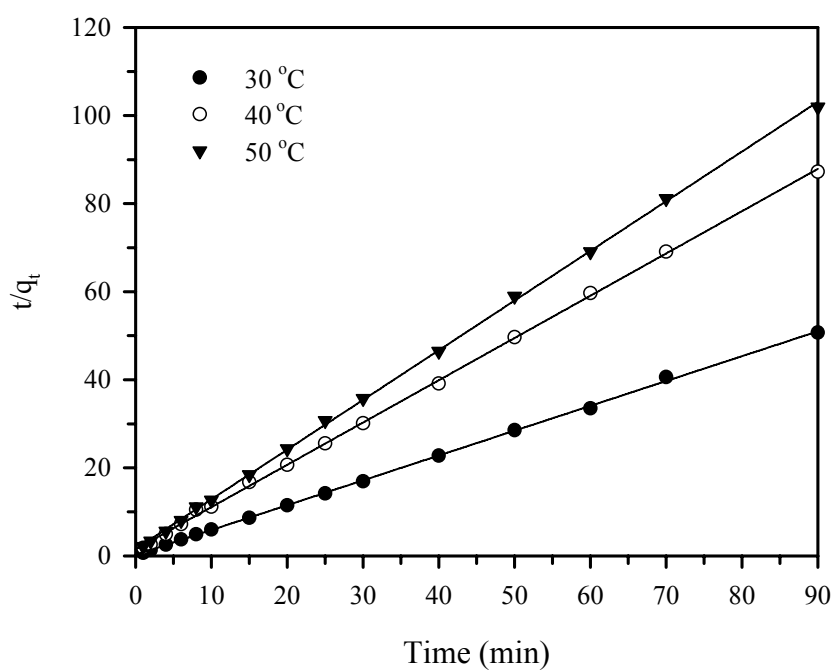


**Figure 4.18** Application of the pseudo second order equation at different temperatures on the adsorption of indigo-urea onto silk.

#### 4.4.2.4 Activation parameters for the adsorption of indigo-urea onto silk

The rate constants  $k_2$  for the pseudo second-order model at different temperatures (Table 4.5) were then applied to estimate the activation energy of the adsorption of indigo-urea onto silk by the Arrhenius equation. The slope of the plot of  $\ln k_2$  versus  $1/T$  (Figure 4.19) was used to evaluate  $E_a$  as listed in Table 4.6.

The magnitude of  $E_a$  may then give an indication of whether a physical or chemical adsorption process is in operation. In physical adsorption (physisorption) the interaction is easily reversible, equilibrium is rapidly attained and its energy requirements are small so  $E_a$  is usually no more than 5-40 kJ/mol, because usually weak intermolecular forces are involved. However, with chemical adsorption (chemisorption) much stronger bonding forces are involved and  $E_a$  values range from 40-800 kJ/mol (Nollet, Roels, Lutgen, Van der Meeren, and Verstraete, 2003). For the  $E_a$  of 46.88 kJ/mol observed we can infer that the adsorption of indigo-urea onto silk is most likely occurring by a chemisorption process.

**Table 4.6** Activation parameters for the adsorption of indigo-urea onto silk at initial dye concentration 20 mg/L.

Temp. (°C)	$k_2$ (g silk/ mg min)	$E_a$ (kJ/mol)	$R^2$	$\Delta H^\#$ (kJ/mol)	$\Delta S^\#$ (J/mol K)	$\Delta G^\#$ (kJ/mol)	$R^2$
30	1.3915					172.62	
40	0.7370	46.88	0.9984	49.58	-406.04	176.68	0.9986
50	0.4388					180.74	



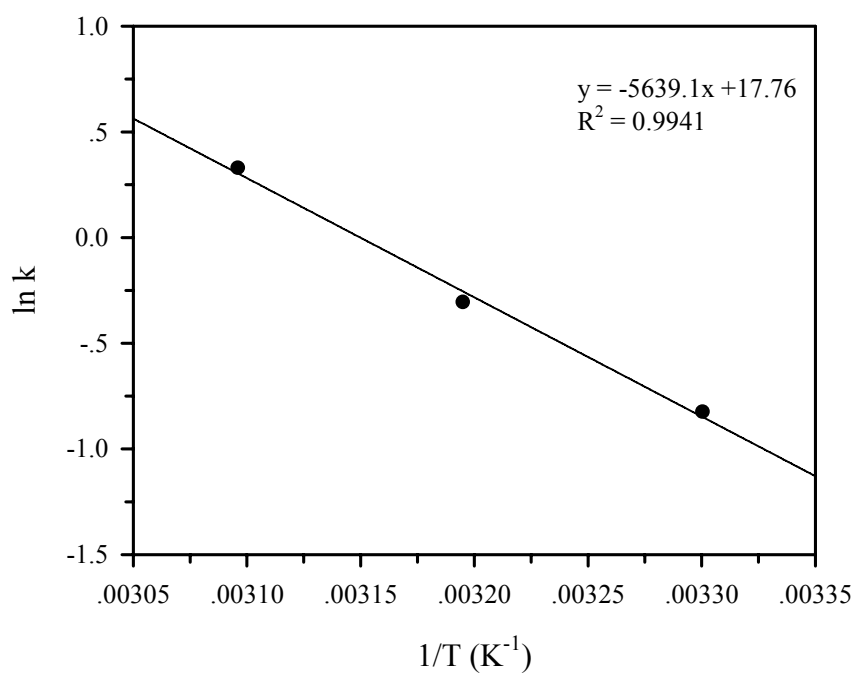


**Figure 4.19** Arrhenius plot for the adsorption of indigo-urea on silk.

From the Eyring equation, the enthalpy ( $\Delta H^\ddagger$ ) and entropy ( $\Delta S^\ddagger$ ) of activation were calculated from the slope and intercept of a plot of  $\ln(k/T)$  versus  $1/T$  (Figure 4.20) as listed in Table 4.6. The value of  $\Delta G^\ddagger$  was calculated at 303, 313 and 323 K by using equation (2.10) and these values are listed in Table 4.6, the negative entropy value ( $\Delta S^\ddagger$ ) reflects more aggregation and the interaction between indigo and the silk yarn.

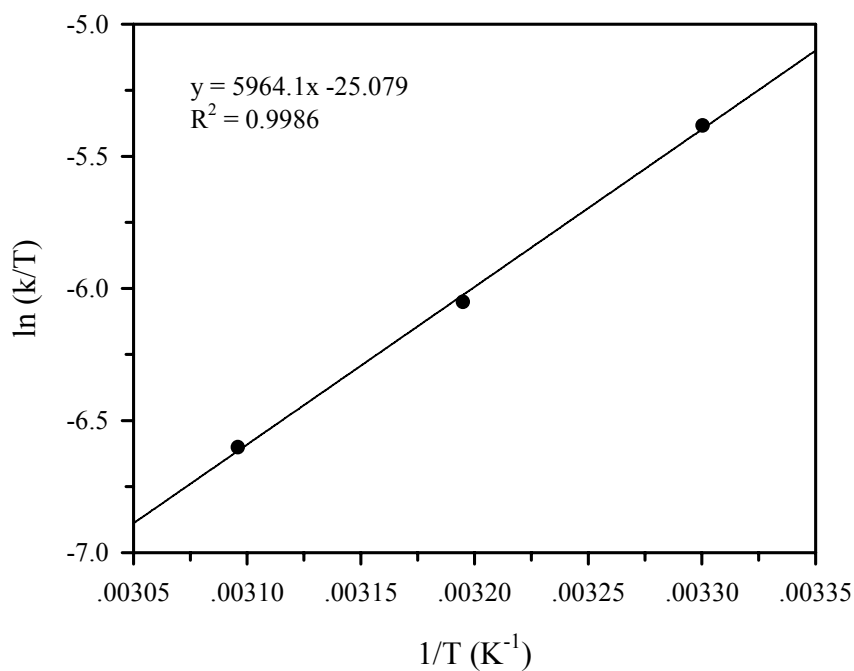


**Figure 4.20** Plot of  $\ln(k/T)$  against  $1/T$  for the adsorption of indigo-urea on silk.

#### 4.4.2.5 Adsorption isotherm for the adsorption of indigo onto silk

The adsorption isotherm of indigo dyeing onto silk under the conditions of an MLR of 1:100 in the initial dye concentration range 20-200 mg/L at 30, 40 and 50°C is shown in Figure 4.21. It was found that the amount of dye adsorbed per unit weight of fibre at equilibrium,  $q_e$  decreased with increasing temperature, thereby indicating the process is exothermic.

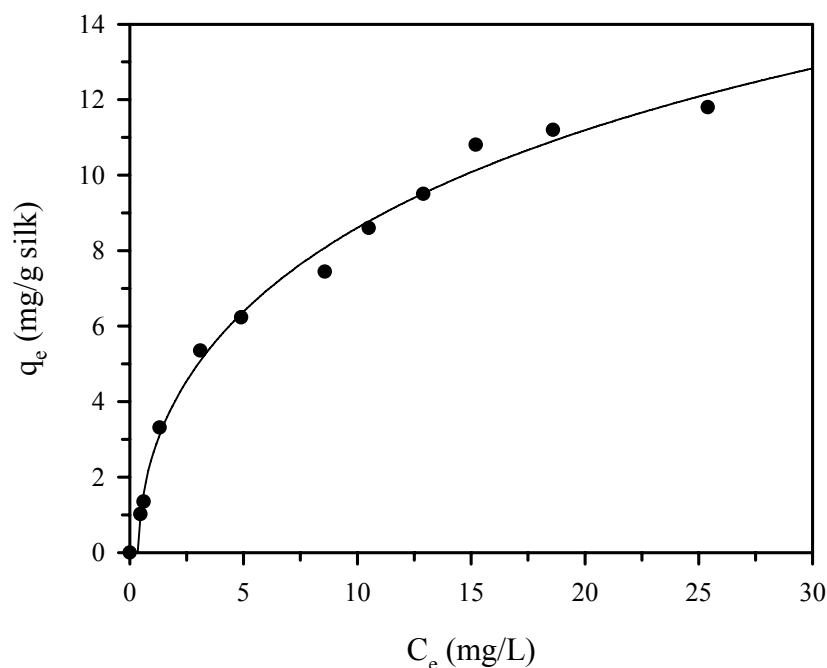


**Figure 4.21** Adsorption isotherms of indigo-urea onto silk at 30°C.

The Langmuir adsorption model was used to describe the characteristic adsorption based on the assumption that adsorption takes place at specific homogeneous sites on the surface. It is then assumed that once a dye molecule occupies a site, no further adsorption can take place at that site. When  $1/q_e$  is plotted against  $1/C_e$  according to the Eq. (2.13), the Langmuir adsorption model fitted the experimental data very well with high correlation coefficients ( $R^2 > 0.99$ ) (Figure 4.22). It was indicated that Langmuir isotherm expression in line with a monolayer coverage of indigo onto silk. The values of the maximum amount of the dye per unit weight of fibre to form complete monolayer coverage on the surface (monolayer capacities,  $Q$ ) and Langmuir constants ( $b$ ) were calculated from the slopes and intercepts of the straight lines, respectively. The calculated results are reported in

Table 4.7. The monolayer capacity,  $Q$  of 15.65 mg/g silk and the  $b$  value of 153.42 mL/mg indicated that the silk yarn has an affinity for indigo dye.

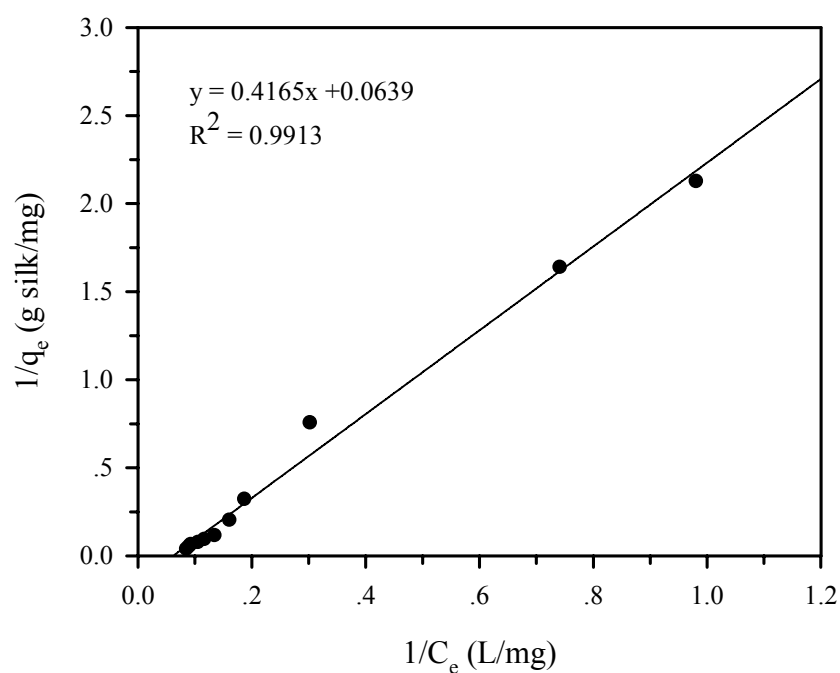


**Figure 4.22** Langmuir adsorption isotherm of the adsorption of indigo onto silk at 30°C.

**Table 4.7** Langmuir and Freundlich isotherm constants for the adsorption of indigo-urea onto silk at 30°C.

Temp. (°C)	Langmuir			Freundlich		
	$Q$ (mg/g silk)	$b$ (mL/mg)	$R^2$	$Q_f$ (mg/g silk)	$n$	$R^2$
30	15.65	153.42	0.9913	2.09	1.67	0.9566

The Freundlich isotherm equation (Eq. (2.15)) was also applied to the results of the adsorption of indigo onto silk. The values of  $Q_f$  and  $1/n$  can be determined from the linear plot of  $\ln q_e$  versus  $\ln C_e$  (Figure 4.23). The magnitude of the exponent  $1/n$  gives an indication of the favourability of adsorption. Values of  $n > 1$  (Table 4.7) obtained represent favourable adsorption conditions (Chairat *et al.*, 2005).

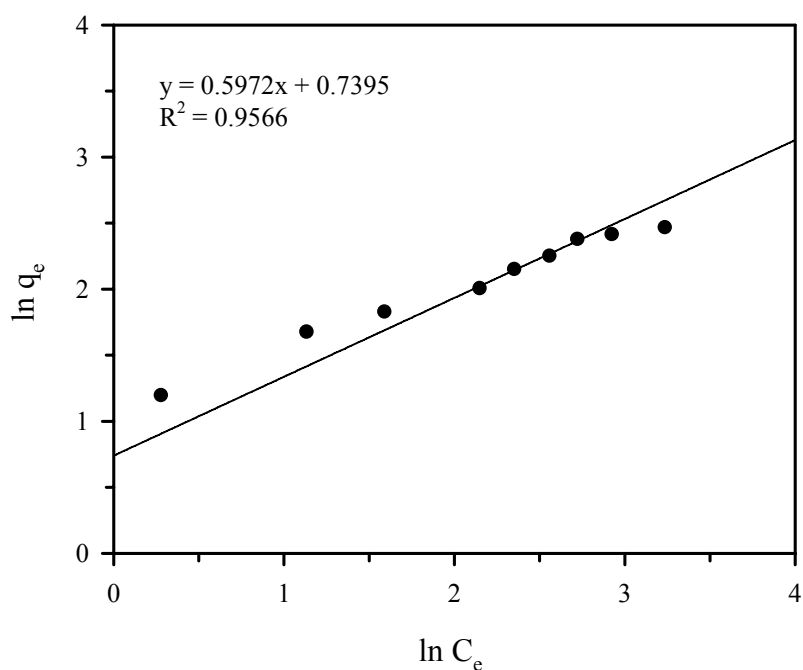


**Figure 4.23** Freundlich adsorption isotherm of the adsorption of indigo onto silk at 30°C.

#### 4.4.2.6 Thermodynamic parameters for the adsorption of indigo-urea on silk

In order to support the exothermic behaviour of the adsorption of indigo onto silk, the thermodynamic parameters,  $\Delta G^\circ$ ,  $\Delta H^\circ$  and  $\Delta S^\circ$  of indigo adsorption after reaching equilibrium were calculated by using the equations (2.16) to (2.19). Enthalpy change ( $\Delta H^\circ$ ) and entropy change ( $\Delta S^\circ$ ) of the adsorption are calculated from the slope and intercept of the van't Hoff plots of  $\ln K_c$  versus  $1/T$  (Figure 4.24). The results are listed in Table 4.8. The negative values of  $\Delta G^\circ$  indicate that the adsorption of indigo on silk is spontaneous. The negative value of  $\Delta H^\circ$  confirms that the adsorption process is an exothermic one. Furthermore, the entropy change ( $\Delta S^\circ$ ) in dyeing represents the entropy difference of the dye molecules within the fibre (Kim, Son, and Lim, 2005). The negative value of  $\Delta S^\circ$  indicates that adsorbed indigo-urea dye become more restrained within the silk fibre molecules than in the dyeing solution.

**Table 4.8** Thermodynamic parameters for the adsorption of indigo-urea onto silk at different temperatures.

Temp. (°C)	$K_c$	$\Delta G^\circ$ (kJ/mol)	$\Delta H^\circ$ (kJ/mol)	$\Delta S^\circ$ (J/mol K)	$R^2$
30	33.12	-9.62			
40	3.32	-3.53	-162.94	-509.29	0.9954
50	0.61	-1.56			

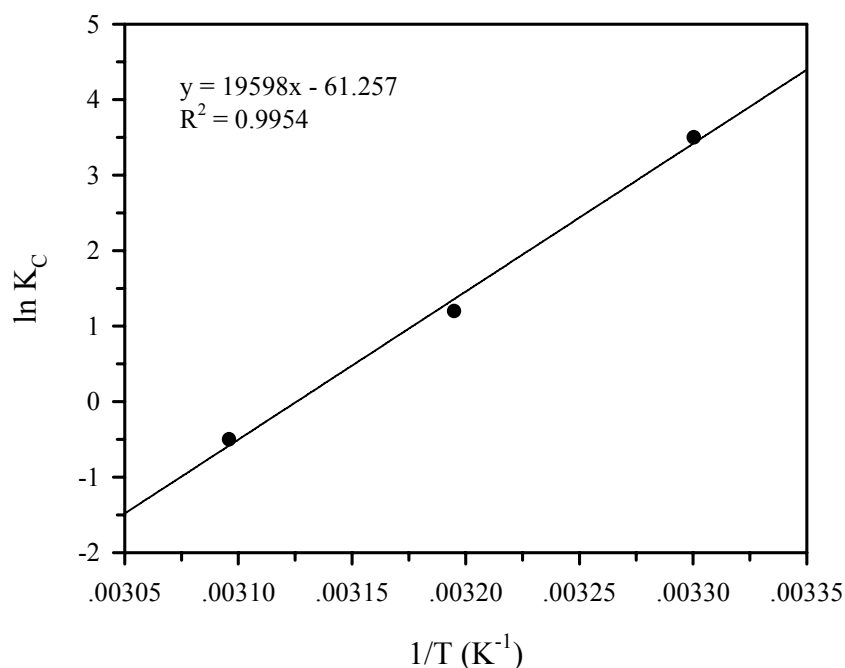


**Figure 4.24** The van't Hoff plots of  $\ln K_C$  versus  $1/T$ .

#### **4.4.3 Adsorption studies of plant extracted indigo-urea direct dyeing onto silk**

In order to investigate the plant extracted indigo-urea direct dyeing onto silk, the experimental parameters including, initial dye concentration, contact time and temperature were determined to find the most suitable dyeing conditions. The mechanism of adsorption of plant extracted indigo-urea direct dyeing onto silk was investigated by using the pseudo first order and pseudo second order kinetic models. In addition, activation parameters and thermodynamics parameters of adsorption have been investigated in this section.

#### **4.4.3.1 Effect of initial dye concentration and contact time on the adsorption of plant extracted indigo-urea onto silk**

The effects of initial dye concentration and contact time on the adsorption of plant extracted indigo-urea onto silk are presented in Figure 4.25. The adsorption capacities at equilibrium,  $q_{e,exp}$ , increased from 0.87-3.10 mg/g silk with an increase in initial dye concentration from 0.52-1.95 g/L (contained ~ 10-40 mg/L indigo) with an MLR of 1:100 at pH 4.0 and 30°C with equilibrium reached after 60 min. The equilibrium time is independent of initial dye concentrations. But in the first 30 min, the initial rate of adsorption was greater for higher initial dye concentrations since diffusion of dye molecules through the solution to the surface of the adsorbents is affected by this concentration (at a constant agitation speed). An increase of the dye concentration accelerates the diffusion of dyes from the dye solution onto adsorbents due to the increase in the driving force of the concentration gradient, as was also observed with indigo-urea adsorption on silk.



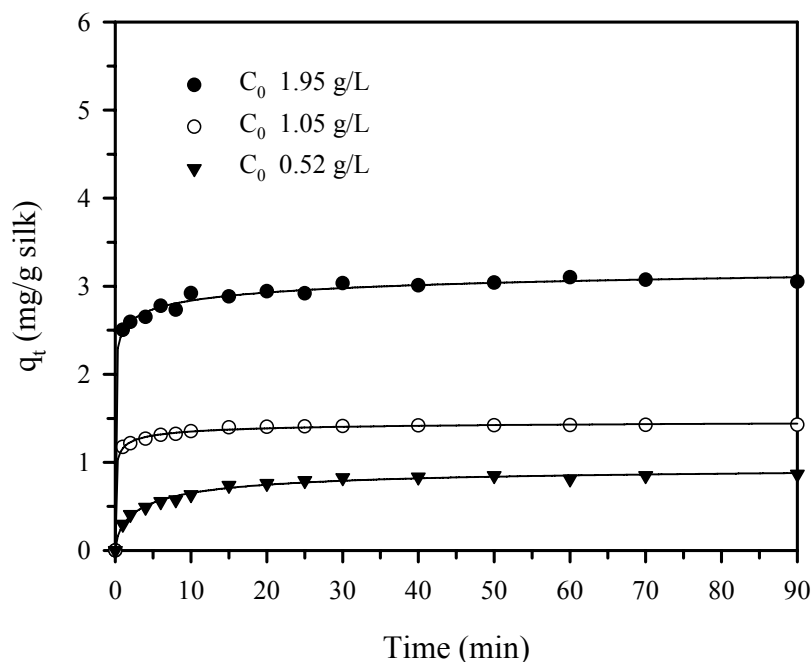


**Figure 4.25** Effect of initial dye concentration on the adsorption of plant extracted indigo-urea onto silk (under dyeing condition MLR = 1:100, pH = 4.0, 30°C).

The characteristic parameters of the pseudo first order and pseudo second order models and correlation coefficients are tabulated in Table 4.9. Plots of the pseudo- first order and pseudo second order equation at different initial dye concentration on the adsorption of plant extracted indigo onto silk are presented in Figures 4.26 and 4.27, respectively. The correlation coefficients ( $R^2$ ) for the pseudo-second order model for all concentrations are higher than for the pseudo first order model and the calculated equilibrium adsorption capacities fit well with the experimental data in the former model. These suggest that the pseudo second order adsorption mechanism is predominant as was the case with indigo-urea adsorption (section 4.4.2.1). The results in Table 4.9 also show  $k_2$ ,  $h_i$  and  $q_e$  as a function of

initial dye concentration. For the pseudo second order model, the rate constant decreases with an increasing of initial dye concentration, while the initial adsorption rate,  $h_i$ , increases with an initial dye concentration. An increase in initial dye concentration results in a significant increase in  $q_{e,cal}$ .

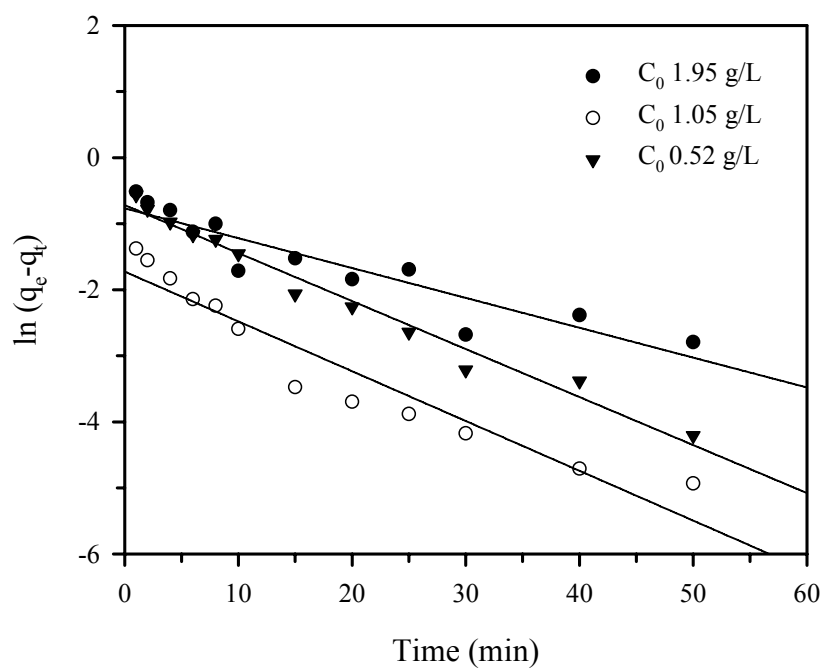


**Figure 4.26** Application of the pseudo first order equation at different initial dye concentration on the adsorption of plant extracted indigo-urea onto silk.

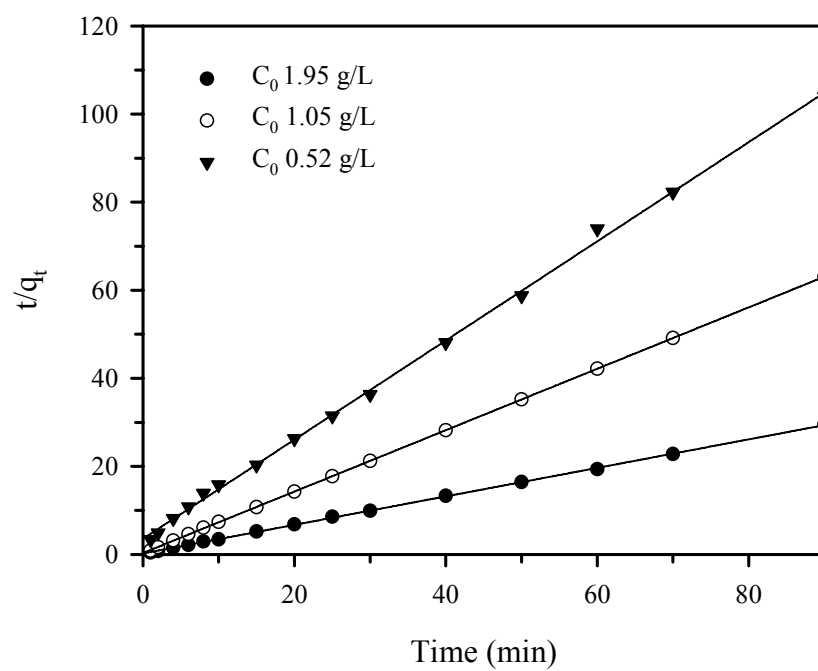


**Figure 4.27** Application of the pseudo second order equation at different initial dye concentration on the adsorption of plant extracted indigo-urea onto silk.

**Table 4.9** Comparison of the pseudo first- and pseudo second-order adsorption rate constants and the calculated and experimental  $q_e$  values for different initial dye concentrations and temperatures for the adsorption of plant extracted indigo-urea onto silk.

Parameter	$q_{e,exp}$ (mg/g silk)	Pseudo first order model			Pseudo second order model			
		$k_1$ ( $\text{min}^{-1}$ )	$q_{e,cal}$ (mg/g silk)	$R^2$	$k_2$ (g silk/mg min)	$q_{e,cal}$ (mg/g silk)	$h_i$ (mg/g silk min)	$R^2$
<i>Initial dye concentration: <math>C_0</math> (g/L): MLR 1:100, temp. 30 °C, contact time 60 min</i>								
0.52	0.87	0.0898	0.47	0.8600	0.3569	0.89	0.2820	0.9987
1.05	1.43	0.0754	0.18	0.9797	1.4708	1.43	3.0266	1.0000
1.95	3.10	0.0452	0.46	0.9197	0.4468	3.09	4.2644	0.9998
<i>Temperature: <math>C_0</math> 1 g/L, MLR 1:100, contact time 60 min</i>								
30	1.43	0.0754	0.18	0.9797	1.4708	1.43	3.0266	1.0000
40	0.88	0.0466	0.21	0.7866	1.1440	0.89	0.5715	0.9995
50	0.63	0.0407	0.14	0.8375	0.8287	0.63	0.4532	0.9996

#### **4.4.3.2 Effect of temperature on the adsorption of plant extracted indigo-urea onto silk**

The effect of temperature on adsorption of plant extracted indigo onto silk has been investigated at an initial dye concentration of 1 g/L (contained ~ 20 mg/L indigo) at pH 4.0 and an MLR of 1:100. A study of the temperature dependence of adsorption gives valuable information about the enthalpy change during adsorption. The effect of temperature on the adsorption rate was studied by carrying out a series of experiments at 30, 40 and 50°C. The adsorption capacities show a different trend at different temperatures (Figure 4.28). The adsorption decreased with increasing the temperature indicating that the adsorption of plant extracted indigo-urea onto silk is controlled by an exothermic process. A similar temperature effect on adsorption trend has also been shown in the case of adsorption of indigo-urea onto silk as described in section 4.4.2.3. The results of rate constant studies for different temperatures calculated by the pseudo first order and pseudo second order models are listed in Table 4.9. The correlation coefficient,  $R^2$ , for the pseudo second order adsorption model (Figure 4.30) has a higher value suggesting the dye adsorption process is predominantly by a pseudo second order adsorption mechanism.

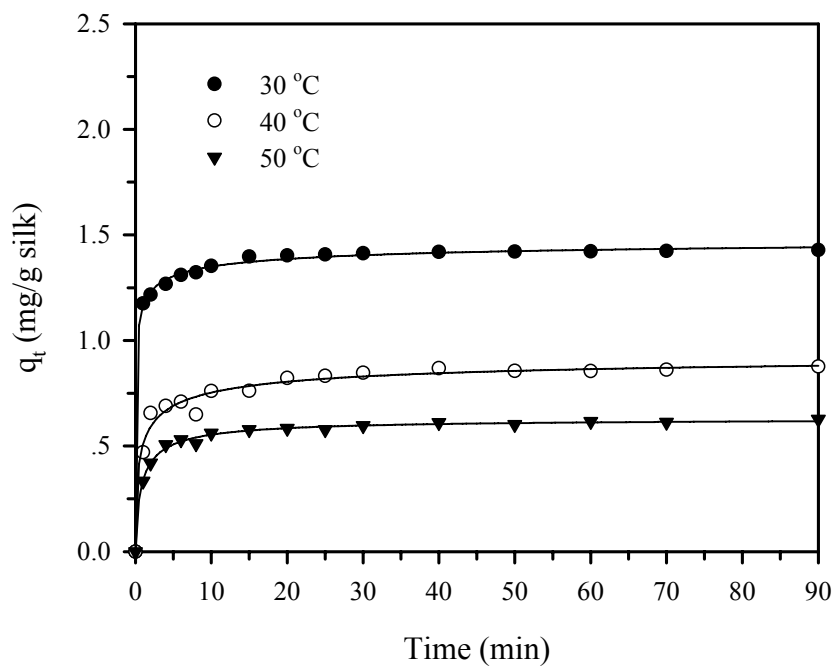


**Figure 4.28** Effect of temperature on the adsorption of plant extracted indigo-urea onto silk (under dyeing condition  $C_0 = 1$  g/L, pH = 4.0, MLR = 1:100).

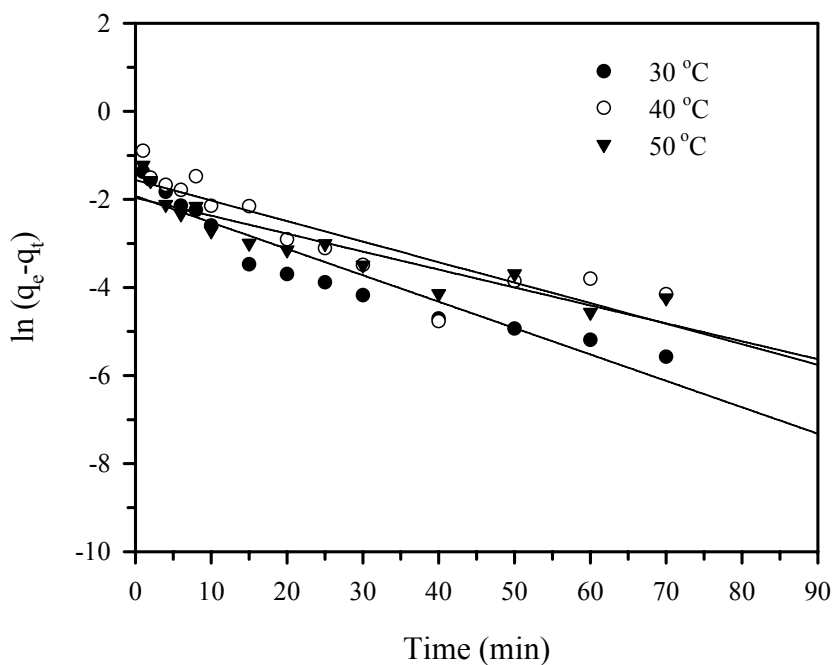


**Figure 4.29** Application of the pseudo first order equation at different temperatures on the adsorption of plant extracted indigo-urea onto silk.

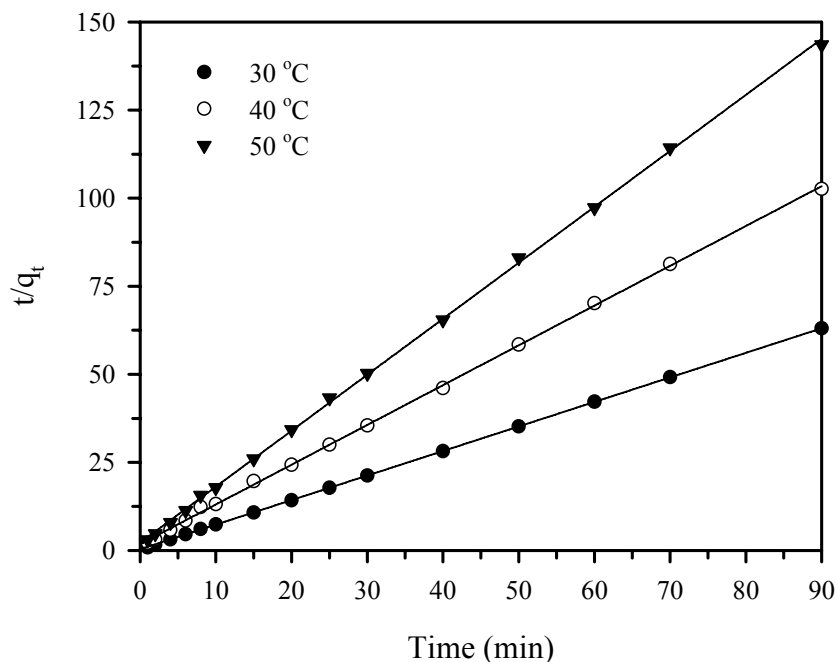


**Figure 4.30** Application of the pseudo second order equation at different temperatures on the adsorption of plant extracted indigo-urea onto silk.

#### 4.4.3.3 Activation parameters for the adsorption of plant extracted indigo-urea onto silk

The activation energy of the diffusion can be describes the dependence of the diffusion coefficient on the dyeing temperature and also represents the energy barrier that the dye molecule should overcome to diffuse into the fibre molecules (Kim *et al.*, 2005). The rate constants  $k_2$  for pseudo second order model at different temperatures listed in Table 4.9 were then applied to estimate the activation energy of the adsorption of plant extracted indigo onto silk by the Arrhenius equation. The slope of the plot of  $\ln k_2$  versus  $1/T$  (Figure 4.31) was used to evaluate  $E_a$  as listed in Table 4.10. For the  $E_a$  of 42.84 kJ/mol observed we can infer that the adsorption of plant

extracted indigo in the presence of urea onto silk is most likely via a chemisorption process as was again the case with the adsorption indigo-urea onto silk as described in section 4.4.2.4.

**Table 4.10** Activation parameters for the adsorption of plant extracted indigo-urea onto silk at initial dye concentration 1 g/L.

Temp. (°C)	$k_2$ (g silk/ mg min)	$E_a$ (kJ/mol)	$R^2$	$\Delta H^\#$ (kJ/mol)	$\Delta S^\#$ (J/mol K)	$\Delta G^\#$ (kJ/mol)	$R^2$
30	1.4708					72.93	
40	1.1440	42.84	0.9997	-47.76	-398.32	76.91	0.9991
50	0.8287					80.90	

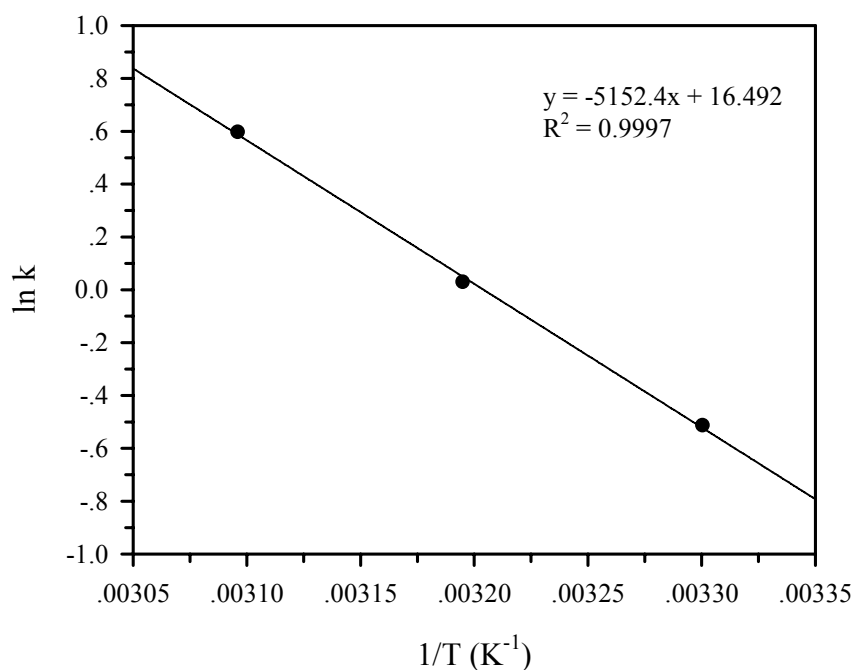


**Figure 4.31** Arrhenius plots for the adsorption of plant extracted indigo-urea on silk.



From the Eyring equation, the enthalpy ( $\Delta H^\ddagger$ ) and entropy ( $\Delta S^\ddagger$ ) of activation were calculated from the slope and intercept of a plot of  $\ln(k/T)$  versus  $1/T$  (Figure 4.32) as listed in Table 4.10. The value of  $\Delta G^\ddagger$  was calculated at 303, 313 and 323 K by using equation (2.10) and these values are listed in Table 4.10, while the negative entropy value ( $\Delta S^\ddagger$ ) reflects more aggregation and the interaction between plant extracted indigo-urea and the silk yarn.

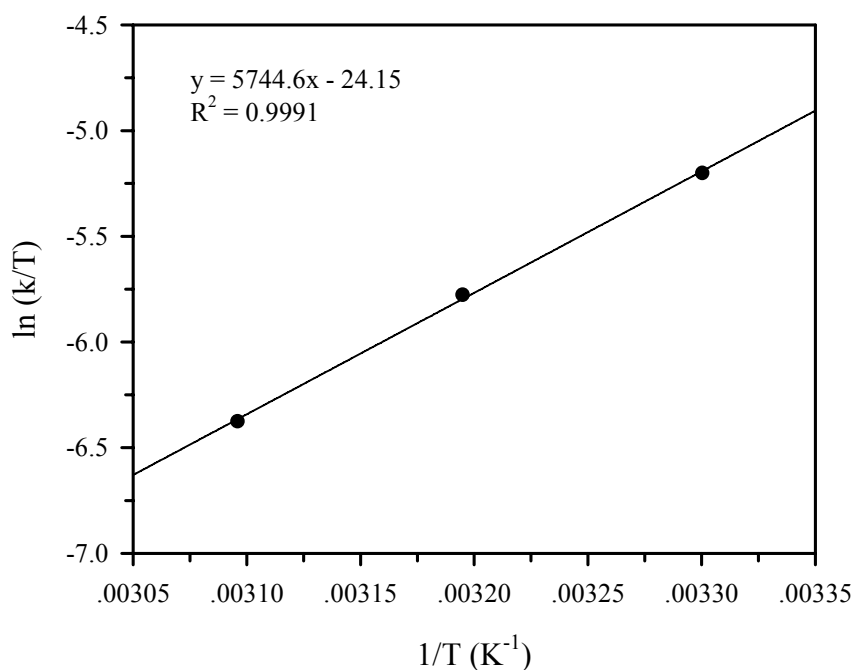


**Figure 4.32** Plot of  $\ln(k/T)$  against  $1/T$  for the adsorption of plant extracted indigo-urea on silk.

#### 4.4.3.4 Adsorption isotherm for the adsorption of plant extracted indigo-urea onto silk

The adsorption equilibrium data of plant extracted indigo-urea dyeing onto silk at 30°C were analyzed using the Langmuir (Figure 4.33) and Freundlich (Figure 4.34) expressions. The adsorption capacities and adsorption constants of plant extracted indigo-urea onto silk are shown in Table 4.11. The experimental data were found to fit well to the Langmuir isotherm, with the former being slightly better as indicated by the higher  $R^2$  values compared with that from the Freundlich expression. The applicability of the Langmuir isotherm suggests monolayer coverage of the dye on the surface of the silk. The Freundlich equation describes heterogeneous systems and reversible adsorption; and is not limited to the formation of a complete monolayer. It can be seen from Table 4.11 that the correlation coefficients for the Freundlich isotherms are less than those obtained for the Langmuir expression, but the Freundlich isotherm cannot be totally rejected in these equilibrium studies. Also the values of  $n$  more than 1 (Table 4.11) indicate favourable adsorption.

**Table 4.11** Langmuir and Freundlich isotherm constants for the adsorption of plant extracted indigo-urea onto silk at 30°C.

Temp. (°C)	Langmuir			Freundlich		
	Q (mg/g silk)	b (mL/mg)	$R^2$	$Q_f$ (mg/g silk)	n	$R^2$
30	2.56	4.98	0.9935	2.05	1.73	0.9527

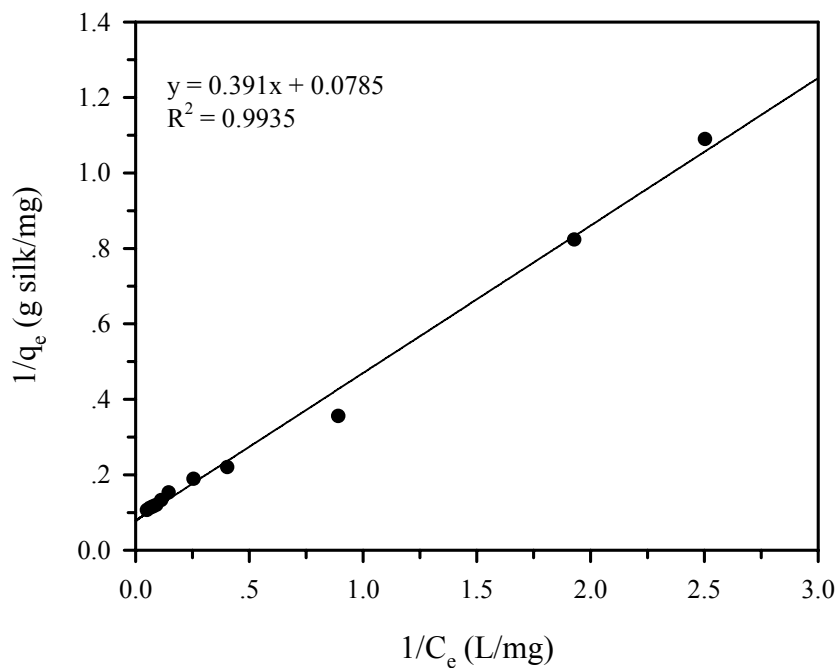


**Figure 4.33** Langmuir adsorption isotherm of the adsorption of plant extracted-urea indigo onto silk at 30°C.

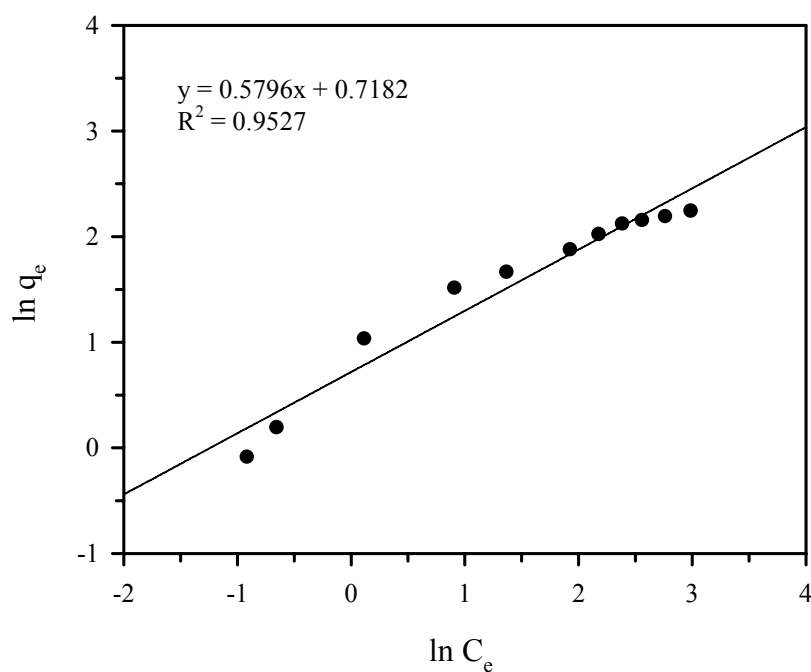


**Figure 4.34** Freundlich adsorption isotherm of the adsorption of plant extracted-urea indigo onto silk at 30°C.

#### **4.4.3.5 Thermodynamic parameters for the adsorption of plant extracted indigo-urea on silk**

In order to provide supporting evidence for the exothermic behaviour of plant extracted indigo-urea adsorption onto silk, after reaching equilibrium, the thermodynamic parameters  $\Delta G^\circ$ ,  $\Delta H^\circ$  and  $\Delta S^\circ$  of plant extracted indigo-urea adsorption were calculated by using the equations (2.16)-(2.19). Enthalpy change ( $\Delta H^\circ$ ) and entropy change ( $\Delta S^\circ$ ) of the adsorption are calculated from the slope and intercept of the van't Hoff plots of  $\ln K_c$  versus  $1/T$  (Figure 4.35). The results are listed in Table 4.12. The negative of  $\Delta H^\circ$  suggests that the adsorption of plant extracted indigo-urea onto silk is an exothermic process. The negative values of  $\Delta G^\circ$  indicate that the adsorption of process is spontaneous. Meanwhile, the entropy change ( $\Delta S^\circ$ ) on dyeing represents the entropy difference of the dye molecules within the fibre (Kim *et al.*, 2005). The negative value of  $\Delta S^\circ$  indicates that adsorbed indigo-urea dye become more restrained within the silk fibre molecules than in the dyeing solution. The result of the thermodynamic parameters for the adsorption of plant extracted indigo-urea on silk were shown the similar of adsorption behaviour to the thermodynamic parameters for the adsorption of indigo on silk that listed in Table 4.12.

**Table 4.12** Thermodynamic parameters for the adsorption of plant extracted indigo-urea onto silk at different temperatures.

Temp. (°C)	$K_C$	$\Delta G^\circ$ (kJ/mol)	$\Delta H^\circ$ (kJ/mol)	$\Delta S^\circ$ (J/mol K)	$R^2$
30	24.80	-8.13			
40	2.66	-2.47	-179.57	-565.83	0.9996
50	0.30	-3.19			

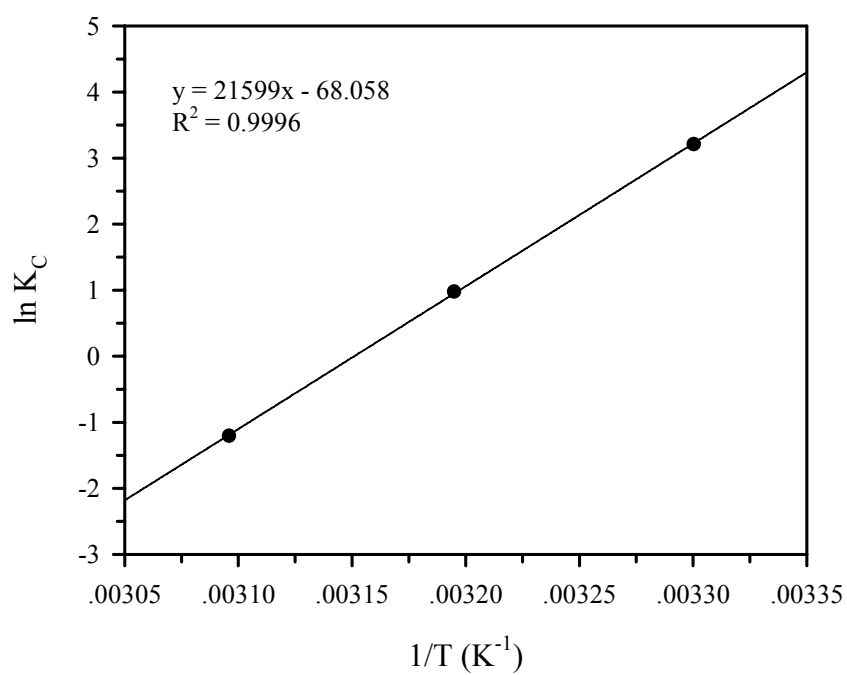


**Figure 4.35** The van't Hoff plots of  $\ln K_C$  versus  $1/T$ .

## 4.5 Conclusion

New ways to increase the water solubility of indigo were found based on the use of additives. These additives included cyclodextrins and derivatives, or simple hydrotropic compounds like urea and nicotinamide. Using these compounds the water solubility of pure indigo and plant extracted indigo could be increased significantly. The addition of urea was then used to develop a new process for the direct dyeing of silk under acidic conditions without the need for an indigo reduction and subsequent oxidation step. The key kinetic and thermodynamic parameters for this dyeing process were obtained, with the kinetics fitting a pseudo second order model. Other parameters were consistent with an exothermic chemisorption process. Whether the urea does more than increase the indigo solubility is as yet not known and could be the subject of future studies. It may, for example, swell the silk fibres and act as a type of organic mordant. Further studies on the colour properties, and wash and light fastness of the directly dyed silk, which is dyed a very attractive blue-green colour, are also required. Direct dyeing of silk using plant extracted indigo and urea could be a potentially viable option for villagers.

## 4.6 References

- Alexandre, G. S. P., Jocilene, D. T., Wlaine, A. F. and Silvia C. L. (2004). Comparative adsorption studies of indigo carmine dye on chitin and chitosan. **Journal of colloid and Interface Science**. 277: 43-47.
- Bassani, V. L., Krieger, D., Duchene, D. and Wouessidjewe, D. (1996). Enhanced water-solubility of albendazole by hydroxyl-propyl- $\beta$ -cyclodextrin complexation. **Journal of inclusion phenomena and molecular recognition in chemistry**. 25: 149-152.
- Bikádi, Z., Kurdi, R., Balogh, S., Szemán, J., and Hazai, E. (2006). Aggregation of cyclodextrins as an important factor to determine their complexation behavior. **Chemistry and Biodiversity**. 3(11): 1266-1278.
- Božič, M. and Kokol, V. (2008). Ecological alternatives to the reduction and oxidation processes in dyeing with vat and sulphur dyes. **Dyes and Pigments**. 76(2): 299-309.
- Brewster, M. E. and Loftsson, T. (2007). Cyclodextrins as pharmaceutical solubilizers. **Advanced Drug Delivery Reviews**. 59(7): 645-666.
- Challa, R., Ahuja, A., Ali, J. and Khar, R. (2005). Cyclodextrins in drug delivery: An updated review. **AAPS PharmSciTech**. 06(02): E329-E357.
- Chairat, M. (2004). **Extraction and Characterization of Lac Dye from Thai Stick Lac and Development of Lac Dyeing on Silk and Cotton**. Ph.D. Thesis, Suranaree University of Technology, Thailand.
- Chairat, M., Rattanaphani, S., Bremner, J. B. and Rattanaphani, V. (2005). An adsorption and kinetic study of lac dyeing on silk. **Dyes and Pigments**. 64(3): 231-241.

- Christie, R. M. (2001). **Colour Chemistry**. UK: Cambridge.
- Christie, R. M. (2007). Why is indigo blue? **Biothechnic and Histochemistry**. 82: 51-56.
- Crini, G. (2003). Studies on adsorption of dyes on beta-cyclodextrin polymer. **Bioresource Technology**. 90: 193-198.
- Crini, G. (2008). Kinetic and equilibrium studies on the removal of cationic dyes from aqueous solution by adsorption onto a cyclodextrin polymer. **Dyes and Pigments**. 77(2): 415-426.
- Davis, M. E. and Brewster, M. E. (2004). Cyclodextrin-based pharmaceuticals: past, present and future. **Nature Reviews Drug Discovery**. 3(12): 1023-1035.
- Domenech, A., Domenech-Carbo, M. T. and Vazquez de Agredos Pascual, M. L. (2007). Indigo/dehydroindigo/palygorskite complex in Maya Blue. **Journal of Physical Chemistry C**. 111: 4585-4595.
- Easton, C. J., Harper, J. B. and Lincoln, S. F. (1998). N,N'-Bis(6<sup>A</sup>-deoxy- $\beta$ -cyclodextrin-6<sup>A</sup>-yl) urea as a molecular template in the formation of indigoid dyes. **New Journal of Chemistry**. 22: 1163-1165.
- Easton, C. J. and Lincoln, S. F. (1999). **Modified Cyclodextrin: Scaffolds and Templates for Supramolecular Chemistry**. London: Imperial college press.
- Easton, C. J. (2005). Cyclodextrin-based catalysts and molecular reactors. **Pure and Applied Chemistry**. 77(11): 1865-1871.
- Gonzalez, G., Nassar, E. J. and Zaniquelli, M. E. D. (2000). Examination of the hydrotropic effect of sodium p-toluenesulfonate on a nonionic surfactant (C<sub>12</sub>E<sub>6</sub>) solution. **Journal of Colloid and Interface Science**. 230: 223-228.



- Hamlin, J. D., Phillips, D. A. S. and Whiting, A. (1999). UV/Visible spectroscopic studies of the effects of common salt and urea upon reactive dye solutions. **Dyes and Pigments**. 41(1-2): 137-142.
- Harper, J. B., Easton, C. J. and Lincoln, S. F. (2003). A cyclodextrin-based molecular reactor to template the formation of indigoid dyes. **Tetrahedron Letters**. 44: 5815-5818.
- Hebeish, A. and El-Hilw, Z.,H. (2001). Chemical finishing of cotton using reactive cyclodextrin. **Coloration Technology**. 117: 104-110.
- Kawahito, M. (2006). Natural and synthetic indigo colour in silk and cotton cloth. **Sen'i Gakkaishi**. 62(1): 43-47.
- Kim, T. K., Son, Y. A. and Lim, Y. J. (2005). Thermodynamic parameters of disperse dyeing on several polyester fibers having different molecular structure. **Dyes and Pigments**. 67(3): 229-234.
- Kongmuang, S. (2002). Hydrotropic Solubilization of riboflavin by urea, nicotinamide and nicotinamide analogues in aqueous systems. **Thai Journal of Pharmaceutical Sciences**. 26(2-2): 61-68.
- Loftsson, T. and Duchene, D. (2007). Cyclodextrins and their pharmaceutical applications. **International Journal of Pharmaceutics**. 329: 1-11.
- Mansur, C. R. E., Pires, R. V., Gonzalez, G. and Lucas, E. F. (2005). Influence of the hydrotrope structure on the physical chemical properties of polyoxide aqueous solutions. **Langmuir**. 21: 2696-2703.
- Muller, B. W. and Albers, E. (1991). Effect of hydrotropic substances on the complexation of sparingly soluble drugs with cyclodextrin derivatives and the influence of cyclodextrin complexation on the pharmacokinetics of the drugs.

**Journal of Pharmaceutical Sciences.** 80(6): 599-604.

Nollet, H., Roels, M., Lutgen, P., Van der Meeren, P. and Verstraete, W. (2003).

Removal of PCBs from wastewater using fly ash. **Chemosphere.** 53(6): 655-665.

Pederson, M. (1993). Effect of hydrotropic substances on the complexation of

clotrimazole with  $\beta$ -cyclodextrin. **Drug Development and Industrial Pharmacy.** 19(4): 439-448.

Savarino, P., Parlati, S., Buscaino, R., Piccinini, P., Degani, I. and Barni, E. (2004).

Effects of additives on the dyeing of polyamide fibres. Part I: [ $\beta$ ]-cyclodextrin. **Dyes and Pigments.** 60(3): 223-232.

Savarino, P., Parlati, S., Buscaino, R., Piccinini, P., Barolo, C. and Montoneri, E.

(2006). Effects of additives on the dyeing of polyamide fibres. Part II: Methyl- $\beta$ -cyclodextrin. **Dyes and Pigments.** 69(1-2): 7-12.

Septhum, C., Rattanaphani, S., Bremner, J. B. and Rattanaphani, V. (2009). An

adsorption study of alum-morin dyeing onto silk yarn. **Fibers and Polymers.** 10(4): 481-487.

Son, Y. A., Lim, H. T., Hong, J. P. and Kim, T. K. (2005). Indigo adsorption

properties to polyester fibers of different levels of fineness. **Dyes and Pigments.** 65: 137-143.

Steingruber, E. (2004). **Indigo and Indigo Colourants: Ullmann's Encyclopedia of**

**Industrial Chemistry.** New York: Wiley-VCH.

Szente, L. and Szejtli, J. Z. (1999). Highly soluble cyclodextrin derivatives:

chemistry, properties, and trends in development. **Advanced Drug Delivery Reviews.** 36(1): 17-28.

Yuan, Z., Zhu, M. and Han, S. (1999). Supramolecular inclusion complex formation and application of [beta]-cyclodextrin with heteroanthracene ring cationic dyes. **Analytica Chimica Acta**. 389(1-3): 291-298.

## CHAPTER V

### CONCLUSION

The adsorption kinetics and thermodynamics of indigo and indigo derivatives dyeing onto silk were investigated in this study. The adsorption capacities are significantly affected by pH, the initial dye concentration, the material to liquor ratio (MLR) and temperature. Detailed kinetic and thermodynamic parameters were determined for the first time for the dyeing of silk using indigo itself and the vat dyeing method. This method involved initial reduction of the indigo with sodium dithionite (indigo:Na<sub>2</sub>S<sub>2</sub>O<sub>4</sub>:NaOH equal to 1:300:300) to give leuco indigo, then immersion of the silk in the aqueous solution of leuco indigo, followed by aerial oxidation to indigo *in situ*. A chemisorption process with an activation energy ( $E_a$ ) of 77.45 kJ/mol was indicated for the indigo dyeing of silk. A comparison of kinetic and thermodynamic data for silk dyeing using plant derived indigo extract obtained from *Indigofera tinctoria* was also made with the data from indigo itself and close similarities were seen. This was consistent with the HPLC analytical data which showed indigo as a major component of the extract. It also indicated that other components in the crude indigo extract were not significantly affecting the dyeing kinetics and thermodynamics. This work obtained the key adsorption parameters for indigo dyeing onto silk which enabled a better understanding of the indigo dyeing process. It also was to provide benchmark data to inform later projected direct dyeing studies with indigo and derivatives.

Detailed kinetic and thermodynamic parameters have been obtained for the first time with respect to the direct dyeing of silk using the commercially available, water soluble blue dye, indigo carmine. The adsorption process with this indigo-derived dye was an exothermic chemisorption one following pseudo second order kinetics. The adsorption capacity was dependent on the pH of the dye solution and optimal uptake on silk occurred at pH 4.0. Another new water soluble blue-green dye was prepared in this work from indigo, which, in contrast to indigo carmine, involved the introduction of polar substituents on nitrogen in the indigo molecule. The particular compound prepared incorporated a carboxylic acid and ester group in separate substituents. In a trial experiment, this compound was shown to dye silk under acidic conditions. Future work could cover optimization of the dyeing process, kinetic and thermodynamic adsorption studies, colour property studies and wash and light fastness investigations. In addition, ways to prepare the diacid analogue in high yield could be further investigated, as this compound would be expected to have higher water solubility at acidic pH and more opportunities for silk-dye interactions.

New ways to increase the water solubility of indigo were found based on the use of additives. These additives included cyclodextrins and derivatives, or simple hydrotropic compounds like urea and nicotinamide. Using these compounds the water solubility of pure indigo and plant extracted indigo could be increased significantly. The addition of urea was then used to develop a new process for the direct dyeing of silk under acidic conditions without the need for an indigo reduction and subsequent oxidation step. The key kinetic and thermodynamic parameters for this dyeing process were obtained, with the kinetics fitting a pseudo second order model. Other parameters were consistent with an exothermic chemisorption process. Whether the

urea does more than increase the indigo solubility is as yet not known and could be the subject of future studies. It may, for example, swell the silk fibres and act as a type of organic mordant. Further studies on the colour properties, and wash and light fastness of the directly dyed silk, which is dyed a very attractive blue-green colour, are also required. Direct dyeing of silk using plant extracted indigo and urea could be a potentially viable option for villagers.

# CURRICULUM VITAE

**NAPARAT JIWALAK**

**E-mail:** naparat406@yahoo.com

**Born:** 30 October 1974 at Nakhon Ratchasima, Thailand

## **Education:**

1993-1998 B.Eng. (Chemical), Suraneree University of Technology, Thailand

2000-2003 M.Eng. (Chemical), Suraneree University of Technology, Thailand

## **Experiences:**

1998-2000 Research Assistant at School of Chemical Engineering, Suraneree University of Technology, Nakhon Ratchasima, Thailand

1998-2001 Teaching Assistant at School of Chemistry, Suraneree University of Technology, Nakhon Ratchasima, Thailand

2007 Ph.D. research experience at the University of Wollongong, Australia

2008 Ph.D. research experience at the Srinakharinwirot University, Thailand

2004-present Lecturer, School of Chemistry, Chiang Mai Ratchabhat University, Thailand

## **Scholarship:**

Support by Chiang Mai Ratchabhat University, Chiang Mai, Thailand and the Ministry of University Affairs, Thailand

## **Publication:**

Jiwalak, N., Rattanaphani, S., Bremner, J. B. and Rattanaphani, V. (2010). Equilibrium and kinetic modeling of the adsorption of indigo carmine onto silk.

**Fibers and Polymers.** 11(4): 572-579.